



UNIVERSITY OF  
**LEICESTER**

**ANALYSIS OF VOLATILE ORGANIC  
COMPOUNDS PRODUCED DURING THE  
DECOMPOSITION OF HUMAN ANALOGUES**

Thesis submitted for the degree of Doctor of  
Philosophy at University of Leicester

By

Omolara O. Okunuga (M. Chem)

Department of Chemistry

University of Leicester

September 2016

## DECLARATION

I hereby certify that this material which I now submit for assessment on the program of study leading to the award of Doctor of Philosophy is entirely my own work, that I have exercised reasonable care to ensure that the work is original, and to the best of my knowledge, does not breach any law of copyright, and has not been taken from the work of others save and to the extent that such work has been cited and acknowledged within the text of my work.

Signed  Mwara Kuunga

Date September 29, 2016

## ABSTRACT

The study of volatile organic compounds (VOCs) associated with decomposing remains is a field of growing interest in forensic science. Over the past decade, there has been an increasing demand to explicate key signatures of decomposition odour in an attempt to improve upon current training kits, aid in the development of an implement which could be used to detect clandestine graves, and to determine the post-mortem interval of a corpse. At present, current research seems to validate the view that the decomposition odour profile is ambiguous because of disparities in the environment in which decomposition occurs, methods of chemical analysis and sample collection techniques.

The purpose of this research was to investigate the odour profile surrounding buried and exposed human analogues in controlled environments, in order to understand how VOCs partition between different mediums. To this effect, a bespoke decomposition chamber was developed and characterised in the Real-time Air Fingerprinting Technology laboratory at the University of Leicester, and decomposition VOCs released into the headspace within chamber were monitored online via the use of Chemical Ion Reaction Mass spectrometry (CIR-MS) and Solid Phase Micro Extraction coupled with Gas Chromatography-Mass Spectrometry (SPME-GC-MS).

Overall, there was an abundance of polysulphides, specifically dimethyl disulphide detected by both CIR-MS and SPME-GC-MS in the buried and exposed experiments. Seven VOCs argued to be key markers of decomposition in the exposed trials comprised of 2-butanone, dimethyl disulphide, methanethiol, trimethylamine, 1-propanol, 1-butanol, and acetone.

In effect, findings from these trials demonstrated that there are distinctive subsets of VOCs released from decomposing carcasses, and soil acts as a sink for majority of these compounds. The use of CIR-MS in the study of decomposition odour was successful, as was the application a novel approach in extracting patterns within the CIR-MS data

## ACKNOWLEDGEMENTS

Firstly, I would like to express my sincerest gratitude to my supervisor Prof. Paul Monks for the continuous support of my PhD study, for his patience, motivation and immense knowledge. His guidance was instrumental in all the time of my research and in the writing of this thesis. Besides my supervisor, I am also indebted to Dr. Rebecca Cordell, for her assistance, teaching and sharing her valuable knowledge; I am truly grateful for all her support in all areas of this study.

Thanks are also due to Dr. Roberto Sommariva, Dr. Robert Blake, Dr. Thomas Adams and Rikesh Panchal for the laughs, encouragements, stimulating discussions and most importantly, for making the research group a pleasure to work and learn in. I acknowledge the contribution of Carl Schieferstein and Praful Chauhan, and all the technical staff for always making time to help and providing the necessary support and resources.

I would like to thank to my family for their love and emotional support, they have always encouraged me to do my best and I appreciate all the time and effort they have dedicated to supporting me. Finally, I must thank Dr William Darler for his unwavering faith, love and encouragement. You understand the ups and downs over the past few years most well. Thank you for caring and sticking with me.

# Contents

<b>1</b>	<b>INTRODUCTION</b> .....	<b>1</b>
1.1	Forensic taphonomy .....	1
1.2	Detection of remains.....	3
1.3	Determination of Post Mortem Interval (PMI) .....	6
1.4	Chemistry of decomposition .....	8
1.4.1	Process of decomposition.....	8
1.4.2	Stages of decomposition .....	11
1.4.3	Factors affecting decomposition process .....	13
1.5	Volatile Organic Compounds .....	17
1.6	Current research on cadaver decomposition VOCs .....	18
1.7	Practitioner- oriented goals.....	21
1.8	Study objectives .....	22
1.9	Chapter 1 Summary .....	23
<b>2</b>	<b>EXPERIMENTAL</b> .....	<b>26</b>
2.1	Decomposition chamber .....	26
2.2	Chemicals and consumables .....	28
2.2.1	Research subjects .....	28
2.3	Analytical methods.....	30
2.3.1	Solid Phase Microextraction (SPME) .....	30
2.3.2	Gas Chromatography-Mass Spectrometry (GC-MS) .....	36

2.3.3	Chemical Ionisation Reaction Mass Spectrometry (CIR-MS)	43
2.3.4	Quantification of results generated by CIR-MS	52
2.3.5	Data handling and statistics	53
2.4	Chapter 2 Summary	57
<b>3</b>	<b>METHOD DEVELOPMENT</b>	<b>59</b>
3.1	Decomposition chamber	59
3.1.1	Design and implementation	60
3.1.2	Characterisation of the decomposition chamber	63
3.2	Characterisation of the CIR-MS instrument	68
3.2.1	Sensitivity	68
3.2.2	Humidity dependence	69
3.2.3	Competing reagent ions	72
3.2.4	Calibration of the CIR-MS instrument	76
3.3	Characterisation of the SPME-GC-MS instrument	82
3.3.1	Choice of SPME fibre	83
3.3.2	Effect of exposure time on VOCs captured by SPME	86
3.3.3	Choosing an internal standard concentration	88
3.3.4	Effect of humidity on VOCs extracted by SPME	92
3.3.5	Effect of ammonia on VOCs extracted by SPME	94
3.3.6	Calibration of SPME-GC-MS	95
3.4	Chapter 3 Summary	100
<b>4</b>	<b>THE ANALYSIS OF VOCS RELEASED FROM MAMMALIAN DECOMPOSITION DURING BURIED HUMAN ANALOGUE TRIALS (BHA)</b>	<b>103</b>

4.1	Introduction .....	103
4.2	Experimental Setup.....	105
4.3	Data Analysis.....	107
4.4	Results and Discussion.....	108
4.4.1	Climatic conditions.....	108
4.4.2	CIR-MS .....	111
4.4.3	SPME-GC-MS.....	126
4.4.4	Reproducibility of decomposition VOCs (BHA trial 3) .....	133
4.4.5	Validation and Quantification of decomposition VOCs.....	135
4.5	Chapter 4 Summary .....	140
<b>5</b>	<b>THE ANALYSIS OF VOCS RELEASED FROM MAMMALIAN DECOMPOSITION DURING EXPOSED HUMAN ANALOGUE TRIALS (EHA).....</b>	<b>143</b>
5.1	Introduction .....	143
5.2	Experimental setup .....	144
5.3	Results and Discussion.....	146
5.3.1	Physical conditions.....	146
5.3.2	CIR-MS .....	148
5.3.3	SPME-GC-MS.....	158
5.3.4	Validation of CIR-MS results .....	167
5.3.5	Reproducibility .....	169
5.3.6	Quantification.....	175
5.4	Chapter 5 summary.....	179
<b>6</b>	<b>CONCLUSIONS .....</b>	<b>181</b>

6.1.1	Feasibility of CIR-MS in the study of decomposition odour..	181
6.1.2	Repeatability of carcass decomposition.....	184
6.1.3	Stages of decomposition from headspace measurements.....	184
6.1.4	Influence of soil on decomposition VOCs. ....	186
6.1.5	Core VOCs associated with buried and exposed decomposition 187	
6.2	Future considerations .....	187
<b>7</b>	<b>BIBLIOGRAPHY .....</b>	<b>190</b>

# List of Tables

1.1.	Summary of some of the methods used in the detection of human remains. Adapted from Killiam 1994 (7) .....	4
1.2.	Relation of Taphonomy to traditional determination of post-mortem interval. Reproduced from Reich <i>et al</i> (23) .....	7
1.3.	Chemical composition of Mammalian Cadavers during life. Measurements of carbon (C), nitrogen (N), phosphorus (P), potassium (K), calcium (Ca), and magnesium (Mg) are presented as grams per kilogram (g/kg) cadaver mass (dry weight). Adapted from Tibbett and Carter (4) .....	10
2.1.	Details of the main experimental trials conducted towards this research project. BHA refers to <i>buried human analogue</i> and EHA, <i>exposed human analogue trials</i> . .....	29
2.2.	Overview of some commercially available SPME fibre coatings. Adapted from Schmidt 2015 (86).....	34
2.3.	Overview of GC columns used in other decomposition studies .....	37
2.4.	Summary of the main product channels formed as a result of protonation using hydronium as the primary ion. Adapted from Ellis et al (89) .....	45
3.1.	Details of five analytical standards tested for on CIR-MS under varied sample humidity. Values for proton affinities were reported from the National Institute of Standards and Technology (NIST) unless otherwise stated. Analytical grade standards were purchased from Sigma Aldrich UK.....	71
3.2.	Details of the twenty standards calibrated for on the CIR-MS instrument. Standards were purchased form Sigma Aldrich, UK.....	78
4.1.	Details of the compounds tentatively assigned in the measurements collected by CIR-MS in BHA trial 4 References are represented symbolically as # (Forbes 2014 (62)), $\diamond$ (Statheropoulos 2011(28)), $\ominus$ =	

	(Perrault 2014 (68)), $\boxtimes$ (Dekeirsschieter 2009 (27)), $\bullet$ (Swann 2010 (115)), and $\#$ (Agapoiu 2015 (58)). .....	123
4.2.	Compounds with greater than 3 occurrences during BHA 4 trial. <i>RT</i> refers to retention time in minutes, <i>R. Match</i> refers to reverse match, % prob refers to percentage probability and MW refers to molecular weight of each compound. Reverse matches and percentage probabilities were reported using the NIST search library. Diazene dimethyl, cyclobutylamine, dimethyl sulphide and hexane only occurred twice during BHA 4 trial. ....	129
4.3.	Overview of the core compounds detected via CIR-MS and SPME-GC-MS across BHA 3 and BHA 4 trials. Mass channels (MW+1) is presented under CIR-MS column.....	135
5.1.	Tentative compound assignment of mass channels detected within the three subsets of EHA trial 3 (CIR-MS). Proton affinity figures are reported from NIST unless otherwise stated, and stages of decomposition were collected from the text within several decomposition articles. These have been references symbolically as $\#$ (Forbes 2014 (62)), $\diamond$ (Statheropoulos 2011(28)), $\ominus=$ (Perrault 2014 (68)), $\boxtimes$ (Dekeirsschieter 2009 (27)), $\bullet$ (Swann 2010 (115)), and $\#$ (Agapoiu 2015 (58)). .....	155
5.2.	Full list of compounds detected by SPME-GC-MS in EHA trial 3. These have been references symbolically as $\#$ (Forbes 2014 (62)), $\diamond$ (Statheropoulos 2011(28)), $\ominus=$ (Perrault 2014 (68)), and $\boxtimes$ (Dekeirsschieter 2009 (27)). .....	160

# List of Figures

Figure 1.1 Typical decay stages followed by pig carcasses in a forest biotope. Reproduced from Dekeirsschieter 2012 [30].....	13
Figure 2.1 Illustrates the schematic of the chamber covering used in the study of the decomposition of human analogues. ....	27
Figure 2.2 Image of the chamber developed for the study of decomposition VOCs associated with pig carcasses .....	27
Figure 2.3 Illustrates the principles of Headspace – Solid-phase Microextraction (a), and (b) Extraction mechanisms for absorbent (liquid) and adsorbent (solid) fibre coating. Image adapted from Schmidt et al [89] .....	33
Figure 2.4 Analysis by solid phase micro extraction-gas chromatography-mass spectrometry (SPME-GC-MS). Image adapted from Schmidt <i>et al</i> [89] .....	35
Figure 2.5 Schematic diagram showing components of a GC instrument. Schematic reproduced from Ellis <i>et al</i> [92].....	37
Figure 2.6 Schematic representation of the chromatographic separation in the GC column. Adapted from McNair 2011 .....	39
Figure 2.7 Side and end views of the rods employed in quadrupole mass analysers. Reproduced from Ellis <i>et al</i> [92].....	41
Figure 2.8 Schematic of the ion source (ED1-ED2) and drift tube region (ED3-ED7) of the CIR-MS instrument employed in this research. Image reproduced form Ellis et al [92] .....	48
Figure 2.9 Schematic of the reflectron end of the time of flight mass analyser used in CIR-TOF-MS instrument utilized in the study of decomposition VOCs .....	50
Figure 2.10 Schematic representation of the University of Leicester CIR-TOF-MS system. Image adapted from Blake et al [100].....	51
Figure 2.11 Representation of the data processing scheme used in this research project .....	56
Figure 3.1 Illustrates the sectioning of the bespoke decomposition chamber used in preliminary decomposition odour experiments which were	

	conducted in early 2012 (a), and (b) the sectioning used to elude fissures in Buried Human Analogue trials 3 and 4. ....	60
Figure 3.2	Previous strategies employed in the design of the bespoke decomposition chamber used in the first Buried Human Analogue trial in 2012 (a), the first Exposed Human Analogue trial conducted in 2012, (c) the second Buried Human Analogue trial in 2013, and (d) the external positioning of the sample lines and electrical wirings.....	62
Figure 3.3	Graphical representation of the differences in the exit flow rate (y-axis) versus entry flow rate (x-axis) of the bespoke decomposition chamber when a range of flow rates were examined. Flow rates tested spanned from 0 L/min to 1 L/min range. Flows were measured by use of an Alicat Scientific mass flow controller with a maximum flow capacity of 10 L/min.....	64
Figure 3.4	Average CIR-MS mass spectra generated over the course of seven days when: (a) synthetic grade air was directly fed into the CIR-MS instrument, (b) synthetic air was bypassed through the decomposition chamber, (c) topsoil added to the decomposition chamber and (d) sand added to the decomposition chamber. 10 minute scans were collected over the 7 days, and all counts were normalised to 1E6 of the counts in mass channel 19.....	66
Figure 3.5	Illustrates the average climatic conditions within the decomposition chamber. Headspace and relative humidity were measured by use of CS215 sensor while soil temperature and volumetric water content (VWC) were monitored by use of CS650 probe. Measurements were logged hourly on CR10X data logger over several weeks .....	67
Figure 3.6	Sensitivity of pyrrole (m/z 68) as measured by the CIR-MS instrument over the course of three years. Tests were conducted at approximately 10% relative humidity. Concentration variations were achieved by altering the flow rate of dilatant gas nitrogen. The flow rate of pyrrole (10 ppm pyrrole mixture in nitrogen) was held constant at 60 ml/min. 1 minute scans were collected for a total of twenty minutes, although data from the first ten minutes were regarded as the equilibration period, and were excluded from the analysis. All counts were normalised to hydronium at mass channel 19. ....	69

Figure 3.7 Graphical representation of the ratio of hydronium ions at m/z 19 to hydrated hydronium cluster ions at m/z 37 when sample humidity in a Tedlar bag was increased from 0.5% (dry) to 89% (humid) relative humidity. 10 minute scans were collected and averaged over a 60-minute period by use of the CIR-MS instrument.....	70
Figure 3.8 Humidity effect on measurements collected by CIR-MS. Varying concentrations of analytical grade standards 1-propanol, dimethyl sulphide, acetone and 2-butanone were tested under dry (0.5% relative humidity) and humid (89% relative humidity) conditions. 10- minute scans were collected for a total of 100 minutes at each concentration and all counts were normalised to 106 of the signal at m/z 19.....	72
Figure 3.9 Illustrates the raw signal intensities for competing reagent ions hydronium ( $H_3O^+$ ) at m/z 19 and ammonium ion ( $NH_4^+$ ) at m/z 18 as a function of concentration of sample gas ammonia. The experiments were conducted in 10 L Tedlar sample bags and 10 minute scans were collected over a 60-minute period. All measurements were observed by use of the CIR-MS instrument. ....	74
Figure 3.10 Graphical representation of the behaviour of four analytical grade standards purchased from Sigma Aldrich UK: hexane, 1-butanol, carbon disulphide (a) and (b) trimethylamine as a function of ammonia gas concentration as measured on the CIR-MS instrument.....	76
Figure 3.11 Sensitivity of the CIR-MS instrument to twenty analytical grade standards: carbon disulphide, trimethylamine, 2-butanone, dimethyl sulphide, 1-propanol, acetone, methanethiol, acetic acid, dimethyl trisulphide (DMTS), dimethyl disulphide (DMDS), decane, hexane, 3-pentanone, alpha pinene, dodecane, butanal 3-methyl, ethyl acetate, pentane, 1-butanol and benzene. Sensitivity was extrapolated from the slope of the respective linear fit, and is reported in normalised counts per second per concentration in ppbV.....	79
Figure 3.12 Typical parameters considered in SPME method development .....	83
Figure 3.13 Total number of VOCs captured on five SPME fibre polymer coatings (expressed in per cent)., Each fibre was exposed in the headspace of the decomposition chamber for 20 minutes, and sampling occurred on the same day (day 6 of BHA trial 4). Compounds present in the background	

(day 0) i.e. prior carcass introduction were excluded from the final count .....	84
Figure 3.14 Schematic of the Carboxen –PDMS SPME fibre. Adapted from Robert <i>et al</i> [87] .....	84
Figure 3.15 Time effect for SPME extraction (a)reproduced from Vas <i>et al</i> [82] and (b) results generated from this work (EHA trial 3) by use of CAR/PDMS fibre .....	86
Figure 3.16 Bar chat illustrating the effect of exposure time of SPME fibre CAR/PDMS on the extraction of decomposition VOCs methanethiol, trimethylamine, dimethyl sulphide, dimethyl disulphide, dimethyl trisulphide and bromobenzene as measured on the SPME-GC-MS instrument during Exposed Human Analogue trial 3 .....	87
Figure 3.17 Illustrates the response of the SPME-GC-MS instrument (CAR/PDMS fibre) when varying concentrations of internal standard bromobenzene was used. Experiments were created by use of 10 L Tedlar sample bags, and at each concentration, triplicate measurements were collected...89	89
Figure 3.18 Illustrates the response of the SPME-GC-MS instrument when 0.6 ppmV (blue), 1 ppmV (red) and 5 ppmV (green) of Internal standard bromobenzene were captured on five SPME fibre coatings: PA, PDMS, PDMS/CAR, PDMS/DVB, PDMS/CAR/DVB. Variables such as sampling height, exposure times and internal oven temperatures of the GC oven were kept constant.....	91
Figure 3.19 Graphical representation to show the humidity dependence of SPME- GC-MS (CAR/PDMS fibre) on four analytical grade standards: 1- propanol, dimethyl sulphide, acetone and 2-butanone when examined under dry (0.5% relative humidity) and humid (89% relative humidity) conditions.....	92
Figure 3.20 Illustrates the response of the CAR/PDMS SPME fibre when varying concentrations of ammonia gas was added to the headspace of a calibration mixture. The calibration mixture consisted of constant concentrations of analytical grade standards hexane, carbon disulphide, trimethylamine and 1-butanol.....	94
Figure 3.21 Sensitivity of the SPME-GC-MS (PDMS/CAR) to analytical grade standards carbon disulphide, trimethylamine, 2-butanone, dimethyl sulphide, 1-propanol, acetone, methanethiol, acetic acid, dimethyl	

	trisulphide (DMTS), dimethyl disulphide (DMDS), decane, hexane, 3-pentanone, alpha pinene, dodecane, butanal, 3-methyl, ethyl acetate, pentane, 1-butanol and benzene. Sensitivity is extrapolated from the slope of the linear fit and 'Area' refers to the ratio of the analyte signal to that of the internal standard signal. ....	96
Figure 4.1	Cross-sectional view of the bespoke decomposition chamber during the Buried Human Analogue trials. ....	106
Figure 4.2	Temperature recordings as measured during Buried Human Analogue trial 4 (BHA 4). Maximum, minimum and mean headspace temperature measurements a) Soil, headspace, and carcass temperature measurements b) Temperature recordings were captured by use of Campbell Scientific CS215 and CS650 sensors. All parameters were logged unto a CR10X data logger. Headspace refers to the air 'pocket' above the soil within the experimental chamber. BHA trial 4 lasted a total of 40 days .....	109
Figure 4.3	Soil Volumetric Water Content recordings as measured by Campbell's Scientific CS650 sensor during BHA 4 trial. Measurements were collected hourly until 40 days passed. Daily VWC averages are shown in per cent .....	110
Figure 4.4	Average CIR-MS mass spectra generated from the decomposition chamber when a) empty, b) half filled with sterile soil, c) buried human analogue trial 4, and d) the time profiles of reagent ion hydronium (m/z 19) and ammonium (m/z 18) - zone B1 represents the first background sample collected with an empty chamber, and B2 with the chamber half filled with soil. Day 1 signifies the first 24 hours after the carcass was buried .....	113
Figure 4.5	Temporal variation of mass channels 136, 137, and 138 (subset 1) as measured by CIR-MS in BHA trial 4. A total of 15 mass channels reported $r^2 > 0.9$ against m/z 136. ....	114
Figure 4.6	Temporal variations of mass channels 79, 81, and 95 (subset 2) as measured by CIR-MS in BHA trial 4. A total of 21 mass channels reported $r^2 > 0.9$ against m/z 79. This subset includes m/z 35, 45, 48, 49, 62, 64, 65, 66, 80, 82, 83, 94, 96, 97, 98, 141, 142 and 143 .....	116
Figure 4.7	Temporal variations of mass channels 223, 297, and 298 (subset 3) as measured by CIR-MS in BHA trial 4. A total of 15 mass channels	

reported $r^2 > 0.9$ against $m/z$ 18. This subset includes $m/z$ 17, 29, 30, 32,163, 224, 225, 281, 299 and 300 .....	118
Figure 4.8 Temporal variations of mass channel 59 (subset 4) as measured by CIR-MS in BHA trial 4. Only $m/z$ 59 is reported as belonging to subset 4. ....	119
Figure 4.9 Temporal variation of mass channel 63 (subset 5) as measured by CIR-MS in BHA trial 4. Only $m/z$ 63 is reported as belonging to subset 5. ....	120
Figure 4.10 Temporal variations of mass channel 37 and 55 (subset 6) as measured by CIR-MS in BHA trial 4. A total of 2 compounds were reported for this subset .....	121
Figure 4.11 Remnants of the carcass at the end of BHA trial 4 .....	125
Figure 4.12 Total number of VOCs grouped by chemical class as measured by SPME-GC-MS during BHA 4 trial. ....	127
Figure 4.13 Distribution of the different chemical classes measured during BHA 4 trial. Total VOC of interest excludes Internal standard, siloxanes, and methylene chloride. Day 0 represents VOCs measured a day before carcass introduction (background). ....	128
Figure 4.14 Temporal variations of decomposition related VOCs with greater than three occurrences during BHA 4 trial as measured by SPME-GC-MS (images a-c). The stability of internal standard bromobenzene over the first 2 weeks is shown in image d. The precision (RSD) of the internal standard was calculated as 17.4%. ....	131
Figure 4.15 Temporal variations of mass channels 79, 94, 95,96,97 and 141 (subset 1) as measured by CIR-MS in BHA trial 3. ....	134
Figure 4.16 Temporal variations of mass channels 37, 55 and 63 (subset 2) of as measured by CIR-MS of BHA trial 3 .....	134
Figure 4.17 Illustrates the concentrations of core decomposition VOCs dimethyl disulphide (DMDS) and dimethylsulfide (DMS) as measured by CIR-MS and SPME-GC-MS during buried human analogue trials (BHA 3 and BHA 4). GC-MS measurements were only collected during BHA trial 4 due to instrument availability .....	138
Figure 4.18 Illustrates the concentration profile of carbon disulphide and pentane as measured by SPME-GC-MS during buried human analogue trial 4. ....	139

Figure 4.19 Stages of decomposition in Buried Human Analogue 4(a) and (b) work conducted on 70 kg carcass left to decompose on the surface of the ground by Perrault et al [68] .....	141
Figure 5.1 Cross-sectional view of the bespoke decomposition chamber during the Exposed Human Analogue trials. ....	145
Figure 5.2 Temperature profile of the sand used as the surface for deposition during Exposed Human Analogue (EHA) trials 2 and 3. Measurements were collected hourly by use of Campbell’s Scientific CS650 sensor and were averaged daily over a period of 40 days during EHA2 and 30 days during EHA 3. ....	147
Figure 5.3 Volumetric water content of the decomposition chamber during EHA trial 3 as measured by Campbell Scientific CS650 sensor. ....	147
Figure 5.4 Average background mass spectrum generated prior to EHA trial 3 a) Average mass spectrum generated during EHA 3 trial b) and the temporal variations of primary ions m/z 19 (hydronium) and m/z 18 (ammonium) as detected during EHA trial 3 c). The x-axis represents m/z in (a) and (b), while (c) corresponds to experimental day. Negative days denote activity in each channel prior carcass introduction. All counts are normalized to total ion count (TIC) and are derived from the CIR-MS instrument. ....	150
Figure 5.5 Temporal variation of three subsets argued to describe the process of decomposition in EHA trial 3. Subset 1 consists of mass channels 18, 33, 44, 49, 79, 80, 94, 114 (a), subset 2 consists of mass channels 39, 40, 41, 43, 57, 61, 63, 71, 73, 75, 88, 89, (b) and (c) subset 3 consists of mass channel 95. ....	152
Figure 5.6 Photograph of the bloated carcass on day 5 of EHA trial 3.....	153
Figure 5.7 Total number of VOCs grouped by chemical class as measured by SPME-GC-MS .....	158
Figure 5.8 Illustrates the distribution of decomposition VOCS when grouped by chemical class as detected by SPME-GC-MS during EHA trial 3.....	159
Figure 5.9 Time profiles of 15 core decomposition VOCs as measured by SPME-GC-MS during EHA trial 3. These include: Methanethiol, Methyl ethyl disulfide, Tetrasulfide dimethyl, Dimethyldisulfide, Dimethylsulfide, Dimethyltrisulfide, Trimethylamine, 1-butanol, 2-butanone, Carbon	

disulfide, Carbamic acid ammonium salt, Acetone, 1-propanol, Pentane and Benzene. ....	163
Figure 5.10 Total number of compounds captured during EHA trial 3 as a function of Accumulated Degree Days (ADD) .....	164
Figure 5.11 Sample chromatograms collected before carcass introduction (day 0), day 2, day 4, day 8, day 16 and day 32 of EHA trial 3 as measured by SPME - GC - MS. Labels 0 refers to remnants of the air peak , 1(carbamic acid ammonium salt, 2 (acetone), 3 (Methanethiol), 4 (carbon disulphide), 5 (Trimethylamine), and 6 (Tetrasulphide dimethyl).....	166
Figure 5.12 Overlay of 7 common VOCS as measured by CIR-MS and SPME-GC-MS during EHA trials 3. Normalised counts represent results generated by CIR-MS. CIR-MS signal was normalized to hydronium, and the integrated area for SPME-GC-MS was ratioed against internal standard bromobenzene. Common compound between CIR-MS and GC-MS include, methanethiol, 1-propanol, 1-butanol, 2-butanone, trimethylamine and acetone.....	168
Figure 5.13 Average CIR-MS mass spectrum gathered from EHA trial 2 (a), and (b) the temporal variations of ammonium and hydronium during EHA trial 2 .....	170
Figure 5.14 The behaviour of methanethiol (m/z 49) and trimethylamine (m/z 60) when under primary ion ammonium (day 15 onwards) in EHA trials 2 and 3 . The proton affinity of methanethiol, trimethylamine and ammonium are 773.7, 948.9 and 853 KJ mol <sup>-1</sup> respectively.....	171
Figure 5.15 Sample chromatogram generated by SPME-GC-MS during EHA trial 2. 1-hour exposure time used.....	172
Figure 5.16 Time profiles of 19 compounds detected during EHA trial 2 as monitored by SPME-GC-MS.....	174
Figure 5.17 Temporal variation of Internal standard bromobenzene (1ppm) during EHA trial 3. ....	175
Figure 5.18 Quantification of trimethylamine, 1-propanol, 2-butanone, acetone and 1-butanol as measured by SPME-GC-MS during EHA trial 3.....	177
Figure 5.19 Quantification of methanethiol, trimethylamine, 2-butanone, 1-propanol, dimethyl disulphide as obtained by CIR-MS .....	178

Figure 6.1 Time profiles of reagent ion at $m/z$ 19, and hydrated hydronium clusters at $m/z$ 37 and 57 during BHA trial 4. ....	182
Figure 6.2 Comparison of the mass spectrum obtained during the days 10-15 versus day 24-27 of BHA 4 tria .....	183
Figure 6.3 Stage of decomposition from the Buried Human Analogue trials .....	185
Figure 6.4 Stage of decomposition as measured during the Exposed Human Analogue trails. ....	185



# 1 INTRODUCTION

The degradation of human matter involves the transformative conversion of large structures such as tissues, muscles, skin and bone into simpler building blocks. This process of soft tissue breakdown results in the release of an assemblage of products including liquids, gases and volatile organic compounds which combine to make up the distinctive odour associated with decomposition.

This thesis explores questions surrounding the determination of key markers of decomposition odour, as a means to understand the combination of compounds perceived by cadaver dogs during the search of clandestine graves. Correspondingly, it also investigates the extraction of distinctive stages of decay exclusively from the VOC profiles measured in the headspace of decomposing human analogues.

This chapter provides context to these measurements through an introduction to forensic taphonomy, chemistry and the factors that affect the process of decomposition.

## 1.1 Forensic taphonomy

The word taphonomy originates from the Greek word *tophos*, meaning grave or burial and *nomos* meaning law [1]. Although it was originally defined in the 1940s by a Russian palaeontologist as the study of the transition of animal remains from the biosphere into the lithosphere [2]. Since then, however, the word taphonomy has adopted several definitions across diverse disciplines including archaeologists, zoo archaeologists and paleoanthropologists, and as a result, the term adopts multiple definitions. Nevertheless, in a forensic context, the adopted definition of taphonomy is the study of

environmental changes to human remains, focusing largely on environmental effects i.e. decomposition in soil or water and the interaction with plants, insects and animals [3]. Forensic taphonomy uses the processes associated with cadaver decomposition to estimate post-mortem interval or post-burial interval, determine cause and manner of death, locate clandestine graves and identify the deceased [4].

The model used in forensic taphonomy is described as having two distinctive requirements, those of temporal and spatial. The temporal element describes events that occurred before or leading up to death i.e. trauma (peri-mortem) and events that occur between death and recovery (post-mortem). Interpretation of these events may be sequential, expressed as intervals (absolute time units), or they may be expressed as a ratio relative to other temporal sequences.

The object dimension considers if the body of the remains belongs to a human (cadaver) or an animal (carcass). It also considers the physical state of the remains at the point of recovery, i.e. is it a complete body or has it been mutilated or separated into body units. The space dimension refers to the environment the remains were discovered in. It considers if the remains were deposited on the surface of the ground, buried in shallow or deep graves, submerged in water, concealed between slabs of concrete or locked up in trunks of cars. The third dimension *modification of the object* studies alterations that may have occurred since death. These include investigating if the corpse remained at the site of death or if it has been transported either deliberately, or as an action of secondary scavengers or by the action of natural phenomena e.g. landslides, avalanches. Finally, *cultural dimension* considers the cause of death, investigator bias in the collection, curation and analysis of any forensic based evidence [5].

To conclude, forensic taphonomy focuses on the detection and recovery of human remains and identification of taphonomic factors affecting the determination of post-mortem interval [6].

## 1.2 Detection of remains

In criminal investigations, the search for human remains is a carefully planned out and meticulous process often involving the specialization of more than one discipline. The identification of the area to be searched begins with an established intelligence achieved by gathering information from the victim's family, suspects and witnesses. Following this, the investigator begins a preliminary search off-site by collecting aerial photographs, maps of the proposed search area, weather forecasts as well as confirming information about ownership of the land to determine accessibility [7]. The order in which search methods are applied is of great importance. Non-invasive methods are applied first to preserve the integrity of any forensic based evidence. These non-invasive methods include, but are not limited to; ground based visual searches, geophysical survey techniques and air-scent dogs. Consequently, intrusive methods like probing, combustible gas vapour detectors and soil analysis to name a few may then be used. A forensic archaeologist may also be called to assist at this point [8]. The forensic archaeologist is able to offer practical advice and assistance in the location, excavation and recovery of human remains. As well as this, he or she is able to maximise the recovery of forensic evidence [8].

As a critical focus of the scientific work contained herein; this thesis focuses on the use of airborne signatures, the merits and shortcomings of the use of human remain detection dogs (HRD or cadaver dogs), and their training aids as it is one of the most relied upon methods used today in the search of human remains [9]. A more comprehensive list of the other methods employed in the search and detection of remains has been discussed in details in Killiam 2004 [7], though a brief overview of some of the methods used in the detection of human remains is provided in Table 1.1.

The use of canines in forensic investigation is not limited to human remain searches alone; air scent canines have been used in the detection of drugs, explosives, accelerants and human remains [10-15]. One of the advantages of using mammals such as canines lies in their olfactory capabilities. For example, bloodhounds have 20 times

more olfactory receptor cells compared to humans thus allowing them to have a more remarkable sense of smell [16] . Rebmann *et al* [16] proposed the scent cone theory to describe how dogs perceive smell. This theory states that the concentration gradient associated with scent becomes more diffused the farther away the object is. As such, canines are able to detect the presence and relative concentrations of scent by following the increasing concentration to its source at the apex of the cone. This explains how HRD canines operate to identify clandestine graves. That said, a number of factors including wind, terrain and time can interrupt or enhance the spread of molecules from the source and thus may distort the scent cone.

**Table 1.1 Summary of some of the methods used in the detection of human remains. Adapted from Killiam 1994 [7]**

<b>Methods</b>	<b>Advantages</b>	<b>Disadvantages</b>
<b>Foot searched and visual signs</b>	Inexpensive, no damage to subsurface evidence, adaptable to any terrain	Difficult to manage, searchers need to be trained, possible damage to surface evidence.
<b>Probing</b>	Adaptable to any terrain, can be done in combination with visual searches	Slow coverage, daytime only, rest and replacement needed, good weather only.
<b>Combustible gas vapour detectors</b>	Easy to operate equipment, thorough search, adaptable to any terrain	Slow coverage, active decomposition must be on underway, requires trained operator.
<b>Penetrometers</b>	Minimal surface damage. Easy to supervise	Hard physical work, slow coverage, daytime and good weather only
<b>Magnetic surveying</b>	Medium coverage speed, minimal surface damage and no subsurface damage	Interferences, requires expert interpretation, expensive equipment.
<b>Ground penetrating radar (GPR)</b>	Results immediately available in the field, medium coverage speed, adjustable to conditions	Very expensive equipment, expert interpretation required, clear ground cover required, daytime and good weather only.
<b>Resistivity surveying</b>	Can determine lateral position and depth of anomaly, some field results available, used as pre-test for GPR	Requires data processing, requires expert interpretation, less useful in cultivated land. Daytime and good weather only.
<b>Infrared scanner imagery</b>	No ground contact or damage, elevated view point, adaptable to any terrain, usually done at night	Very expensive equipment, limited availability, requires expert operator, interference from radio waves.

Similarly, HRD canines can be trained to locate anything from a drop of blood to an entire human body and can also be used to detect residual odour from soil and surfaces long after the decomposing remains have been removed [17]. Alexander *et al* [17] observed that HRD canines were able to detect the odour of remains up to 667 days post removal with 75% - 100% accuracy rate [18]. The dogs give visual displays to their handlers who must also be sufficiently trained to interpret and guide the dogs. Although the dog will follow the ideal scent cone, it is up to the handler to analyse the environmental context and anticipate the dogs response [16].

The benefits of employing HRD canines in criminal investigations are extensive, however their limitations must also be considered. One of the greatest drawbacks in the use of HRD canines lies in the lack of sufficient training aids to train the dogs with. It remains unclear what exact compounds or combination of compounds HRD canines detect [19]. Training aids currently used include human bones, gauze soaked in decomposition fluid, blood, and clothing previously in contact with remains. However these items can be difficult to obtain and as such access is limited by legal restrictions and are considered to be potential biohazards [10]. To circumvent this, chemical pseudo scents are employed as training aids.

Two synthetic scents pseudo corpse scent formulation I and II supplied by *Sigma Aldrich* are often used as canine training aids for the detection of corpses [9]. However, evaluation of the composition of these pseudo scents has revealed that their chemical composition is far too simplistic and thus not a true reflection of the VOCs released from a decomposing corpse [6, 10, 20]. In fact, It was observed by Stadler *et al* [20] that none of the constituents of the pseudo corpse scents had been previously reported as volatile products of decomposition. In formulation I, the major components identified were 2-pyrrolidone and 4-aminobutanoic acid; whereas in formulation II putrescence, cadaverine, butyrolactone and tridecylamine were detected [9, 20]. These compounds are not an accurate representation of the dynamic nature of decomposition VOCs and as a result, there is a demand to further the research and development of canine training aids. One consequence of using inaccurate and ineffective aids is that it can confound cadaver training thus having adverse effects on criminal investigations [10].

### 1.3 Determination of Post Mortem Interval (PMI)

The determination of an accurate post-mortem Interval is central to any homicide investigation because it is used by law enforcement personnel to corroborate witness testimonies, eliminate possible assailants and may even aid in the identification of the deceased. At present, there are multitudes of methods used to estimate PMI (table 1.2), however they are not without their limitations. Entomology, botany, taphonomy, visual inspection (section 1.4.1), inorganic and organic chemical methods, anthropology and odontology are some of the offered approaches. Generally, the more accurate the method, the longer and more complicated the analysis is, thus potentially delaying criminal investigations. As a result, there is a desire to develop a method that is not only accurate, but one that is also rapid in order to aid law enforcement agencies [21].

Vass [21] developed a rough estimate for determining PMI for aerobic (surface deposition) and anaerobic (buried) decomposition. His formula relies upon an estimation of soft tissue decomposition in percent, an empirically developed accumulated degree-days (ADD) value, temperature and humidity (Equation 1.1 and Equation 1.2). In spite of its successes when applied in forensic case studies, it must be noted that its application, specifically the anaerobic PMI equation is limited only to the eastern section of the United States because of the similarities in soil moisture, soil type and vegetation to the research facility in University of Tennessee where the formulae was developed

$$PMI_{\text{Aerobic}} = \frac{1285 \times \left(\frac{\text{decomposition}}{100}\right)}{0.0103 \times \text{temperature} \times \text{humidity}} \quad \text{Equation 1.1}$$

$$PMI_{\text{Anaerobic}} = \frac{1285 \times \left(\frac{\text{decompositiion}}{100}\right) \times 4.6 \times \text{adipocere}}{0.0103 \times \text{temperature} \times (\text{soil moisture})} \quad \text{Equation 1.2}$$

Forensic entomology is another well-utilised approach used in PMI determination. It relies upon the succession and development of cadaveric specific insects. The theory is that since insects appear in distinct sets at defined periods and succeed each other

during cadaver decomposition, identification of a particular fauna present at a certain decomposition stage might correlate with the period since death [4]. Since odours emanating from a corpse change as the body decomposes, some insect species become less attracted to the body as time progresses. For example, blowflies tend to arrive shortly after death but quickly lose their attraction once the remains have passed a certain stage of decomposition, or become mummified or dry [22]. This approach is particularly useful when determining PMI of a corpse left to decompose on the surface of the ground (exposed). However, in the case of buried corpse where microorganisms, scavengers and insects are limited, forensic entomology is restricted. In addition, other considerations worth noting when adopting this method are biotic and abiotic factors known to influence carrion insect growth and activity [22].

**Table 1.2 Relation of Taphonomy to traditional determination of post-mortem interval. Reproduced from Reich *et al* [23]**

<b>Time interval</b>	<b>Observational Phenomena</b>	<b>Methodology</b>
<b>Minutes-Hours</b>	Enzymatic changes, Cellular respiration	Biochemistry Cell biology
<b>Hours - One day</b>	Classic Triad (Algor/livor/rigor mortis)	Forensic Pathology
<b>One Day - One week</b>	Gross post-mortem decomposition	Forensic pathology Ecology Taphonomy
<b>Weeks – Months</b>	Disarticulation or Skeletisation	Anthropology Taphonomy Archaeology
<b>Months - Years</b>	Weathering or Burial	Taphonomy Archaeology Paleoecology
<b>Years - Eons</b>	Fossilization or Digenesis	Archaeology Palaeontology Mineralogy

Anthropology is particularly useful in establishing the period of interment, which typically is the same as the time since death. Likewise, anthropology is used to make the distinction between modern and ancient remains. In a criminal context, skeletal remains older than 50 years post mortem are not usually subject to forensic investigations [24]. Chemical analysis of decomposition products specifically soil

solutions is another growing field used to estimate PMI. Microbial produced volatile fatty acids (VFAs) such as propionic, iso-valeric and n-valeric acids are released in set patterns into soil solutions during decomposition. A combination of VFA ratios, temperature and a description of the corpse can provide the required information needed to determine the stage of decomposition and hence the time of death [4].

Furthermore, a range of ions including  $\text{Na}^+$ ,  $\text{Cl}^-$ ,  $\text{NH}_4^+$ ,  $\text{Ca}^{2+}$ , and  $\text{Mg}^{2+}$  have been noted to form in ratios during specific stages of decomposition, allowing an approximate time since death to be estimated. An advantage to using this technique is that unpredictability in the environmental conditions does not affect results. A limitation of this technique, however, is that results are mostly accurate on corpses closer to being skeletonised [4].

In conclusion, this section highlights the importance of the ability to accurately determine PMI in a criminal context, as well as some of the methods currently used in estimating the time since death. Once the body becomes decomposed, it becomes more difficult to estimate PMI. A drawback of majority of these techniques is that investigations have been based solely on surface decomposition, which regrettably cannot always be applied in buried decomposition. As a result, more research is necessary to establish a reliable method for determining PMI in buried environments.

## **1.4 Chemistry of decomposition**

### **1.4.1 Process of decomposition**

Decomposition is a multidimensional process which encompasses physical, chemical and biological transformations occurring within a body as it is transformed from flesh into skeleton. Just as a living body relies on complicated but complementary reactions occurring simultaneously during life to sustain it, the same can be said for the process of decomposition.

The onset of decomposition has been noted to occur as early as 4 minutes after death [25]. Once the heart function ceases, levels of oxygen in the body declines and aerobic microorganisms deplete tissues of the body of any remaining oxygen. In doing so, the body begins to destroy itself in a process known as autolysis. Cells with high enzyme content such as the liver initiate the process, and other cells of the body subsequently follow in a similar manner. Eventually, the body reaches optimal conditions for anaerobic microorganism such as *Clostridium sp.* and bactericides from the gastrointestinal and respiratory tract to take over [4]. The inception and interval of autolysis is heavily dependent on temperature and moisture. As autolysis progresses, the body temperature drops to ambient levels (*algor mortis*), the rate of which depends on the size of the corpse and the presence of any associated materials (e.g. clothing, soil) [26]. Successively, liquid blood settles in the lowest parts of the body resulting in the discolouration of the skin (*livor mortis*). Body stiffening (*rigor mortis*), which is governed by temperature and the metabolic state of the body, causes a chemical change resulting in the conversion of ATP to ADP. As a consequence, lactic acid is produced and pH in the body is lowered [26].

Despite the subject of most corpse decomposition studies being human analogues, the process of decomposition aforementioned describes the processes occurring in within a human cadaver. Table 1.3 illustrates some of the similarities in the chemical composition of humans and other mammalian cadavers; particularly pigs.

A direct result of autolysis in the abdomen is the production of  $H_2S$ , which combines with haemoglobin in the blood to form sulfhaemoglobin; causing a greenish discolouration of the skin. This is usually indicative of the beginning of putrefaction. Putrefaction refers to the action of microorganisms in the destruction of soft tissues in the body and the ensuing catalytic conversion of tissues into gases, liquids and simple macromolecules.

**Table 1.3 Chemical composition of Mammalian Cadavers during life. Measurements of carbon (C), nitrogen (N), phosphorus (P), potassium (K), calcium (Ca), and magnesium (Mg) are presented as grams per kilogram (g/kg) cadaver mass (dry weight). Adapted from Tibbett and Carter [4]**

<b>Organic resource</b>	<b>H<sub>2</sub>O (%)</b>	<b>C:N Ratio</b>	<b>N (g/kg)</b>	<b>P (g/kg)</b>	<b>K (g/kg)</b>	<b>Ca (g/kg)</b>	<b>M (g/kg)</b>
<b>Humans</b>	60	5.8	32	10	4	15	1
<b>Pig (age 56 days)</b>	80	7.70	26	6.5	2.9	10	0.4
<b>Pig (age 28 days)</b>	78	N/A	29	7.4	2.7	10	0.4
<b>Rabbit (age 70 days)</b>	78	N/A	29	7	3.2	12	N/A
<b>Rat (age 70 days)</b>	75	N/A	3.2	6.5	3.5	12	N/A

During this process carbohydrates, lipids, and proteins are transformed into organic acids such as propanoic acid and lactic acid [25]. The outcome of this stage besides distension of tissues is gas and fluid accumulation, which eventually results in bloating of the body. Ultimately, the process of putrefaction compromises the integrity of the skin leading to purging of the body through its natural openings (e.g., eyes, nose and rectum) [4].

Putrefaction is mostly associated by anaerobic fermentation. Ruptures in the skin allow for reintroduction of oxygen into the body, thus creating the ideal environment for aerobic metabolism to progress. At this point, the body is considered to be in the decay stage. Insects, scavengers and cadaveric specific organisms plague the body thereby aiding the process of decomposition [4]. Bacterial action initiates the breakdown of protein and fats into amino acids and volatile fatty acids [25]. Researchers in the field including Vass [25] have noted that not all stages of the process are always observed, and the complete absence of some stages are not uncommon. As mentioned, decomposition is a highly complex process dependent on many factors, including the taphonomy of the corpse.

Essentially, decomposition is the breakdown of complex structures composed of proteins, carbohydrates and lipids into their simplest form. Broadly, it can be divided into four main groups, which are; autolysis, putrefaction, decay and digenesis. Digenesis, the breakdown of bone has not been discussed here, because the most

relevant processes pertaining to this research are putrefaction and decay, particularly as the highest numbers of decomposition by-products and thus volatile organic compounds are reported to be released during these stages [4]. Soft tissue decomposition has been reported to cease at  $1285 \pm 110$  accumulated degree-day [21].

Nonetheless, the above classifications merely describe a general overview of the decomposition process. Putrefaction and decay process can be further divided into smaller fractions to better summarise the physiochemical changes occurring within the corpse.

## **1.4.2 Stages of decomposition**

The process of corpse decomposition is a continuum; although researchers have adopted a classification system as a means to easily describe and discuss the process, particularly for the benefit of court proceedings, there are no strict boundaries between the stages of decomposition. Depending on the researcher, geographical location, and temperate conditions, the number of stages of decomposition reported can vary with up to nine groupings [26], albeit five broad stages have been repeatedly discussed in detail in the literature [27]. These stages are: fresh, bloated, decay (covering both active and advanced decay), post decay and skeletisation [26]. The first four stages of the decay process are depicted in figure 1.1. The onset and duration of each stage is dependent on parameters such as environmental conditions, corpse size, trauma, associated materials and the metabolic state of the body. Determination of these stages were conducted by characterising physical parameters of a decomposing corpse deposited on the surface of the ground (exposed).

The fresh stage begins from death until the first signs of bloating. In the case of exposed cadavers, insect invasion is possible via natural openings of the body (eyes, nose, and mouth) and eggs are deposited inside the corpse. Given appropriate conditions, eggs hatch and internal feeding commences. Flies are also attracted to the body (usually the head) and wound openings [26]. During this stage, the cadaver undergoes autolysis [27]. Putrefaction commences in the bloated stage. Once the heart stops pumping, there is

an oxygen deficit within the corpse, and as such there becomes prevalence in the activity of anaerobic bacteria which typically originates from the digestive and respiratory systems. This stage is characterised by colour changes as well as the onset of marbling (purple to greenish discolouration) [28] resulting from the breakdown of macromolecules such as carbohydrates, lipids and proteins [29]. A consequence of the metabolic process of self-digestion by anaerobic bacteria is the production of gases, which in turn causes inflation of the abdomen and the whole body. Eventually, internal pressures will cause ruptures in the skin and natural openings of the body. Expulsion of internal fluids into the surrounding environment will affect the pH and microbial community the burial substrate. At this stage, decomposition specific organisms invade the body, and there is usually a strong smell associated with the release of some decomposition gases and fluids [26].

The decay stage is considered to begin when the outer layer of skin breaks, and gases from the abdomen escape. This is usually denoted by deflation of the abdomen. During this stage, there is a strong presence of decomposition organisms such as Diptera larvae and Coleoptera; predators like Staphylinidae and Histeridae; necrophages Calliphoridae and Sarcophagidae are also evident. The strongest odours of decomposition are often attributed to this stage of decay. At the end of the decay stage most of the skin will have been removed revealing only cartilage [26]. Post decay introduces a different species of microorganisms Dermestidae that feed on the remaining dried flesh and cartilage. The types of organism present at all stages are heavily dependent on the surrounding areas of the carcass. Given enough time and under appropriate conditions, the remnants of the corpse will only be bones and hair. This period is classified as the skeletonization stage [26].



Figure 1.1 Typical decay stages followed by pig carcasses in a forest biotope. Reproduced from Dekeirsschieter 2012 [30]

Despite the aforementioned classification, it must be considered that the start and termination points for each stage of decomposition is largely subjective. Although most researchers in the field refer to a total of five stages of decomposition, the classification of each stage varies depending on the investigator. In some cases, there is no distinction between post decay and skeletisation, and the decay stage may be further divided into active and advanced decay [27].

### 1.4.3 Factors affecting decomposition process

The rate of post-mortem decay is affected by a multitude of variables, which can be grouped into two distinctive categories: intrinsic and extrinsic factors. Intrinsic factors describe elements concerning the corpse itself i.e. age, gender, diet and cause of death; whereas extrinsic factors describe environmental elements, scavengers, and fauna. All

of these elements affect the rate of decomposition and hence the succession of VOCs. More importantly, however, is the fact that modification of the decomposition process inevitably alters the estimation of the time of death.

The effect of carcass mass on decomposition rate is highlighted in the work conducted by Spicka *et al* [31] and Matuszewski *et al* [32], although conclusions on whether decomposition proceeds quicker in smaller carcasses is still a subject of contention between researchers. Some researchers argue that neonatal and carcasses weighing approximately 20 kg or less decompose more rapidly than larger masses {40 kg} [31-34], whereas the findings of Hewadikaram *et al* [35] suggest the contrary. The effect of age, constitution, cause of death and the integrity of corpse have been succinctly summarized elsewhere [36].

Temperature is frequently considered as one of the most important factors governing the rate of cadaver decomposition [21, 37]. It is influenced by seasons, altitude, burial depth, and presence of water, vegetation and clothing. An increase in cadaver breakdown rate is often associated with an increase in temperature perhaps because of the number and type of carrion insects in association with the cadaver [4]. As well as this, temperature also affects chemical reaction rates. The relationship between temperature and chemical reactions is best described by Arrhenius equation, which (for typical activation energies) shows that the rate of chemical reactions doubles for a 10 °C rise in temperature [4]. The optimal temperature for the development of bacteria ranges between 25°C and 35°C [36].

The effect of temperature on the rate of decomposition is a phenomenon that has been agreed by authors in the field worldwide, to the extent that the interval of decomposition is often reported in units of degree-days (DD) instead of time. Michaud *et al* [38] observed that temperature records could be used to accurately predict decomposition stages, and thus developed a reliable-degree day index which is now widely used in the study of decomposition-related processes [39-41]. ADD is the accumulation of thermal energy needed for chemical and biological reactions to take place in soft tissue decomposition. It measures the energy that is placed into a system as accumulated temperature over time. Accumulated Degree-Days refers to heat

energy units needed to propel biological processes and is calculated as the summation of daily temperature averages above a threshold value for all days from death until cadaver recovery [40]. One-degree day is one entire day where the temperature stays above the baseline temperature threshold by one degree. The baseline temperature threshold used differs across various disciplines; for example, forensic entomologist's use 10°C or 6°C as it is the expected temperature carrion species would cease to grow and develop. Theoretically decomposition should still proceed even in temperatures as low as 0° C owing to the concentration of salts in the cadaver, however a suppression in decomposer activity and hence a reduced rate of decomposition has been reported [42]. The application of degree-day indices allows researchers to compare decomposition-related data such as the onset of decay stages regardless of climatic variability.

Another factor considered to influence the rate of decomposition is moisture content. Extremely dry and extremely wet conditions promote desiccation and the formation of adipocere respectively. Both of these processes are well known to inhibit cadaver decomposition [4]. Egyptians for example have used desiccation for thousands of years as a way to preserve cadavers via mummification [43]. Conversely, findings from Carter *et al* [44] imply that cadaver decomposition is slower in dry soils. The discussion of the availability of moisture in the decomposition process is often interlinked with soil texture specifically because of gas diffusion rates [4, 45]. Coarse textured soils (sandy) have a high rate of gas diffusivity and as such gases and moisture move rapidly through the soil matrix [4]. Similarly, decomposition in fine textured soil (clay) is retarded as the rate of O<sub>2</sub> is exchanged with CO<sub>2</sub> is insufficient to meet aerobic demands [46].

The consequence of associated materials such as clothing has again been contested. Some researchers contend that the presence of clothing increases the rate of decomposition. The argument is that clothing provides a shaded area for maggots to feed [4], it slows down post-mortem body cooling which in turn favours putrefaction [36]. On the other hand, Matuszewski *et al* [32] reported that clothing had little influence on decomposition specifically during the advanced stage of decay.

The importance of the activity of arthropods particularly necrophagous arthropods have been the subject of many methods used in the approximation of post-mortem interval, perhaps because the succession of each arthropod group can be associated with a particular decomposition stages [36]. Necrophagous arthropods such as Diptera typically originating from the enteric community of microorganisms, combined with activity of intrinsic enzymes are primarily responsible for the degradation of body tissues [4]. Soil microorganisms on the other hand are reported to have a minor role in cadaveric decay, as they are mainly responsible for returning CO<sub>2</sub> from soil organic matter to the atmosphere [4].

The influence of soil has been described to reduce decomposition rates from the perspective of water content and oxygen availability [4]. A change in moisture content has been associated with fluctuations in microbial activity. Tibbet *et al* [4] noted that without water biological processes would cease. As with temperature, where extremely low or high temperatures impede decomposition, the same has been observed with moisture. In extremely wet soils, microbial activity is limited owing to low solubility and a slow diffusion rate of O<sub>2</sub>. In the soil of graves where the cadaver provides a concentrated organic source, there runs the possibility that the rate of O<sub>2</sub> consumption during aerobic respiration will exceed the rate of O<sub>2</sub> diffusion at the decomposition site. The net result of this is that anoxic conditions will be favoured [4]. Haglund *et al* [5] noted that the rate of decomposition in soil proceeds eight times slower than above ground decomposition predominantly because of the limitation of carrion insect and animal activity, thus breakdown of tissues is primarily a result of autolysis and bacterial putrefaction. Furthermore, soil provides a barrier to solar radiation and therefore stabilises temperature variation. At depths of less than a foot, temperatures tend to be similar to those above ground.

In conclusion, there are numerous factors known to govern the rate of decomposition and although only a fraction has been discussed here in detail. It is generally accepted that temperature, moisture and insect activity are amongst the most important parameters to control when experimentally studying the rate of decomposition. Perhaps this is because the results of the effects of some of the other variables are still

inconclusive. The limited understanding of the effect of these variables sheds some light onto the challenges associated with reproducibility in this field.

## 1.5 Volatile Organic Compounds

There are diverse definitions of VOCs in the US, Canada and European Union (EU). However, the EU defines VOCs as volatile organic compounds having an initial boiling point of less than or equal to 250°C measured at a standard pressure of 101.3kPa. The EU also defines organic compounds as compounds containing at least the element carbon and one or more of hydrogen, oxygen, sulphur, phosphorus, silicon, nitrogen, or a halogen, with the exception of carbon oxides and inorganic carbonates and bicarbonates [47]. VOCs are ubiquitous, varied and include almost all chemical classes.

The boiling point of compounds is the temperature at which the vapour pressure equals atmospheric pressure [48]. Vapour pressures signify the likeness for a compound to enter the gaseous phase, thus as the vapour pressure increases, so does the volatility of the compound [49]. The amount and strength of molecular interactions such as Van der Waals attractions and hydrogen bonding within the compound dictates changes in boiling points and thus volatility [49].

Despite some VOCs occurring naturally, government agencies regulate the production of anthropogenic VOCs as they are known to cause adverse health effects [50-52], and can be dangerous to the environment. In the environment, VOCs undergo photochemical reactions in sunlight to form secondary pollutants such as ozone (O<sub>3</sub>) which contributes to air pollution [53].

## 1.6 Current research on cadaver decomposition

### VOCs

The current literature on the study of volatile organic compounds associated with cadaver or carcass decomposition is somewhat limited, although there continues to be a growing interest in the field. The approach into answering the questions 1) what are the key markers of decomposition, and 2) can the PMI of a deceased be inferred solely from the VOC profile of a deceased, has been varied.

Some authors have focused primarily on studying the decomposition of human cadavers [21, 25, 33, 54-56], but the vast majority have used human analogue surrogates [27, 28, 30, 57-63] owing to ethical restrictions. The majority of studies conducted in the field of taphonomy have been through the use of pig carcasses as human surrogates, predominantly because of the similarities in chemical composition (see Table 1.3). Notwithstanding, in 2012 Cablk *et al* [64] compared the results generated from decomposition of human remains and different animal tissues (cows, pig and chicken) and the results indicated that VOC signatures from chicken tissues were most similar to human samples. In spite of this, there is no other evidence to support this claim.

So far, the principal instrumentation used in the study of cadaveric VOCs has been GC-MS [61, 65, 66]. Passive and dynamic sampling techniques have been used [27], as well as a range of collection techniques including triple sorbent traps [54], thermal desorption [27, 57, 58, 65], and solid phase micro extraction [67]. The collection technique used in decomposition VOCs significantly impacts on the number and types of compounds captured. Perrault *et al* [68] reported that the two collection techniques sorbent tubes and SPME were complementary. In addition, there is an emphasis on the use of more than one technique as it provides an advantage in identifying the complete VOC profile of decomposition odour.

More recently, however, there has been a push for the use of two-dimensional gas chromatography (GCxGC-MS) as its resolution supersedes that of the classical single

dimensional gas chromatography, an attribute that is particularly beneficial in the analysis of complex cadaveric VOCs [65, 66, 69, 70]. One reoccurring limitation of the traditional GC-MS in this type of work is that it suffers from insufficient peak capacity to accurately separate the large number of analytes present in decomposition odour profile, thus it provides low mass spectral matches and often leads to compound misidentification. Stefanuto *et al* [70] documented the use of high resolution GCxGC-MS in a longitudinal study of decomposition odour and noted that despite the GCxGC HR-TOF-MS being valuable in improving compound identification, the main challenges were in data storage, computational resources and processing time as the size of the each data file produced was approximately 40 GB.

Aside from the differences in the objects used in the study of decomposition (human or animal analogue), the space i.e. manner of deposition or burial has also been diverse, and as a consequence the resulting VOCs have been difficult to reproduce. In the work conducted by Dekeirsschieter *et al* [30], a total of 832 VOCs were released from a 25 kg domestic pig left to decompose on the surface of a forest biotope located in Belgium. The main classes of compounds identified were oxygen containing (including alcohols, acids, ketones, aldehydes and esters), sulphur and nitrogen containing compounds. 1H-indole in particular was the most prevalent compound with eight occurrences (8 days) and represented a quarter of the volatile emissions. Conversely, Forbes *et al* [62] studied the evolution of VOCs from a 70 kg domestic pig during the summer months in Australia. Samples were collected from the soil below and the headspace above the decomposing carcass. Despite a total of 249 compounds being identified, only 58 compounds were common to both soil and air samples. These findings demonstrate that soil and air samples produce distinct VOC subsets, which contribute to the overall decomposition odour. Thus, sample collection from more than one matrix is necessary to enhance the accuracy of the decomposition odour profile. The Sulphur containing compounds dimethyl disulphide (DMDS) and dimethyl trisulphide (DMTS) were amongst the VOCs consistently observed in both soil and air matrices.

Agapiou *et al* [58] adopted a slightly different approach whereby the carcasses were placed in concrete tunnels to simulate entrapment conditions of collapsed buildings.

One carcass was covered in soil while another was placed in an open body bag. The result of this work yielded a total of 288 VOCs of which the majority were aliphatic, aromatics and nitrogen compounds. That said, sulphur containing compound methanethiol was the most prominent compound detected on the first day of decomposition (carcass in open body bag), whereas sulphur compounds were not detected until the fourth day of decomposition of the buried carcass. DMDS, acetone, xylene and benzene were amongst the detected compounds. This finding provides evidence of the importance of the space dimension associated with the study of cadaveric decomposition VOCs.

Similarly, Statheropoulos *et al* [28] studied the decomposition of buried pig carcass in conditions of entrapment in collapsed buildings. However, there were differences in the types of pigs used (domestic and farm pigs). It was reported that decomposition in farm pigs progressed more rapidly than the domestic pigs and the odour was more intense. Despite the fact that over 150 compounds were detected in total, the most prominent VOCs differed across the two types of pig carcasses. In domestic pigs the most prevalent VOCs were DMDS, pyridine, dodecane, hexane and benzene whereas from the farm pig it was DMTS, DMDS, formamide, methyl ethyl disulphide and trimethylamine. The differences in the types of VOCs detected demonstrate the effect skin microflora and the environment from which the pig originated have on the decomposition process.

Notwithstanding the differences in the methodology applied in the study of cadaveric decomposition VOCs, the end goal remains the same. The underlying thread in the literature is a desire to fully develop the understanding of odour signature associated with decomposing remains regardless of the space dimension (manner of death or burial). Current, HRD canines are being utilised in the search human remains as they have superior olfactory capabilities compared to humans. HRD dogs have been reported to have a greater than 75% success rate in determining not only the location of a grave but also the odour of the human remains up to 667 days post removal from soil surface [19]. The latter point can be attributed to the HRD canines high sensitivity to odours (1pptV) [71]. Regrettably, however, the combination of compounds the dogs smell is still unknown.

In addition to understanding the signature odour associated with decomposition, there is a drive to create a portable chemical sensor capable of mimicking canine olfaction. Furthermore, the net result of this type of work could be the determination of post mortem interval; which HRD dogs are unable establish.

It is clear from the literature that there is a restriction on the reproducibility of VOCs emanating from decomposing carcasses. The geographical diversity and wide spectrum of decomposition environments reveals the necessity for continuing research towards elucidating the decomposition odour profile in order to better understand the chemical profile of death.

## **1.7 Practitioner oriented goals**

Aside from deepening the knowledge of decomposition odor in the field of forensic science which the work in the body of this thesis addresses, there are also specific practitioner-oriented objectives, which are also relevant to this work and its conception.

To begin with, the current commercially available synthetic decomposition odor mixture used in the training of cadaver dogs is very simplistic and is not an accurate depiction of the compounds released from human decomposition. There is also evidence to support the notion that cadaver dogs sometimes do not yield positive responses to these formulations when tested under scenarios [9]. The consequences of using inadequate training tools would have adverse effects on the rate of recovery of sub surface and surface deposited remains.

To this end, the work in this thesis, provides an alternative route to the development of more accurate training aids by better understanding some of the signature compounds released during the process of soft tissue decomposition. Albeit the subjects of decomposition in this study have been pig carcasses, the concept is easily applicable to human remains.

Furthermore, from a holistic perspective, this type of work which examines the signature chemical profile of decomposing remains serves as the basis for the development of electronic noses to mimic the olfactory ability of canines. Electronic nose technology has already been employed in a multitude of areas like food and medicinal science [72-74]. The application of electronic nose technology in this field would yield several benefits; for example, the electronic nose would be void of fatigue, temperament and can be operated under any weather condition. Additionally, it would also be cost-saving as it would eliminate the financially cumbersome process associated with training dogs and their handlers for the purpose of searching for remains.

## 1.8 Study objectives

The objective of this study was to investigate the use of the real time mass spectrometric technique called chemical ionization time-of-flight-mass spectrometry (CI-TOF-MS) and the more traditional applied gas chromatography (GC-MS) in the study of VOCs emanating from decomposing human analogues (pig carcasses). To achieve this, an environmentally controlled decomposition chamber capable of housing whole carcasses was developed and characterised in the Real-time Air Fingerprinting Technologies laboratory (RAFT) at the University of Leicester and CI-TOF-MS was used online to monitor the real time succession of VOCs released during the process of decomposition, in combination with GC-MS for enhancing species determination.

Human analogue trials were conducted in two categories; the first trial investigated the VOC profile in the headspace of buried carcasses (buried human analogue (BHA) trials), while the second trial observed the VOC profile in the headspace of carcasses left to decompose on the surface of the ground (exposed human analogue (EHA) trials). Comparison of the results generated from the two trials elucidated the effect soil had on decomposition. Subsequently, the use of burial and exposed headspace VOC was assessed as a marker for decomposition stage.

Finally, the sequence of VOCs emitted during the decay process was examined to determine if the dynamic VOC profile of decomposing carcasses could be used quantitatively as a marker of decay time.

## 1.9 Chapter 1 Summary

Taphonomy is a growing discipline, however despite its diverse definitions, the objective of forensic taphonomy has always been the following: 1) to develop the understanding of the transformative processes involved in converting a once living form (human or animal) into skeletal remains, 2) an appreciation for the interaction between the sites ecology and the process of decomposition, and 3) to develop an accurate and reliable estimation of the time and circumstances since death.

Current methods used in estimating post-mortem interval and the methods used in the detection of remains revealed the necessity for further research in this field. In addition, there is a clear need to improve upon the development of accurate canine training aids, and possibly the need to devise a portable handheld device capable of mimicking canine olfactory abilities. However, the later point remains an elusive goal owing to the fact that the compounds and combination of compounds HRD dogs detect is still largely unknown.

There are significant issues surrounding repeatability of carcass decomposition, specifically in the natural environment (field/outdoor). Geographic, climatic, and even microbial variations to mention a few are some of the governing parameters affecting the process and thus rate of decomposition. Consequently, the VOCs released as a result of carcass decomposition reported by studies conducted in Greece [28, 55, 75], compared with studies in Canada [6, 57, 65], Cyprus [58], Belgium [70, 76], Australia [45, 61, 62, 77], and the USA [54, 64, 67] have been vastly different. Similarly, very little work has been conducted on the VOCs released from the headspace of buried carcasses [76] i.e. VOCs partitioning between soil and air.

The work conducted in the upcoming chapters aims to bridge some of these gaps in the literature. The approach was to develop and characterise an indoor environmental

chamber capable of housing human analogues (pig carcasses) and study the succession of VOCs released into the headspace environment as the carcass passed through the various decomposition stages. In doing so, geographical variations are eliminated, climatic conditions are better controlled, and external microbial communities are restricted if not completely eliminated. The net result would be an increase in the reproducibility of carcass decomposition by better controlling these variables.

Furthermore, a novel real-time spectrometric technique CIR-MS was employed to follow the dynamic succession of carcass volatile organic compounds during the early post-mortem stages of decomposition; and finally, gas chromatography-mass spectrometry was utilised as a complementary technique to enhance the identification of a complete decomposition odour profile.



# 2 EXPERIMENTAL

## 2.1 Decomposition chamber

A bespoke experimental chamber was developed to house each carcass used in this project (figure 2.1 and figure 2.2). The chamber was constructed from a polyethene container purchased from ESPO. The overall size of the container was 1040 x 700 x 840 mm (*wxdxh*). In the case of the buried trials, the chamber was half filled with 100 L of commercially available sterilized topsoil. In the exposed trials, horticultural grade lime free silica sand was chosen as the surface for decomposition. Both materials were purchased from Homebase (Putney road, Leicester, UK). Internal environmental parameters such as ambient temperature and relative humidity were monitored hourly by use of Campbell Scientific CS215 sensor. Soil temperature and volumetric water content were also recorded using a Campbell scientific CS650 Water Content Reflectometer. The retrieved data from both sensors were logged on Campbell Scientific CR10X data logger, which was connected to a laptop running Microsoft Windows XP adjacent to the carcass chamber.

The chamber cover was fabricated in the workshop in the chemistry department of the University of Leicester. It comprised of 6 mm Perspex (800 mm x 1100 mm) and the outer perimeter was lined with 12 mm black closed cell neoprene sponge. Both the perspex and neoprene were purchased from SBA Ltd. (Leicester, UK). The Perspex covering was perforated seven times to provide sampling ports. The first port was connected to a transfer line leading into the CIR-MS instrument. This transfer line was constructed from an 1/8<sup>th</sup> inch Teflon (perfluoroalkoxyalkane) tubing which was heated to 37 °C using an intertwined heating tape. Teflon has been proven to be the best material for inlet systems as it minimises memory effects on surfaces [78].

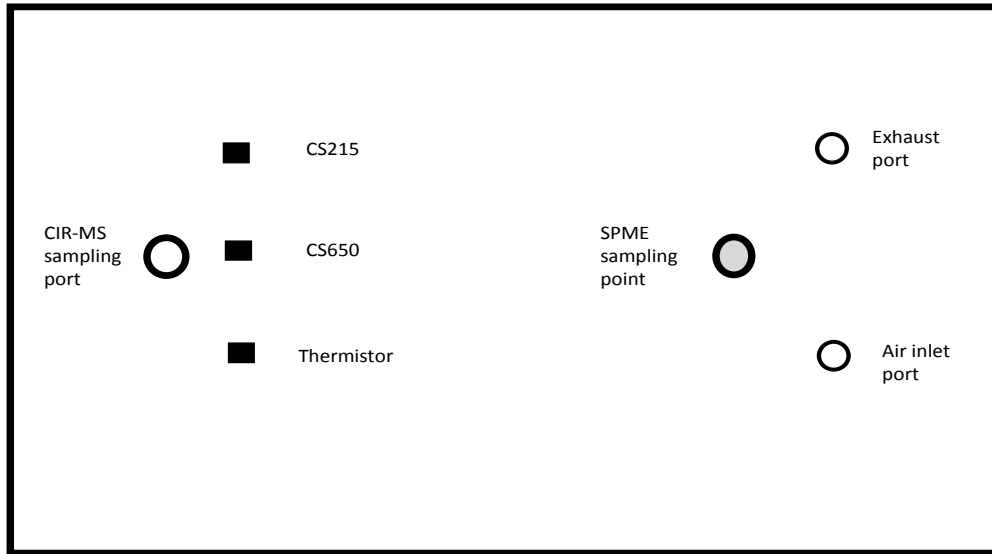


Figure 2.1 Illustrates the schematic of the chamber covering used in the study of the decomposition of human analogues.



Figure 2.2 Image of the chamber developed for the study of decomposition VOCs associated with pig carcasses

## 2.2 Chemicals and consumables

All volatile samples to be analysed by GC-MS were sampled using SPME fibres comprising of an assortment of commercially available coatings. SPME fibres were purchased from Supelco, a division of Sigma Aldrich UK. The selection of fibres allowed for a wide range of VOCs to be collected. Details on the types of VOCs collected by each fibre are discussed in detail in Chapter 3.

A cylinder of 10 ppmV. bromobenzene in synthetic zero air calibration mix was purchased from BOC Limited and was used as internal standard. This compound was chosen as it is not produced in soft tissue decomposition, and is not naturally present in the air. Moreover, bromobenzene has been the internal standard of choice in other decomposition studies [61, 65]. Bromobenzene was diluted further in BTCA 178 synthetic air by a factor of 10 to produce a final concentration of 1 ppmV.

Synthetic air and bromobenzene were fed into the headspace of the chamber at a combined flow rate of 300 sccm per minute to simulate wind dispersion. Bromobenzene did not co-elute with other compounds and produced a reasonably sized peak when analysed by SPME-GC-MS. Analytical grade chemicals were purchased from Sigma Aldrich (Dorset, England) and used as standards in the calibration of the CIR-MS and GC-MS instrument.

### 2.2.1 Research subjects

Owing to ethical reasons surrounding the use of human cadavers for this type of research, pig carcasses were employed as analogues. There is strong evidence in the literature suggesting that pigs are the most suitable analogue to simulate human decay, based upon internal anatomy composition, chemical composition and gut fauna [79, 80]. Furthermore, one of the most important similarities previously noted by other decomposition authors is the common decay route of pig and human corpse. These similarities might explain why pigs are one of the most viable candidates employed as

human surrogates in the field of taphonomy [28, 58, 62, 63, 68]. In addition, not only do both mammals follow the same decay route i.e. stages of decomposition, Stokes *et al* [81] has documented commonalities in the types of VOCs released during decomposition in both mammals.

The pig carcasses (*Sus scrofa*) used in this study were purchased from a local butcher in Leicestershire. Arrangements were made such that all pigs were of the same gender and were raised on the same farm. In addition, the method of slaughter remained the same. Each carcass was transported to the laboratory within 4-6 hours of death. In order to limit the inclusion of insects, carcasses were wrapped in plastic bags before being transported to the laboratory. At the site, the weight of each carcass was recorded (Table 21.) before introduction into the chamber.

**Table 2.1** Details of the main experimental trials conducted towards this research project. BHA refers to *buried human analogue* and EHA, *exposed human analogue trials*.

Trials								
Sample ID	BHA 1	EHA 1	BHA 2	BHA 3	EHA 2	BHA 4	EHA 3	
Weight (kg)	7.14	27.6	11.62	36	11.7	7.48	27	
Start of experiment (m/y)	09/12	12/12	01/14	04/14	10/14	07/15	01/16	
Experimental Mode	Buried	Exposed	'Heaped' burial	Buried	Exposed on sand	Buried	Exposed on sand	
Analytical Methodology	CIR-MS	CIR-MS	CIR-MS	CIR-MS	CIR-MS, GC-MS	CIR-MS, GC-MS	CIR-MS, GC-MS	

## 2.3 Analytical methods

### 2.3.1 Solid Phase Microextraction (SPME)

SPME has been long established as being one of the simplest yet most effective sampling techniques used in analytical science. Perhaps its successes are attributed to the fact that it operates without need for solvents, or that it is compatible with an array of analytical instruments. SPME integrates sample extraction, concentration and sample introduction into the analytical instrument in a single solvent-free step Figure 2.3 and Figure 2.4 [82].

Arthur and Pawliszyn [83] first developed SPME in 1989 and subsequently the technique has been utilised in numerous applications ranging from food, pharmaceuticals, toxicology, environment and forensic analysis [84-86]. SPME is able to concentrate trace analytes by adsorption and absorption onto specially coated fibres (Figure 2.3b). SPME was an attractive candidate for this research project because of its ability to detect low concentrations of decomposition VOCs, its ease of operation, especially because of the possibility of automation, the ease in transportation to potential burial sites, and its straightforward coupling to GC-MS [87].

SPME sampling involves two steps: first, a thin fused silica fibre coated with a thin polymer film (extracting phase) is exposed in the sample headspace and target analytes partition from the sample matrix to the coating (Figure 2.3a). The quantity of analyte extracted is proportional to its concentration, and the type of analyte extracted depends on the selectivity of the coating and the extraction time used [82]. At present, there is a restriction to the types of coatings commercially available. The current range includes a mixture in thickness and combinations of: polydimethylsiloxane (PDMS), typically suitable for extracting non-polar volatile compounds; poly acrylate (PA) for polar semi volatiles; carboxen polydimethylsiloxane (CAR/PDMS) for bipolar gases and volatiles; divinylbenzene (DVB) and carboxen (CAR) for volatiles.

Once the fibre has been exposed to the sample environment and after a defined time or when equilibrium is reached, the fibre is retracted into the metal needle for

protection. Following this, the SPME fibre is transferred to the injection port on the analytical instrument, in this instance the GC-MS; where the analytes are desorbed and separated. 65  $\mu\text{m}$  PDMS/DVB, 50/30  $\mu\text{m}$  DVB/CAR/PDMS, 85  $\mu\text{m}$  PA, 75  $\mu\text{m}$  CAR/PDMS and 100  $\mu\text{m}$  PDMS were investigated as fibre choices for the extraction of VOCs released into the headspace of decaying carcass. The capabilities of these fibres in relation to decomposition VOCs are explored in detail in Chapter 3.

The kinetics of SPME relates to the speed in which analyte are extracted from the sample matrix i.e. extraction rate. The process is governed broadly by parameters such as film thickness, extraction time and agitation [82]. There is a directly proportional relationship between the thickness of the fibre and extraction time i.e. as the thickness of the fibre increases, so does the required extraction time. It takes longer to reach equilibrium with a thicker coating compared to a thin coating, although volatile analytes require a thick coating to retain them longer, and thin coatings are preferred for extraction of high-molecular weight analytes [87]. Longer extraction times generally correspond with higher sample recoveries. The time of extraction is independent of the concentration of the analyte in the sample, and the relative number of molecules extracted at any distinct time is also independent of the concentration of the analyte [82]. Although higher recoveries are possible with longer extraction times, efforts are usually made to reduce extraction times, which in turn reduces overall sampling times. To achieve this, the thinnest possible fibre film is often employed [82].

Other approaches used to increase the rate of extraction by SPME involve increasing the temperature of the sample or by agitation. Both methods help increase analyte transport from the sample matrix into the headspace [88] and thus into the extracting phase of the SPME fibre.

SPME can be used for aqueous or gaseous (headspace) samples. In both cases, extraction is based on the partition of analytes between the sample matrix and the stationary phase of the fibre [88]. The micro extraction process is considered complete when the analyte concentration reaches equilibrium in the sample matrix and the fibre coating [88].

The distribution or partition coefficient  $K_{fs}$  is described in Equation 2.1, where  $C_f^\infty$  and  $C_s^\infty$  are equilibrium concentrations in the fibre coating and the sample respectively. Quantification using SPME is achieved by application of Equation 2.2 which states the number of moles of analyte extracted onto the fibre coating ( $n$ ) is linearly proportional to the analyte concentration in the sample ( $C_0$ ). When the sample volume ( $V_s$ ) is unknown or very large as is the case in this study, Equation 2.2 becomes simplified to Equation 2.3 [88]

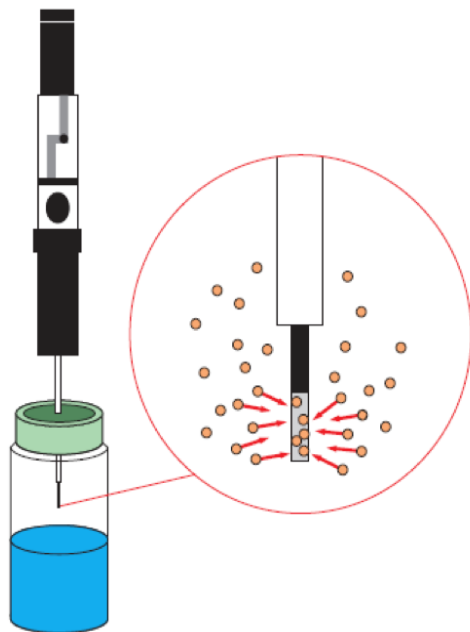
$$K_{fs} = C_f^\infty / C_s^\infty \quad \text{Equation 2.1}$$

$$n = C_f^\infty V_f = C_0 (K_{fs} V_s V_f / K_{fs} V_f + V_s) \quad \text{Equation 2.2}$$

$$n = K_{fs} V_f C_0 \quad \text{Equation 2.3}$$

Thermodynamically, SPME operates on the principle that all chemical extractions involve the distribution of the analyte between the sample matrix and the extraction phase. Such distribution constants can be estimated using isothermal GC retention times on a column with a stationary phase identical to the fibre coating material, especially as the partitioning process in GC is analogous to the partitioning process in SPME. Absorbent type coatings consist solely of a liquid polymer coating (Figure 2.3b). Analytes migrate into and through this polymer based on their affinity (polarity). Larger analytes are retained longer in absorbent fibres because of the slower migrations times required to travel through the stationary phase. In addition, smaller molecules can also be retained longer, however this depends on the thickness of the coating i.e. the thicker the liquid coating, the higher the retention of smaller analytes.

(a)



(b)

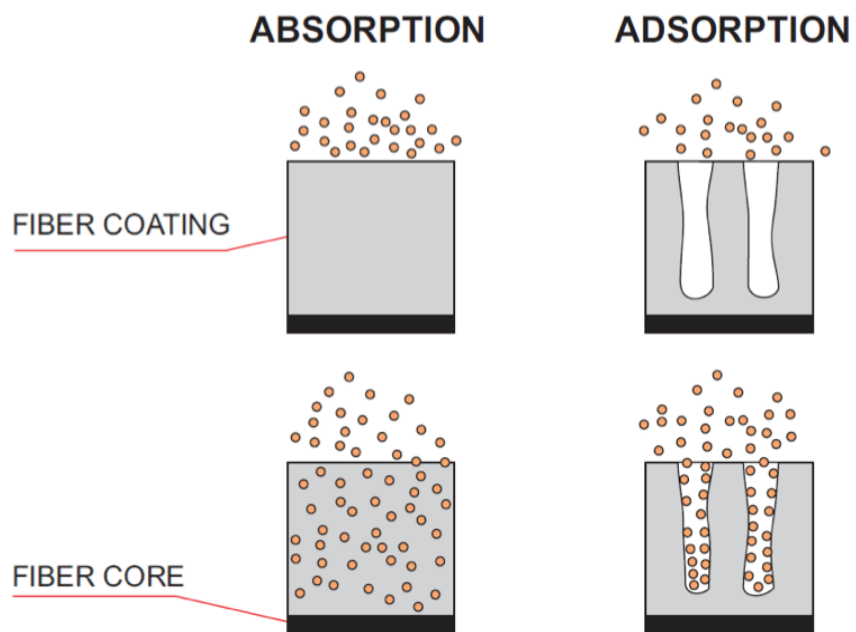


Figure 2.3 Illustrates the principles of Headspace – Solid-phase Microextraction (a), and (b) Extraction mechanisms for absorbent (liquid) and adsorbent (solid) fibre coating. Image adapted from Schmidt et al [89]

Table 2.2 Overview of some commercially available SPME fibre coatings. Adapted from Schmidt 2015 [89]

Polymer coating and thickness	Recommended application	Mechanism	Target	
			MW Range	Polarity
100 µm PDMS	Volatiles	Absorbent	60-275	Non-polar
30 µm PDMS	Non-polar semi volatiles	Absorbent	80-500	Non-polar
85 µm PA	Polar semi volatiles	Absorbent	125-600	Non-polar
75 µm CAR/PDMS	Gases and low molecular weight compounds	Adsorbent	30-225	Bipolar
65 µm PDMS/DVB	Volatiles, amines and nitro-aromatic compounds	Adsorbent	50-300	Bipolar
50/30 µm DVB/CAR/PDMS	Flavor compounds: volatiles and semi-volatiles, C3-C20	Adsorbent	40-275	Bipolar

In contrast, adsorbent-type fibre coatings consist of a solid porous polymer either made from carbon or silica. This polymer is bonded to a liquid material coated on the fibre core. Analyte molecules travel from the sample into the pores of the adsorbent and interact with its particles via hydrogen,  $\pi$ - $\pi$ , or van der Waals bonding (figure 2.3b). Retention of the analyte in adsorbent based fibres is based on the size of the molecules, the diameter of the pores and the amount of porosity. Table 2.2 outlines the extraction mechanism of some commercially available SPME fibres [89].

Following extraction of analytes by either adsorption or adsorption mechanism, and after a suitable extraction time, the SPME fibre is retracted into the metal casing where it is protected. The SPME fibre is then transferred to the separation instrument, typically gas chromatography where the analytes are desorbed (Figure 2.4)

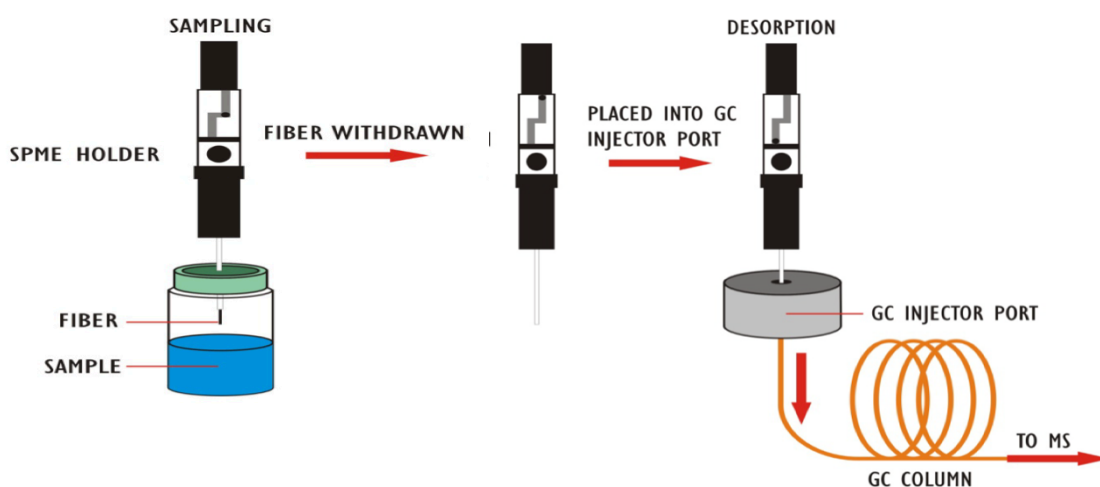


Figure 2.4 Analysis by solid phase micro extraction-gas chromatography-mass spectrometry (SPME-GC-MS). Image adapted from Schmidt *et al* [89]

## 2.3.2 Gas Chromatography-Mass Spectrometry (GC-MS)

### 2.3.2.1 The Basics

Gas chromatography is a well-established analytical technique that was first pioneered in 1941 by Martin Archer and Richard Synge; although the first article describing the first gas chromatograph was not published until 1950s [90]. Fundamentally, GC separates the components in a sample based on the differences in the partition coefficient between the analyte and the coating of the column in the GC [91]. The GC-MS system used in this research project was a 7890A Gas Chromatography coupled to a 5975C mass spectrometer equipped with a CTC-PAL auto sampler purchased from Agilent technology, Wokingham, UK.

The sample is introduced into the instrument via the inlet port (Figure 2.5) which is temperature controlled. The high temperature of the inlet ensures that the sample gas volatilises or in the case of SPME is thermally desorbed before being swept into the column by the carrier gas which acts as the mobile phase. The inlet port is connected to the head of the column, which contains the stationary phase. The mobile phase serves to carry analytes of the mixture through the heated column, and is typically in the form of an unreactive gas (He, N<sub>2</sub> or H<sub>2</sub>), set at a predetermined flow rate or pressure. The inlet of the GC can be operated in split or split less mode. In split mode, the percentage of sample entering the column can be controlled for more efficient peaks separation, and high reproducibility. It also increases the lifetime of the detector, by reducing detector saturation, but does so at the cost of reduced sensitivity. In the column, separation is based on the affinity of components within the analyte sample and the stationary phase [91].

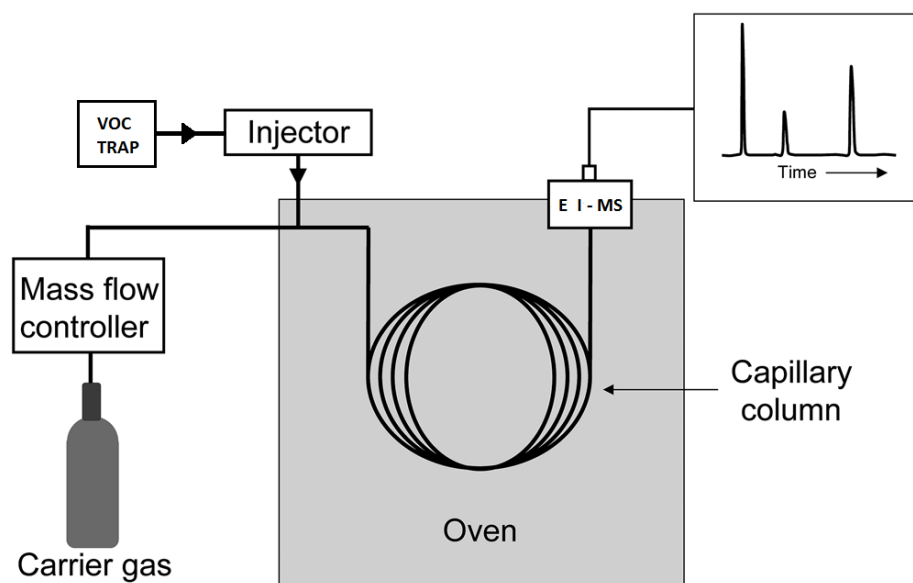


Figure 2.5 Schematic diagram showing components of a GC instrument. Schematic reproduced from Ellis *et al* [92]

Table 2.3 Overview of GC columns used in other decomposition studies

GC column	Stationary phase	Polarity	Ref
MXT-624	6% cyanopropylphenyl and 94% dimethyl polysiloxane	Non-polar	[27]
RTX-5	5% diphenyl/95% and Dimethyl polysiloxane	Non polar	[30]
DB-225ms	5% Phenyl 95% dimethylarylene siloxane	Non polar	[29]
RTX-1PONA	100% dimethyl polysiloxane	Non-polar	[93]
DB-wax	Polyethylene glycol (PEG)	Polar	[94]
DB-5ms	5% Phenyl 95% dimethylarylene siloxane	Non-polar	[94]

Chromatography involves a separation method in which components of a sample partition between two immiscible phases i.e. mobile (moving) and stationary (non-moving). The mobile phase in gas chromatography is a high purity inert gas, although in other types of chromatographic separation the mobile phase can be a liquid or supercritical fluid. The stationary phase may be in the form of a liquid supported by a porous or inert material, or an adsorptive, inert solid.

The degree of partitioning in gas chromatography depends on each compound's affinity to the mobile and stationary phases. The sample to be separated is carried by the flow of the mobile gas, and is percolated over the stationary phase. In doing so, each compound within the sample interacts with the stationary phase to different degrees, depending on their respective affinity for the stationary phase. Compounds with greater solubility or affinity for the stationary phase will move with lower velocity through the chromatographic system and thus will take longer to emerge than compounds with less affinity. Ultimately, it is this difference in migration velocity that leads to the physical separation of components within a sample [95, 96]. The tendency for a compound to be attracted to the stationary phase is referred to as the partition coefficient or distribution constant. The greater the value of the partition coefficient, the greater the affinity to the stationary phase [97].

Schematic representation of the chromatographic process is shown in Figure 2.6. The horizontal lines represent the column, and each line is like a snapshot of the process at a different time. Each component partitions between the two phases (above = mobile phase, below = stationary phase). Compound A has a greater distribution in the mobile phase and thus is carried through the column faster than compound B. On the other hand, compound B has a greater affinity for the stationary phase, and as a consequence compound B has a lower migration velocity through the stationary phase. Eventually, both components A and B leave the column and reach the detector. The time at which each component reaches the detector is recorded and is often referred to as the retention time. The output signal of the detector is a chromatogram shown on the right hand side of Figure 2.6

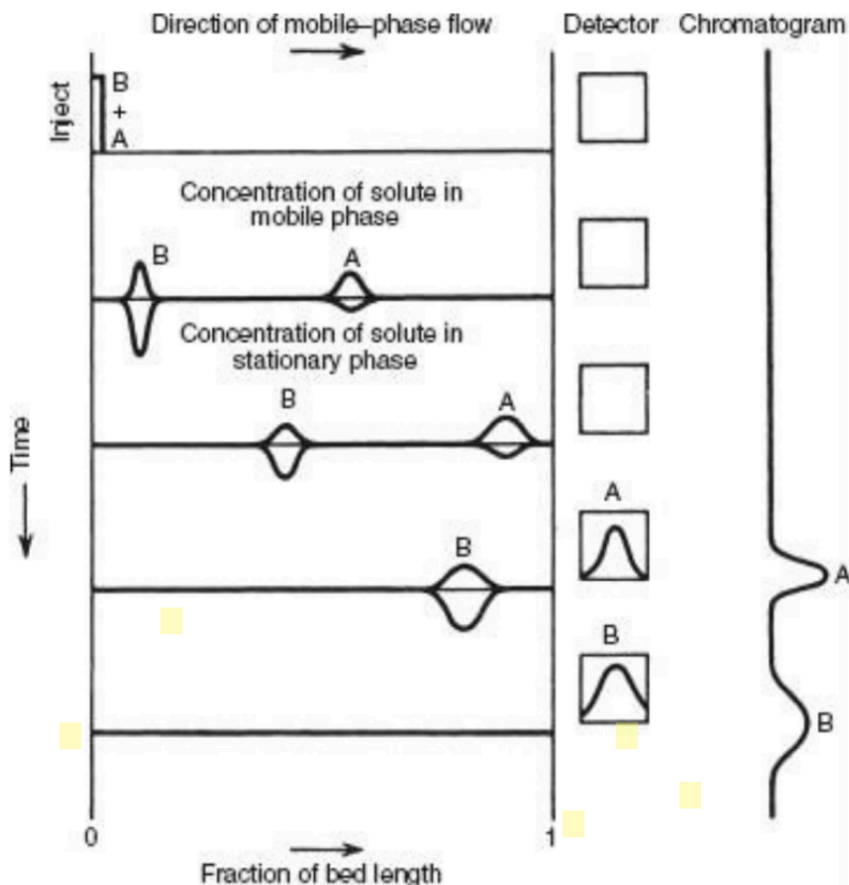


Figure 2.6 Schematic representation of the chromatographic separation in the GC column. Adapted from McNair 2011

The difference in the broadening of the resulting peaks which corresponds to compound A and B in the chromatogram depicted in Figure 2.6 can be broadly characterized as being due to contributions from the dead volume and the chromatographic column. Dead volume relates to all the volumes outside of the column but within the chromatographic system i.e. tubing used to connect components, volumes in the detector cell etc. All these volumes contribute to peak broadening especially because they are not related to the separation process occurring in the column. The other source of peak broadening is due to the chromatographic column and can be divided into four areas: longitudinal diffusion, eddy diffusion, mass transport broadening in the stationary phase and mass transport broadening in the mobile phase. Each of these have been discussed in much detail elsewhere [98].

In simpler terms, 'like will attract like' such that polar compounds will be well retained on a polar based column, and non-polar compounds to a non-polar column. Components that do not retain well onto the column will reach the detector first, whereas substances that have a strong affinity for the column will move slowly through and will not reach the detector at the end of the column until much later. The column is contained in an oven, which can operate by isothermal or temperature gradient programming. Application of temperature gradients ensures that all analytes are eluted from the column. As well as this, an isothermal hold enhances the resolution of any early eluting peaks.

Thus far, there have been a diverse range in the polarity of columns used to study decomposition VOCs (table 2.3). The capillary column used in this study was a DB-5MS (30m long x 0.250 mm diameter, 0.25  $\mu\text{m}$  film thickness) purchased from Agilent Technology, Wokingham, UK.

### 2.3.2.2 The Theory

Gas chromatography operates on the theory of gas-liquid separation. It is governed by a number of parameters including partition coefficient ( $K_x$ ), selectivity factor ( $\alpha$ ), retention factor ( $k'$ ) theoretical number of plates ( $N$ ), reduced plate height ( $h$ ), reduced velocity ( $v$ ), and resolution ( $R_s$ ) [91].

The distribution coefficient or partition coefficient ( $K_x$ ) measures the affinity of an analyte to the stationary phase. If the partition coefficient is sufficiently large, the analyte is retained longer on the column, and thus better separated. The relationship between the concentration of the analyte in the stationary, mobile phase and the partition coefficient is described by the following equation  $K_x = \text{mol}_s / \text{mol}_m$  where  $\text{mol}_s$  and  $\text{mol}_m$  are the moles of the solute in the stationary and mobile phase respectively [98]. Details of the other characteristics affecting separation by gas chromatography have been discussed in great detail by several authors [91, 98].

The choice of detector in gas chromatography can help increase the probability of positive compound identification, especially as it is possible for two or more compounds to bear the same retention time. The most common detector used in gas chromatography is a mass spectrometer; which operates by further separating elutants from chromatography based on their mass to charge ratio.

Mass spectrometers typically operate under three principles; ionization, mass separation and ion detection. First, elutants from chromatography are ionised by bombardment with energetic electrons in the ion source region of the mass spectrometer; this leads to the formation of positively charged ions. It is worth mentioning that there are numerous alternative approaches to ionise a molecule, however the most commonly employed in GC-MS is electron impact ionisation (EI). Once molecules are ionised, electromagnetic fields are used to separate the ions according to their mass to charge ratio. One of the most utilised form of mass analyser employed is a quadrupole (figure 2.6). The quadrupole operates by exploiting DC and RF potentials on the quadrupole rods such that only a selected mass will have a stable trajectory through the quadrupole to reach the detector while all other ions will collide with the rods never reaching the detector. Quadrupole mass analysers can operate synchronously in selected ion monitoring mode (SIM) or full scan mode.

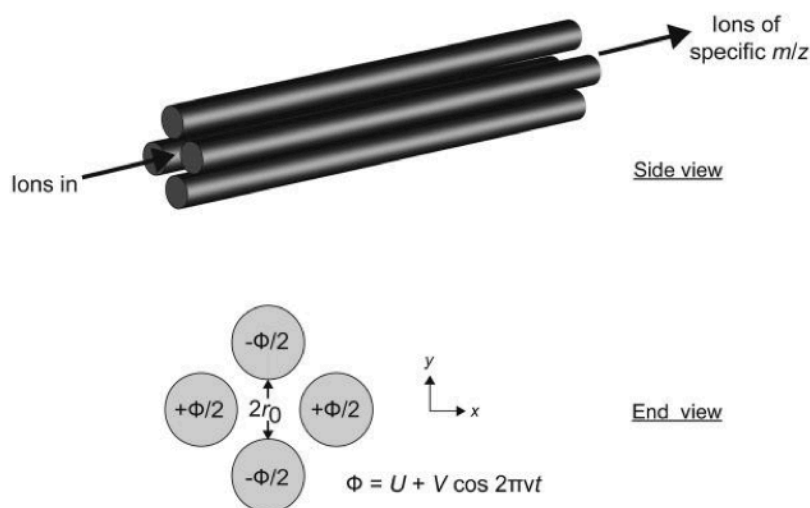


Figure 2.7 Side and end views of the rods employed in quadrupole mass analysers. Reproduced from Ellis *et al* [92]

### 2.3.2.3 The Analysis

Once the components of the sample have been sufficiently separated, the detector sends an analogue signal to the data system where the signal is digitised, amplified and plotted against time (retention time). The result of this is what is commonly referred to as the total ion chromatogram (TIC). The data system is also usually capable of performing various quantitative and qualitative operations on the chromatogram, assisting with sample identification and quantification.

Compounds that are retained on the column eventually elute as gaussian shaped peaks (ideal) although fronting and tailing are also possible. Fronting and tailing are forms of Langmuir isotherms which results from overloading the stationary phase (fronting) and Anti-Langmuir (tailing) a result of injecting a sample that is too highly concentrated [98].

Retention times provide the qualitative aspect of the analysis because the retention time of a compound is constant under identical chromatographic separations. In addition, separation by mass together with the fragmentation patterns observed by the mass spectrometer also enhances compound identification. Typically, both chromatographs and mass spectrums are compared against those stored in libraries such as National Institute of Standard Technologies (NIST).

For quantification, the chromatographic peak area is measured as it directly relates to the quantity (concentration) of the analyte present [99]. However, accurate identification and quantification cannot be determined solely by comparisons with search libraries. Search libraries only allow for tentative assignments so for accurate determination of the compound, retention times and peak areas should be compared against standards of known concentrations.

One of the limitations with analysis of a sample by gas chromatography-mass spectrometry is time resolution. The time it takes components of a sample to pass through the chosen column in a GC oven takes typically tens of minutes [100]. This coupled with the time taken to collect the sample (exposure times in the case of SPME) before injection into the GC further increases the duration of the analysis. Gas chromatography-mass spectrometry is therefore not the most suitable technique to use

when temporal resolution is a significant factor [100]. As well as this, the method of ionization (typically EI) can be disadvantageous as the excess energy can cause extensive fragmentation. This means in a complex sample consisting of different components there is an increased likelihood that the different components will produce fragments with similar masses, further increasing the complexity of analysis especially as information of the molecular ion peak is often not represented. To add to this, common constituents of the air  $N_2$ ,  $O_2$ ,  $CO_2$  at masses 28, 32 and 44 respectively usually overwhelm the GC at the lower mass range.

The most important drawback of SPME-GC-MS, however, is the biased nature of the technique. This can be considerably limiting especially when analysing complex matrixes such as the volatile compounds associated with carcass decomposition. It quickly becomes clear that there is not one sampling collection technique, or column that is highly sensitive and selective to all the expected chemical classes produced as a result of carcass decomposition. The selectivity of each individual component aforementioned suggests that there is a need to implement a technique that is not only fast, but one that can simultaneously detect a multitude of chemical classes at levels as low as parts per trillion (ppt).

### **2.3.3 Chemical Ionisation Reaction Mass Spectrometry (CIR-MS)**

Chemical ionisation reaction-mass spectrometry (CIR-MS) was first introduced in 1966, and since then it has been developed into a powerful and versatile tool that has found extensive applications in numerous fields ranging from medical, biochemistry, environmental and chemistry [101].

Chemical ionisation itself is a blanket description for a collection of chemical processes which produce low energy ionisation reagents. It involves gas phase ion molecule interactions where the sample of interest is affected by a reagent ion rather than by

electron impact as occurs in EI. In EI, bombardment of a gaseous sample consisting of polyatomic species at pressures of  $\approx 10^{-5}$  Torr produces an assembly of molecular ions that possess high internal energies ranging from 0 eV to 70 eV [102]. As a direct result of this high internal energy, molecular ions fragment extensively to what is observed in an EI spectrum. To this end, using EI, the molecular ion of the species is often poorly represented in the resulting spectrum. Although review of the fragmentation pattern observed in EI-MS can assist with structure elucidation, identification of the molecular mass can be somewhat challenging. On the other hand, ionisation by gas phase ion-molecule reactions (CI) is a much softer technique, resulting in significantly less fragmentation. This in turn produces information about the mass of the molecular ion, and a simpler spectra which can be easily interpreted [103].

The three most prominent processes of chemical ionisation are proton transfer, charge transfer and hydride extraction [101]. All of these processes involve the transfer of entities from the ion to the molecule of interest. In the instance where ionisation occurs via proton transfer, the extent of fragmentation relies on the exothermicity of the proton transfer reaction between the reagent ion and the molecule being ionised.

This document focuses primarily on proton reaction reactions. Details of other chemical ionisation processes have been discussed by other authors [101].

### **2.3.3.1 Proton Transfer Reaction (PTR)**

As the name suggests, proton transfer reactions involve the transfer of a proton from one compound to another (Equation 2.4). The reaction is best described as an ion-molecule interaction consisting of a rich proton donor (ion) and a neutral molecule (sample). The thermodynamics of the reaction can be explained based on the difference in proton affinity of the ion and the molecule [100].

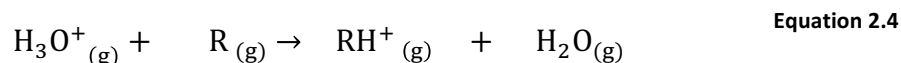
While other proton donors have been previously used in PTR reactions [92, 100, 104],  $\text{H}_3\text{O}^+$  remains one of the most widely used reagent ion because it possesses a low proton affinity, is readily available, inexpensive and non-toxic. The low proton affinity

of water ( $691 \pm 3 \text{ kJ mol}^{-1}$ ) positions it as a good candidate to ionise most organic compounds ( $< 900 \text{ kJ mol}^{-1}$ ) especially as most inorganic compounds have a much lower proton affinity. The use of  $\text{H}_3\text{O}^+$  as the primary ion in PTR means that the technique is transparent to common inorganic constituents of the air, thereby reducing any interferences [100].

**Table 2.4 Summary of the main product channels formed as a result of protonation using hydronium as the primary ion. Adapted from Ellis et al [92]**

Functional group	Reaction products
<b>Alkanes</b>	No reactions with acyclic alkanes with $\text{C}_5$ or less Species with $> \text{C}_6$ give only association products.
<b>Alkenes</b>	100% $\text{MH}^+$ product for $< \text{C}_7$ species. Fragmentation must be considered for alkenes with 7 or more carbons.
<b>Alkynes</b>	Endothermic for $\text{C}_2$ or less species, but fast for larger alkynes dominated by $\text{MH}^+$
<b>Aromatic hydrocarbons</b>	100% production of $\text{MH}^+$
<b>Alcohols</b>	Dehydration for species with 3 or more carbons
<b>Ethers</b>	Mainly $\text{MH}^+$ products can be calculated providing the ratio of ion counts between hydronium and the molecular
<b>Aldehydes</b>	100% production of $\text{MH}^+$ for $\text{C}_3$ or lower aldehydes, but increasing tendency to lose water for $\text{C}_4$ or higher species
<b>Ketones</b>	100% production of $\text{MH}^+$
<b>Carboxylic acid</b>	Mostly $\text{MH}^+$ formation, although some dehydration is possible
<b>Esters</b>	Mostly $\text{MH}^+$ for small esters. Major ion fragmentation if alcohol group has 3 or more carbons
<b>Nitriles</b>	100% of $\text{MH}^+$
<b>Amines</b>	Mainly $\text{MH}^+$ product, although some loss of alkene or $\text{H}_2$ is possible
<b>Organosulphur compounds</b>	100% production of $\text{MH}^+$
<b>Organohalides</b>	Aromatic halides form 100% $\text{MH}^+$ products.

If the proton affinity of the reagent molecule (R) is larger than the donor ion ( $\text{H}_3\text{O}^+$ ) the proton transfer reaction will be exothermic and is expected to be spontaneous (Equation 2.4). The magnitude of the exothermicity is controlled by the choice of reagent ion, thus by choosing a suitable reagent ion for the sample being investigated, the amount of energy produced as a result of the proton transfer reactions can be reduced so that it is sufficiently small to preclude extensive fragmentation [92].



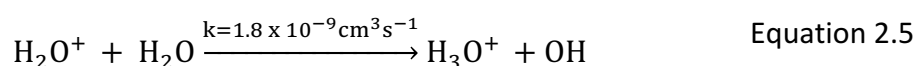
In spite of hydronium being the reagent ion of choice,  $\text{RH}^+$  is not the only possible product channel upon reacting with organic compounds. For instance, depending on the chemical class of the organic compound and its number of carbons, it is possible to observe the removal of water (dehydration) or association reactions (Table 2.4). This needs to be considered when interpreting the mass spectrum generated by PTR-MS.

The forthcoming section discusses the design of the apparatus required to perform proton transfer reaction mass spectrometry. An overview of the PTR-MS schematic can be found in Figure 2.9

### 2.3.3.2 The Ion source

The ion source and drift tube assembly used in this research was fabricated at the University of Leicester. The ion source positioned at the top end of the drift tube used hydronium as the reagent ion, produced by the passage of water over a low-level  $\alpha$  particle emitter source  $^{241}\text{Am}$ .  $^{241}\text{Am}$  was embedded within a thin metal strip housed in a stainless cylinder ( $\approx 44.4\text{mBq}$ , standard film, NRD incorporated, Grand Island NY) between regions ED1 and ED2 of the drift tube (Figure 2.7). The high energy  $\alpha$  particles (5 MeV) interact with an incoming flow of nitrogen and water vapour to cause a chain of multiple ion-molecule reactions which ultimately yields  $\text{H}_3\text{O}^+$  in secondary reactions (Equation 2.5) [92]. The high flow of zero grade nitrogen (BOC, BTCA 1178 grade) and

high purity de-ionized water vapour (30 sccm per minute) was used to ensure that a sufficient flow of gas was achieved to prevent back streaming of the analyte gas into the ion source region. Having said this, the ingress of small amounts of the constituents of air, N<sub>2</sub> and O<sub>2</sub> into the ion source region of the CIR-MS instrument was inevitable, although it is reduced by use of a radioactive ion source compared with a hollow cathode discharge ion source.



### 2.3.3.3 The Drift tube

The drift tube located from region ED3-ED7 Figure 2.7 provides a suitable pressurized environment for ion-molecule reactions between the proton donor ion H<sub>3</sub>O<sup>+</sup>, produced in the ion source region (ED1-2), and the analyte gas to occur. The drift tube used in this work was constructed from stainless steel and insulating spacers and was 15 cm long. It consisted of equally spaced ring electrodes programmed to a set electric field gradient. The electric field provided the ions with kinetic energy to induce ion-molecule collisions. The decreasing potential on each successive electrode was such that ions entering the drift tube are drawn in a downward stream towards the aperture leading to the mass spectrometer end. In addition, the drift tube was continually pumped to maintain a constant high pressure of 6 mbar. The pump, located at the bottom end of the drift tube provided a pressure gradient which further enhanced the direction of the stream. A mass flow controller was used to deliver a constant flow of analyte gas of 150 sccm transverse to the H<sub>3</sub>O<sup>+</sup> ion velocity.

However, in spite of the electric field applied (E), collisions between ions and molecules in the drift tube cause a decrease in velocity. A decrease in ion velocity means a reduced rate of collisions and as such, a higher proportion of formed water cluster molecules, otherwise known as hydrated hydronium ions, are preserved (H<sub>3</sub>O<sup>+</sup>.(H<sub>2</sub>O)<sub>n</sub>). Aside from the fact that water cluster molecules possess higher proton affinities than H<sub>3</sub>O<sup>+</sup>,

hydrated hydronium clusters are not restricted to proton transfer alone, ligand switched reactions are also possible, complicating the interpretation of the generated mass spectra [100].

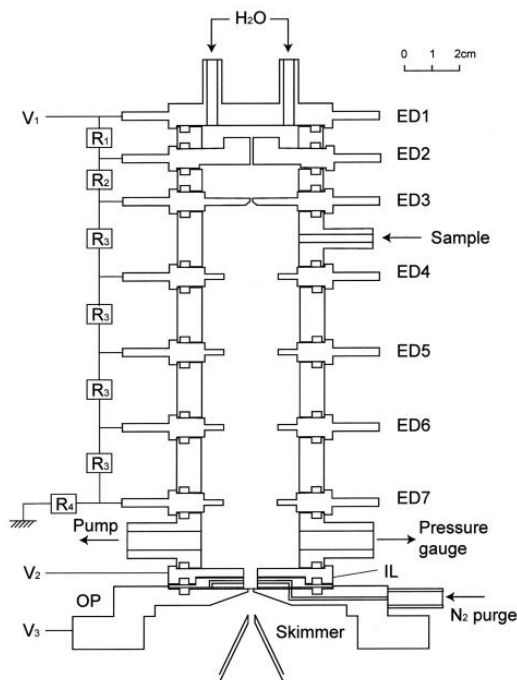


Figure 2.8 Schematic of the ion source (ED1-ED2) and drift tube region (ED3-ED7) of the CIR-MS instrument employed in this research. Image reproduced from Ellis *et al* [92]

In order to circumvent this issue of hydrated hydronium clusters, the design of the drift tube was such that it incorporated a collision induced dissociation (CID) region towards the end of the drift tube region of the CIR-MS instrument. The design of the CID was similar to that of Warneke *et al* [78]. Unlike the electric field applied to the ring electrodes encompassing the main length of the drift tube, in the CID region, a steep electrical gradient is applied so as to allow the possibility of collision-induced dissociation of the ions exiting the drift tube.

E/N refers to the energy delivered to ion-molecule collisions in the drift tube to preclude excessive clustering of hydrated hydronium clusters.  $E$  is the applied energy and  $N$  the density of gas molecules present, per unit volume in the drift tube. The ratio of E/N is typically reported in units of Townsend (Td) where  $1 \text{ Td} = 10^{-17} \text{ Vcm}^2$ . The application of a high E/N over a short distance helps breakup any hydronium cluster ions that might have formed, thereby simplifying the mass spectrum. Typically drift tube lengths range

between 8-10 cm [105], however, the longer drift tube adopted here provides a longer reaction time for a given E/N, and enhances sensitivity. In this work, the operating E/N was 97.72 Td with a CID region of 154 Td. Such low E/N helped retain the formation of protonated parent ions produced in the drift tube.

#### **2.3.3.4 The Transfer Chamber**

The ions exit the drift tube through a 200- $\mu\text{m}$  orifice to maintain the pressure differential, after which they are passed through a second 3 mm orifice into the transfer chamber of the CIR-MS system. A three element einzel lens help focus the ions between the back plate and the extractor grid Figure 2.9. By rapidly switching the potential between the back plate and the extractor grid, the protonated ions are driven through a set of spatial focusing electrodes and steering plates before passing into the flight tube region of the system [105].

#### **2.3.3.5 The Flight tube**

In the flight tube, protonated ions are separated based on their mass. A 'packet' of ions leaving the drift tube is introduced orthogonally into the space between the two plates (repeller and extractor). The repeller and extractor electrodes are first given the same electrical potential, after which the potential of the repeller plate is increased thus creating an electrical gradient. This gradient sends pulses of ions into the flight tube, which has no electrical field, and the detector at the end of the flight tube measures the response time of each ion. The measurement of time allows for the determination of  $m/z$  (mass to charge ratio) by application of Equation 2.6, where  $m$  is the ion mass,  $l$  is length of the flight tube and  $t$ , the time taken [92]. Despite the description given above, not all ions receive the same energy.

A reflectron time of flight mass spectrometer was used in the CIR-MS instrument because it provided higher resolution over the conventional linear form.

The reflectron end consisted of a two-stage acceleration zone to accommodate for the energy drop between the plates. As well as this, electrodes are used in the flight tube to reverse the direction of the ions. In doing so, more energetic ions of the same mass would penetrate deeper in the reflectron zone, hence increasing their flight paths. The net result of this is that all ions of the same mass will arrive at the detector at the same time. The development of the TOF system to include a reflectron end

Figure 2.9) enhances the resolution of the mass analyser [92].

$$t = \sqrt{\frac{l^2}{2eV}} \cdot \frac{m}{z} \quad \text{Equation 2.6}$$

A multi-channel plate (MCP) detector connected to the end of the flight tube generates an output, which is sent to a time digital converter. Overall, the PTR-TOF-MS acts a multichannel instrument capable of collecting a whole mass spectrum at once with no compromise in sensitivity unlike quadrupole mass spectrometers such as found in the GC-MS instrument. This coupled with its resolving power in excess of  $m/\Delta m$  1000 makes it an ideal candidate in the analysis on complex mixtures such as that expected in the headspace of decomposing carcasses.

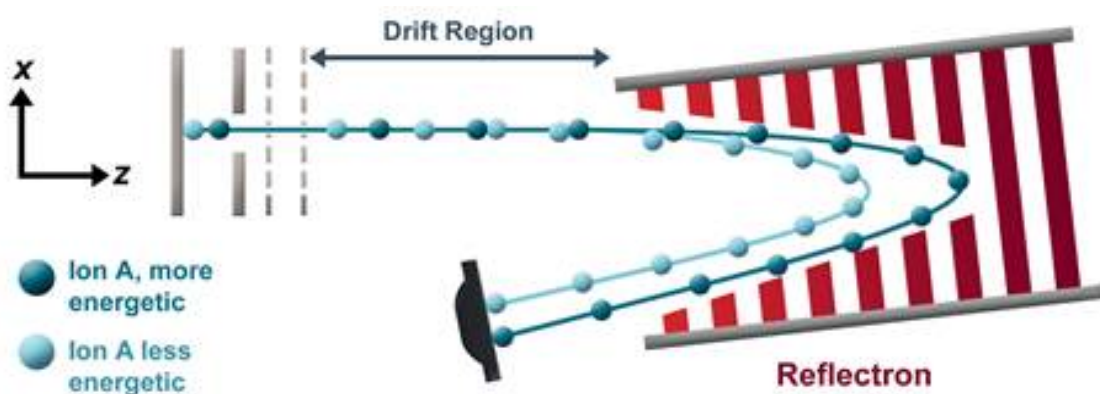


Figure 2.9 Schematic of the reflectron end of the time of flight mass analyser used in CIR-TOF-MS instrument utilized in the study of decomposition VOCs

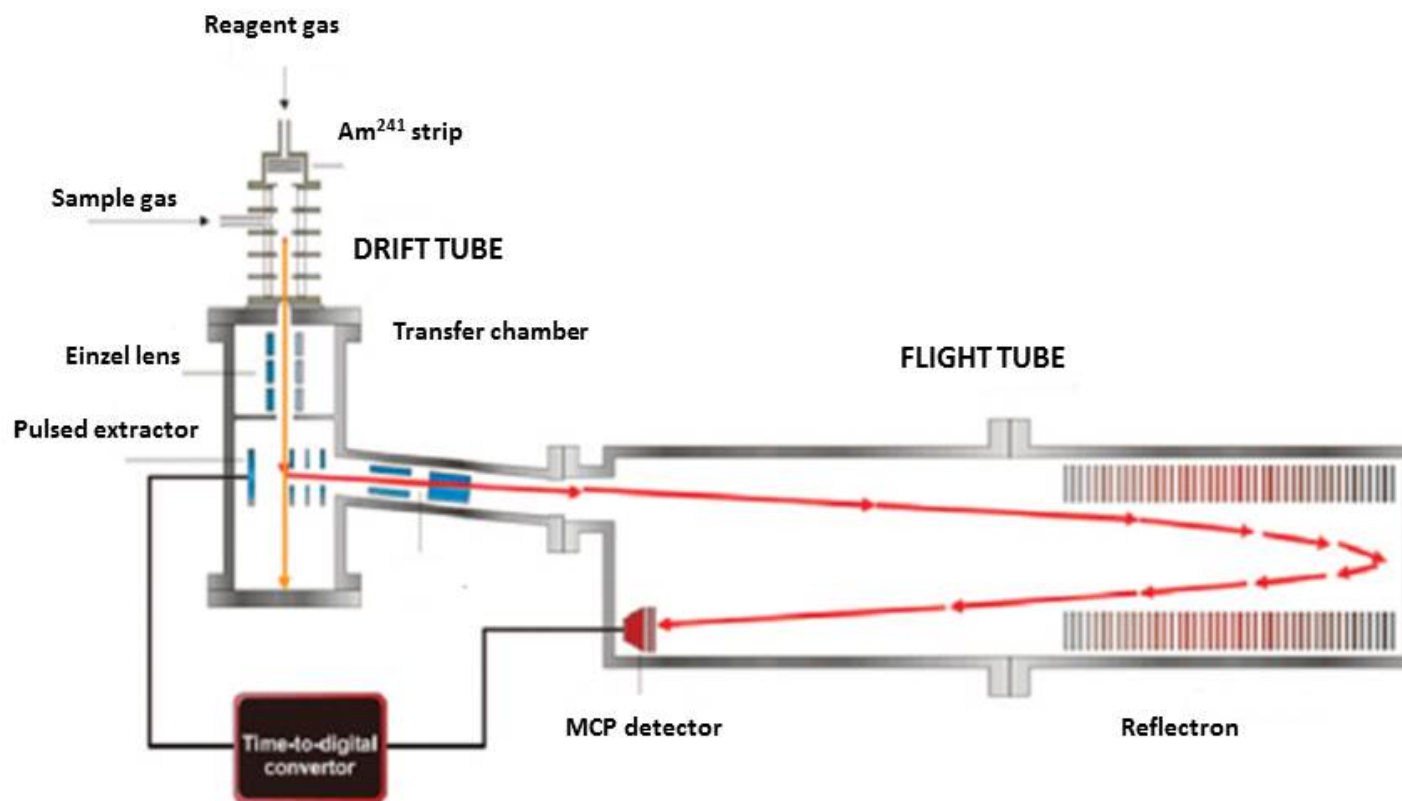


Figure 2.10 Schematic representation of the University of Leicester CIR-TOF-MS system. Image adapted from Blake et al [100]

### 2.3.4 Quantification of results generated by CIR-MS

One of the attributes of CIR-MS, particularly PTR-MS instruments is its potential to determine absolute concentrations without the need for calibrations. As outlined in Equation 2.7 and Equation 2.8, the volume mixing ratio (VMR), used to denote concentration of species (M) can be calculated providing ( $i(MH^+)/i(H_3O^+)$ ), rate coefficient (k), reaction time (t) in the drift tube, and the number density ( $N_d$ ) ( $N_a$ ,  $p$ ,  $T$  represents the pressure temperature and Avogadro's number respectively) are known [92].

However, a limitation of this approach for quantitative analysis is that Equation 2.7 only considers one product ( $MH^+$ ) resulting from the proton transfer reactions. This leads to a certain degree of uncertainty as it does not consider fragment or cluster ions which are also possible. As well as this, Equation 2.7 only calculates the concentration within the drift tube, although the required concentration is of species **M** in the sample [92]. Hence, calibrations are necessary to reduce such uncertainties and to improve the reliability of the PTR-MS.

$$VMR_m = \frac{i(MH^+)}{i(H_3O^+)} \frac{1}{kt} \frac{10^9}{N_d} \quad \text{Equation 2.7}$$

$$N_d = \frac{pN_a}{RT} \quad \text{Equation 2.8}$$

In order to calibrate the CIR-MS instrument, varying concentrations of known standards are fed into the CIR-MS under the same operational settings as the sample to be analysed. A typical calibration plot for CIR-MS shows the response of the instrument on the y-axis as normalised counts per second (ncps) and concentrations in volume mixing ratios (ppmV, ppbV, pptV) on the x-axis [92]. Providing the instruments response is linear, the calibration factor can be extracted from the slope of the fit.

Normalisation in ncps, refers to the count rate of  $MH^+$  relative to  $H_3O^+$ . The main reason CIR-MS users quote this relative value rather than absolute ion count rates is because the count rates of  $H_3O^+$  are not stable over the course of one day, and from one day to the next, although PTR theory assumes the counts and thus concentration of hydronium is constant [92].

As evident from Table 2.1 experiments conducted on the CIR-MS instrument towards this research spanned a total period of four years. Hence the decision to normalise was apparent as it allowed for better comparisons of the instruments response between the different trials. All CIR-MS data discussed in the upcoming chapters were normalised by multiplying the ratio of ion counts from  $MH^+$  and  $H_3O^+$  by  $10^6$  [92].

### **2.3.5 Data handling and statistics**

As outlined in the section 1.8, the objective of this research was to monitor, evaluate and quantify the evolution of VOCs during the early post mortem stages of carcass decomposition. To achieve this, measurements generated by both CIR-MS and GC-MS instruments needed to be analysed in a manner that aligned with this objective. At the time this research was conducted, there was no documented record of CIR-MS being used as an instrumental technique to study decomposition VOCs, and as such the approach in handling the resulting data from the trials here is novel. GC-MS on the other hand has been the primary instrumentation used by other decomposition authors, thus there is some evidence to support the data analytical process. Some of the more recent studies conducted on decomposition VOCs have been by use of GCxGC-MS instruments which have advanced comparison algorithm software such as ChromTOF, built in to assist with data analysis [30, 61, 76].

One of the most challenging aspects of this research project was in developing a system to identify patterns within the dataset. Ten minute scans collected over the course of, on average, 30 days per trial (7 trials in total) via CIR-MS eventually amounted to what can be considered big data. Consequently, it was crucial to develop a method of

managing the data, through data reduction, without losing decomposition relevant information. An overview of the data processing step is illustrated in (Figure 2.11).

CIR-MS is a technique that lacks the ability to definitively identify compounds. As such compound assignment can only be tentative. The beginning of the data reduction process of CIR-MS data involved averaging each ten-minute scan into daily readings. This step was possibly via the use of a built in function on the CIR-MS computer. Following this, the data set was normalised to the reagent ion hydronium ( $m/z$  19) providing there was evidence to support the fact that the reagent ion peak was not sufficiently depleted at any point during the trial by constituents of the analyte gas to make the PTR equation void (*step 5 in the process*). Ion counts were always normalised to one million of the counts at  $m/z$  19 for reasons discussed in section 2.3.4.

Next, standard deviations and one-way ANOVA tests were applied to all 500 monitored mass channels. One-way ANOVA tests if the means of each measurement are statistically different from each other. The output from ANOVA reveals a  $p$ -value, and  $p$ -values less than 0.05 are interpreted as being statistically different.  $P$ -values are also associated with Fisher ratios (F-ratio), which is the difference between groups divided by the difference within groups [106]. Some decomposition authors have employed the use of fisher ratios in the data analysis process [107]. Regrettably however, ANOVA as a statistical operation did not inform on which of the mass channels were statistically different [106].

To circumvent this, initially post hoc tests as described by Tukey and Scheffe [106] were applied as a means to identify and group mass channels with similar patterns. However, examination of the time profiles of the mass channels within the groups created by the post hoc tests revealed discrepancies in the mass channels proposed to share the same time profile. There was no clear trend in the time profiles of the mass channels within the grouping systems generated by Scheffe and Tukey. This finding suggested that groupings based on means was insufficient in describing patterns within each mass channel. This disagreement was akin to the results generated by K-clustering.

Consequently, it became clear that the techniques aforementioned could not be used to accurately extract patterns within the monitored mass channels. As a result, the decision to classify mass channels based on their characteristic time profiles was reached. Since it was expected that the process of decomposition would constantly change, it was plausible that compounds (mass channels) would vary in appearance and abundance as the carcasses passed through the different stages of decomposition.

To achieve this, a small selection of the data was first inspected. The top 20 varied mass channel were used as a way of pre-determining signature mass channels based on their time profiles (*step 6*). Extraction of the top 20 varied mass channels provided an insight into some of the patterns within the dataset. At this stage, the data was described as being locally classified. Subsequently, Spearman's correlation coefficient comparisons were conducted on the entire population (*step 7*). Spearman's correlation is a non-parametric method which supplies information about the strengths and directions of relationships by using a range of -1 to +1 [93]. The profiles identified from the top 20 mass channels were used as guidelines when the full dataset was examined. Spearman's correlation coefficient greater than or equal to 0.96 was used and consequently, the local classification system previously created was enhanced by inclusion of other mass channels regardless of variance. At this stage, the data was considered as being globally classified (*step 8*). The final step was validation of the global classifications system created as a result of step 8. Comparisons of the time profiles of all the mass channels proposed to belong to each global subset were made. At this stage, the data had also been sufficiently reduced.

IBM® SPSS® statistics version 24 was used to conduct one-way ANOVA tests and R programming (versions R 3.1.0) was used to graph outputs of the correlation calculations. Finally, Igor Pro version 6.37 and graph pad version six were used to produce final graphical representations.

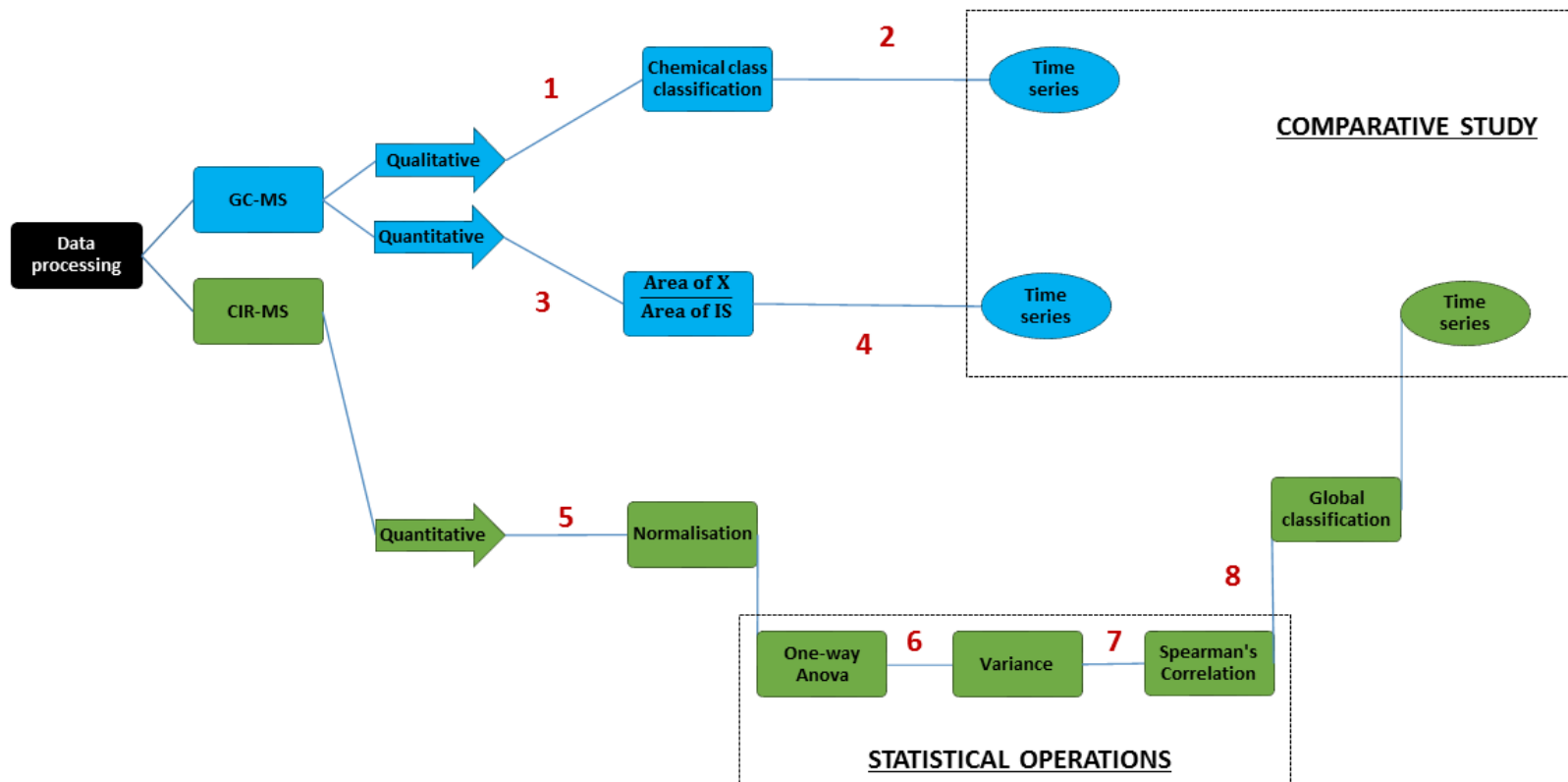


Figure 2.11 Representation of the data processing scheme used in this research project

## 2.4 Chapter 2 Summary

The development of an indoor decomposition chamber used in the study of decomposition odour was somewhat novel. The design of the chamber was such that the multitude of factors known to govern the rate of decay were limited, so as to increase reproducibility of the decay process.

Admittedly, there is an obvious conflict in the design of the decomposition chamber, especially from a forensic perspective, as it raises questions about how realistic decomposition in a confined environment is. However, at this initial stage, some compromise had to be made in relation to conducting realistic trials versus increasing reproducibility. Evidently, the decision to focus on the latter was reached as repeatability seems to be a reoccurring issue in the field of carcass and cadaver decomposition.

CIR-MS is a fast analytical technique capable of detecting almost all chemical classes at sensitivities as low as parts per trillion. That said, the most compelling attribute of CIR-MS is its ability to monitor VOCs in real-time. The speed of analysis by CIR-MS is unprecedented as it is capable of producing a mass spectrum in seconds. The combination of the aforementioned reasons positioned CIR-MS as a technique that could potentially be advantageous in the study of decomposition VOCs.

Long-standing powerful GC-MS was also incorporated alongside CIR-MS for speciation and validation of the results generated by CIR-MS. Though, there is an emphasis on the selectivity. Selectivity issues persist around the technique used to collect samples for analysis by GC-MS, in this case SPME, the choice of packing material in the column, oven conditions and other GC-MS operational settings. These parameters can significantly affect the types of VOCs detected by SPME-GC-MS.

In spite of all of the above, the combination of the two techniques CIR-MS and SPME-GC-MS could be beneficial in the drive towards elucidating a signature profile of decomposition odour.



# 3

## METHOD DEVELOPMENT

This chapter describes the characterisation of the analytical instruments CIR-MS and SPME-GC-MS, together with the design and implementation of the decomposition chamber developed towards the study of decomposition VOCs. It also includes the experimental work carried out towards calibration of both CIR-MS and SPME-GC-MS instruments

### 3.1 Decomposition chamber

As mentioned in Section 2.1, the experimental design of this project included a decomposition chamber that was fabricated and developed in the University of Leicester. Details of the materials used in its development have also already been discussed in chapter 2. Although the final version of the decomposition chamber is shown in Figure 2.1, the design slowly evolved over the course of this research project.

The upcoming sections briefly discuss the design history. The objective in reviewing this process is to provide clarity to the reader on some of the design decisions made. Ultimately, the goal was to create an indoor burial environment with relatively stable internal conditions, in terms of temperature and humidity, and to exclude environmental fauna and flora - factors which have been established to alter the rate of decomposition [5, 37, 38, 45]. As a result, each carcass within the same experimental treatment would undergo decay at the same rate, thus improving the reproducibility of the VOCs released during the process of decomposition.

### 3.1.1 Design and implementation

A preliminary buried experiment was conducted to test the feasibility of the experimental design idea and although the results from this study are not included in this thesis, a cross sectional view of the chamber at the time is shown in Figure 3.1a. One of the disadvantages noted from this initial chamber design was the presence of multiple fissures on the surface of the soil (overburden), which occurred as the carcass passed through the different stages of decomposition. Consequently, there was an increased degree of uncertainty surrounding determination of these VOCs as those associated with buried or exposed decomposition. This outcome formed the foundation of the first decomposition chamber design (Figure 3.2a).

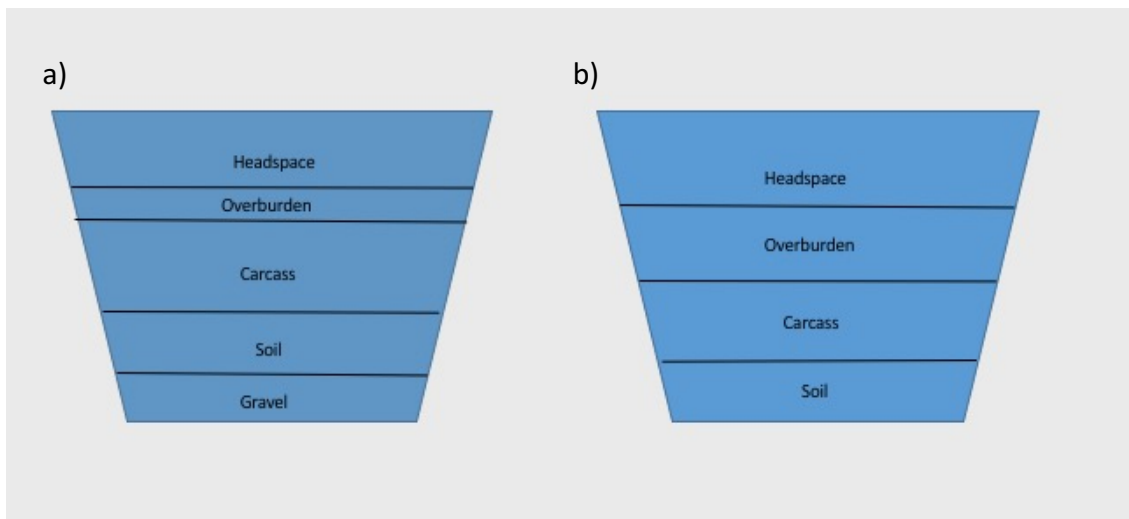


**Figure 3.1** Illustrates the sectioning of the bespoke decomposition chamber used in preliminary decomposition odour experiments which were conducted in early 2012 (a), and (b) the sectioning used to elude fissures in Buried Human Analogue trials 3 and 4.

The first buried human analogue experiment (BHA 1) conducted towards this research project occurred in late 2012. The design of the chamber included a plastic matrix similar to an enlarged egg tray, pictured in (Figure 3.2a). The purpose of this structure was to prevent the overburden (soil added on top of the structure) from developing similar fissures to that described above. This in turn ensured that the VOCs released from the carcass underneath the plastic matrix had sufficiently permeated the soil above before entering the headspace region of the chamber. Although practically this

implementation was acceptable, it was later dismissed because it was deemed as being too unrealistic from a forensic perspective.

Following this, was the first attempt at designing the experimental setup for the exposed human analogue trial (EHA 1). The purpose of this trial was to assist in the understanding of the differences between the VOCs emanating from carcasses buried in soil and VOCs released into the headspace when soil was excluded entirely. In some regards, the exposed trials can be considered as control experiments. The design for EHA trial 1 is illustrated in Figure 3.2b. The carcass was placed on a bed of aluminium to prevent the liquid products of decomposition from seeping into the internal structure of the chamber. As well as this, the sample line was extended until it was approximately 7-8 cm away from the head of the carcass. Regrettably however, the results generated from this set-up were unusable. This was because the performance of the CIR-MS instrument was compromised by unintentionally introducing liquid decomposition products into the instrument via the sample line. As a consequence, the decision to exclude an extending sample line inside the chamber was reached. In addition, subsequent EHA trials were re-designed such that the pig carcass was deposited on the surface of chemically inert sand, mainly to absorb the liquid products of decomposition.

By 2014, BHA 2 trial was piloted (Figure 3.2c) In an attempt to recreate a more realistic burial, the carcass was buried with a mound of soil (barrow). This type of burial is often associated with archaeological graves [108]. At this stage also, the positions of the ports used to allow entry of the sample line and environmental sensors were changed from being on the side of the chamber (Figure 3.2d) to the covering of the decomposition chamber (Figure 2.1). In doing so, it meant the decomposition chamber could be easily replaced without the need to reconstruct the entry points. Again, although there were no practical issues with this set-up, there were questions surrounding how forensically realistic a mound burial was in relation to clandestine graves.

The overall conclusion from these design strategies was the decision to ensure that the overburden used in the buried trials was sufficient enough to circumvent fissures (Figure 3.1b) and in the exposed trials, to introduce an inert material such as sand to absorb liquid by-products of decomposition. As well as this, sample lines extending

inside the chamber were eliminated across both buried and exposed trials, and all entry ports were constructed on the covering to allow multiple uses of the decomposition chamber.

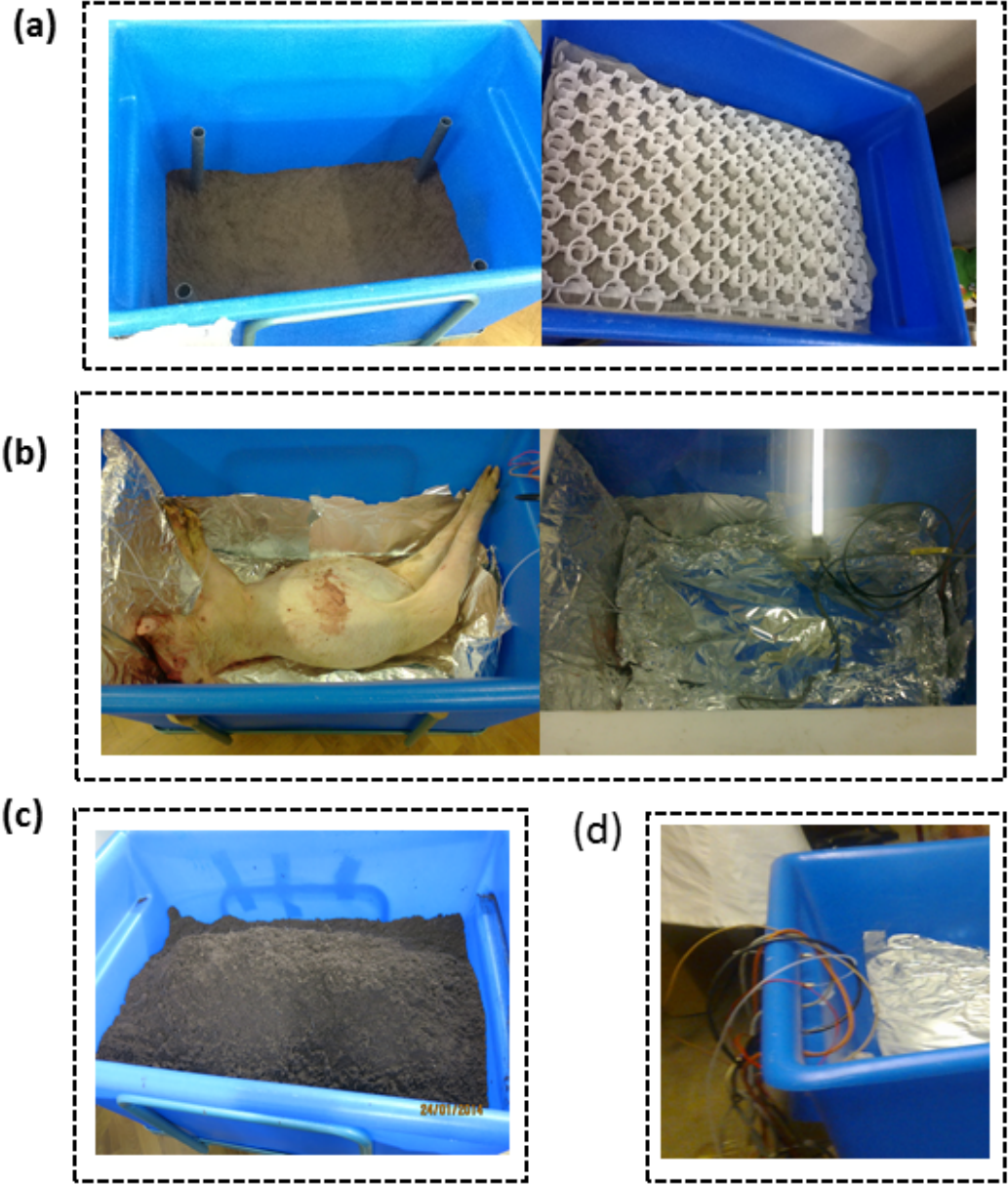


Figure 3.2 Previous strategies employed in the design of the bespoke decomposition chamber used in the first Buried Human Analogue trial in 2012 (a), the first Exposed Human Analogue trial conducted in 2012, (c) the second Buried Human Analogue trial in 2013, and (d) the external positioning of the sample lines and electrical wirings

## 3.1.2 Characterisation of the decomposition chamber

The following subsections describe the steps taken in characterising the final decomposition chamber used in the study of decomposition VOCs. Experiments were conducted to determine the types of VOCs released from the materials used to construct the chamber, as well as to define background VOCs (compounds released when soil and sand were added to the chamber). In addition, smaller scale experiments were piloted to determine how leak proof the chamber was, and to define the climatic conditions within the decomposition chamber before introduction of the decomposition objects (carcasses).

### 3.1.2.1 Leak tests

Owing to the nature of the experimental setup and the location of the instruments (particularly CIR-MS used for online sampling), it was necessary that the decomposition chamber was kept inside the RAFT laboratory. For this reason, it was important to ensure that the chamber was leak-proof. To assess this, a simple experiment using the decomposition chamber, N<sub>2</sub> and a mass flow controller (Alicat Scientific - flow capacity 10 standard litres per minute) was conducted to test the difference in entry and exit flow rates when the chamber was sealed. A range of entry flow rates (0-1 Lmin<sup>-1</sup>) were used, and the results indicated that the decomposition chamber was relatively airtight across this range (Figure 3.3a, slope= 0.813), although there was an even better fit on the lower end of the flow scale (Figure 3.3b). As a result, the decision to use a total combined flow rate of 0.3 L min<sup>-1</sup> of N<sub>2</sub> and C<sub>6</sub>H<sub>5</sub>Br to simulate wind dispersion within the chamber as it would be in the case of an outdoor burial was reached.

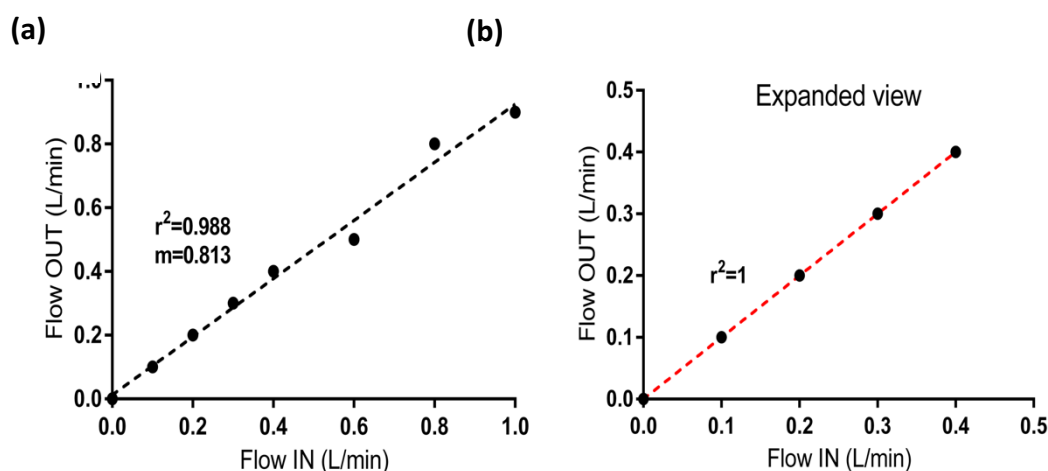


Figure 3.3 Graphical representation of the differences in the exit flow rate (y-axis) versus entry flow rate (x-axis) of the bespoke decomposition chamber when a range of flow rates were examined. Flow rates tested spanned from 0 L/min to 1 L/min range. Flows were measured by use of an Alicat Scientific mass flow controller with a maximum flow capacity of 10 L/min.

### 3.1.2.2 Background VOCs

Since CIR-MS was the principal instrumentation used to study the succession of VOCs released from carcasses as they decomposed in the bespoke chamber, it was crucial to define the VOCs released from the materials of the chamber and the burial substrates as a means of determining the background VOCs. Although CIR-MS is lacking in a definitive identification perspective, it was possible to elucidate the major mass channels associated with VOCs released from the chamber prior the introduction of the carcass.

Background samples were collected in sequence, starting with synthetic air used as the inflow gas to simulate wind dispersion. Synthetic air was fed directly into the CIR-MS instrument. Following this, synthetic air was bypassed through the decomposition chamber before sampling. The third sequence consisted of synthetic air, decomposition chamber and topsoil; and in the last sequence, topsoil was replaced with sand. Each sequence lasted a week, and the CIR-MS operational settings used were consistent with those used in the human analogue trials (Chapters 4 and 5). All ion counts recorded by CIR-MS were normalised to  $10^6$  of the counts in mass channel 19 which corresponded to the reagent ion  $H_3O^+$ .

The results illustrated in Figure 3.4 show that mass channels 18, 29, 47, 121 and 136 were amongst the most prominent when the decomposition chamber was flushed with synthetic air ( Figure 3.4 a and b). Mass channel 37 relates to hydrated hydronium ion ( $\text{H}_3\text{O}^+(\text{H}_2\text{O})$ ), and was used to estimate the humidity within the drift tube region of the CIR-MS instrument [92].

The compound corresponding to the behaviour observed in mass channel 61 appears to be unique to the decomposition chamber, suggesting it was released from one of the components of the chamber. It can also be seen that addition of topsoil and sand significantly alters the contributions from the previously measured mass channels (Figure 3.4 c and d). Furthermore, it was observed that inclusion of soil and sand decreased the signal in all mass channels by more than half with the exception of hydrated hydronium signal which increased. Similarly, the humidity of the CIR-MS instrument also doubled in the sand experiment.

The results from these background measurements imply that the activity in these mass channels correspond with VOCs released in the decomposition chamber. Although this is true, it is also plausible that VOCs bearing similar masses to those measured here are also released during carcass decomposition. As such, the results collected here merely serve as a tentative suggestion of the possible sources of these VOCs. Consequently, these mass channels were not eliminated during analysis of the decomposition dataset; instead, examination of their behaviour over time was used to determine if their activities related to the process of carcass decomposition

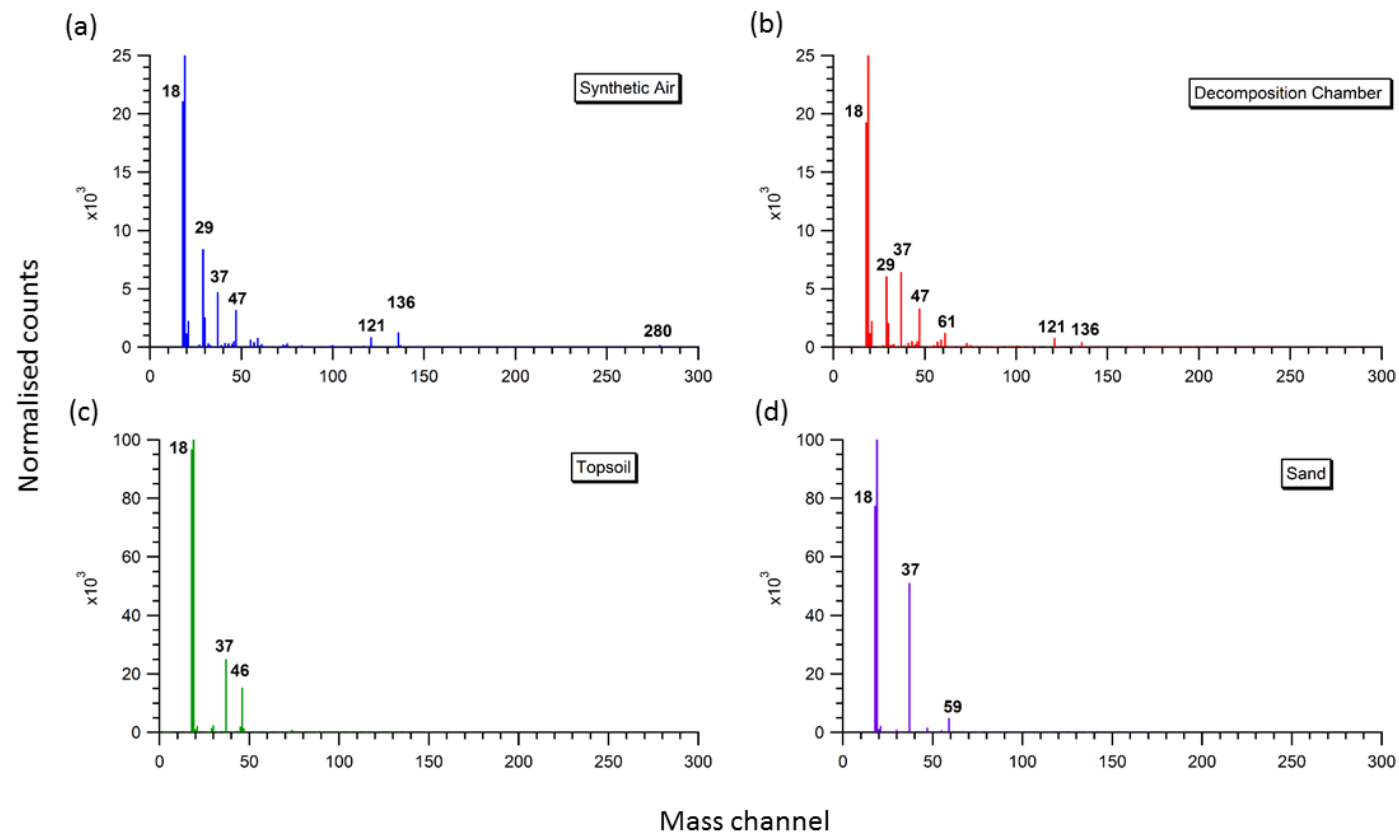


Figure 3.4 Average CIR-MS mass spectra generated over the course of seven days when: (a) synthetic grade air was directly fed into the CIR-MS instrument, (b) synthetic air was bypassed through the decomposition chamber, (c) topsoil added to the decomposition chamber and (d) sand added to the decomposition chamber. 10 minute scans were collected over the 7 days, and all counts were normalised to  $1E6$  of the counts in mass channel 19

### 3.1.2.3 Climatic conditions

Climatic conditions such as headspace temperature, relative humidity, volumetric water content and soil temperature were defined in the decomposition chamber before introduction of the carcass. Measurements were collected hourly over several weeks by the use of Campbell Scientific sensors described earlier (Section 2.1). The average readings collected over this time period is presented in (Figure 3.5).

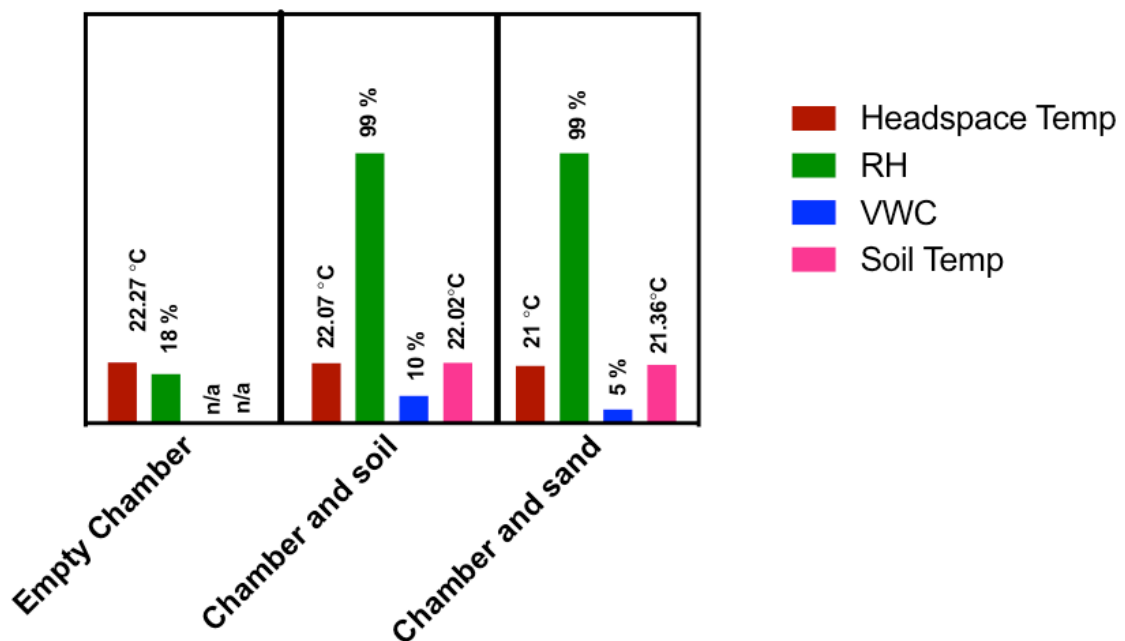


Figure 3.5 Illustrates the average climatic conditions within the decomposition chamber. Headspace and relative humidity were measured by use of CS215 sensor while soil temperature and volumetric water content (VWC) were monitored by use of CS650 probe. Measurements were logged hourly on CR10X data logger over several weeks

To validate the performance of the sensors, a CS251 probe was used to record the relative humidity in the RAFT laboratory before it was inserted into the decomposition chamber. The relative humidity recorded by the instrument was approximately 56% which is expected for an indoor environment in the UK. Unsurprisingly, the relative humidity of the environment within the decomposition chamber fell to 18% when only synthetic air was flowing through it. This value increased to 99% when soil and sand were added to the chamber. There was a five-fold increase in the relative humidity between the measurements taken when the chamber was empty and when soil was added. This increase correlates with the surge in humidity within the drift tube of the

CIR-MS instrument measured by the activity of mass channel 37 (discussed in detail in section 3.2.2). Conversely, the volumetric water content of sand was measured as half the amount in soil.

## 3.2 Characterisation of the CIR-MS instrument

### 3.2.1 Sensitivity

The result generated from CIR-MS sensitivity tests with pyrrole between 2014 and 2016 showed significant fluctuations in the instruments performance. The slopes of the linear fits (Figure 3.6) imply that the sensitivity of the CIR-MS instrument improved with each consecutive year, with the greatest change occurring between 2015 and 2016. CIR-MS operation parameters such as drift tube pressure; voltage and temperature were constant across the years, and the calculated E/N was between 93 - 98 Townsend.

Review of the ratio of primary ion ( $m/z$  19) to its first cluster ( $m/z$  37) provides an insight into the relative humidity within the drift tube. Despite the sample air being dry ( $\approx 10$  % RH) during all three investigations, a small percentage of unreacted water molecules particular at  $m/z$  37 entered the reaction chamber from the ion source region. The ratio of the ion counts at  $m/z$  19 to  $m/z$  37 was on average 179, 132 and 589 normalised counts per second in 2014, 2015 and 2016 respectively. These findings imply that there was approximately a 4-fold increase in the amount of hydrated hydronium cluster ion ( $m/z$  37) between 2015 and 2016, thus the system was more humid. CIR-MS measurements are known to have a high dependency on humidity, particularly for compounds such as pyrrole [109]. Sinha *et al* observed that the sensitivity of pyrrole on PTR-MS increases with an increase in humidity.

Between the years 2015 and 2016, the apparatus used to generate water vapour for the CIR-MS instrument was re-designed. This redevelopment might explain the source of increased water cluster ions, as the new apparatus generated more gaseous water particles.

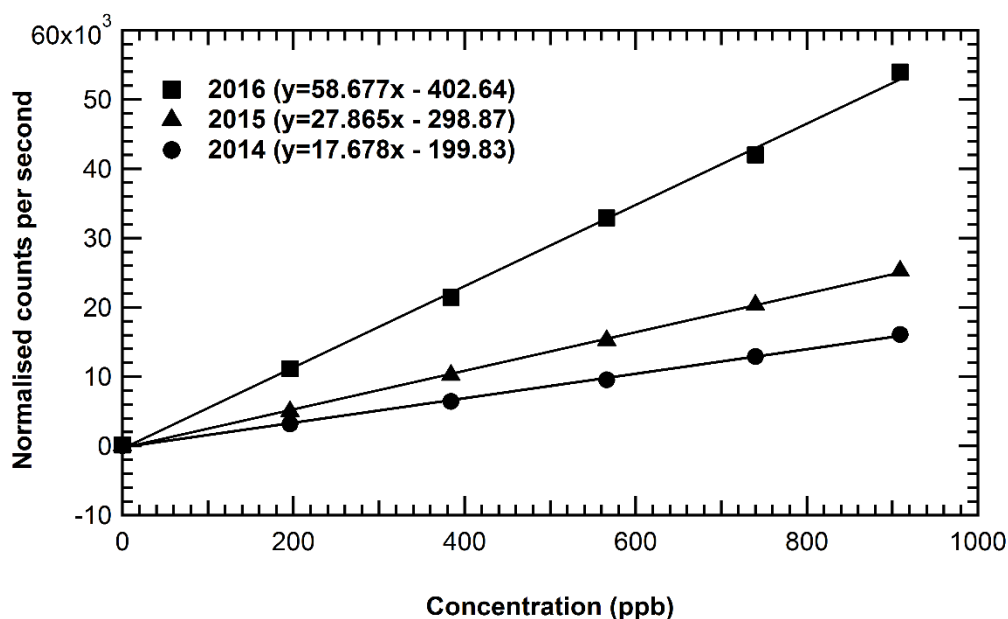


Figure 3.6 Sensitivity of pyrrole ( $m/z$  68) as measured by the CIR-MS instrument over the course of three years. Tests were conducted at approximately 10% relative humidity. Concentration variations were achieved by altering the flow rate of dilutant gas nitrogen. The flow rate of pyrrole (10 ppm pyrrole mixture in nitrogen) was held constant at 60 ml/min. 1 minute scans were collected for a total of twenty minutes, although data from the first ten minutes were regarded as the equilibration period, and were excluded from the analysis. All counts were normalised to hydronium at mass channel 19.

### 3.2.2 Humidity dependence

It has been well established that the humidity of a sample analysed by CIR-MS significantly affects the sensitivity of VOCs captured on thermodynamic grounds [92]. Humid air means the increased abundance of water molecules, which have a tendency to interact with the reagent ion hydronium to create hydrated hydronium clusters in the form  $H_3O^+(H_2O)_n$ ; where  $n = 1, 2, 3$ . The presence of water molecules in the drift tube region of the CIR-MS instrument is not uncommon as it is also possible for a small quantity of non-ionised water molecules to gain entry from the ion source. This explains why even in dry samples with reported relative humidity of approximately 0.5%, a fraction of hydrated hydronium clusters (typically at  $m/z$  37) is still observed [92].

The humidity dependence on detection sensitivity in CIR-MS measurements is a subject that is very often examined in the literature as it can have significant effects on the ion chemistry occurring in the drift tube and hence affects the analysis of the resulting mass

spectra. Since the transfer of protons in proton transfer reactions is based on the differences in proton affinities, hydrated hydronium ions sometimes behave like the reagent ion, by transferring a proton to analytes possessing higher proton affinities. In such instances where the proton affinity of the analyte is greater than hydrated hydronium cluster at  $m/z$  37, the product ion is still  $MH^+$ , and the resulting mass spectra is still relatively straight forward to analyse. However, for molecules possessing proton affinities less than the hydrated hydronium cluster ( $808 \text{ kJ mol}^{-1}$ ), the proton transfer reaction becomes forbidden on energetic grounds. It is because of this differential that humidity effects in CIR-MS are referred to as being compound specific [78].

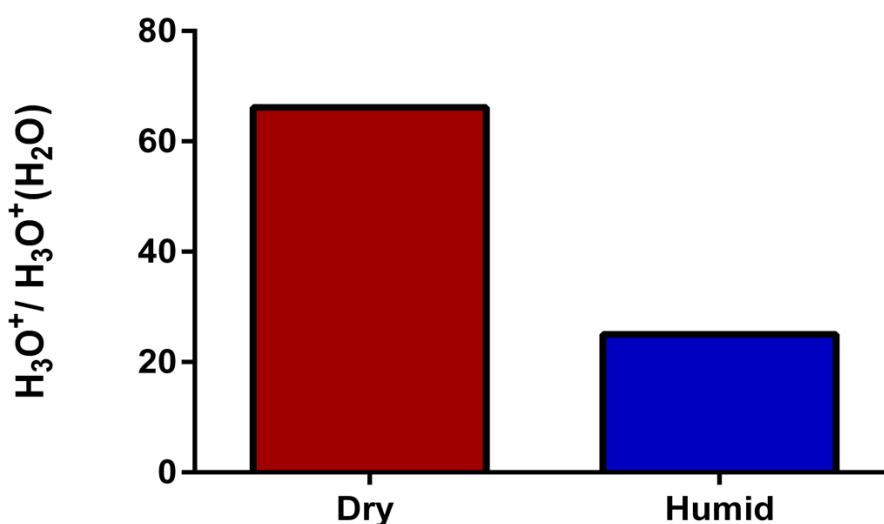


Figure 3.7 Graphical representation of the ratio of hydronium ions at  $m/z$  19 to hydrated hydronium cluster ions at  $m/z$  37 when sample humidity in a Tedlar bag was increased from 0.5% (dry) to 89% (humid) relative humidity. 10 minute scans were collected and averaged over a 60-minute period by use of the CIR-MS instrument.

When a humid sample is being analysed, there is likely to be an increase in the proportion of hydrated hydronium cluster, particularly at  $m/z$  37, and a decrease in  $H_3O^+$  as most of the reagent ion will be tied up in the hydrated form ( $H_3O^+(H_2O)$ ) (Figure 3.7). A consequence of this is that there will be less  $H_3O^+$  available to undergo proton transfer reactions particularly for those compounds possessing proton affinities less than that of the hydrated clusters, and the net result would be a reduced sensitivity of these ions. Another outcome of having a system with an increased proportion of

hydrated hydronium clusters is that it opens up more product channels as proton transfer reaction is not the only reaction that can occur. Reverse proton transfer reactions and ligand switching are some of the possible pathways available when there is an increased abundance in hydrated hydronium ions [92]. The combination of the reasons aforementioned makes an increase in the abundance of water molecules in the drift tube region of the CIR-MS instrument undesirable.

To assess the humidity dependence of the CIR-MS instrument used to study the evolution of cadaveric VOCs, the sensitivity of four analytical standards were investigated under dry (0.5 % RH) and humid (87-89% RH) conditions. Details of the standards investigated are listed in (Table 3.1). The conditions at which the CIR-MS instrument was operated during these measurements were drift tube pressure of 6 mbar, voltage of 2190 V and E/N of 93.83 (154) Td. The value in parenthesis represents the E/N in the collision induced dissociation end of the drift tube. The concentrations used in this calibration covered the range expected to be released during carcass decomposition.

**Table 3.1** Details of five analytical standards tested for on CIR-MS under varied sample humidity. Values for proton affinities were reported from the National Institute of Standards and Technology (NIST) unless otherwise stated. Analytical grade standards were purchased from Sigma Aldrich UK

Compound name	Cas. No	Molecular weight		
Dimethyl sulphide	75-18-3	62	830.9	139.9
1-propanol	71-23-8	60	786.5	95.5
2-butanone	78-93-3	72	827.3	136.3
Acetone	67-64-1	58	812	121.0
H <sub>3</sub> O <sup>+</sup>	7732-18-5	18	691	0.0
(H <sub>3</sub> O <sup>+</sup> (H <sub>2</sub> O))	N/A	36	808	117.0

The slope of the linear fit of the calibration curve (Figure 3.8). shows that there is no humidity dependence on dimethyl sulphide; 2-butanone and acetone. On the other hand, 1-propanol shows a reduced sensitivity under humid conditions. Sensitivities are extracted from the slope of the linear fits in units of ncps ppbV<sup>-1</sup>. These results align with what is expected, and have been corroborated by other CIR-MS users [78]

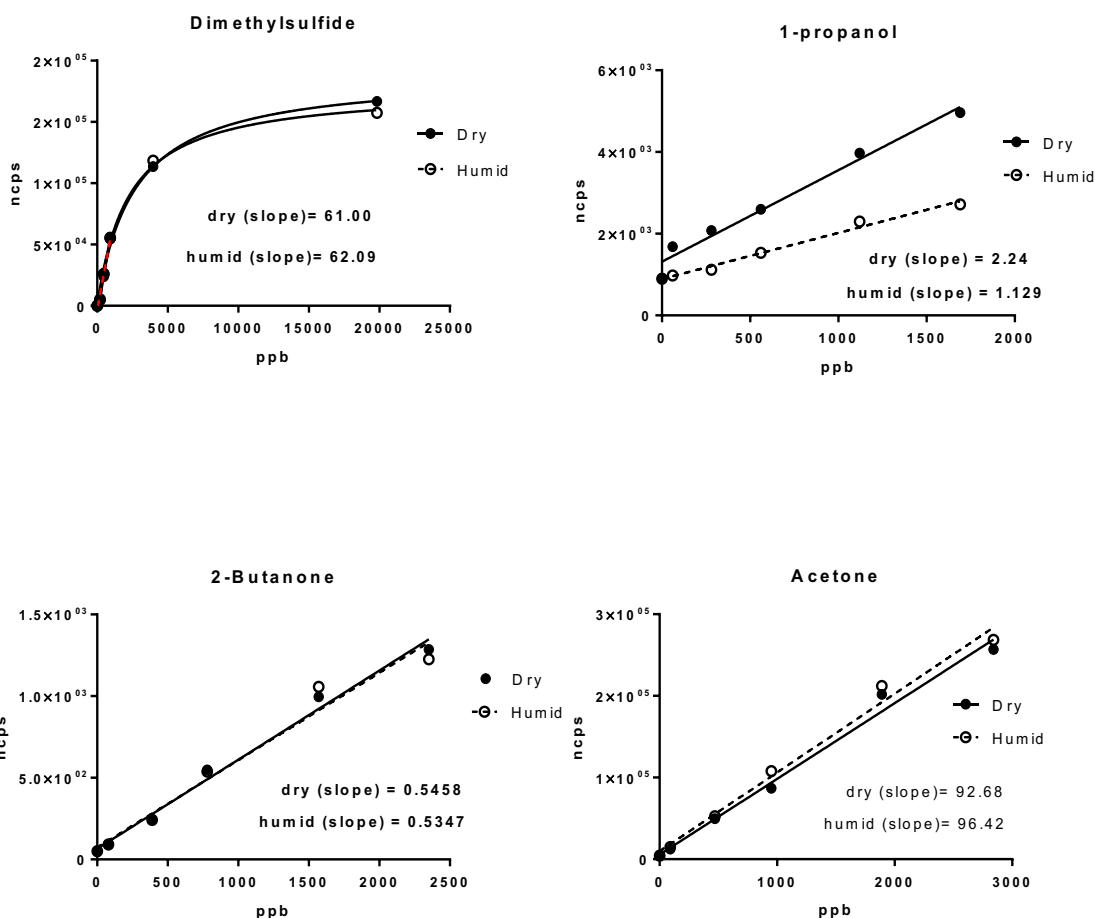


Figure 3.8 Humidity effect on measurements collected by CIR-MS. Varying concentrations of analytical grade standards 1-propanol, dimethyl sulphide, acetone and 2-butanone were tested under dry (0.5% relative humidity) and humid (89% relative humidity) conditions. 10- minute scans were collected for a total of 100 minutes at each concentration and all counts were normalised to 106 of the signal at  $m/z$  19.

### 3.2.3 Competing reagent ions

The reagent ion used in CIR-MS is not limited to  $H_3O^+$  alone. There have been documented evidence of the use of alternate reagent ions such as ethanol [110],  $O_2^+$  [111], and  $NH_4^+$  [112]. Owing to the nature of the overall experimental design of this project, high concentrations of decomposition VOCs are expected to be produced into the headspace region of the chamber, particularly in the exposed trials. In such instances, it is necessary to investigate the consequence high concentrations of analyte gas has on the ion-molecule chemistry occurring in the drift tube region of the CIR-MS.

When there is an excessive abundance of more than one reagent ion, the system is referred to as having competing or alternate reagent ions. The effect of having competing reagent ions can be beneficial as the difference in proton affinities of the primary ions can be used to distinguish between molecules with identical nominal masses [92]. That said, the most important consequence of having high concentrations of analyte gas is that the premises of proton transfer reaction with  $\text{H}_3\text{O}^+$  can no longer be fulfilled especially when VMR ratios surpass a threshold of 10 ppmV (typically) [110]. The two crucial parameters for PTR reaction via  $\text{H}_3\text{O}^+$  are as follows: 1] the ionisation process is dominated by reactions from hydronium to organic molecules to form  $\text{MH}^+$ ; and 2] the primary ion signal is not depleted by reactions with organic molecules [110].

In addition to the two previous points, proton transfer is not the only possible reaction pathway possible with alternating or competing reagent ions. Other reaction pathways such as charge transfer, hydride abstraction and association reactions are also possible [92]. When association reactions occur (preferred route when organic compounds with proton affinities less than  $853.6 \text{ KJ mol}^{-1}$  react with alternate proton donor such as  $\text{NH}_4^+$ ), the outcome is the formation of  $\text{M.NH}_4^+$  adducts. Proton transfer reactions from  $\text{NH}_4^+$  are only feasible for compounds with proton affinities higher than that of ammonia. This added reaction pathway makes the resulting mass spectra even more challenging to interpret, as it causes reduced sensitivities of compounds with proton affinities less than ammonium, the formation of  $\text{MH}^+$  ions for compounds that can accept a proton from ammonium and the formation of products other than  $\text{MH}^+$  in other compounds. For these reasons, having an environment with competing reagent ions in this type of non-target analysis is highly undesirable.

In an attempt to provide evidence for the response of the CIR-MS instrument used in the research project to an environment where there is more than one primary reagent ion, small scale experiments were conducted to investigate the effect of having competing ion ammonium alongside hydronium in the drift tube region of the CIR-MS instrument. To create such an environment, concentrations of hydronium, and four analytical grade standards were kept constant while the concentration of ammonia gas fed into the drift tube region of the instrument increased sequentially until a maximum

concentration of 9000 ppbV was reached. Each chosen standard represented a different chemical class and had a distinctive molecular mass. Hexane, carbon disulphide, trimethylamine and 1-butanol were chosen to represent alkanes, organosulphurs, amines, and alcohols respectively. These compounds were chosen because they represented a good range of proton affinities. Hexane for example has a proton affinity of  $672 \text{ KJ mol}^{-1}$  [113], carbon disulphide  $681 \text{ KJ mol}^{-1}$ , trimethylamine (TMA)  $948 \text{ KJ mol}^{-1}$ , and 1-butanol  $789 \text{ KJ mol}^{-1}$ . As well as this, the protonated parent ion of these standards are distinctive so as to elude overlapping peaks, although there is still the possibility of fragmentation, thus overlays of fragment ions cannot be completely avoided.

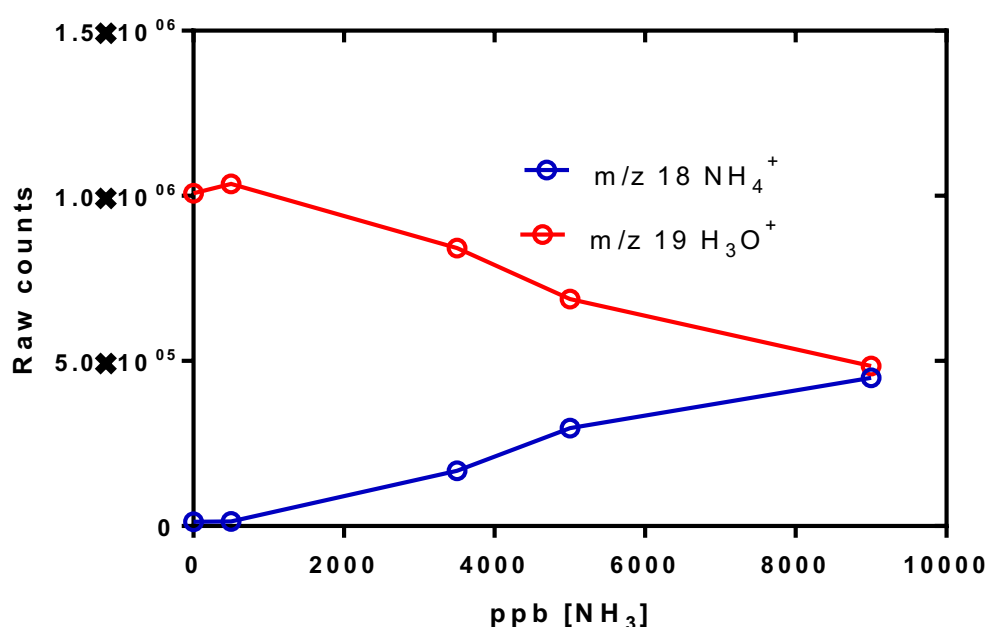


Figure 3.9 illustrates the raw signal intensities for competing reagent ions hydronium ( $\text{H}_3\text{O}^+$ ) at  $m/z 19$  and ammonium ion ( $\text{NH}_4^+$ ) at  $m/z 18$  as a function of concentration of sample gas ammonia. The experiments were conducted in 10 L Tedlar sample bags and 10 minute scans were collected over a 60-minute period. All measurements were observed by use of the CIR-MS instrument.

Figure 3.9 illustrates the behaviour of primary ions hydronium ( $m/z 19$ ) and ammonium ( $m/z 18$ ) as the concentration of ammonia was increased. It was observed that as the concentration of  $\text{NH}_3$  increased,  $\text{H}_3\text{O}^+$  became depleted by reactions with the large quantity of  $\text{NH}_3$  present. As mentioned earlier (section 2.3.3), during proton transfer reactions alcohols have an increased tendency to lose a molecule of water. As a direct

result, 1-butanol was observed at  $m/z$  57. Hexane, 1-butanol, and carbon disulphide declined as the concentration of ammonia increased (Figure 3.10a). This is because as more ammonia was fed into the drift tube, an increasing amount of hydronium was used up through protonation of  $\text{NH}_3$ . This meant less hydronium was available as a reagent ion to protonate these analytes, a point which is especially relevant for hexane, 1-butanol and carbon disulphide as their proton affinities are significantly lower than that of ammonia, and as such can only accept a proton from hydronium. TMA on the other hand, is able to receive a proton from both hydronium and ammonium, thus it was not affected by the changing concentrations of ammonia

Regrettably, owing to the setup of this investigation, the maximum achievable ammonia concentration was 9000 ppb. At this concentration it was possible to achieve a 1:1 ratio of two reagent ions hydronium and ammonium. The results of this experiment provide an evidence of the effect of having competing reagent ions operating within the drift tube of the CIR-MS instrument.

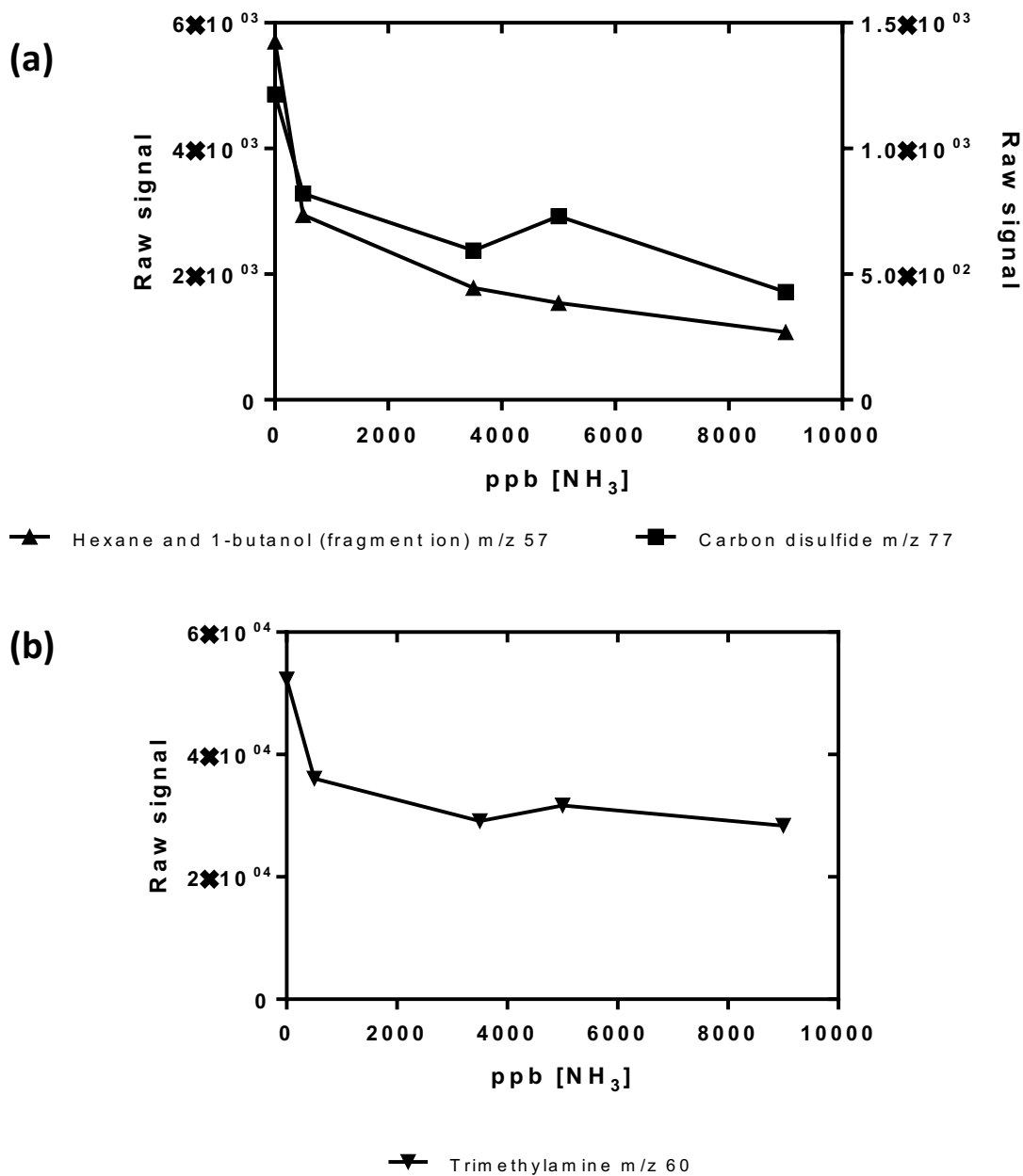


Figure 3.10 Graphical representation of the behaviour of four analytical grade standards purchased from Sigma Aldrich UK: hexane, 1-butanol, carbon disulphide (a) and (b) trimethylamine as a function of ammonia gas concentration as measured on the CIR-MS instrument

### 3.2.4 Calibration of the CIR-MS instrument

Twenty chemical standards were purchased from Sigma Aldrich, UK. These standards were selected to represent the types of compounds expected to be released during the

process of carcass decomposition. They consisted of a range of chemical classes including alkanes, aldehydes, ketones, esters, alcohols, aromatics, amines and organosulphur. The choice of concentrations used was also a reflection of the range expected to be produced across both buried and exposed decomposition trials. Calibration mixtures were made in 25 L Tedlar bags, details of which are provided in Table 3.2.

To achieve the desired concentrations, each standard was diluted in humidified synthetic air (89% RH) similar to the recorded relative humidity in the decomposition chamber. The gaseous standards were fed into the CIR-MS instrument and ten minute scans were collected for a total of sixty minutes at each concentration. A six concentration point calibration curve was produced, and the first point corresponded to the signal generated from sampling Tedlar bag when no standard added.

Of the twenty standards calibrated for, twelve standards showed good linearity ( $r^2 > 0.9$ ), although for some standards the instrument response was only linear within a defined concentration range. The calibration factor extracted from the slope of the linear fit denotes the sensitivity of the CIR-MS instrument towards each compound. Unless otherwise stated, plots shown in Figure 3.11 correspond to signals observed for the parent ion of each standard ( $MH$ )<sup>+</sup>. Carbon disulphide, trimethylamine, 2-butanone, dimethyl sulphide (DMS), 1-propanol, acetone, acetic acid, 1-butanol and butanal, 3-methyl produced a good linear response across the full concentration range tested. In contrast, the instruments response was non-linear above approximately 900 ppbV for dimethyl disulphide (DMDS) and above 1000 ppbV for methanethiol and dimethyl trisulphide (DMTS) respectively.

**Table 3.2** Details of the twenty standards calibrated for on the CIR-MS instrument. Standards were purchased from Sigma Aldrich, UK

Bag No.	Compound	Cas No.	Proton affinity (kJ/mol)	Fragment ions
1	Benzene	71-43-2	750.2	77
1	Dimethyl sulphide	75-18-3	830.9	47
1	1-Propanol	71-23-8	786.2	31
1	2-Butanone	78-93-3	827.3	43
1	Acetone	67-64-1	812	43
2	Hexane	110-54-3	N/A	57, 43
2	Carbon disulphide	75-15-0	681.9	43, 42
2	Trimethylamine	75-50-3	948.9	58
2	Pentane	109-66-0	N/A	43
2	1-Butanol	71-36-3	789.2	56, 31
3	Butanal, 3-methyl	590-86-3	N/A	44, 43
3	Ethyl Acetate	141-78-6	835	43
3	Decane	124-18-5	N/A	57, 43
4	3-Pentanone	96-22-0	836.3	57, 29
4	Alpha Pinene	80-56-8	N/A	93
4	Dodecane	112-40-3	N/A	57, 43
5	Dimethyl trisulphide	3658-80-8	N/A	79,45
5	Dimethyl disulphide	624-92-0	815.3	79,45
6	Methanethiol	74-93-1	773.4	47
6	Acetic acid	64-19-7	783.7	43,45

Unsurprisingly, the CIR-MS response to alkanes generally was poor, specifically pentane. This is because there is no proton transfer reaction with acyclic alkanes with five carbons or less [92]. Although reactions with larger alkanes are thermodynamically feasible, dodecane (C<sub>12</sub>) has a molecular weight of 171 and was most likely lost on the walls of the Tedlar bag. 3-methyl butanal does not form MH<sup>+</sup> ion upon reacting with hydronium, instead it has an increasing tendency to lose water. As such the fragment ion at m/z 69 is reported here. Likewise, 1-butanol also undergoes dehydration and its parent ion is rarely observed in proton transfer reactions. The poor response reported for benzene can be attributed to its dependence on humidity. Findings from Warneke et al [78] support the view that sensitivity of CIR-MS instrument is significantly reduced for benzene when there is an increased humidity in the sample air. The deviation observed in the 4<sup>th</sup> calibration point of alpha pinene and 3-pentanone suggest there was an error associated with the sample preparation step, although the reasons for poor sensitivity observed for ethyl acetate is still unknown.

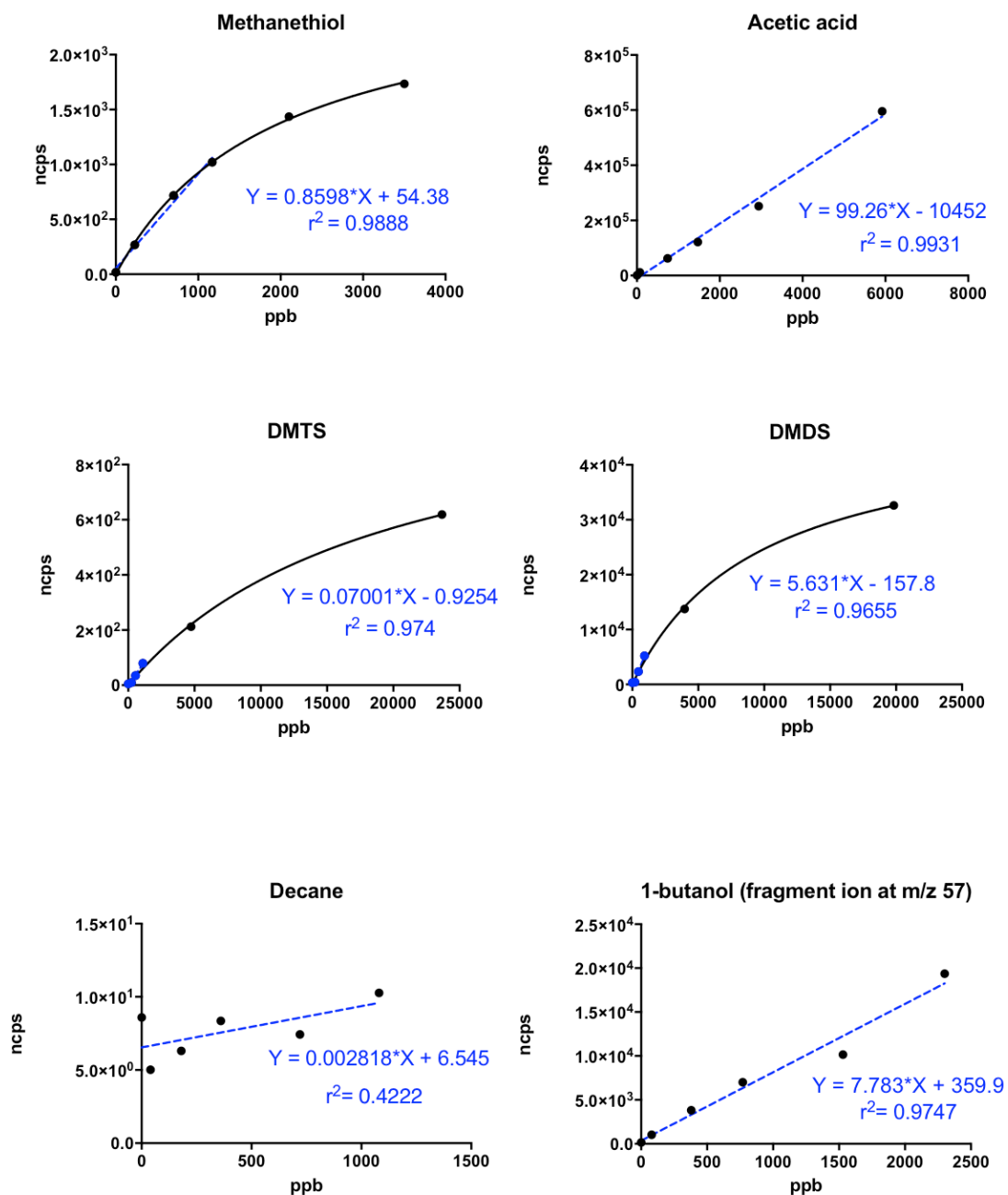


Figure 3.11 Sensitivity of the CIR-MS instrument to twenty analytical grade standards: carbon disulphide, trimethylamine, 2-butanone, dimethyl sulphide, 1-propanol, acetone, methanethiol, acetic acid, dimethyl trisulphide (DMTS), dimethyl disulphide (DMDS), decane, hexane, 3-pentanone, alpha pinene, dodecane, butanal 3-methyl, ethyl acetate, pentane, 1-butanol and benzene. Sensitivity was extrapolated from the slope of the respective linear fit, and is reported in normalised counts per second per concentration in ppbV.

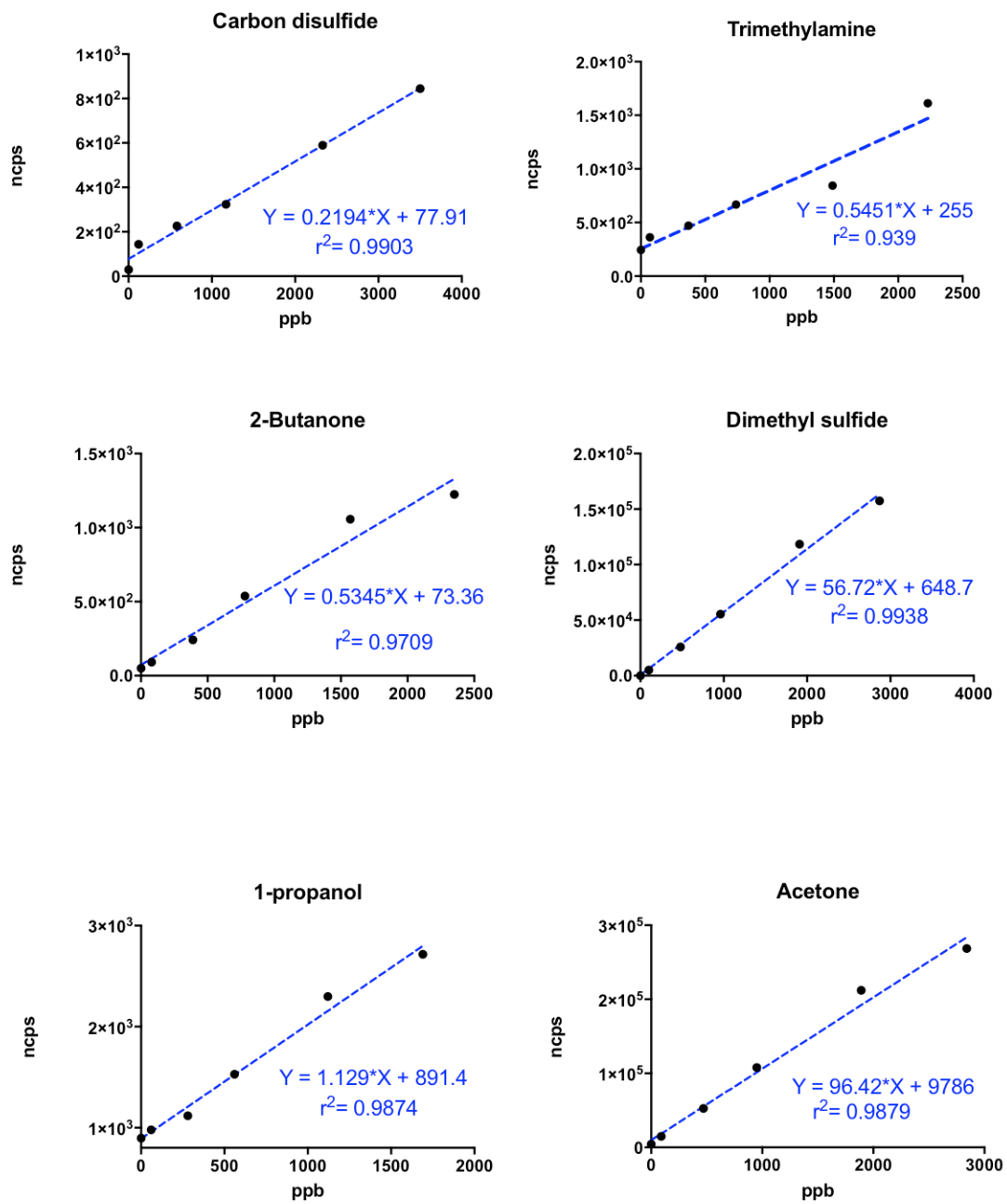


Figure 3.11 continued

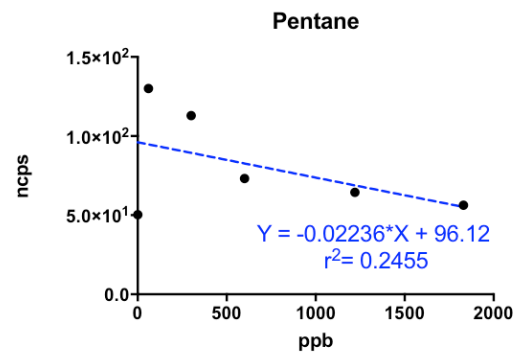
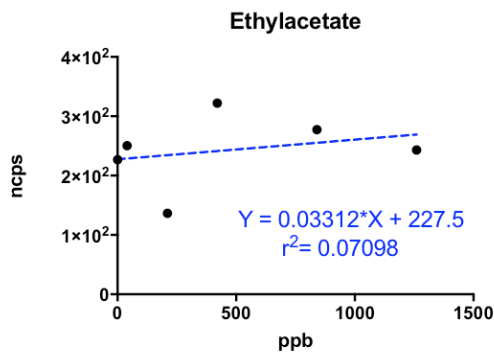
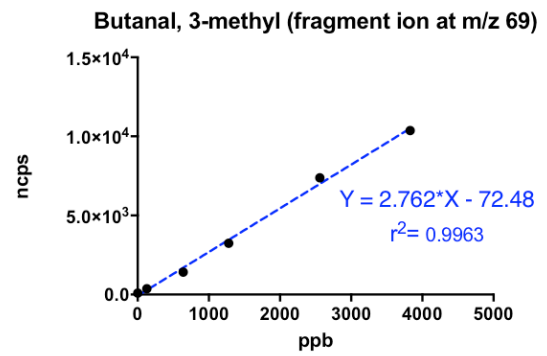
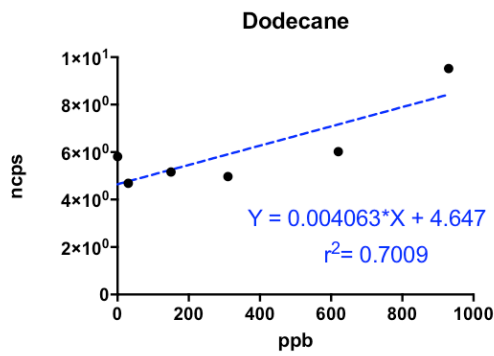
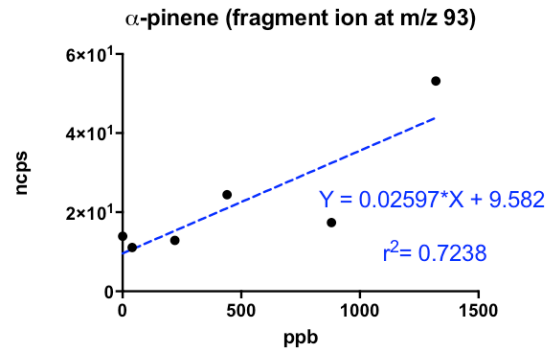
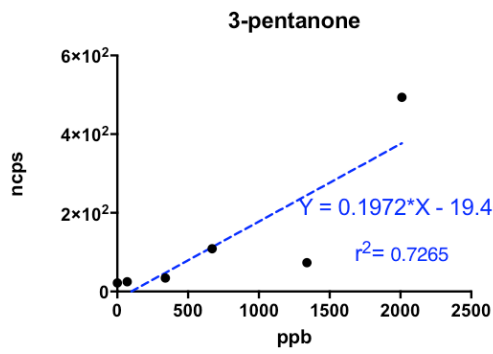


Figure 3.11 continued

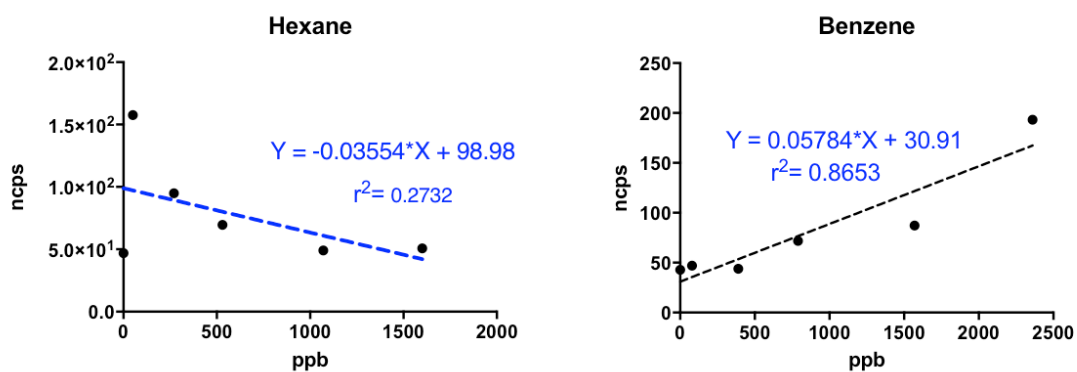


Figure 3.11 continued

### 3.3 Characterisation of the SPME-GC-MS instrument

In order to develop a suitable SPME-GC-MS method to be used for the study of carcass decomposition VOCs, several parameters must be considered. To begin with, in the sample collection step, a decision on the choice of fibre coating, extraction and desorption conditions and a selection of a suitable calibration method to mention a few must be reached (Figure 3.12). Within the GC-MS, decisions on the most appropriate column coating, mobile phase flow rates, oven conditions and MS scan ranges must also be considered.

Although not all of the aforementioned parameters were thoroughly investigated in this study, mostly due to time restrictions and sample availability, considerations on the most suitable SPME coating, extraction or exposure time, internal standard concentrations, sample humidity effects, high concentration of competing analyte gas and calibration methods were given. The upcoming sub-sections describe the steps taken in developing these parameters.

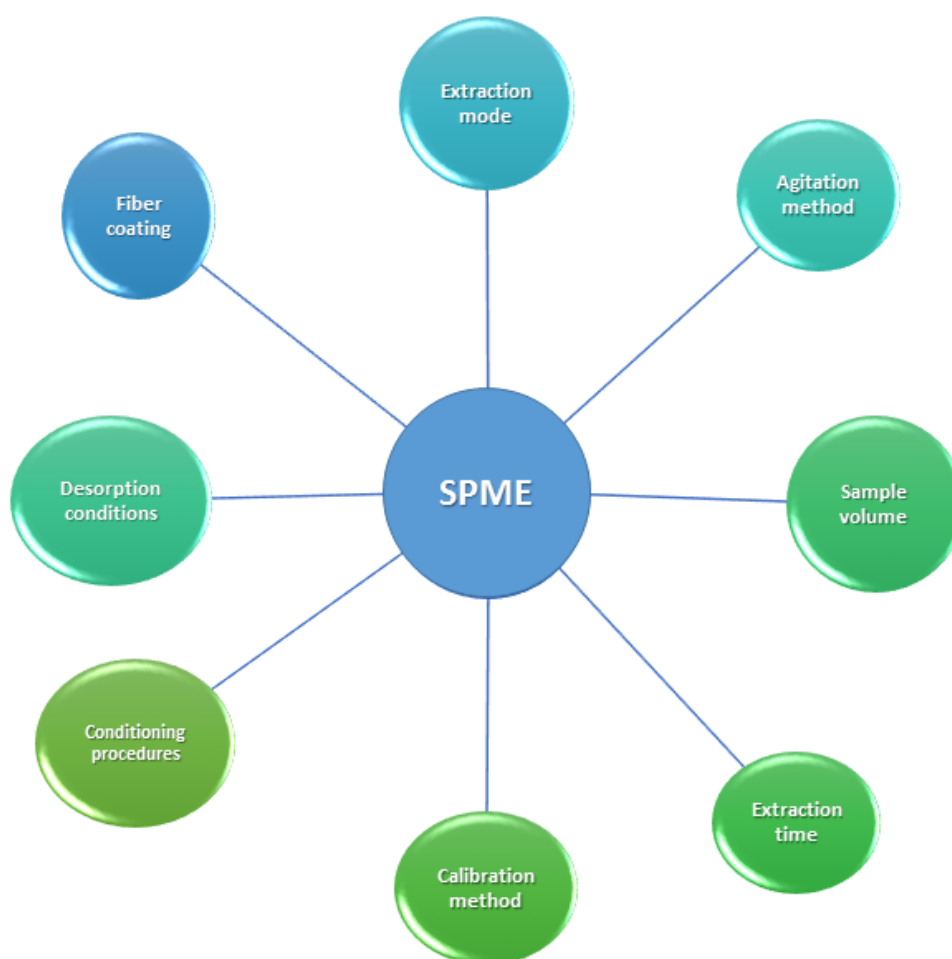


Figure 3.12 Typical parameters considered in SPME method development

### 3.3.1 Choice of SPME fibre

Five SPME fibre coatings were sampled on the same day (day 6) during Buried Human Analogue trial 4 (BHA 4). Each fibre was exposed at the same height and for the same length of time (20 minutes) in the headspace above the decomposing carcass. Oven conditions, injection volumes and all other GC parameters were kept constant throughout the sampling period. The fibres varied in coating, thickness, core and assembly type. Full details of the specifics of each fibre has been presented elsewhere (Table 2.2).

The results as demonstrated in Figure 3.13 show that the combination of fibre coatings specifically polydimethylsiloxane and carboxen was most effective as it captured 21% more decomposition VOCs on average compared to the other types tested.

Unsurprisingly, the types of compounds captured by each fibre varied, predominantly because of the differences in polarity and extraction mechanisms; for example, absorbent fibres with PA and PDMS coatings require the migration of analyte in and out of the liquid polymer coating which is slow [87]. This invariably means a longer exposure time would be needed. In contrast, adsorbent type fibres like PDMS/CAR, PDMS/DVB and PDMS/CAR/DVB, extraction is accomplished by trapping the analytes in internal pores ( Figure 3.14). Here, analytes migrate into the pores of the adsorbent and retention of the analyte depends upon the size of the analyte and the pore diameter.

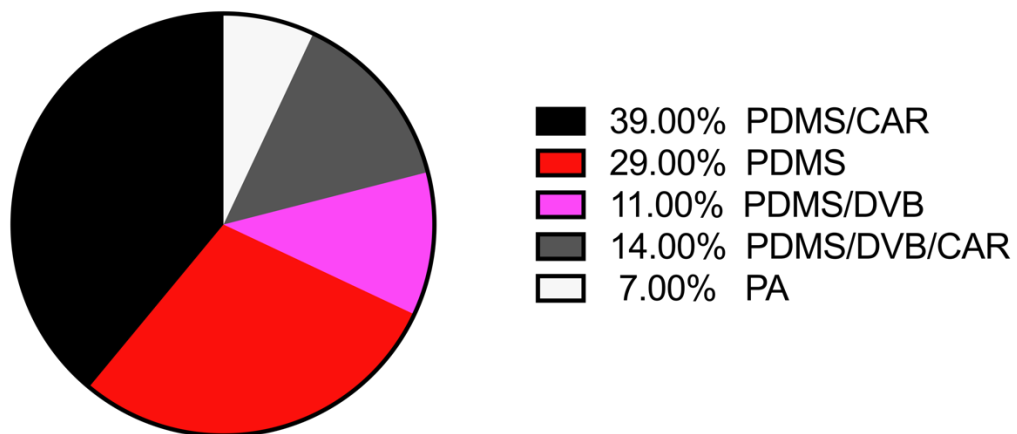


Figure 3.13 Total number of VOCs captured on five SPME fibre polymer coatings (expressed in per cent)., Each fibre was exposed in the headspace of the decomposition chamber for 20 minutes, and sampling occurred on the same day (day 6 of BHA trial 4). Compounds present in the background (day 0) i.e. prior carcass introduction were excluded from the final count

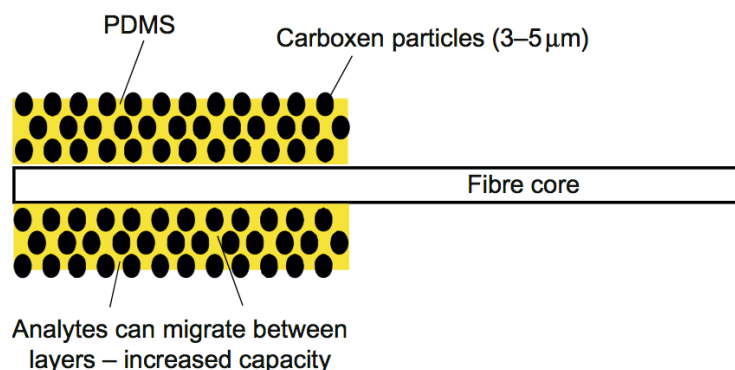


Figure 3.14 Schematic of the Carboxen –PDMS SPME fibre. Adapted from Robert *et al* [87]

The only compound detected on more than one fibre was dimethyl disulphide, which was consistently captured on PDMS/CAR, PDMS/DVB and PDMS/CAR/DVB fibres. That said, the highest sensitivity for dimethyl disulphide on day 6 was observed on the PDMA/CAR fibre coating. Dimethyl disulphide has been continually reported as one of the core VOCs released from decomposing carcasses regardless of methodology or location [4, 29, 30, 58, 61, 75]. The adsorbent mechanism and bipolarity resulting from mixing fibre coatings helps extend the range and types of VOCs that can be detected. This later point is particularly useful in the analysis of complex matrices such as decomposition.

However, in spite of the advances in SPME as an analytical technique, it becomes clear that there are limitations on the selection of commercially available fibre coatings. The net result of this is that there will always be a degree of bias in the extraction of analytes particularly in non-target analysis such as carcass decomposition.

Despite the fact that only the results generated from day 6 out of  $\approx$  30 days of carcass decomposition is discussed here, it is important to remember that the process of decomposition is constantly changing. As a consequence, it is plausible that the ratio of VOCs extracted per fibre will also vary to reflect the dynamicity of decay. Therefore, the decision to adopt a fibre type over another was not made entirely on the total number of VOCs captured on one decomposition day. The strong signal observed for frequently reported decomposition product such as dimethyl disulphide on the PDMS/CAR fibre coating, made it a good candidate for this work.

Finally, since the amount of time each fibre is exposed into the headspace of the carcass chamber has significant effects on the number of VOCs captured by the fibre, the next section discusses the results generated when different SPME fibre exposure times were explored.

### 3.3.2 Effect of exposure time on VOCs captured by SPME

As mentioned earlier, one of the most important factors governing quantification by SPME is the amount of analyte extracted by the fibre, especially as it is proportional to the concentration of the compounds in the sample. SPME can be used quantitatively before equilibrium between the headspace phase and the polymer film on the fibre is reached, or after equilibrium. Often, however, SPME users adopt the pre-equilibrium approach as it allows for shorter sampling times. In this approach, sampling time (exposure or extraction time) is critical as small changes in time significantly affect the amount of analytes adsorbed onto the fibre.

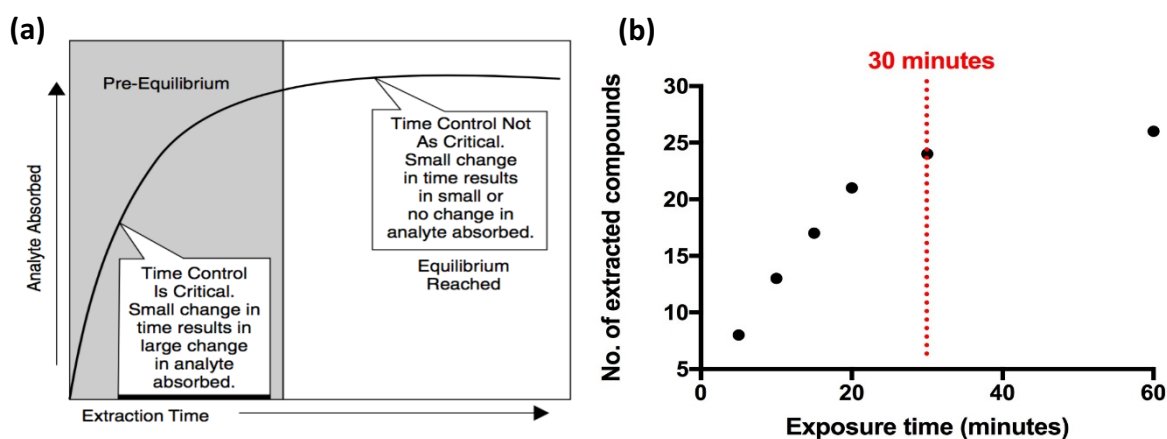


Figure 3.15 Time effect for SPME extraction (a) reproduced from Vas *et al* [82] and (b) results generated from this work (EHA trial 3) by use of CAR/PDMS fibre

Figure 3.15a shows the typical relationship between extraction time and amount of analyte absorbed/adsorbed onto the fibre [82]. The amount of analytes extracted when six different exposure times (5, 10, 15, 20, 30 and 60 minutes) were tested revealed that there were little changes in the analytes adsorbed onto the CAR/PDMS fibre when exposure time exceeded 30 minutes. In other words, the results imply that the diffusion equilibrium between analytes in the headspace phase of the decomposition chamber and the fibre polymer was achieved at approximately 30 minutes (Figure 3.15b). In addition to the amount of analytes extracted at different exposure times, the amounts of specific VOCs extracted were also examined.

Figure 3.17 shows the effect exposure times had on the extraction of methanethiol, trimethylamine, dimethyl sulphide, dimethyl disulphide, dimethyl trisulphide and bromobenzene (internal standard). These compounds were extracted on the same decomposition day during EHA trial 3. The y-axis represents integrated areas of the peaks corresponding to each of the compounds listed above. The objective of this investigation was to determine the optimum time for extraction of headspace decomposition VOCs as well as the internal standard, whilst keeping the overall sampling time relatively short.

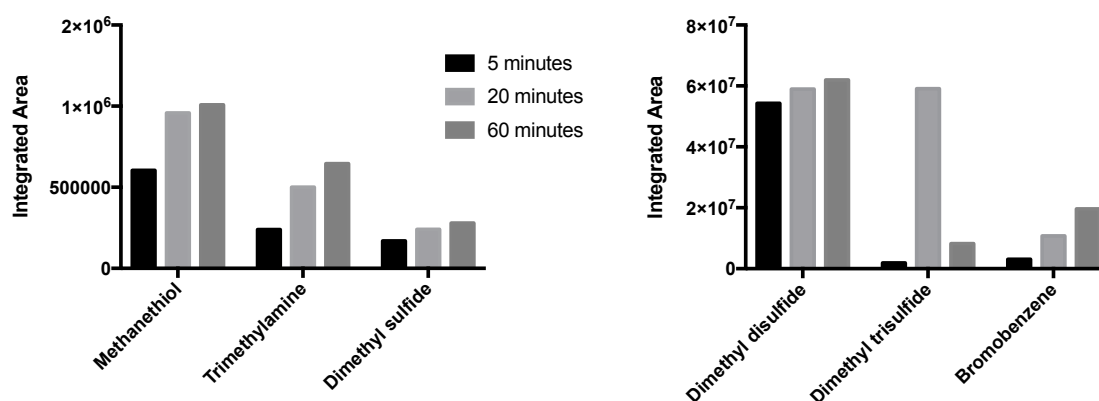


Figure 3.16 Bar chart illustrating the effect of exposure time of SPME fibre CAR/PDMS on the extraction of decomposition VOCs methanethiol, trimethylamine, dimethyl sulphide, dimethyl disulphide, dimethyl trisulphide and bromobenzene as measured on the SPME-GC-MS instrument during Exposed Human Analogue trial 3

The findings depicted in Figure 3.16 suggests that an exposure time of 20 minutes was the most appropriate for this work. At this time, good peaks which correlated to concentrations of five relevant decomposition VOCs were achieved. For methanethiol, dimethyl sulphide and dimethyl disulphide, there was a small difference in their extracted amounts beyond 20 minutes. In contrast, the amounts of trimethylamine and bromobenzene adsorbed onto the fibre increased proportionately with time. This implies that the equilibrium point varies for different compounds and it is feasible that even at 60 minutes, equilibrium was not reached for trimethylamine and bromobenzene. One of the other considerations of using high extraction times is that desorption of high concentrations of compounds onto the analytical instrument, in this case GC-MS could lead to detection saturation.

In conclusion, at 20 minutes was deemed as a suitable exposure time to be use in this study. This is because it allowed for quicker sampling and more importantly, the amount of analyte adsorbed unto the fibre from the headspace of the decomposition chamber at this time was a good representation of the VOCs associated with carcass decomposition.

### **3.3.3 Choosing an internal standard concentration**

Addition of an internal standard of known concentration to an unknown sample matrix is a long-standing but highly effective technique employed by analytical chemists to account for fluctuations in detector response, and sampling variability. Since the internal standard is exposed to the same instrumental conditions as the unknown analyte, it is expected that the effect of natural occurring variations (random error) in the detectors response will be constant for both standard and analyte i.e. the relative response of the detector to internal standard and analyte is constant over a wide range of concentrations. In chromatography, the concentration of the analyte can be calculated from the relative signals of the areas from analyte and internal standard. Furthermore, addition of internal standards improves precision and accuracy [99].

The choice of internal standard is crucial, and as such only a compound that is chemically similar to the target compounds is chosen. Similarly, the internal standard must not be naturally present in the sample being analysed. An isotopically labelled (deuterium) analogue of the target compounds makes for the most ideal internal standard, however they are not available for every compound and co-elute with the non-labelled target compound in chromatography [114]. However, using a mass analyser (detector) with high resolution circumvents the latter point. For this work, bromobenzene was not expected to be produced as a result of carcass decomposition, and has been used as an internal standard repeatedly by other decomposition authors [61, 65, 66].

Determination of the most appropriate concentration of internal standard to add to the sample relied to some extent on trial and error. Firstly, the internal standard was

sampled under the same conditions as the trials to ensure it did not co-elute with any of the analyte peaks. This was especially challenging, as the matrix obtained from cadaveric decomposition is complex with almost all chemical classes represented at different retention times. Although bromobenzene has been used as the internal standard in other decomposition work, the retention time of the compound is specific to the column, oven condition and other gas chromatographic parameters. In this work, bromobenzene eluted from the DB-5MS column at  $\approx 12.5$  minutes.

0.6 ppm, 1 ppm, and 5 ppm of bromobenzene concentrations were initially tested on SPME fibres with PDMS, PMDS/CAR, PDMS/DVB, PDMS/CAR/DVB, and PA polymer coatings to determine which concentration and which polymer coating produced reasonable Gaussian peaks. The results illustrated in Figure 3.18 show that SPME fibres with PA and PDMS coatings produced poor signals relative to other elutants, whereas fibres with mixed polymer coatings produced good signals with respect to internal standard bromobenzene.

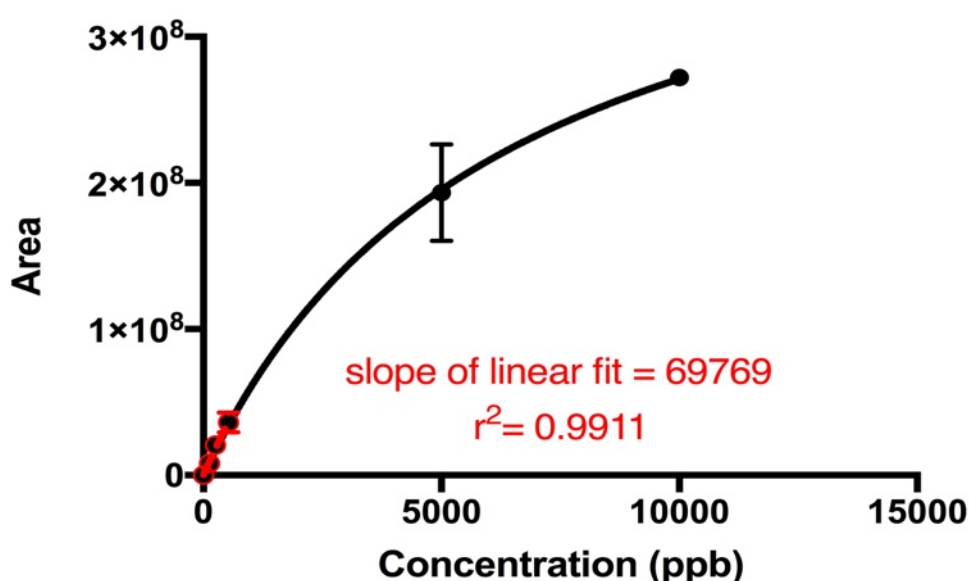


Figure 3.17 Illustrates the response of the SPME-GC-MS instrument (CAR/PDMS fibre) when varying concentrations of internal standard bromobenzene was used. Experiments were created by use of 10 L Tedlar sample bags, and at each concentration, triplicate measurements were collected.

Following this, tests were conducted to investigate the linearity of bromobenzene on CAR/PDMS fibre. Concentrations between 0-10 ppmV were examined and the results depicted in Figure 3.17 illustrates the response of the SPME-GC-MS instrument (CAR/PDMS fibre) when varying concentrations of internal standard bromobenzene shows that bromobenzene concentration exceeding 1000 ppbV fell outside the linear range of the CAR/PDMS fibre. Overall, it was decided that 1000 ppbV of bromobenzene was an appropriate concentration to use as an internal standard because it produced a distinctive peak at 12.5 minutes, did not co-elute with other decomposition VOCs, was within the linear range of CAR/PDMS fibre, and produced a reasonable sized peak in relation to other elutants.

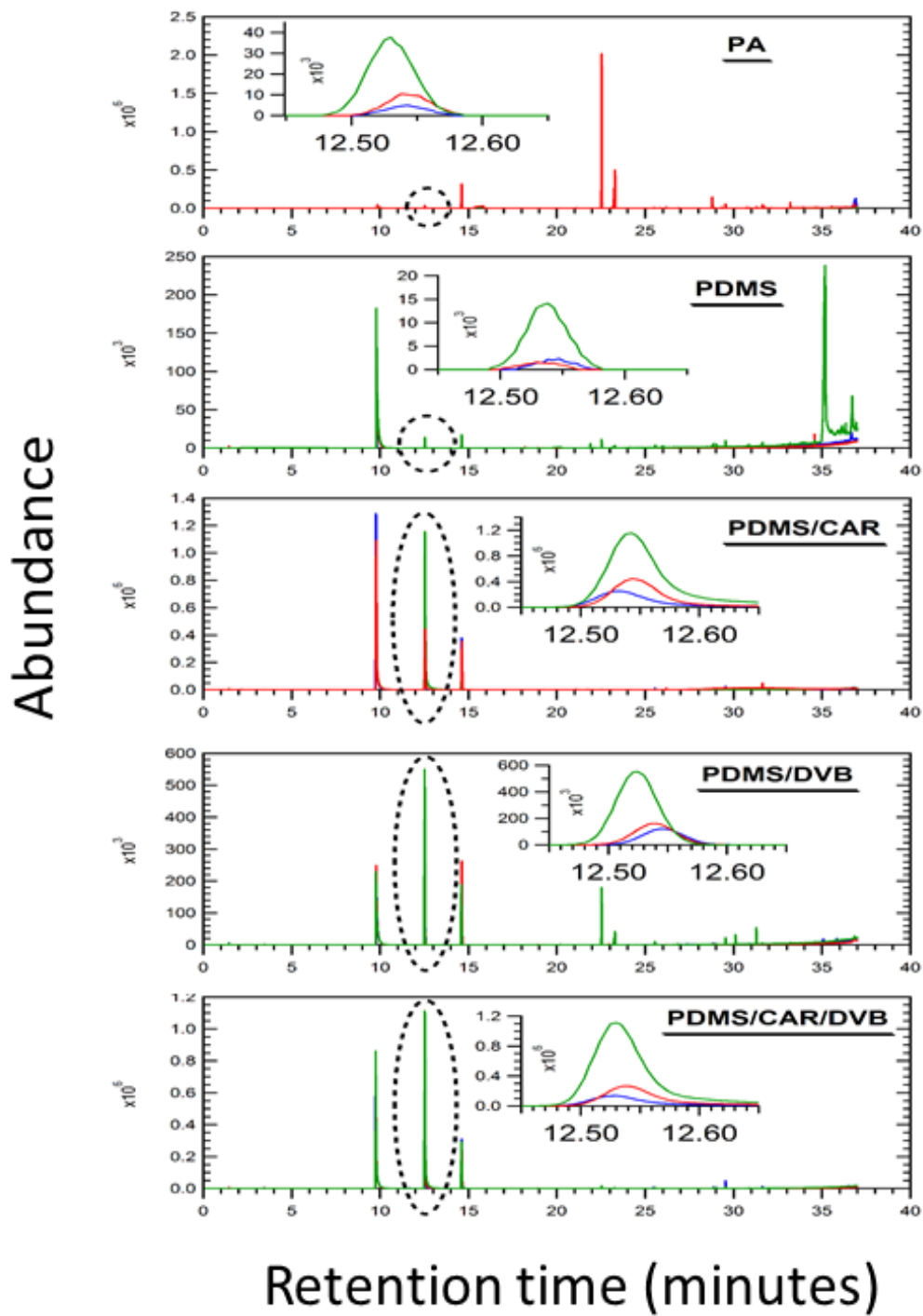
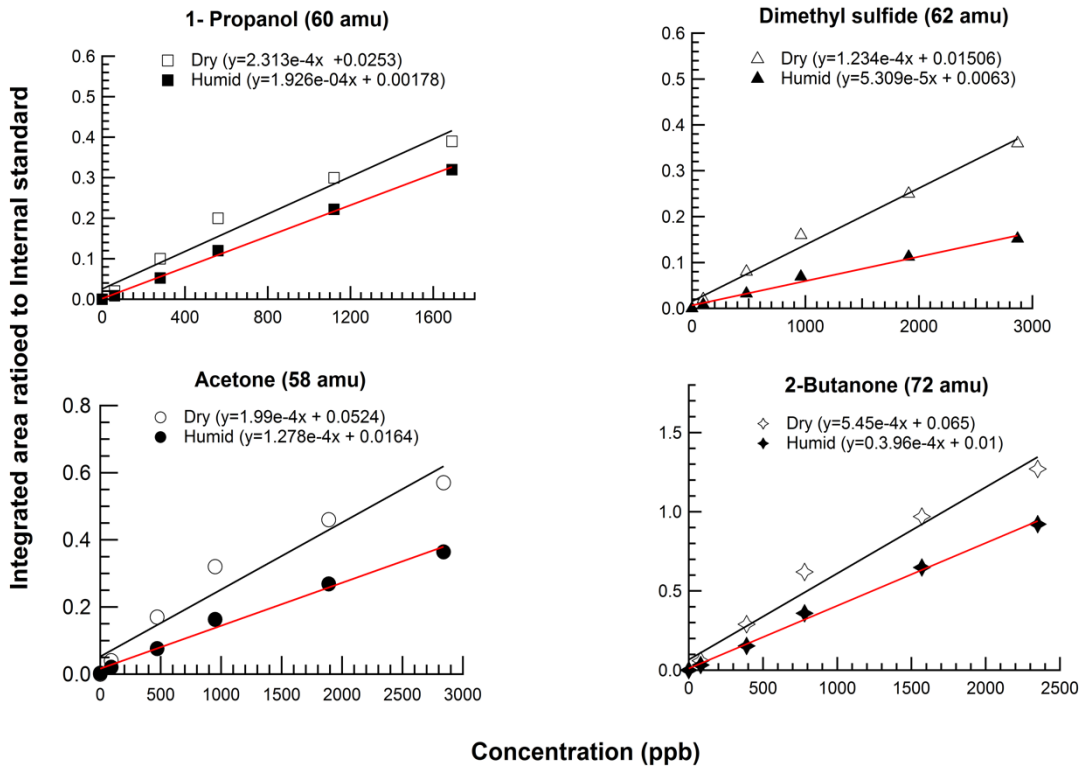


Figure 3.18 Illustrates the response of the SPME-GC-MS instrument when 0.6 ppmV (blue), 1 ppmV (red) and 5 ppmV (green) of Internal standard bromobenzene were captured on five SPME fibre coatings: PA, PDMS, PDMS/CAR, PDMS/DVB, PDMS/CAR/DVB. Variables such as sampling height, exposure times and internal oven temperatures of the GC oven were kept constant.

### 3.3.4 Effect of humidity on VOCs extracted by SPME

There are a number of factors that affect the uptake of VOCs on to SPME fibres. Type of fibre coating, thickness, exposure times, and temperature are amongst a few of elements governing the types and amounts of VOCs captured. Earlier sections of this chapter have discussed the effect of fibre coatings and exposure time. The decision not to investigate the effect of temperature on SPME performance in this work will become clearer in the upcoming chapters (Chapters 4 and 5) as the nature of the chamber like set-up used in this study of carcass decomposition proved to stabilise temperature at around 22 °C. That said, relative humidity was measured to be consistently high at 99.8 % in the background chamber. Considering most ambient air measurements are conducted in the range of 30 - 80 % relative humidity [115], it is plausible that such a high relative humidity as that measured in the trials, might affect VOC uptake on the CAR/PDMS fibre.



**Figure 3.19 Graphical representation to show the humidity dependence of SPME-GC-MS (CAR/PDMS fibre) on four analytical grade standards: 1-propanol, dimethyl sulphide, acetone and 2-butanone when examined under dry (0.5% relative humidity) and humid (89% relative humidity) conditions.**

Four analytical grade standards representative of the type of VOCs detected during carcass decomposition were purchased from *Sigma Aldrich UK*. These included 1-propanol, dimethyl sulphide, acetone and 2-butanone. These standards readily vaporised under standard conditions. In order to achieve the desired concentration ranges, synthetic grade air was used as the dilutant gas. 1 ppmV bromobenzene was also added to the mixture as the internal standard. All dilutions were conducted in 25 L Tedlar bags purchased from *Thames Restek Ltd, Wycombe, UK*. Ideally a range of relative humidity would have been investigated, however, the apparatus available at the time of this study was only able to control relative humidity in the region of 87-89%. The apparatus (not shown) was fabricated by use of a water bubbler, a vessel and a relative humidity sensor. In the humid experiments (87% RH) the diluent gas was passed through the water bubbler, whereas in the dry experiments (0.5 % RH) the apparatus used to create water vapour was disconnected. 75µm CAR/PDMS fibre was exposed into each bag for a period of 20 minutes before being desorbed into the GC-MS instrument. Overall, the standards were subjected to the same instrumental conditions as the trials. The peak areas of the standard at each concentration were manually integrated and were ratioed against the area of the internal standard peak. Six-point calibration curve was used including the value obtained in the blank (when no standard was added).

In the four standards tested, the results indicated that the detection sensitivity (gradient of the slope) is reduced in the humid environment (Figure 3.19). This must be considered when discussing the results generated from the experimental trials as this finding suggests that the sensitivity of the VOCs captured by SPME during carcass decomposition is likely to be reduced due to the high relative humidity measured within the chamber during the trials.

Owing to the adsorbent nature of the CAR/PDMS fibre, at high relative humidity, water molecules interfere and compete with analyte mass uptake. Relative humidity higher

than 90% has been reported to reduce adsorption of analytes by as much as 10% [116]. Although this preliminary investigation was conducted at a maximum relative humidity of 89%, the relative humidity measured during carcass decomposition in the trial was in excess of 99%. However, the results generated here serve as a good estimation of the humidity dependence of SPME. It has also been argued that there is the possibility that the characteristics of the SPME fibre alters due to adsorption of water by the fibre in environments with high relative humidity [115].

These results align with the conclusions generated from the work of Prosen *et al* [116] which states that humidity of the air has an impact on the effectiveness of extraction by SPME.

### 3.3.5 Effect of ammonia on VOCs extracted by SPME

The response for hexane, trimethylamine, and 1-butanol and carbon disulphide as depicted in Figure 3.20 shows that increasingly high concentrations of ammonia gas in the sample headspace had little to no effect on the extraction via SPME. That said, of the fourth concentration (5000 ppb) was lower in all four standards, possibly a reflection of error associated with the sample preparation steps. Results of T-tests confirmed that there was no significant difference in the 4<sup>th</sup> concentration recorded for carbon disulphide

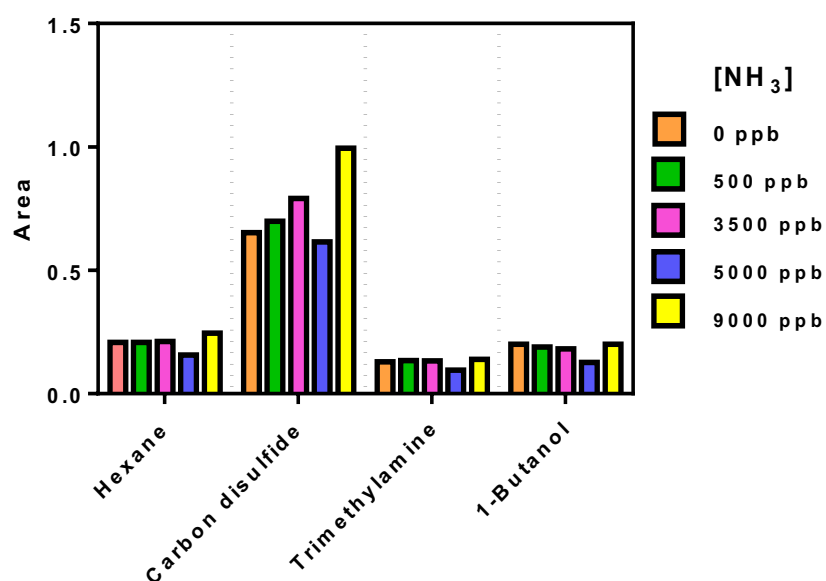


Figure 3.20 illustrates the response of the CAR/PDMS SPME fibre when varying concentrations of ammonia gas was added to the headspace of a calibration mixture. The calibration mixture consisted of constant concentrations of analytical grade standards hexane, carbon disulphide, trimethylamine and 1-butanol

### 3.3.6 Calibration of SPME-GC-MS

Calibration curves are plotted such that the vertical axis (y) represents integrated area ratioed to internal standard and standard concentrations in ppbV on the horizontal (x) axis. All signals were normalised to internal standard bromobenzene. The slope of the linear fit corresponds to the sensitivity of SPME-GC-MS with respect to each standard. Six concentration point calibration curves for twenty analytical grade standards are illustrated in Figure 3.21. Details of the standards have already been presented elsewhere (Table 3.2). Each standard was prepared in 25L Tedlar bags under humid conditions (89 %RH) to simulate similar environment to that of the decomposition chamber. 1ppmV bromobenzene was also included into the mixture as the internal standard. At each concentration, samples were collected in triplicates and the associated error bars (1 standard deviation) are included in the calibration curves.

The CAR/PDMS fibre was exposed for twenty minutes at each concentration, after which it was desorbed into the inlet of the GC for five minutes. The oven in the GC was set at 35 °C for 6 minutes, then ramped to 80 °C at a rate of 5°C per minute. Following this, secondary ramp was applied at a rate of 10 °C per minute until 300 °C. The total GC-MS runtime was 37 minutes. Data was acquired in full scan mode, as it would be in the case of the human analogue trials, between 20- 400 amu.

The results of the calibrations provide an indication of the response of the chosen analytical method to known concentrations of standards. When the response is linear, i.e. the instrument response is proportional to analyte concentration, the equation of the calibration fit (straight line) can be used to deduce the concentration of the analyte present in an unknown sample

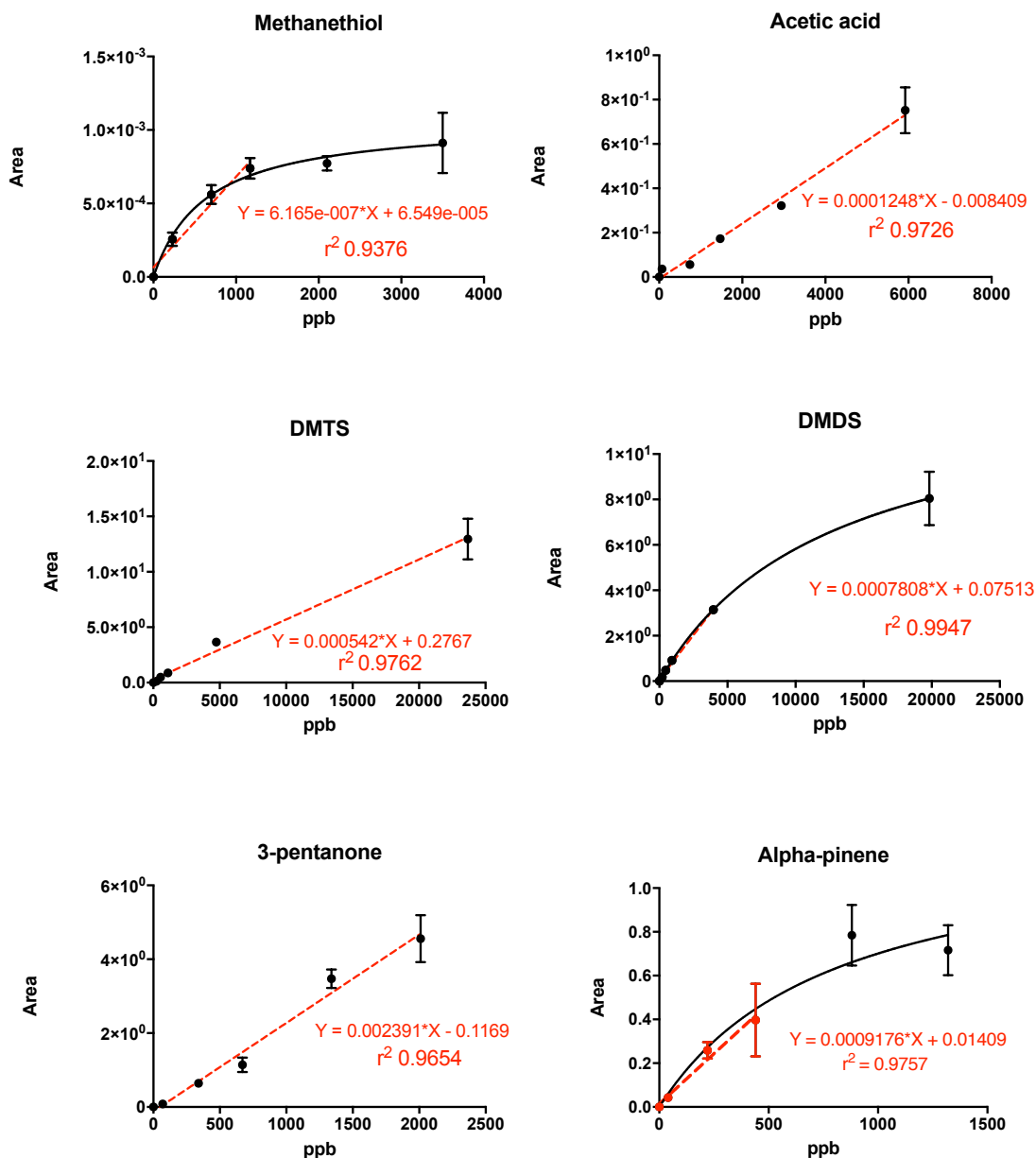


Figure 3.21 Sensitivity of the SPME-GC-MS (PDMS/CAR) to analytical grade standards carbon disulphide, trimethylamine, 2-butanone, dimethyl sulphide, 1-propanol, acetone, methanethiol, acetic acid, dimethyl trisulphide (DMTS), dimethyl disulphide (DMDS), decane, hexane, 3-pentanone, alpha pinene, dodecane, butanal,3-methyl, ethyl acetate, pentane, 1-butanol and benzene. Sensitivity is extrapolated from the slope of the linear fit and 'Area' refers to the ratio of the analyte signal to that of the internal standard signal.

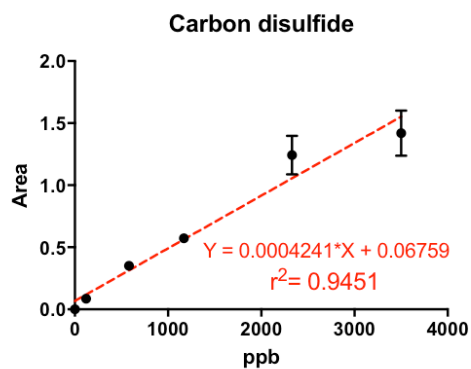
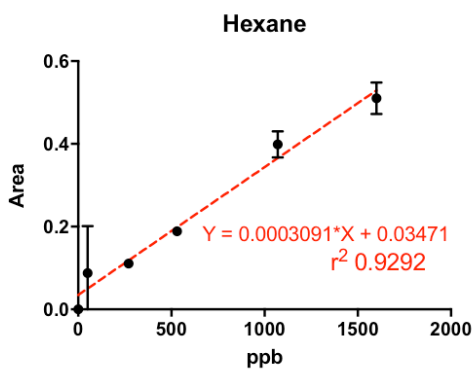
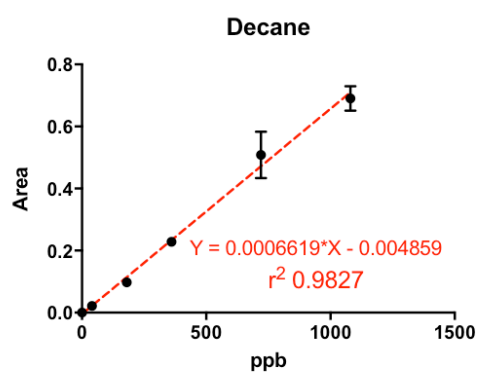
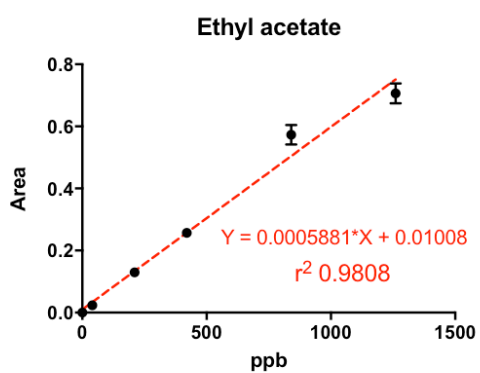
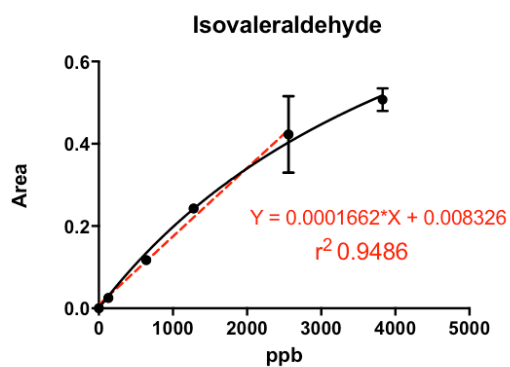
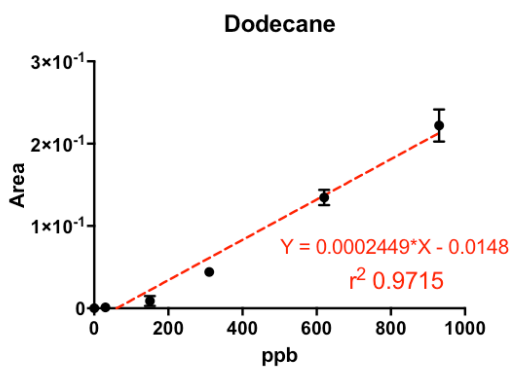


Figure 3.21 continued

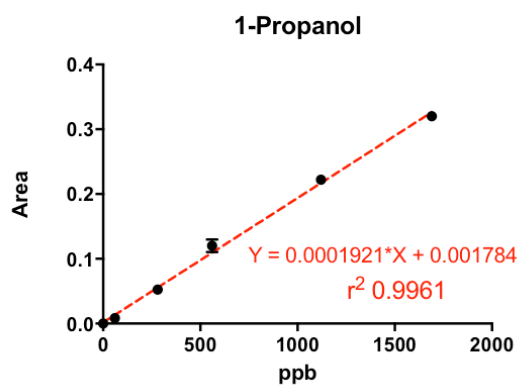
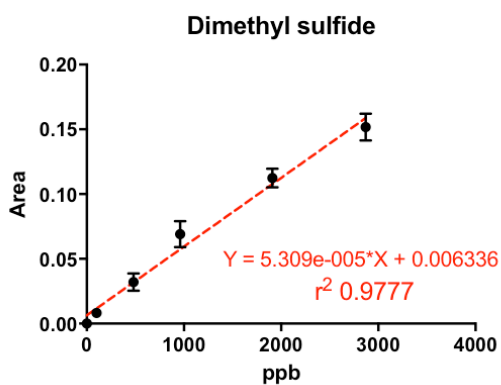
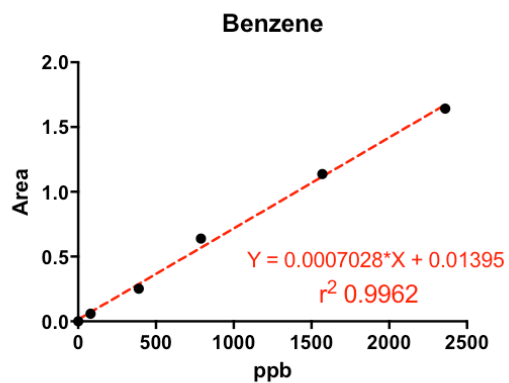
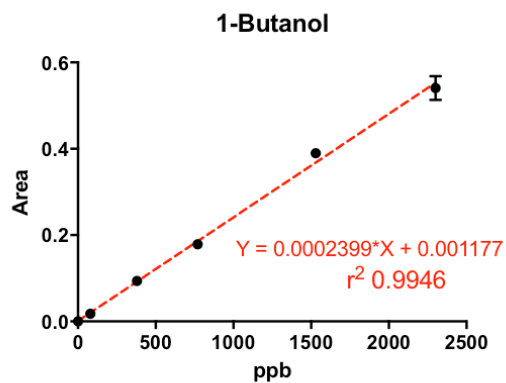
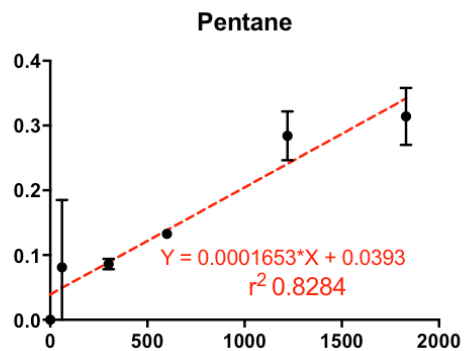
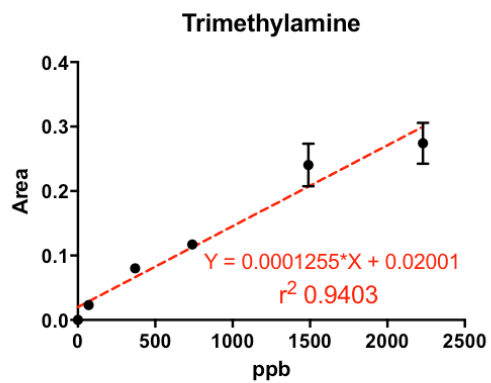


Figure 3.21 continued

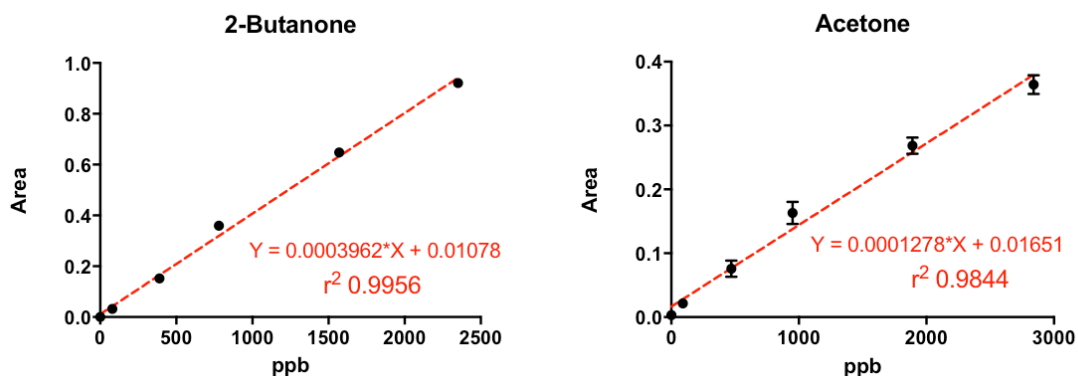


Figure 3.21 continued

The measured concentration ranges of methanethiol, dimethyl disulphide,  $\alpha$ -pinene and isovaleraldehyde appeared to be outside the linear range of the CAR/PDMS fibre [117]. Concentrations above 1200 ppbV, 4000 ppbV, 900 ppbV and 2800 ppbV for each compound respectively cannot be deduced by use of the equation from the linear fit. This is because the CAR/PDMS fibre become saturated at higher concentrations. The adsorbent nature of the fibre means there are limited sites for adsorption, as such the fibre is mostly suited to trace analyte concentrations. One methods of increasing the linear range of CAR/PDMS is to reduce the extraction time. When the extraction time was reduced from 15 minutes to 2 minutes, the linear range of CAR/PDMS could be extended from 1000 ppb to 25000 ppb. However, a caveat to reducing extraction times is that the amount of analyte adsorbed is also significantly reduced [117].

In contrast, the response of the analytical method to acetic acid, dimethyl trisulphide, 3-pentanone, dodecane, ethyl acetate, decane, carbon disulphide, trimethylamine, 1-butanol, pentane, benzene, dimethyl sulphide, 1-propanol, 2-butanone and acetone were within the linear range. This means that the concentration of these compounds in the human analogue trials can be deduced by use of the equation of the linear fits generated from the calibration graphs (Figure 3.21)

### 3.4 Chapter 3 Summary

Experiments conducted towards characterisation of the decomposition chamber, revealed that the chamber was relatively airtight, allowing it to be stored in the laboratory. Background VOCs gathered in sequence within the chamber showed that soil and sand absorbed majority of the VOCs released from the chamber. This attribute must be considered when reviewing the results obtained from the buried and exposed trials. As well as this, the relative humidity of the chamber was measured as high as 99% in the background.

As expected, sample humidity had significant effects on CIR-MS measurements and the uptake of VOCs by SPME. In both instruments, a reduced sensitivity was observed with an increase in sample humidity. In CIR-MS humidity effects were measured from the signal of hydrated hydronium ions at mass channel 37. Between 2014 and 2016, the humidity within the CIR-MS instrument (ratio of  $m/z$  19 to 37) was noted to have increased by three folds. This would affect the sensitivity of decomposition VOCs in the buried and exposed trials especially as the effect of humidity proved here, appeared to be compound specific. Owing to the high relative humidity measured in the background chamber, all calibrations were conducted under humid environments. The results from the linear fits from the calibrations will be used to deduce quantitative information on decomposition specific VOCs in the upcoming human analogue trials.

Aside from the investigations on humidity dependence, the effect of having a high concentration of analyte gas ammonia, was also tested on both techniques. In SPME, there was no significant effect in VOC uptake, however, in CIR-MS the high concentrations of ammonia referred to as competing reagent ion affected the chemistry occurring within the drift tube, which further complicated analysis of the results obtained by CIR-MS. Consequently, having competing reagent ions was considered unfavourable at this stage of this research.

In SPME-GC-MS, results from the method development process revealed that use of a mixture of fibre coatings was the best choice for this type of non-target analysis.

Therefore, CAR/PDMS fibre was chosen at an exposure time of 20 minutes. Having said that, saturation was observed for methanethiol, dimethyl disulphide,  $\alpha$ -pinene and isovaleraldehyde on CAR/PDMS fibre above a certain concentration. This is a particular attribute of CAR/PDMS which is mostly suited for quantification of trace analytes. Overall, the performance of both CIR-MS and SPME-GC-MS were as expected. Almost all twenty compounds calibrated for showed a positive response, with the exception of alkanes in CIR-MS.



# **4 THE ANALYSIS OF VOCS RELEASED FROM MAMMALIAN DECOMPOSITION DURING BURIED HUMAN ANALOGUE TRIALS (BHA)**

## **4.1 Introduction**

Characterisation of odour in itself is a challenging analytical task given as odour consists of a mixture of many different gases at low concentrations. Hence, to be able to quantify odour, the composition and concentration of the gas mixtures will need to be measured. This is even more complicated when the critical components of malodour are only present in trace levels within a complex matrix of volatiles [118]. Such is the case with the odour associated with a decaying corpse.

Until recently, much of the focus of odour profiling of decomposition has been from surface deposited carcasses [27, 30, 57, 65]. So far, findings from these studies have been instrumental in expanding the understanding of the physical and chemical processes associated with carcass decomposition. In particular, it has been useful in illustrating that it is the combination of gases released from a decaying corpse that attracts forensic relevant insects and human remains detection canines (HRD or cadaver dogs). Unfortunately however, the unique composition of VOCs associated with decomposition and responsible for attracting scavengers and predators to a corpse is still largely unknown [59]. In addition, soil decomposition has been poorly

characterised and there still is considerably variation in the observed VOC profile across published literature [119].

In an attempt to bridge this gap, laboratory scale experiments using the bespoke decomposition chamber described in section 2.1 were conducted to study the evolution of headspace VOCS released from carcasses when buried (shallow buried) in soil. From a criminal perspective, it is more probable, that an offender would attempt to conceal a corpse in some manner, either by burying or submerging in water. Presently, techniques such as soil probing [69], soil solution [33], soil analysis [4, 62, 63] are used to investigate soil decomposition VOCs. However, a caveat to these techniques are that they are can be invasive and destructive, particularly in the case of soil analysis which requires that a sample of soil be removed from the ground, stored and transported to the laboratory for further analysis. Aside from the lengthy time taken to conduct such analysis (typically hours or days), there runs a high risk of soil contamination and/or VOC losses from within the soil if improperly stored during transit.

The objective of this BHA study was to understand the partitioning of VOCs from the soil into the headspace region within the chamber, as it has been evidenced that it is this distinctive assemblage of compounds perceived above ground by HRD dogs which enables them to locate graves (scent cone theory) [16]. The hypothesis is that decomposition VOCs capable of permeating the soil to reach surface level might give a better indication of the unique markers responsible for attracting forensic relevant insects, scavengers, and HRD dogs to the location of a body and clandestine grave. It would also allow for the possibility to identify and quantify the VOCs associated with carcass decomposition in soil. The net result would be the ability to define stages of decomposition without visual examination, and hence, be able to determine the post burial interval of a corpse.

## 4.2 Experimental Setup

The genesis of BHA trials under controlled chamber environments began in 2012 in the RAFT laboratory of the Department of Chemistry at University of Leicester. Since then, the development, characterization and application of an environmentally controlled decomposition chamber used in the analysis of VOCs from human analogues has evolved to what has been discussed in preceding chapters. From the onset, the aim has been to improve upon the knowledge and understanding of VOCs emanating from carcasses, with particular interest in the effect soil has on the resulting VOC signatures when measured in headspace.

To address this, trials were structured such that pig carcasses (*Sus scrofa*) were used as surrogates to humans. The first trial (BHA 3) took place on 11<sup>th</sup> of April through until 19<sup>th</sup> of May 2014, allowing a total of 5 weeks of data collection, and the second trial (BHA 4) began on the 30<sup>th</sup> July 2015 until 8<sup>th</sup> September 2015. Both carcasses were shallow buried using commercially available sterilised topsoil. Two gilt piglets were stunned by penetrative captive bolt; before slaughter. The pigs were buried within 6 hours in the RAFT laboratory at the University of Leicester. All experimental pigs were of the same breed and were raised on the same farm to ensure consistency in their feed. The pigs weighed 36 kg (BHA 3) and 7.48 kg (BHA 4) respectively, and immediately after euthanasia, the carcasses were bagged in plastic bags to avoid insect colonisation during transportation to the experimental chamber. The carcasses were laid on their left side and placed on a bed of sterilised topsoil. A needle thermistor was fitted subcutaneously on the upper surface of each carcass to measure temperature variations before covering with the remaining topsoil. The depth of burial was consistent across both trials, in that it simulated a shallow grave of a human victim (Figure 4.1).

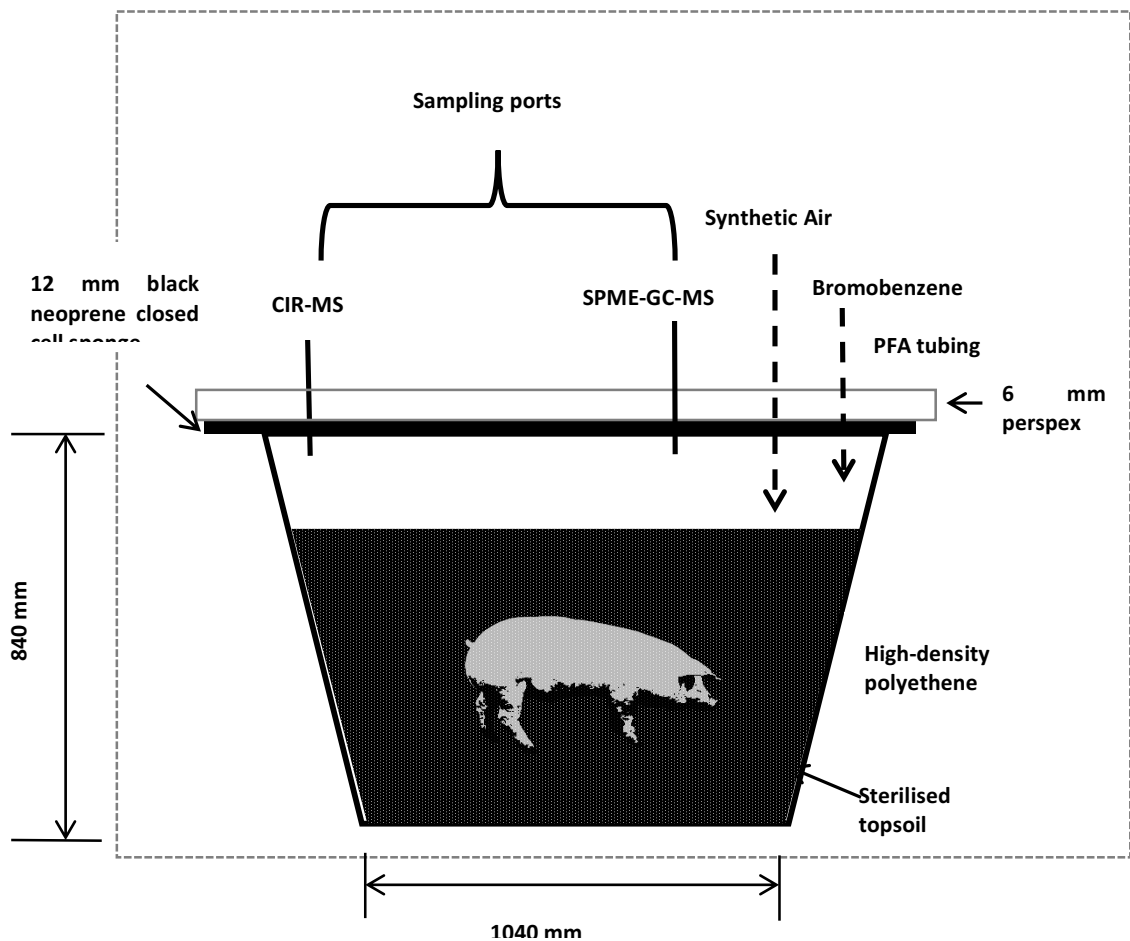


Figure 4.1 Cross-sectional view of the bespoke decomposition chamber during the Buried Human Analogue trials.

A combination of synthetic air (BTCA 178 grade) and internal standard (1 ppmV bromobenzene) were pumped into the headspace of the chamber at a rate of 300 sccm to mimic wind dispersion, as it would be in the case of an outdoor burial. Background samples were collected from the chamber when empty, and when filled with topsoil. Headspace VOCs were passed into the CIR-MS instrument by use of a temperature controlled (27°C) eighth inch perfluoroalkyl transfer line. In addition, headspace VOCs were also sampled offline by the use of HS-SPME-GC-MS. SPME fibres were manually inserted into the inlet port of the chamber and sampling was carried out at noon on a daily basis for two weeks, after which samples were taken every 3 days until 40 days had passed. A full description of the SPME-GC-MS method used has been described in

section 3.3. Ambient temperature and relative humidity within the chamber were measured by use of Campbell scientific CS 215 probe, whereas soil temperature and volumetric water content was monitored through the use of CS 650 sensor. All measurements were logged hourly on Campbell Scientific CR10X data logger.

Owing to the nature of the setup, i.e. burial within a confined site, access to scavengers, environmental fauna and flora were restricted. The introduction of soil organisms was limited through sterilisation of the soil; and as a result, the only bacterial contribution to the decomposition process originated from the carcass. The decision to exclude all other environmental factors typically affecting the rate of decomposition was deliberate, as it was believed that in doing so, the already convoluted process of decomposition could be better controlled, consequently increasing the reproducibility of the trials.

## 4.3 Data Analysis

From the results collected by CIR-MS, reagent ion hydronium at  $m/z$  19 was the most dominant ion across both BHA 3 and BHA 4 trials, and as such, all analyte peaks were normalised to 1 million counts of the reagent ion signal. Following this, patterns were extracted based on the characteristic time profiles of the monitored mass channels (0-500 amu mass range) and as a result, subsets (groupings) were created to describe the process relating to carcass decomposition. The approach adopted in analysis of the CIR-MS dataset was described in Chapter 2.

On the other hand, SPME-GC-MS dataset is reported as a ratio of analyte peak area to internal standard peak area. All peaks were background subtracted to remove interferences from common constituents of the air ( $N_2$ ,  $O_2$ ). MSDS Chemstation and NIST library searches were used for qualitative analysis, and all identifiable compounds from GC-MS are reported. The results generated by SPME-GC-MS were used to validate those obtained by CIR-MS.

## 4.4 Results and Discussion

### 4.4.1 Climatic conditions

As mentioned earlier, temperature is regularly reported as being the most important parameter to affect the rate of carcass decomposition as it disturbs both biological activity and biochemical reactions [37], particularly when over the mesophilic range of 15°C and 35°C. Nevertheless, to observe the effect of temperature on a biochemical system, there must be an increase of at least 10 °C often described as Van't Hoff temperature coefficient Q10 [120].

The ambient temperature as measured by the CS215 sensor within BHA 4 trial was fairly stable throughout the study with an average of 22.5 °C, a minimum of 22.03 °C and a maximum of 22.9 °C. Soil, headspace and carcass temperatures were also relatively constant with a maximum difference of 1 °C between each temperature sensor (Figure 4.2). This minimal temperature change meant that the rate of chemical reactions occurring within the carcass, as it passed through different stages of decomposition were not significantly affected by temperature in this setup. It can therefore be concluded that temperature was not the governing factor on the rate of carcass decomposition in these experiments.

That said, the temperature profile of BHA 4 trial was within the optimum range for putrefaction. The optimum range for putrefaction was reported to be between 21°C and 38 °C. Below 10 °C and above 40 °C putrefaction is significantly retarded on the grounds of reduced microbiological activity [4]. In spite of the negligible change in temperature, standardization of the decomposition rate using the concept of accumulated degree-days (ADD) as adopted by other forensic authors was still applied. Accumulated degree-days were used to represent time and accounts for the effect of temperature on the rate of decomposition. ADD was calculated by totalling the number of degree-days the average temperature was greater than the lower threshold value of 0°C [33, 40].

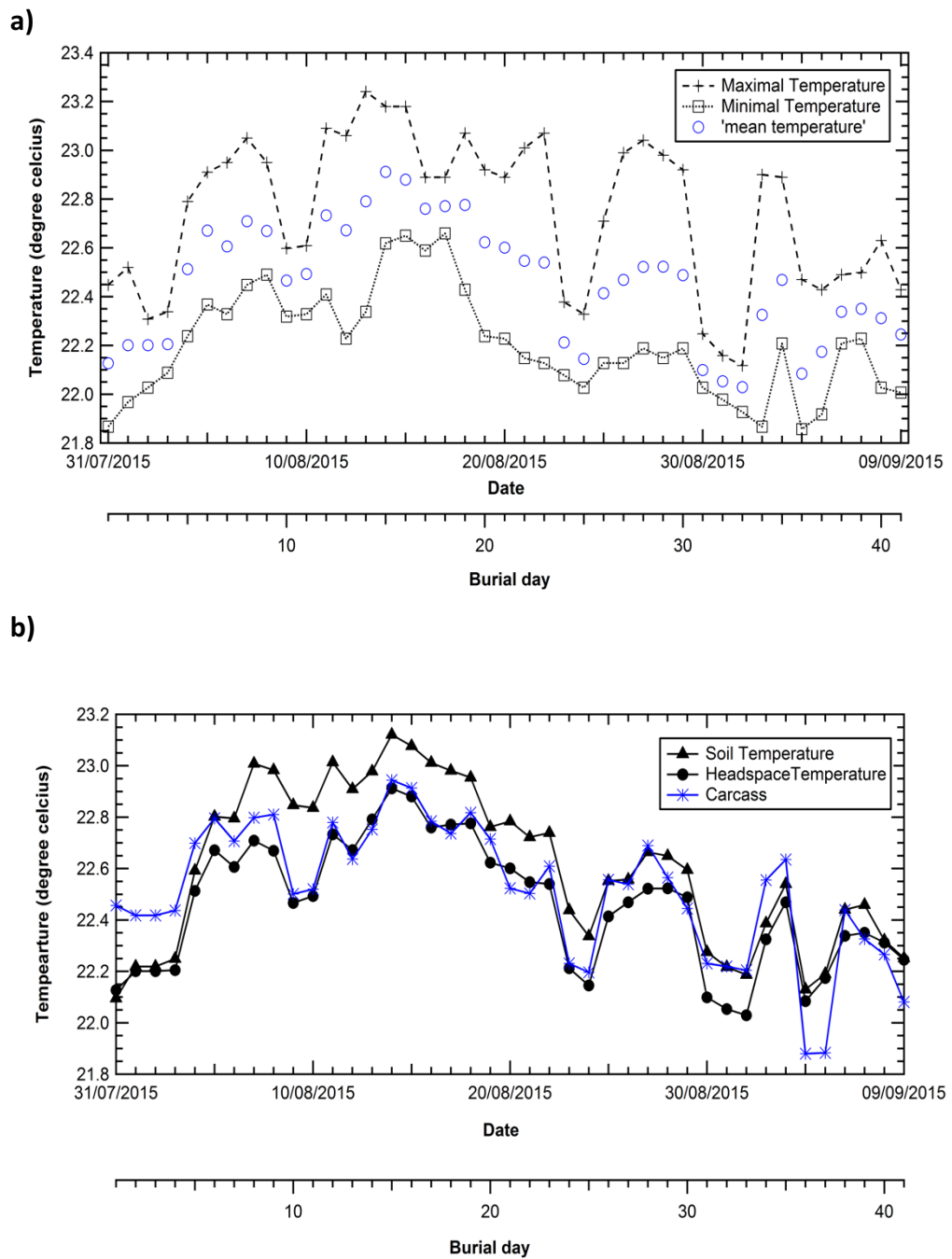


**Figure 4.2** Temperature recordings as measured during Buried Human Analogue trial 4 (BHA 4). Maximum, minimum and mean headspace temperature measurements a) Soil, headspace, and carcass temperature measurements b) Temperature recordings were captured by use of Campbell Scientific CS215 and CS650 sensors. All parameters were logged onto a CR10X data logger. Headspace refers to the air 'pocket' above the soil within the experimental chamber. BHA trial 4 lasted a total of 40 days

Relative humidity (RH) recordings in the headspace of the chamber were also collected with the CS 215 sensor. Prior to the start of this trial, RH measurements in the RAFT laboratory were recorded as 56 % on average, a typical value for an indoor environment in the UK. By feeding dry synthetic air into the empty chamber, RH readings declined to 18%. However, once topsoil was introduced to the chamber, RH recordings increased to 99.8% and remained constant at this value throughout the entire duration of the study. The rise in the relative humidity of the chamber was visually noticeable as condensation occurred on the inner surface of the chamber covering. RH measurements remained constant from background sampling through until the end of the experiment. Subsequently, alternative methods described in section 3.2.2 were adopted to estimate the overall effect of relative humidity on the CIR-MS instrument. Hydrated hydronium clusters at  $m/z$  37 and  $m/z$  55 were used as proxies to estimate the effect of humidity in the pig chamber had on the CIR-MS

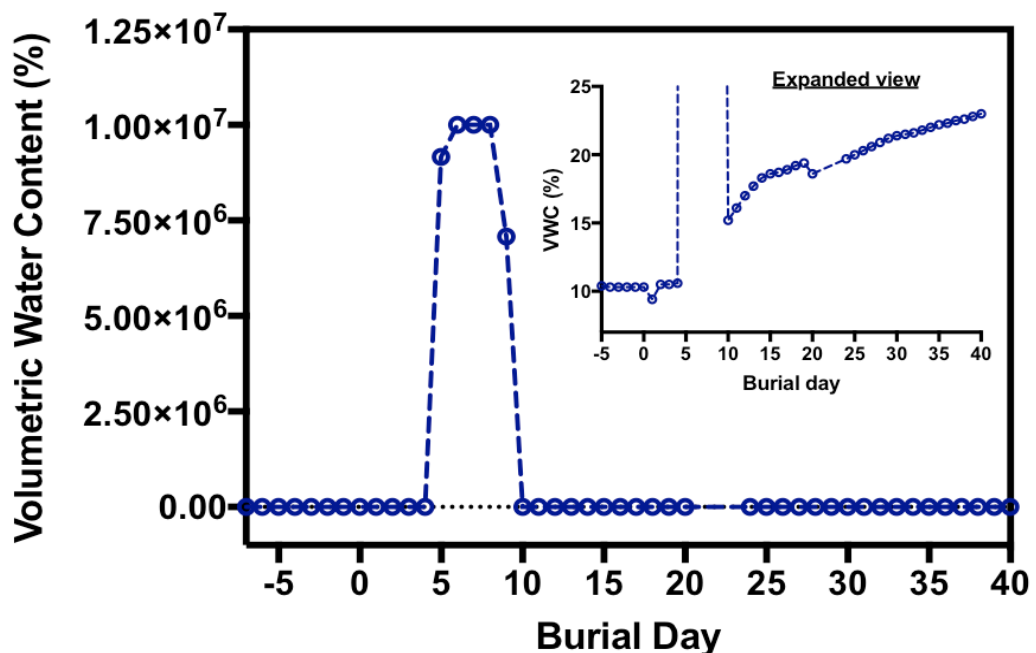


Figure 4.3 Soil Volumetric Water Content recordings as measured by Campbell's Scientific CS650 sensor during BHA 4 trial. Measurements were collected hourly until 40 days passed. Daily VWC averages are shown in per cent

Average volumetric water content (VWC) measured in the soil before the carcass was introduced was about 10%. A steep increase in the water content of the soil was observed from day 4 until day 10 following burial (Figure 4.3). This behaviour implies that a physical transformative process occurred within the carcass during this period, possibly an indication of the end bloated phase of decay and the onset of active decay. At the end of the bloated stage, there is a release of accumulated pressure within the carcass through the natural openings of the carcass i.e. eyes nose, rectum. A consequence of this is the liberation of gaseous and liquid decomposition by-products into the soil. Beyond day 10, VWC decreased to about 15%. This value slowly increased again to about 25% until the end of the trial.

## 4.4.2 CIR-MS

### 4.4.2.1 Background VOCs

Background VOCs were defined as volatile compounds present in the environmental chamber prior to the introduction of the carcass. These VOCs were determined by collecting samples from the chamber when empty and with the burial material (sterile soil). The first background sample lasted a total of 20 days (Figure 4.4a), after which sterilised soil was added and sampling continued for a further 7 days (Figure 4.4b). When the chamber was empty, there was a significant contribution from  $m/z$  18, commonly associated with ammonium ( $\text{NH}_4^+$ ,  $m/z$  18). The presence of ammonia recorded in the background chamber was a direct result of carry over interference from the previous carcass experiment particularly as ammonia was measured in high concentrations (see Chapter 5). Other significant channels detected when the chamber was empty included  $m/z$  29, 26 and 73. Interestingly, the resulting mass spectrum upon addition of soil was very different. The relationship between  $m/z$  18 and 19 was altered, such that the contribution from  $m/z$  18 was reduced. The same was observed for contributions at mass channels 29, 46 and 73, as they were no longer detected (Figure 4.4b). This implies that the soil acted as a sink, trapping volatile compounds either

within soil gas, or VOCs adhered unto soil particles. This phenomenon has been noticed in another decomposition study [63]. The effect of soil on ammonia ( $m/z$  18) is emphasised in Figure 4.4d where B1 refers to contributions from the background chamber when empty, and B2 when topsoil was added.

The difficulty associated with definitive compound identification by CIR-MS, meant the aim this stage, was simply to differentiate the most prominent compounds generated as a result of carcass decomposition compared to those present in the background. Average normalised counts plus three times standard deviation of each mass channel in the background signal was used to determine the background (noise) level, and subsequently signals higher than this calculated value were assumed to be released as a result of carcass decomposition. Overall, scans were collected every 10 minutes, after which, daily averages were calculated. All data presented were normalized from raw data to 1 million counts of the hydronium ion signal ( $H_3O^+$ ,  $m/z$  19).

#### 4.4.2.2 Decomposition VOCs

Through the application of a novel approach in data reduction and pattern recognition, it was possible to extract six distinctive patterns (subsets) within the data generated by CIR-MS in BHA 4. Subsets 1-5 were proposed to describe specific events occurring during decomposition process, while subset 6 predominately explained contributions from hydrated hydronium clusters. Owing to the nature of interment, visual determination of the stages of decay could not be established. Hence the aim was to distinguish if the VOCs which partitioned from the soil into the headspace region within the chamber could be used to denote the stages of decomposition.

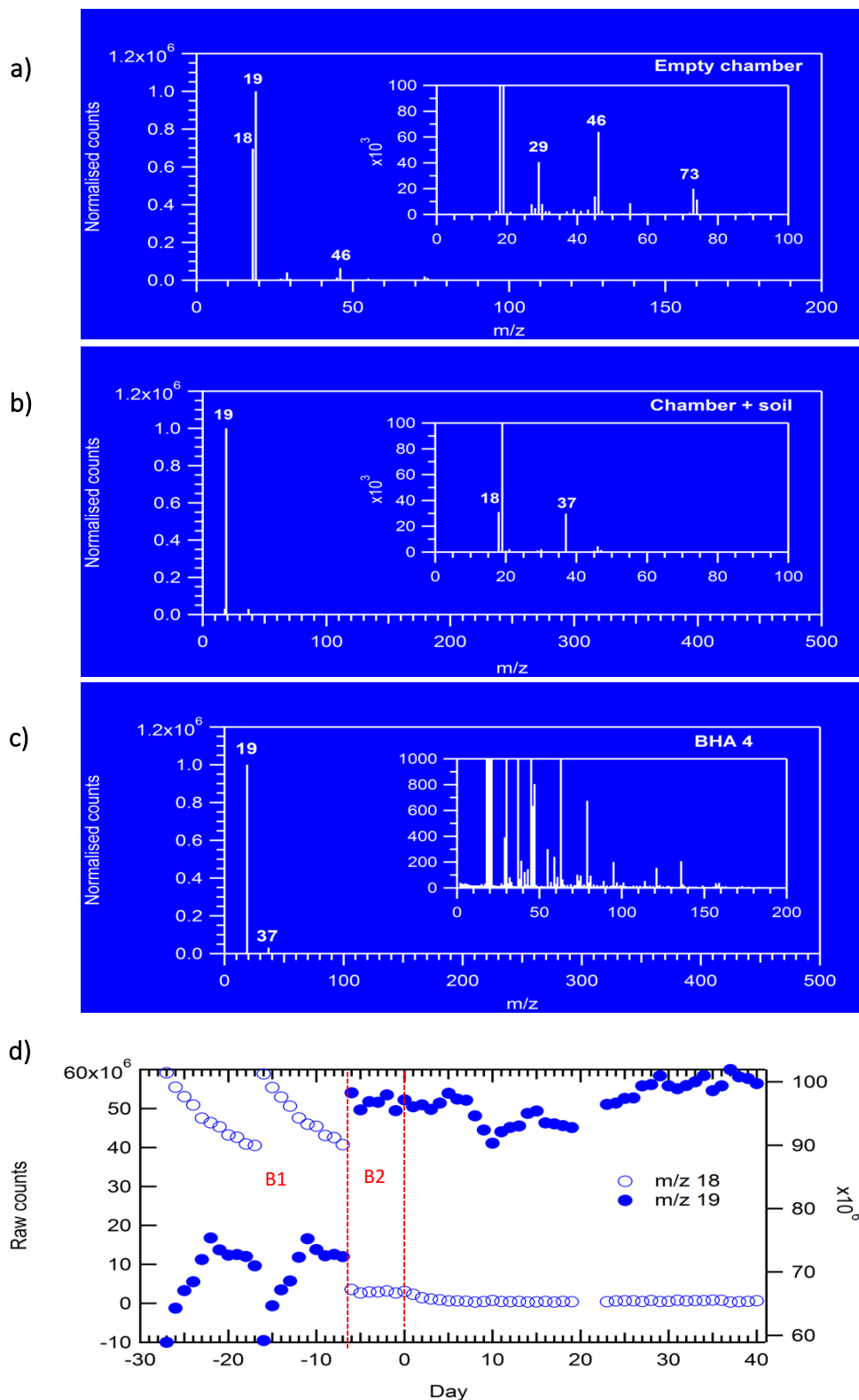
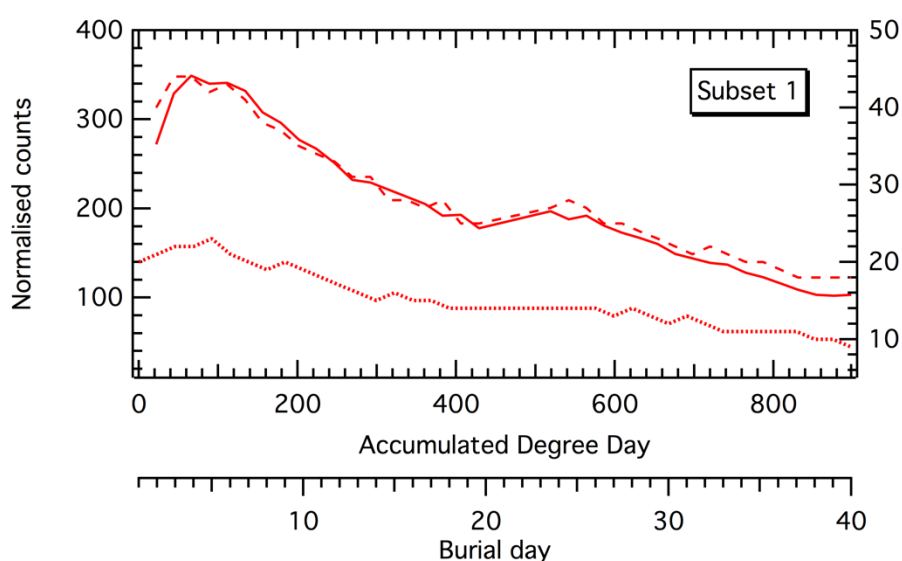


Figure 4.4 Average CIR-MS mass spectra generated from the decomposition chamber when *a)* empty, *b)* half filled with sterile soil, *c)* buried human analogue trial 4, and *d)* the time profiles of reagent ion hydronium ( $m/z$  19) and ammonium ( $m/z$  18) - zone B1 represents the first background sample collected with an empty chamber, and B2 with the chamber half filled with soil. Day 1 signifies the first 24 hours after the carcass was buried

Subset 1 consisted of fifteen mass channels (Figure 4.5). The signals of the mass channels within this subset showed a sharp rise in the first 3 days, after which they declined at a steady rate until the end of the trial. Though a total of fifteen mass channels were reported with a spearman's correlation coefficient greater than 0.9, only m/z 136, 137 and 138 produced signals higher than the instruments signal to noise ratio (S/N). The signal to noise for each mass channel was calculated using the chamber and soil background dataset as blank. The S/N is reported as the mean  $\pm 3\sigma$  (where  $\sigma$  represents standard deviation).



**Figure 4.5** Temporal variation of mass channels 136, 137, and 138 (subset 1) as measured by CIR-MS in BHA trial 4. A total of 15 mass channels reported  $r^2 > 0.9$  against m/z 136.

The trend observed in this subset suggests that the compounds responsible for the signal in m/z 136, 137 and 138 were released as by-products of carcass decomposition, perhaps as a consequence of the fresh or bloated stage of decomposition. That said, very few VOCs have been previously reported during autolysis (fresh stage of decomposition) [27], thus it is probable that compounds with molecular mass of 135, 136 and 137 were related to the VOCs released during the bloated stage of decay, which according to Figure 4.5, occurred between day 2 and day 3 following burial. Benzothiazole and N-Methylbenzamide both have a molecular mass of 135 while phenyl acetic acid,  $\alpha$ -pinene and d-Limonene have a mass of 136. These compounds have been

previously detected by other decomposition authors [27, 28, 68, 121], thus they were considered as likely candidates responsible for the trend observed in their respective mass channels in BHA 4 trial.

The trend observed in subset 2 (Figure 4.6) was the most distinctive throughout the BHA 4 trial. Twenty-one mass channels were recorded within this subset and each showed a dramatic increase from day 4 with the highest signal on day 6. By day 8, contributions fell to the same level as present in the background. Mass channels within this subset included but were not limited to  $m/z$  94, 95 and 141. The temporal variation observed in this subset aligns with the physical changes occurring at the end of the bloated stage and signifies the onset of the active phase of decomposition. During this stage, the skin has ruptured and as a consequence there is a sharp release of decomposition products into the surrounding environment [27]. Similarly, the pattern observed in subset 2 is similar to the profile of the VWC discussed earlier (Figure 4.3) supporting the conclusion that a physical transformation which signifies the begin of the active phase of decay occurred between day 4 and day 10.

Previous work conducted by other decomposition authors suggest that the signals observed in mass channels 94, 95 and 141 imply the presence of 3-methylpyridine, phenol or dimethyl disulphide and methenamine respectively [28, 61, 62, 68]. In addition, these authors have specifically detected dimethyl disulphide, phenol and methenamine in the active phase of carcass decomposition. At this stage, compound identification by CIR-MS is merely tentative although there is the added complexity of discriminating between compounds of similar masses. The latter point is particularly relevant for phenol and dimethyl disulphide as both compounds share the same molecular weight of 94, exhibit the same time profile in BHA 4 trial, and have both been attributed to the active stage of carcass decomposition [28, 30, 62, 68]

Another significant aspect of the pattern observed within subset 2 worth considering is the time frame in relation to other decomposition studies. Perrault et al [68] observed the onset of the active stage of a 70 kg carcass left to decompose on the surface of the ground early as day 4 (106 ADD) until day 8 (196.8 ADD). Although the carcass in this trial was about 10 times smaller (7.48 kg) and buried in a shallow sterile grave, the rate

of decomposition during this time period is argued to be comparable to that of Perrault et al [68].

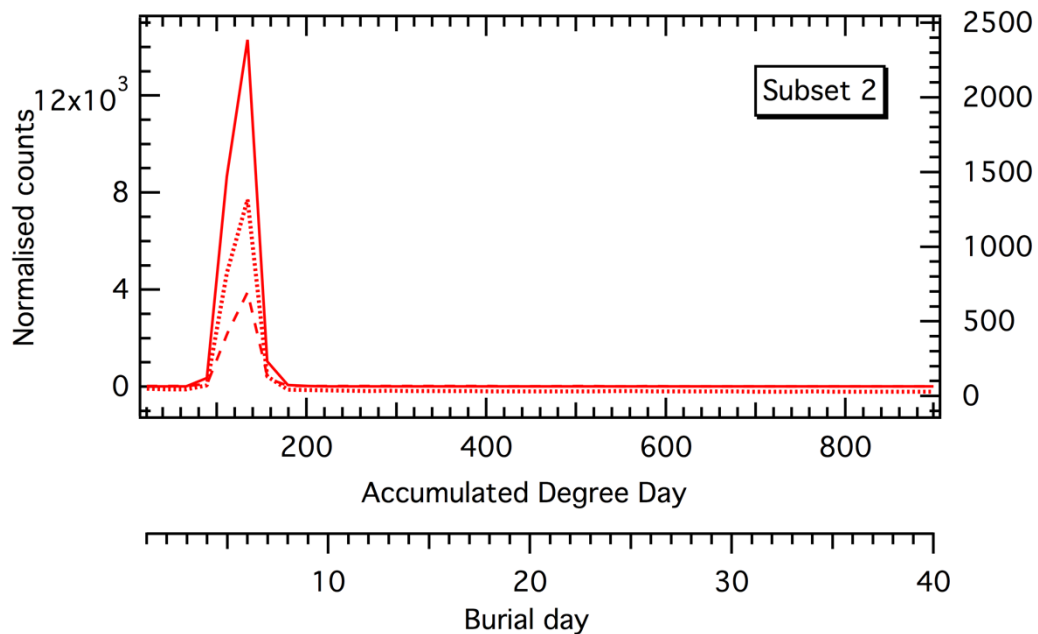


**Figure 4.6** Temporal variations of mass channels 79, 81, and 95 (subset 2) as measured by CIR-MS in BHA trial 4. A total of 21 mass channels reported  $r^2 > 0.9$  against  $m/z$  79. This subset includes  $m/z$  35, 45, 48, 49, 62, 64, 65, 66, 80, 82, 83, 94, 96, 97, 98, 141, 142 and 143

Likewise, the onset and duration of the active stage of decay in the work of Forbes et al [62] is also similar. In Forbes et al [62], four pig carcasses were surface deposited and it was noted through visual examination that the active stage of decay began from day 4 (ADD 106.95) and continued until day 10 (ADD 244.28). The trend observed within subset 2 of BHA 4 trial began on day 4 (80 ADD) and lasted until day 8 (180 ADD).

The similarities between the rate of decomposition of this BHA 4 trial and other decomposition studies [62, 68], poses questions about the effect carcass size, manner of burial and environmental fauna have on the rate of decomposition. According to Spicka et al [31], carcasses of masses < 20 kg (BHA 4 trial) decompose more rapidly within the first 6 days than larger carcasses (>40 kg) because they contain less material for insects to consume. This conclusion has also been supported by Vass [33] and Simmons [34]. Yet, the results generated within subset 2 of BHA 4 trial suggests the

contrary, which is that the rate of decomposition of a 7.48 kg carcass is similar to that of a 70 kg carcass.

Admittedly, the setup of this trial was different to those conducted by the aforementioned authors, in the sense that the object of decomposition in this trial was interred in soil throughout the decomposition process. This is an important distinction as the rate of decomposition in soil has been described as progressing eight times slower in soil compared to above ground decomposition [5]. However again, the result generated within BHA 4 trial contradicts the finding of Haglund [5], as it is evidenced here that the rate of decay, particularly the onset and end of the active stage is equivalent in carcasses that have been shallow buried or surface deposited.

Aside from the differences in the manner of burial between this trial and the literature (buried versus exposed), there is also a distinction in the availability of insects and environmental fauna. The soil used to bury the carcass in this trial was sterilised so as to limit soil based microorganisms from contributing to decay process. That said, soil microorganisms were not expected to be significant factor governing the rate of carcass decomposition [4].

Finally, dimethyl disulphide which was first observed on day 4 during BHA 4 trial (subset 2) is a primary polysulphide based product of decomposition that has been regularly detected by almost every author in the field [6, 33, 62, 68, 69], so much so that some authors recommend that dimethyl disulphide might be a potential marker for soft tissue decomposition [28, 65]. Polysulphides such as dimethyl disulphide are released as decomposition by-products from the degradation of proteins. Proteins are broken down into amino acids, peptones, polypeptides and proteases, although it is the continued breakdown of proteases that results in the formation of sulphur compounds [27]. Dimethyl disulphide is also one of the most prominent compounds released from decomposing human remains [122], and has been found in the headspace analysis of blood, bone, skin, adipocere, and testicles [67].

In contrast, fifteen mass channels recorded within subset 3 declined rapidly after day 1 (Figure 4.8). By day 8 contributions from these mass channels had returned to the same

levels as the background. One possible explanation for this trend could be these VOCs were produced during day 1 as a result of carcass decomposition and their transient nature coupled with the early release could be indicative of the rapid progression of the fresh stage of carcass decay. However, there is a limited record of VOCs documented to be released in the fresh stage of decomposition. Equally, in all of the previously identified VOCs in the literature, there is no record of compounds with masses equivalent to those observed within subset 3 (regardless of stage of decay). Alternatively, these VOCs could be a reflection of contamination or interferences from the laboratory especially as the chamber was opened to introduce the carcass on day 0. Given that approximately half the chamber was filled with topsoil, the total headspace volume was calculated as 306.67 litres. Synthetic air (270 sccm) and bromobenzene (30 sccm) were fed into the chamber, and 150 sccm was extracted every minute for sampling by CIR-MS instrument. Assuming the chamber was air tight with no leaks, it would have taken approximately 28 hours for the air pocket above the soil to be replaced entirely. This implies that any interference from the laboratory at the time of carcass burial would be represented in the analysis up to at least 24 hours after burial. Thus, there is a possibility that the VOCs exhibiting highest signals on day one were a direct result of this.

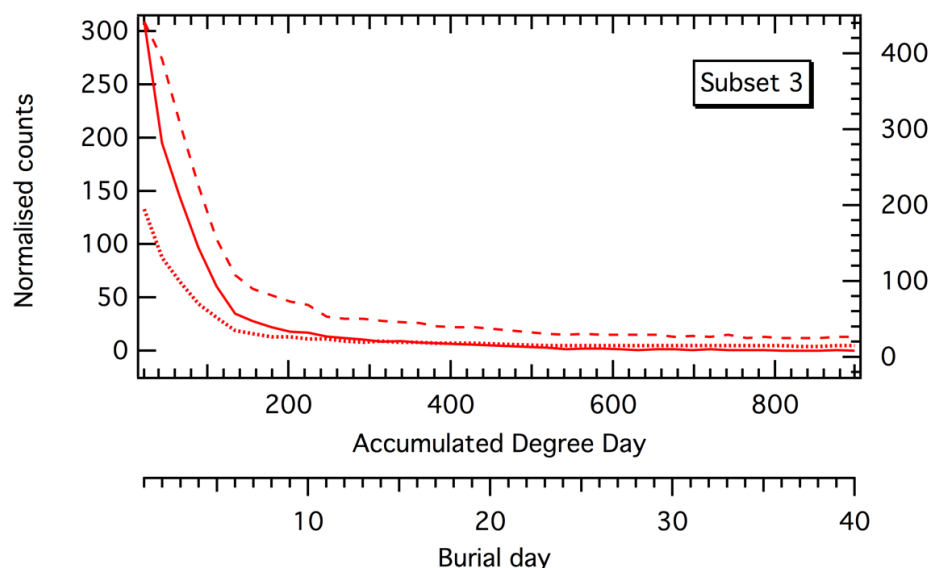


**Figure 4.7** Temporal variations of mass channels 223, 297, and 298 (subset 3) as measured by CIR-MS in BHA trial 4. A total of 15 mass channels reported  $r^2 > 0.9$  against  $m/z$  18. This subset includes  $m/z$  17, 29, 30, 32, 163, 224, 225, 281, 299 and 300

The pattern observed within  $m/z$  59 of subset 4 (Figure 4.8) showed two distinctive trends. The signal observed in the first 9 days was consistent with the levels observed in the background chamber. Following this, the first significant peak was seen between days 18-23; and a secondary peak was detected on day 33. Acetone and 2-propen-1-ol both have a molecular weight of 58 and have been previously detected during the decay of pig carcasses [27, 28, 68]. However, 2-propen-1-ol ( $C_3H_6O$ ) is more likely to undergo dehydration rather than proton transfer reaction with hydronium (Table 2.4) and thus would not be observed at  $m/z$  59.; whereas acetone forms 100 %  $MH^+$  ions. Ketone products such as acetone are frequently a result of aerobic decomposition of fat and muscle [122]. Owing to the nature of burials, there is typically a reduced availability of oxygen to the corpse and decomposition often progresses anaerobically. However, as the corpse advances through the stages of decomposition, specifically after the carcass has been purged, there is a re-introduction of oxygen through the openings of the corpse to facilitate aerobic breakdown [4]. The delayed activity of acetone in  $m/z$  59 might be an indication of the advanced stage of decomposition.

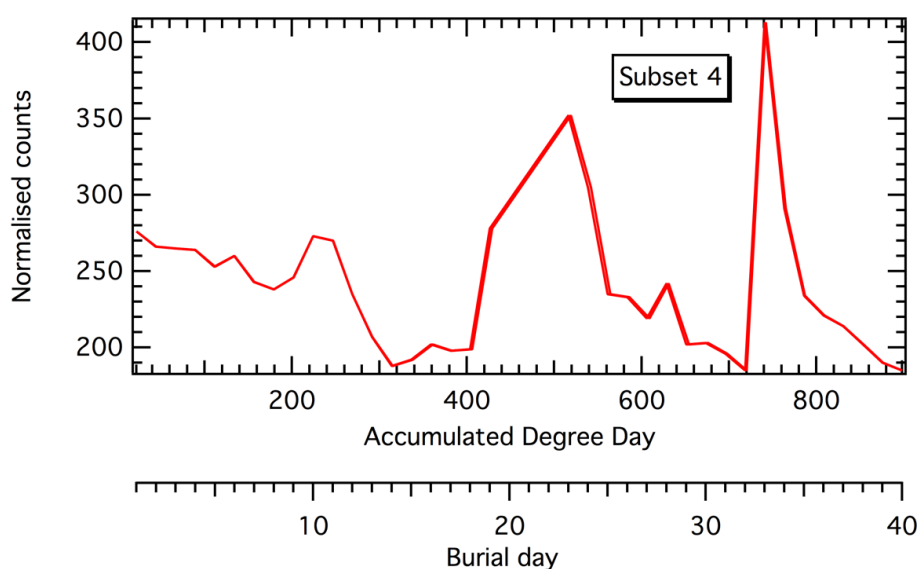


**Figure 4.8** Temporal variations of mass channel 59 (subset 4) as measured by CIR-MS in BHA trial 4. Only  $m/z$  59 is reported as belonging to subset 4.

Subset 5 (figure 4.9) consisted only of m/z 63. The signal in m/z 63 rose considerably from day 2, and peaked on day 6. Unlike the trend in subset 4, the signal at m/z 63 declined at a slower rate until the end of the trial although a secondary peak was seen on day 13. A fourteen-fold increase from the signal observed in the background chamber strongly suggests that the compound at m/z 63 was directly related to the decomposition process. Dimethyl sulphide which has a molecular weight of 62 is another member of the polysulphide family that is routinely argued as possibly being one of the key markers of decomposition [28, 68]. Statheropolous et al [28] detected dimethyl sulphide on day 4, 5, 6 and 9 during the decay of a piggery farm carcass, which coincided with the bloated stage of decay, whereas Perrault et al [68] did not detect dimethyl sulphide until the skeletonised stage on day 24 ( 557.8 ADD) and day 45 (1078.5 ADD). The early release of dimethyl sulphide in this BHA 4 trial implies that it was first released in the bloated stage, however, highest concentrations were observed on day 6 which coincides with the active stage of decomposition in this trial. That said, the slow decline of dimethyl sulphide suggests that it was present throughout the stages of decomposition, albeit at lower concentrations. By the end of the trial (day 40), its levels were still higher than they were in the background.

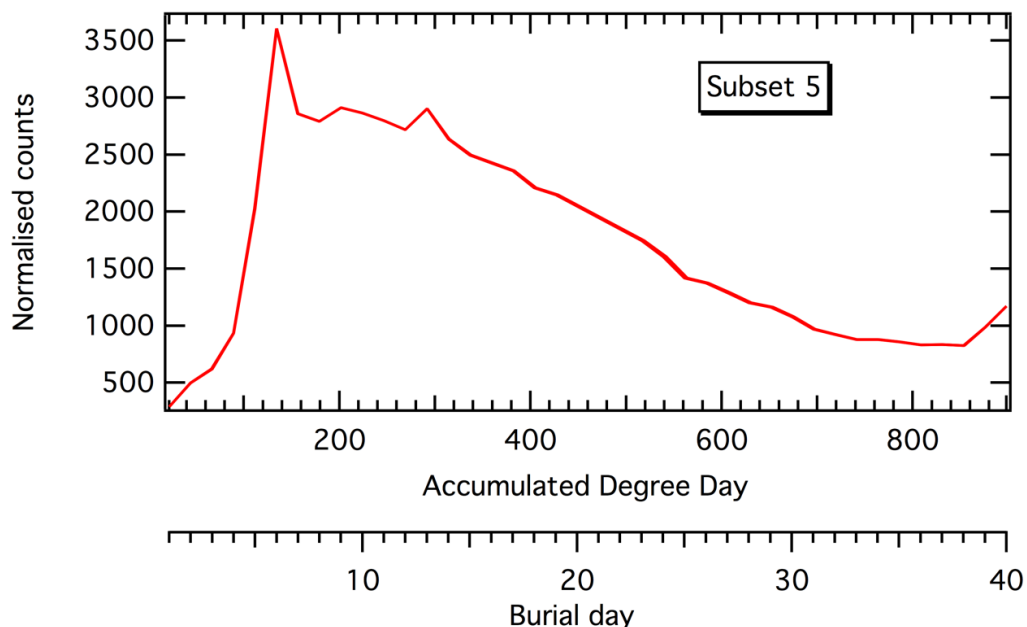


Figure 4.9 Temporal variation of mass channel 63 (subset 5) as measured by CIR-MS in BHA trial 4. Only m/z 63 is reported as belonging to subset 5.

Subset 6 (Figure 4.10) describes the behaviour of mass channels 37 and 55. The activity of these ions rose steadily from day 1 until day 10, with the highest peak on day 9. After day 10, the signal fell at a moderate rate until the end of trial. Secondary peaks were seen on days 18 and again on day 25. Mass channels at 37 and 55 are likely dominated by hydrated hydronium ions  $\text{H}_3\text{O}^+(\text{H}_2\text{O})$  and  $\text{H}_3\text{O}^+(\text{H}_2\text{O})_2$  respectively. As mentioned in section 4.4.1, the relative humidity probe (CS215) was consistently high at 99.8% throughout, hence  $m/z$  37 and 55 were used as proxies for humidity readings as they typically represent hydrated hydronium ions. As far as relative humidity measurements are concerned, when the chamber was empty the average humidity measured by the sensors was 18%. This rose to 99.8% when soil and carcass was introduced. This upsurge in humidity recordings as measured by the sensors suggests that both the soil and carcass might have contributed to the number of unreacted water molecules in the drift tube region of the CIR-MS instrument. However, there was only 0.56 % difference between counts of hydronium and hydrated hydronium cluster at  $m/z$  37 when the background mass spectrum (chamber and soil) was compared against the spectrum generated on the most humid day of the trial (day 9). The ratio of cluster at  $m/z$  55 remained the same.

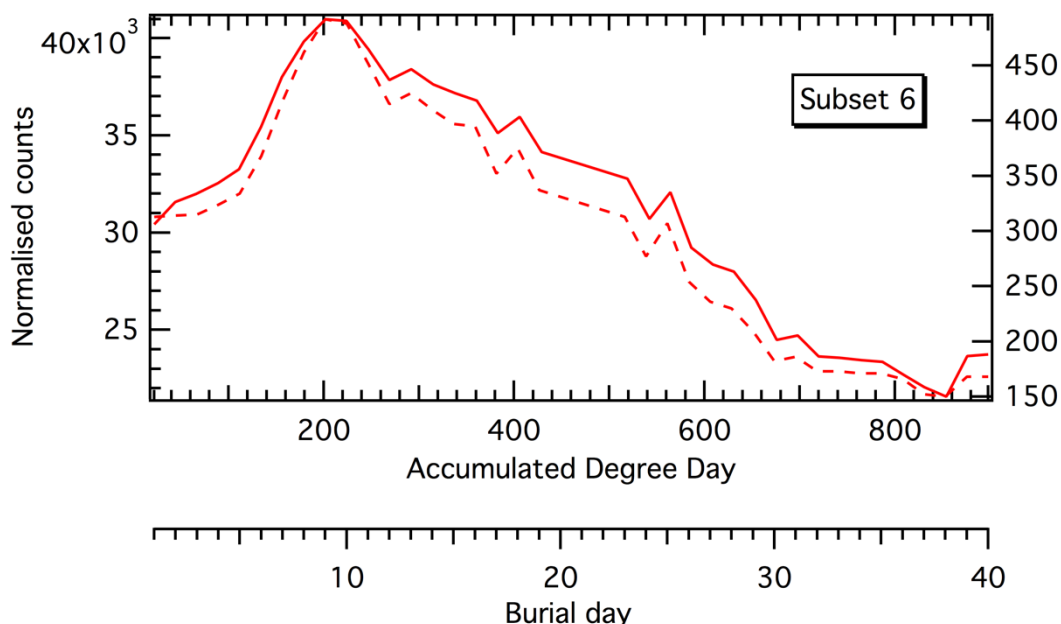


Figure 4.10 Temporal variations of mass channel 37 and 55 (subset 6) as measured by CIR-MS in BHA trial 4. A total of 2 compounds were reported for this subset

The consequences of having an increased in hydrated hydronium clusters in the drift tube of the CIR-MS has already been discussed in detail in section 3.2.2. Nevertheless, comparisons of the mass spectrum generated on day 9 versus day 15 and 24 were conducted and the results indicated that there were no differences in the mass channels detected. This finding, coupled with the minor increase in hydrated hydronium cluster at  $m/z$  37 suggests that the humidity of the CIR-MS instrument was uncompromised during the trial. That said, there is still a possibility that the signal observed at  $m/z$  37 and 55 were a combination of hydronium clusters ions and decomposition VOCs: for example, the protonated parent ion of 1,2-butadiene is at  $m/z$  55, and it has been previously detected during carcass decay [28]. A full list of the compounds tentatively assigned by CIR-MS measurements are illustrated in Table 4.1.

Despite the lack of visual examination of the carcass, many of the compounds present in the profile of the headspace of the carcass in BHA 4 trial have not only been previously identified in the literature, but their sequence of occurrence relating to the physical stage of decomposition was somewhat comparable. The chamber-like experimental setup in this study provides evidence that extrinsic factors such as temperature known to alter the rate of decomposition can be relatively stabilized. Likewise, examination of the dynamic process of decomposition by monitoring the succession of VOCs in the headspace profile of a buried pig carcass through the use of CIR-MS proves that major compounds and trends are comparable regardless of methodology.

From BHA trial 4, it was possible to extract a distinctive group of VOCs behaving similarly from day 4, which is proposed to correspond to the onset of active decay (subset 2). The carcass in this trial was characterised as being fresh from day 0-1 (ADD 22), bloat stage from day 2 -3 (ADD 46), and the beginning of active stage from day 4 (ADD 89), through until day 8 (ADD 179). Localised advanced decay was observed from day 8 - 12 (ADD 179-269), and the skeletonised stage (pictured Figure 4.11) beyond day 32 (ADD 720). As expected, majority of the decomposition VOCs were observed in the active stage.

Table 4.1 Details of the compounds tentatively assigned in the measurements collected by CIR-MS in BHA trial 4. References are represented symbolically as † (Forbes 2014 [62]), ◇ (Statheropoulos 2011[28]), ⊕ (Perrault 2014 [68]), ▫ (Dekeirsschieter 2009 [27]), • (Swann 2010 [121]), and ‡ (Agapoiu 2015 [58]).

Molecular mass	Protonated parent ion	Compound name	Proton affinity (KJ/mol)	Stage of decay	Subset
135	136	Benzothiazole ◇	N/A	N/A	1
135	136	N-Methylbenzamide ▫	N/A	N/A	1
136	137	Phenylacetic acid•	N/A	N/A	1
136	137	α-pinene◇⊕	N/A	Active, Advanced, Skeletonization	1
136	137	β-pinene ⊕	N/A	Advanced	1
136	137	1-methyl-4-(1-methylethyl)-1,4-cyclohexadiene ⊕	N/A	N/A	1
136	137	2,2-dimethyl-3-methylene-bicyclo(2.2.1)heptane ⊕	N/A	N/A	1
136	137	d-Limonene ◇	N/A	N/A	1
48	49	Methanethiol ◇▫	773	N/A	2
64	65	Sulphur dioxide ‡▫	672	Bloat, Active Decay	2
78	79	Benzene ‡◇	750	Skeletonization	2
78	79	Dimethyl sulfoxide ◇	884	N/A	2
79	80	Pyridine ▫	930	N/A	2
82	83	Furan, 2-methyl ‡	866	N/A	2
93	94	3-Methylpyridine ▫◇⊕	943	Active	2
94	95	Phenol ▫◇⊕†	817	Active Decay, Advanced Decay	2
94	95	Dimethyl sulfone ◇	N/A	N/A	2
94	95	Dimethyl disulphide ▫◇⊕†	815	Bloat, Active Decay, Advanced Decay, Skeletonization	2

Table 4.1 continued

Molecular mass	Protonated parent ion	Compound name	Proton affinity (KJ/mol)	Stage of decay	Subset
96	97	Cycloheptene †	N/A	N/A	2
96	97	Cyclohexene, 3-methyl †	N/A	N/A	2
96	97	Cyclohexene, 4-methyl †	N/A	N/A	2
96	97	Cyclopentene, 1,5-dimethyl †	N/A	N/A	2
140	141	Methenamine ‡	N/A	Active Decay, Skeletonization	2
140	141	2-(Methylthio), phenol ◊	N/A	N/A	2
140	141	1-decene ⊖	N/A	N/A	2
140	141	Methyl (methylthio) methyl disulphide ◊	N/A	N/A	2
142	143	Nonanal ⊖	N/A	Active, Advanced, Dry	2
142	143	2-nonanone ▫⊖	N/A	Advanced active	2
142	143	Decane ◊*	N/A	N/A	2
142	143	Nonane, 3-methyl ◊	N/A	N/A	2
31	32	Methylamine ◊	899	N/A	3
280	281	Linoleic acid •	N/A	N/A	3
58	59	Acetone ▫◊	812	N/A	4
58	59	2-propen-1-ol ⊖	N/A	N/A	4
62	63	Dimethyl sulphide ◊⊖	830.9	N/A	5
54	55	1,2-Butadiene ◊	778.9	N/A	6



Figure 4.11 Remnants of the carcass at the end of BHA trial 4

The trends observed in this trial, together with the tentative assignment of compounds such as dimethyl sulphide, acetone, linoleic acid, nonanal, 2-nonanone, 1-decene, cyclohexene 3-methyl, cycloheptene, dimethyl disulphide, dimethyl sulphone, phenol, 3-methylpyridine, furan, 2-methyl, pyridine, benzene, dimethyl sulphoxide and 1,2-butadiene previously identified by other studies provides evidence that the CIR-MS is a technique that needs to be explored further in decomposition studies. More importantly, these provisional compounds identified here, suggest that some of the suggested key markers of decomposition remain unambiguous regardless of methodology or instrumentation.

The CIR-MS technique used in this study was effective in monitoring the range of chemical classes expected in pig carcass decomposition odour. However, it should be emphasised that CIR-MS characterises compounds only by their mass, which is not sufficient for definitive identification. The next step involved incorporating an additional technique such as GC-MS capable of increasing the probability of compound identification.

### 4.4.3 SPME-GC-MS

#### 4.4.3.1 Background VOCs

Background samples were collected in a similar fashion to that described in section 4.4.2.1. Methylene chloride and dibutyl phthalate are amongst the VOCs measured in the chamber before the carcass was introduced. Methylene chloride was confirmed to be one of the major components of the adhesive used in binding neoprene to the perspex lid of the chamber, and as a result, methylene chloride was excluded from further analysis. For qualitative purposes, internal standard bromobenzene and compounds that resulted from the SPME coating bleed or column bleed were removed during pre-processing. For example, silicon containing compounds, specifically siloxanes originated from the coating of the SPME fibre and as such were not related to carcass decomposition [123].

#### 4.4.3.2 Decomposition VOCs

Following this, a total of 55 VOCs were identified using SPME-GC-MS (Figure 4.12). The compounds varied across compound classes and almost all chemical families were represented (in parenthesis, the number of chemical compounds identified); sulphur containing compounds (4), nitrogen containing compounds (21), alkanes (6), aromatic compounds (1), halogenated compounds (3), ketones (2), alcohols (4), esters (9), aldehydes (1) and others (i.e. unclassified compounds) (4).

Of the total number of VOCs detected by SPME-GC-MS, 26 chemical compounds were only detected once. 2 compounds were detected twice, and 17 compounds were detected more than three times. From the perspective of defining signature VOCs associated with carcass decomposition, this study defined core VOCs as those with greater than three occurrences. This applied threshold of > 3 occurrences is similar to that employed by other decomposition authors [30, 58]. A compiled list of compounds with three or more occurrences is presented in Table 4.2.

Sulphur containing compound carbon disulphide was detected every day of the trial. N-Morpholinomethyl-isopropyl-sulphide was visible on day 5, 6, 22 and 34. Contributions from dimethyl disulphide were noticed from day 4-7 only, whereas dimethyl sulphide was only detected on days 5 and 6. These findings suggest that days 4 and 7 were the most important for the sulphur containing compounds during BHA trial 4.

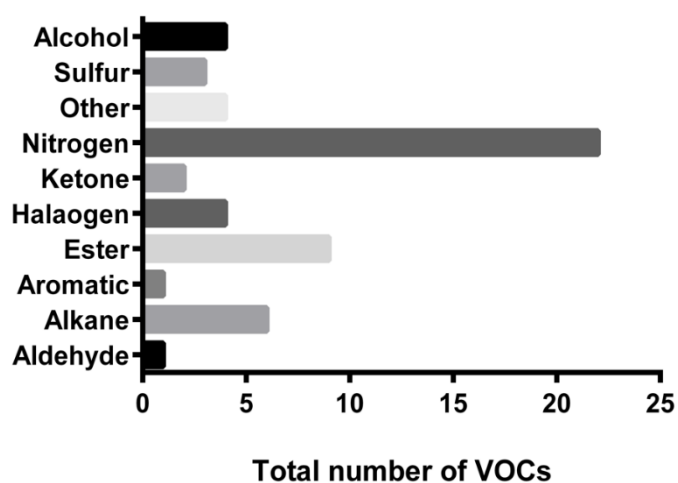


Figure 4.12 Total number of VOCs grouped by chemical class as measured by SPME-GC-MS during BHA 4 trial.

Although nitrogen-containing compounds accounted for majority of the compounds detected (Figure 4.12), only three compounds occurred more than three times. These included N-methylimidazole, ethanethioamide and butanamide N-methyl-4-(methylthio)-2-(2,2-dimethylpropylidene) amino. N-methylimidazole was detected from day 10 until 13, whereas other nitrogen based compounds were sporadic in appearance. In the alkane family, the most common hydrocarbon detected with five occurrences was pentane. The first signal was observed on day 2 and lasted until day 5 before finally reappearing again on day 8 of the trial. In the ketone class, acetone was detected only on day 8, while ketene was seen on day 10, 12 and 18. Formic acid represented the carboxylic acid class and was first detected on day 10. Finally, in the aromatic class, naphthalene was the only compound detected.

Nitrogenous based compounds occur as a result of the breakdown of nucleic acids [27] and hydrocarbons are frequently associated with the active stage of decay [62, 122]. Carboxylic acid such as formic acid is formed through the metabolic conversion of

alcohols into acids, which only occurs in the presence an appropriate metabolizing bacteria and oxygen. Aldehydes and ketones on the other hand are regularly reported as products of fat and muscle degradation [122].

The results generated by SPME-GC-MS showed no clear trend in terms of a particular chemical class evolving at a specific time during the decay process (Figure 4.13). This supports the narrative that the process of decomposition is constantly changing, a point that is often discussed by other decomposition authors. That said, it could be argued that sulphur containing compounds dimethyl sulphide and dimethyl disulphide showed highest contributions between days 4-7. A plausible explanation for the dynamicity of VOCs released into the headspace of a decomposing corpse when buried in soil could be that decomposition by-products adsorb unto soil particles and in turn, there is a retention time factor associated with the release of these VOCs for detection in the headspace. This is especially valid for burials in soil as compounds can coexist in a liquid state between soil particles, as a vapour in soil gas and as a solid adsorbed unto soil particles [68].

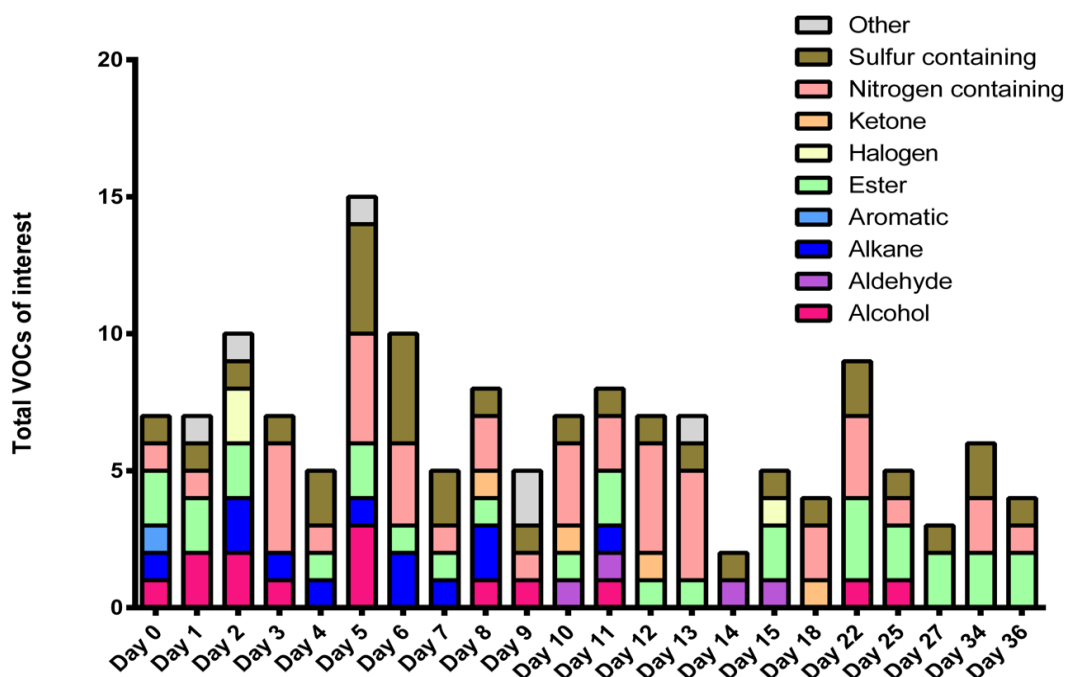


Figure 4.13 Distribution of the different chemical classes measured during BHA 4 trial. Total VOC of interest excludes Internal standard, siloxanes, and methylene chloride. Day 0 represents VOCs measured a day before carcass introduction (background).

This might explain why there is no pattern in the distribution of different chemical classes during this trial (Figure 4.13). In fact, it is for this reason that forensic teams utilise probing techniques during the search of clandestine graves. Once a specific site is suspected to contain a buried corpse, soil probes are inserted into the ground in an attempt release decomposition gas that might be trapped within the soil gas and subsequently cadaver dogs are then employed [69]. In this BHA 4 setup however, the soil surface was left undisturbed as the carcass passed through the different stages of decomposition. The net result of burial in soil is that volatile emissions are significantly reduced compared with the VOCs monitored in an exposed trial (surface deposition).

**Table 4.2** Compounds with greater than 3 occurrences during BHA 4 trial. *RT* refers to retention time in minutes, *R. Match* refers to reverse match, % prob refers to percentage probability and *MW* refers to molecular weight of each compound. Reverse matches and percentage probabilities were reported using the NIST search library. Diazene dimethyl, cyclobutylamine, dimethyl sulphide and hexane only occurred twice during BHA 4 trial.

Compound name	RT	R.Match	% Prob	MW
Pentane	1.76	927	78.3	72
Carbon disulphide	1.92	923	96.3	76
Formic acid hydrazine	2.14	795	85.1	60
Ketene	2.18	999	60.5	42
1H-Imidazole, 1-methyl	2.52	999	6.73	82
Ethanethioamide	3.46	999	15	75
Disulphide, dimethyl	4.77	935	97	94
Diethyl Phthalate	25.57	838	58.8	222
2,6-Bis (1,1-dimethylethyl)-4-(1-oxopropyl) phenol	26.01	844	95.4	262
Butanamide, N-methyl-4-(methylthio)-2-(2,2-dimethylpropylidene) amino	26.17	552	10.5	230
2-trifluoromethylbenzoic acid, 6-thyl-3-octyl ester	26.18	606	21.5	330
N-Morpholinomethyl-isopropyl-sulphide	28.85	840	20	175
2-Morpholinomethyl-1, 3-diphenyl-2-propanol	28.85	827	17.6	311
Dibutylphthalate	29.53	919	15.3	278
Ethaneperoxic acid, 1-cyano-1-(2-(2-phenyl-1,3-dioxolan-2-yl)ethyl) pentyl ester	29.53	850	43.7	347
Phthalic acid, butyl cyclobutyl ester	29.53	888	15	276
Phenol, 4,4 -(1-methylethylidene) bis-	31.61	873	89.8	228
Diazene dimethyl	1.735	961	78.2	58
Cyclobutylamine	1.762	881	59.6	71
Dimethyl sulphide	1.842	888	71.4	62
Hexane	2.286	861	55.9	86

Common VOCs detected in this study when compared with the literature comprised of pentane [28, 62, 68], disulphide dimethyl [28], dimethyl sulphide [28, 68] and hexane [28, 62, 68]. A plausible explanation for the low number of shared VOCs between this

work and the literature could be attributed the differences in sample collection technique and instrumentations used. Carcass decomposition in non-sterile soils has been reported to be greater compared with soils without soil microorganisms. In the results generated by Carter 2005 [46] soil microbiota began to participate in later phases of carcass breakdown following the reduced activity of cadaveric microbes in the early phase of decomposition. The decomposer population in this study was comprised entirely of carcass microbes and invertebrates which typically burrow into the grave to reach the organic matter (corpse) were excluded. Therefore, the rate of gas transfer, specifically O<sub>2</sub>, within the soil was significantly limited. This in turn would promote anoxic conditions and the prevalence of anaerobic microbial activities. Thus, it could be argued that the buried human analogue trials proceeded predominantly under anaerobic conditions. However, considerations must also be given to the presence of free O<sub>2</sub> within synthetic air which flowed through the headspace of the decomposition chamber. As a result, diffusion of oxygen through the soil would promote aerobic metabolisms.

The time profiles of 10 compounds with greater than 3 occurrences during BHA 4 trials is illustrated in Figure 4.14. Samples were collected daily from day 1- 15, and periodically afterwards depending on availability of the GC-MS instrument (days 18, 22, 25, 27, 34 and 36). Day 36 marked the last day samples were collected for analysis by SPME-GC-MS.

The time profiles of the 2,6-Bis (1,1-dimethylethyl)-4-(1-oxopropyl) phenol, pentane and phenol, 4,4 -(1-methylethylidene) bis- suggest that the fresh and bloated stage occurred between days 1-3. Active stage was denoted by the behaviour dimethyl disulphide and dimethyl sulphide between days 4-7 and advanced decay is proposed to have occurred between days 18 and 34 by the activity of carbon disulphide pentane, 2,6-Bis (1,1-dimethylethyl)-4-(1-oxopropyl) phenol, N-Morpholinomethyl-isopropyl-sulphide and 2-trifluoromethylbenzoic acid 6-thyl-3-octyl ester.

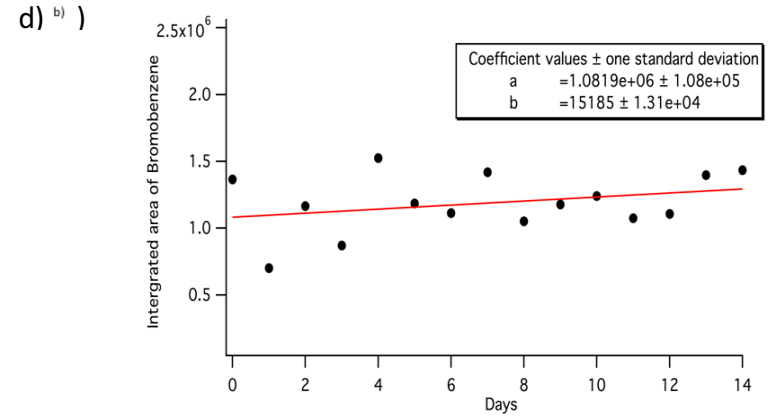
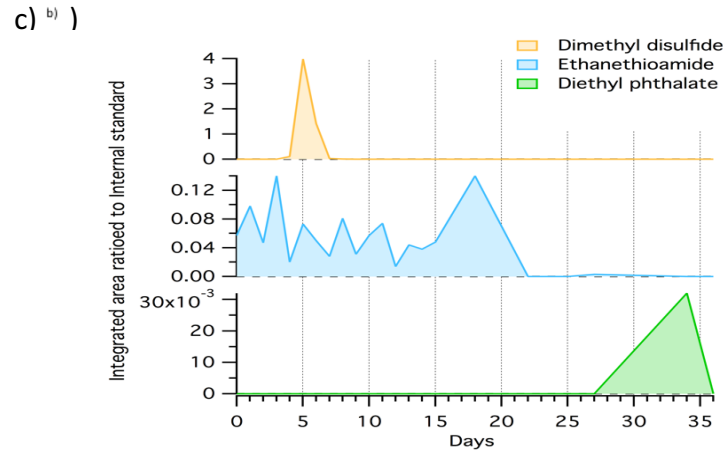
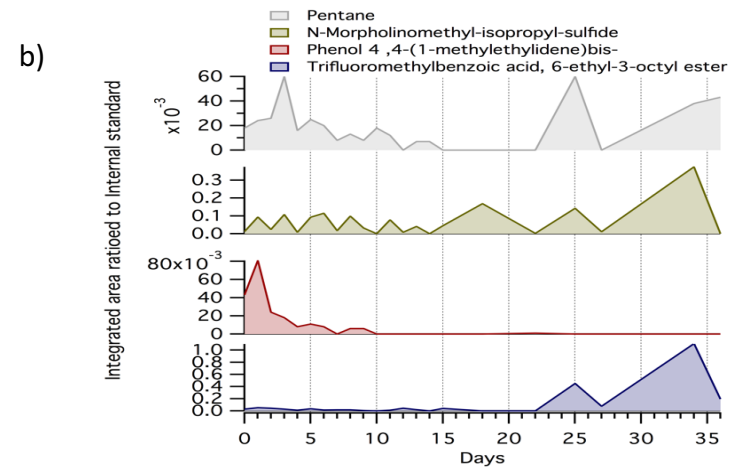
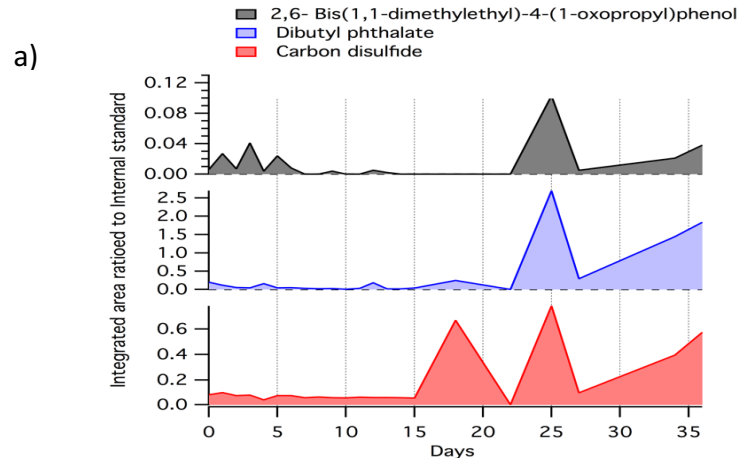


Figure 4.14 Temporal variations of decomposition related VOCs with greater than three occurrences during BHA 4 trial as measured by SPME-GC-MS (images a-c). The stability of internal standard bromobenzene over the first 2 weeks is shown in image d. The precision (RSD) of the internal standard was calculated as 17.4%

In conclusion, majority of the VOCs detected by SPME-GC-MS in the headspace of BHA trial 4 have not been previously documented in the literature, perhaps a reflection of the nature of the experimental setup of this trial, collection technique and operational settings used.

Initially, the primary instrumentation used to follow the succession of decomposition VOCs in this research project was CIR-MS because of its real-time capabilities and simultaneous detection of almost all classes of compounds. However, identifications of compounds based solely on molecular mass presented challenges especially in complex matrixes such as those produced during carcass decomposition. VOCs with identical molecular masses overlap at the same mass channel, as well as fragment ions. This makes compound identification increasingly complex. As a means to circumvent this problem, SPME-GC-MS was incorporated to aid in speciation of the VOCs detected by CIR-MS.

The results collected by SPME-GC-MS in this BHA 4 trial emphasises the selectivity of the technique. The type and amount of VOCs extracted from the headspace of the decomposition chamber is heavily dependent on the composition of the SPME fibre coating and column packing material, as well as other experimental parameters such as exposure times, GC oven temperature and humidity. This might explain why only four of the VOCs detected by SPME-GC-MS (dimethyl disulphide, dimethyl sulphide, hexane and pentane) have been previously documented by other decomposition authors. Hexane and pentane were previously detected in the skeletonised stage of decay [62, 68]; however in this trial, hexane was detected much earlier (day 6 and 7) and pentane on day 3 and 25. Conversely only dimethyl sulphide and dimethyl disulphide produced in the active stage in this trial are in line with other decomposition studies [28, 68].

Finally, the high relative humidity within the decomposition chamber might have increased competition between decomposition VOCs and water molecules for sites on the fibre. In addition, characteristics of the SPME fibre could also have been altered due to adsorption of water molecules [115, 116].

#### 4.4.4 Reproducibility of decomposition VOCs (BHA trial 3)

To assess the reproducibility of the decomposing VOCs, the buried human analogue trial was duplicated. BHA trial 3 began on 11<sup>th</sup> April through until May 2014 and the manner of death was identical to the carcass used in the previous trial. The carcass weighed 36 kg at the beginning of the trial and CIR-MS was used to monitor the succession of VOCs in the headspace above the buried carcass. At the time of this trial, the GC-MS was unavailable and as such only results generated by CIR-MS are discussed in the next sections.

Two unique groupings were determined from the results generated by CIR-MS in BHA trial 3. The first subset described the behaviour of six parent ions;  $m/z$  79, 94, 95, 96, 97 and 141 (Figure 4.15). The time profiles of these compounds were most pronounced between days 4 and 8 of the trial. Subset 2 consisted of mass channels 37, 55 and 63 (Figure 4.16.). As described in section 3.2.2,  $m/z$  37 and 55 are routinely related to hydrated hydronium clusters in CIR-MS measurements.

The time of occurrence, duration, and the concentration profiles of the mass channels monitored within subset 1 and 2 of BHA 3 (figure 4.15 and figure 4.16) were similar to that observed in subsets 2 and 5 of BHA 4 trial (Figure 4.6 and figure 4.9). This result provides evidence that this particular phase of decomposition (active stage) is reproducible in this experimental setup.

Overall, the results obtained by CIR-MS in the buried trials illustrate that there is a characteristic time frame during decomposition of a carcass buried in sterile soil where specific decomposition volatiles are released. The two independent trials demonstrate that one of the most distinctive periods of carcass decay occurs between days 4 and day 8 (80- 160 ADD).

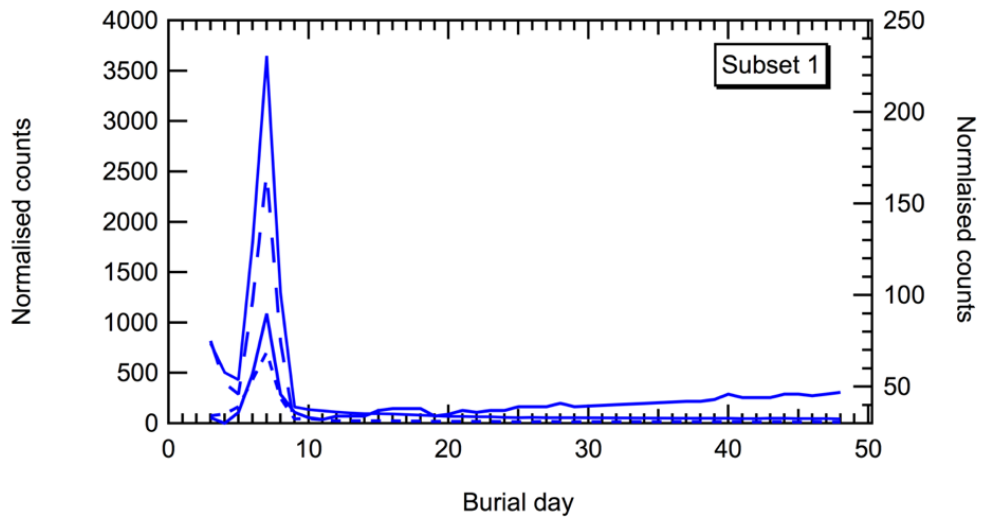


Figure 4.15 Temporal variations of mass channels 79, 94, 95, 96, 97 and 141 (subset 1) as measured by CIR-MS in BHA trial 3.

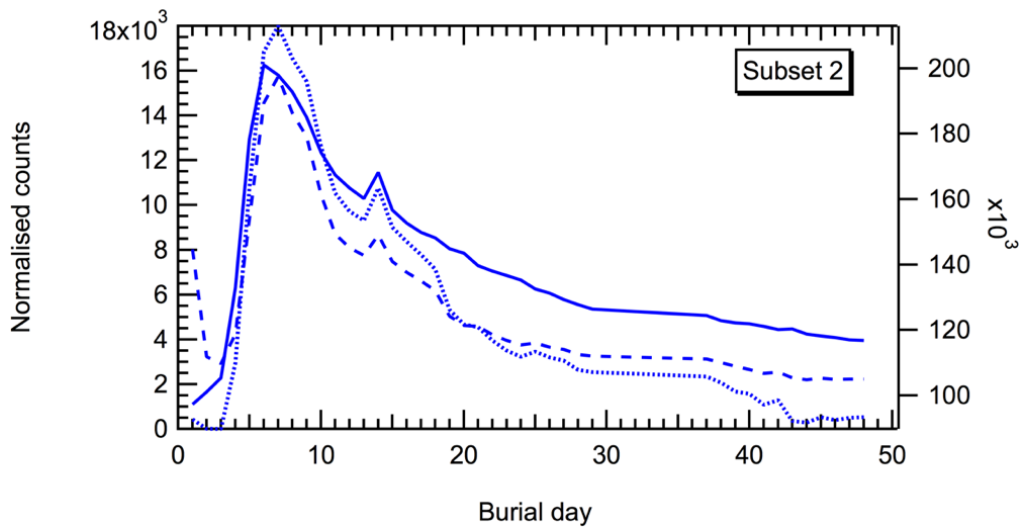


Figure 4.16 Temporal variations of mass channels 37, 55 and 63 (subset 2) of as measured by CIR-MS of BHA trial 3

## 4.4.5 Validation and Quantification of decomposition

### VOCs

As mentioned in Chapter 3, twenty compounds expected to be released during carcass decomposition were purchased and used as standards to calibrate both CIR-MS and SPME-GC-MS instruments. Full details of these standards have already been provided in Table 3.2. The results of the linear fits from the calibration curves (Figure 3.11) for each respective standard was used to yield quantitative information.

DMDS and DMS were detected via both instruments in both BHA trials. However, this cohesiveness was not observed for all compounds; for example, mass channel 49, tentatively assigned as methanethiol, was detected by CIR-MS in BHA 4, but not by GC-MS or by CIR-MS in BHA 3. Whereas the equivalent mass channels for acetone and decane detected by GC-MS were seen via CIR-MS only in BHA 4. Unsurprisingly, alkanes hexane and pentane could not be detected by CIR-MS. An overview of the relationship between mass channels observed by CIR-MS (BHA 3 and 4) and compounds detected by GC-MS (BHA 4) are presented in Table 4.3.

**Table 4.3 Overview of the core compounds detected via CIR-MS and SPME-GC-MS across BHA 3 and BHA 4 trials. Mass channels (MW+1) is presented under CIR-MS column.**

BHA 4		BHA 3
CIR-MS	GC-MS	CIR-MS
49		
59	Acetone	
63	DMS	63
79	Thiourea	79
94		94
95	DMDS	95
96		96
97		97
137		
141		141
143	Decane	
	Carbon disulphide	
	Pentane	
	Hexane	

According to the results obtained by SPME-GC-MS, acetone was only detected on day 8, decane on day 0 (background) and hexane on days 6 and 7. This suggests that the behaviour observed in m/z 59 within subset 4 of BHA 4 (Figure 4.8 ) and m/z 143 of subset 2 in BHA 4 (Figure 4.6) were not associated with acetone and decane respectively.

Through application of the equation of the linear fit generated from the calibration curves of DMS, DMS, carbon disulphide and pentane (figure 3.11 and figure 3.21) concentrations in units of ppbV were calculated for measurements collected by CIR-MS and SPME-GC-MS across both BHA trials. These are illustrated in the form of concentration maps in Figure 4.17 and Figure 4.18.

It is clear from Figure 4.17 that measurements collected for DMDS were not only in agreement across both buried human analogue trials, also the time frame DMDS was released was consistent regardless of the instrumentation used. Hence, it can be concluded that the most important days for the production of DMDS in this experimental set-up was between days 4 and 8 (80- 180 ADD). This time period denotes the active stage of decomposition. Likewise, DMS can be attributed to a similar time frame, although it was first observed a day earlier (day 4, 60 ADD) and its concentration slowly declined until the end of the trial.

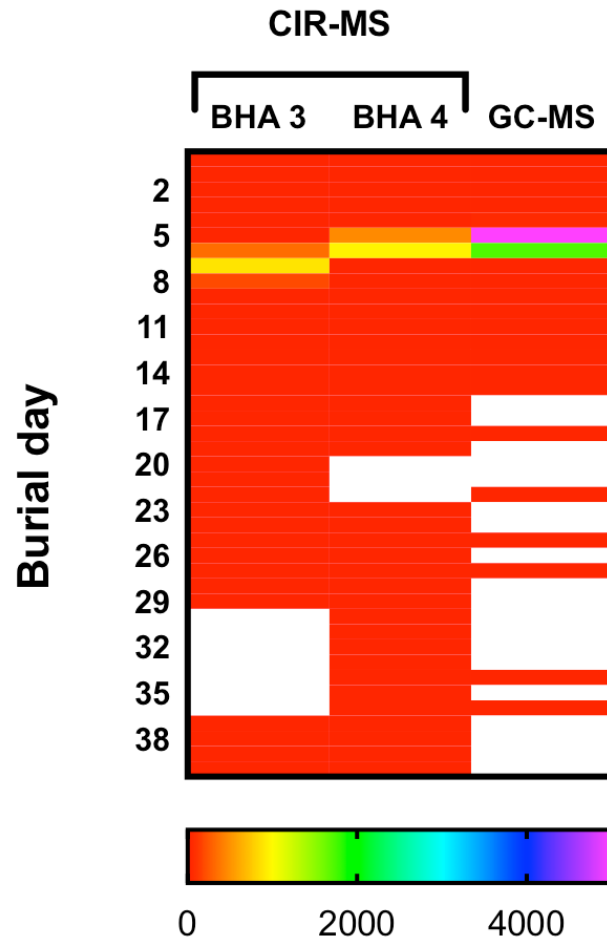
The concentration of DMDS measured by CIR-MS was similar across both BHA 3 and BHA 4 trials (1000 ppbV), although the reported concentrations measured by SPME-GC-MS is approximately 4 times higher than CIR-MS. Figure 4.17 suggests the concentration of DMDS was as high as 5000 ppbV on day 5, although results of the calibration curve in Figure 3.21 indicated that concentration of DMDS above 4000 ppbV fell outside the linear range of the CAR/PDMS fibre used. Thus, the only conclusion that could be drawn from DMDS is that its concentration was in excess of 4000 ppbV on day 5.

Despite observing the highest concentration of DMS between days 4 and 10 in CIR-MS, the absolute concentration differed between the trials. In BHA 3, it was estimated that the highest concentration of DMS was approximately 300 ppbV, whereas in BHA 4, it

was only 60 ppbV. Since the weight of the carcass used in BHA trial 3 was approximately 5 times larger than that of BHA 4, it is feasible that the difference in the concentration of DMS can be attributed to the disparity in composition of muscle in the carcass. This is especially relevant for polysulphides such as DMS as it is released as a product of protein degradation [27].

In contrast, DMS was only observed on day 6 in BHA 4 via SPME-GC-MS, with a concentration of approximately 150 ppbV. Humidity, evidenced to have an effect on the uptake of VOCs by SPME, might explain this discrepancy. From Figure 3.19 the findings from the study on the effect of humidity on VOC uptake by SPME revealed that the sensitivity of DMS decreased with increasing humidity. Although a maximum relative humidity of 89% was investigated in the humidity study, the relative humidity of the decomposition chamber was in excess of 99.8% throughout BHA trial 4. Aside from the RH reading collected by CS215 sensor,  $m/z$  37 and 55 used as proxies for humidity also verified the upsurge in humidity in the chamber from day 4 to day 11 (Figure 4.10). As a consequence, it is possible that competition between DMS and water molecules for adsorption sites on the CAR/PDMS fibre, resulted in the absence of DMS beyond day 6 of BHA 4 trial 4.

## DMDS



## DMS

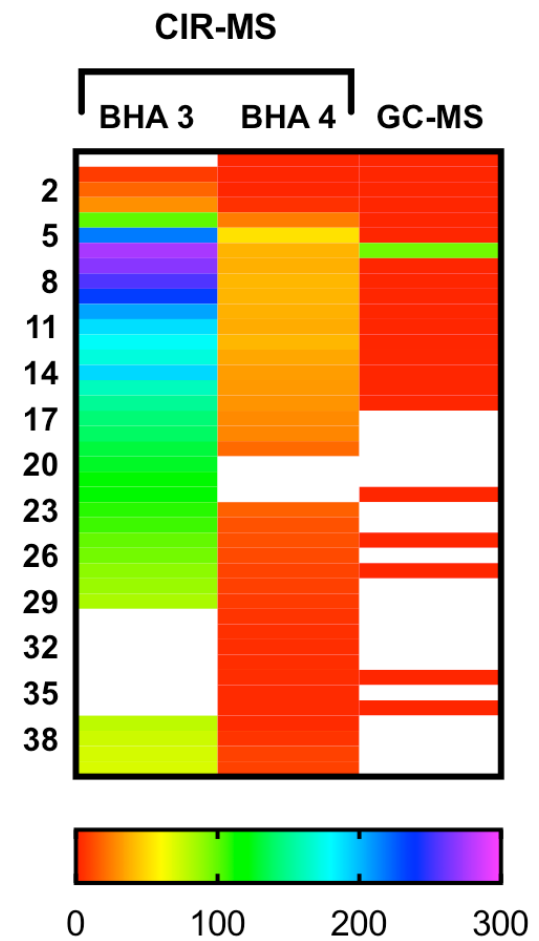
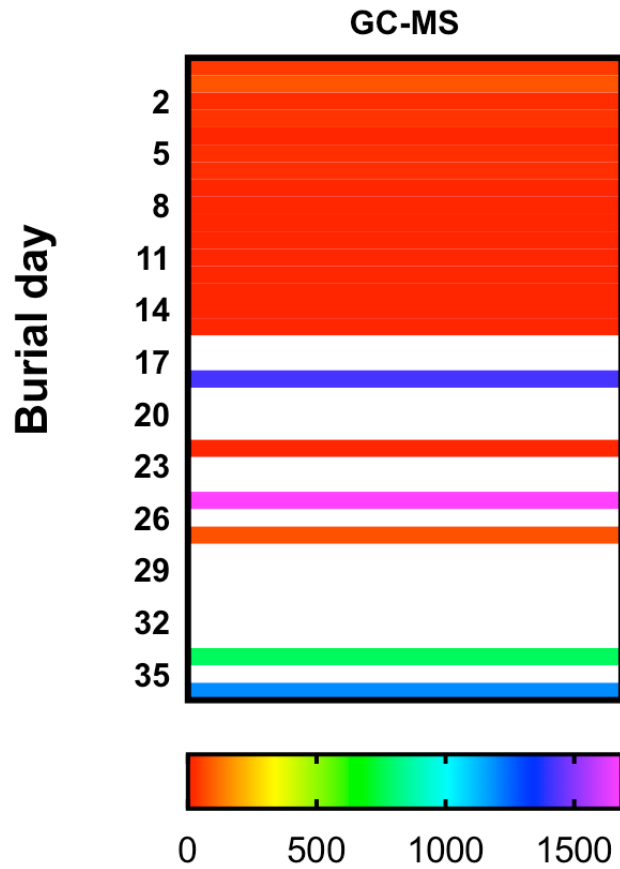


Figure 4.17 Illustrates the concentrations of core decomposition VOCs dimethyl disulphide (DMDS) and dimethylsulfide (DMS) as measured by CIR-MS and SPME-GC-MS during buried human analogue trials (BHA 3 and BHA 4). GC-MS measurements were only collected during BHA trial 4

## Carbon disulfide



## Pentane



Figure 4.18 Illustrates the concentration profile of carbon disulphide and pentane as measured by SPME-GC-MS during buried human analogue trial 4.

Finally, carbon disulphide and pentane were not detected on CIR-MS in either studies. This is unsurprising for pentane as hydrocarbons with C<sub>5</sub> or less are not typically observed when hydronium is used as the reagent ion in proton transfer reaction [92]. In SPME-GC-MS, Carbon disulphide was significantly noticeable on day 18, but by day 25 concentration as high as 1500 ppbV could be seen. Pentane on the other hand was sporadic in appearance. The highest pentane concentrations of 120 ppbV was observed on day 3 and day 25 of the trial.

## 4.5 Chapter 4 Summary

The process of decomposition of two pig carcasses were independently followed by examination of the VOCs released into the headspace of a bespoke decomposition chamber. The nature of burial and experimental setup in both trials were identical. Both carcasses were purchased from the same farm, and as such it is argued that their nutritional make-up would have been similar during their lifetimes. There was no record of ailments in either carcass at the time of purchase, and the method of slaughter was the same. The only difference between the carcasses in BHA trial 3 and BHA trial 4 was their mass pre-burial. The carcass used in BHA 4 trial weighed 7.48 kg and in BHA 3 trials the carcass weighed 36 kg. The evolution of VOCs into the headspace region of the chamber was monitored simultaneously by CIR-MS and SPME-GC-MS.

In BHA 4 trials 4, a total of 59 mass channels were extracted from the CIR-MS dataset as being pertinent to decomposition. While SPME-GC-MS identified a total of 55 compounds. Comparison of the time profiles generated by each analytical technique showed that only the measurements for dimethyl disulphide was in agreement across both instruments. A possible explanation for the variability in the types and compounds detected by each technique, specifically SPME-GC-MS could be attributed to any one of the following; choice of SPME fibre coating, exposure time, sample humidity, GC operating temperatures and column choice. That said, review of the results generated by SPME-GC-MS independently, showed that four compounds (pentane, disulphide

dimethyl, dimethyl sulphide and hexane) detected in BHA trial 4 had been previously identified by other decomposition authors.

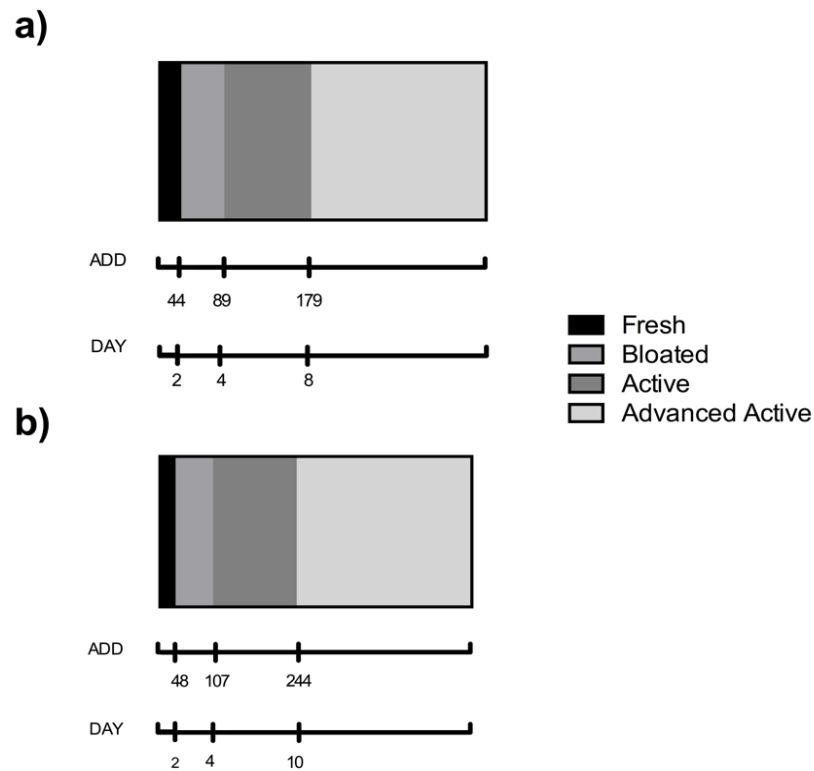


Figure 4.19 Stages of decomposition in Buried Human Analogue 4(a) and (b) work conducted on 70 kg carcass left to decompose on the surface of the ground by Perrault et al [68]

The results generated by CIR-MS in both BHA 3 and BHA 4 trials were similar. Despite the difference in weight of the carcasses, the rate of decomposition from a temperate perspective was comparable to each other, as well as to work conducted by other decomposition authors [68] (Figure 4.19). The findings generated by CIR-MS showed that both carcasses released six common VOCs between days 4 and 8, with dimethyl sulphide and dimethyl disulphide amongst this group. In addition, the compounds released and the duration of this characteristic time period in both carcasses led to the conclusion that the active stage of decay occurred between days 4-8 in this set up.



# 5 THE ANALYSIS OF VOCS RELEASED FROM MAMMALIAN DECOMPOSITION DURING EXPOSED HUMAN ANALOGUE TRIALS (EHA)

## 5.1 Introduction

As outlined in chapter 1, one of the main objectives of this research project was to study the evolution of VOCs from buried carcasses as a way to understand the influence soil has on the release of decomposition compounds. Therefore, it was deemed necessary to first determine the VOCs released from unburied carcasses (exposed human analogue trials). There is still a rapidly growing literature concerning the elucidation of core decomposition VOCs regardless of the nature of deposition; which will significantly improve upon current canine training aids [6, 20]. In some regard, the work discussed in this chapter can be viewed as control experiments to the buried trials already reviewed in Chapter 4.

Coupled with the above point, there is the additional aim to determine if under-represented CIR-MS is a viable technique to be used in the study of decomposition. To assess this, exposed human analogue trials were piloted and CIR-MS was used as an online technique to follow the succession of VOCs released from the decaying carcasses. The data gathered were then used comparatively against SPME-GC-MS measurements collected within the same trial. Despite this assessment qualifying as an initial validation check, comparisons of the VOCs observed in the headspace of the exposed trials were

extended across the literature, especially as the vast majority of documented VOCs thus far have relied on results generated from surface deposited carcasses.

That said, consideration must be given to the nature of the experimental setup within EHA trials, specifically because of the use of an indoor decomposition chamber. Aside from the apparent exclusion of environmental fauna and flora, and the differences in carcass mass, the internal conditions of the chamber are different to anything that has previously been documented. Therefore, it can be expected that the carcass within these exposed trials might progress through decomposition at a different rate, meaning the onset and duration of each decomposition stage and the number and types of VOCs released may differ from what is already known.

Nonetheless, these differences were embraced, as it served as a reflection of the dynamicity encountered in real forensic cases.

## 5.2 Experimental setup

The first exposed human analogue trial (EHA 2) was conducted on October 3<sup>rd</sup> until November 10<sup>th</sup> 2014, while the second trial (EHA 3) took effect from January 14<sup>th</sup> until 10<sup>th</sup> February 2016. The carcasses were of the same species (*sus scrofa*) and weighed < 15 kg and 27 kg respectively. In addition, both carcasses were raised on the same farm suggesting some degree of consistency in their diet when alive, and the manner of death remained unambiguous. Illustrated in Figure 5.1 is the chamber setup of the exposed trials.

Horticultural grade lime free silica sand was chosen as the surface of deposition, and 1 ppmV of bromobenzene (internal standard) diluted in artificial air (zero grade) were passed over the carcass at a combined flow rate of 300 sccm to simulate wind dispersion. Campbell Scientific CS 215 probe was used to measure ambient temperature and relative humidity, while CS 650 sensor was used to monitor sand temperature and volumetric water content (VWC).

CIR-MS was the principal instrument used to follow the succession of VOCs from the decomposing carcasses, predominantly because of its ability to monitor compounds from almost all chemical classes quickly and simultaneously [100]. When available, headspace VOCs were also analysed concurrently by use of SPME-GC-MS. SPME samples were collected at noon every day for a total of 14 days, during EHA trial 3, after which sampling occurred on alternate days until a total of 27 days had passed. A full description of the SPME-GC-MS method used has already been discussed in detail in Chapter 3.

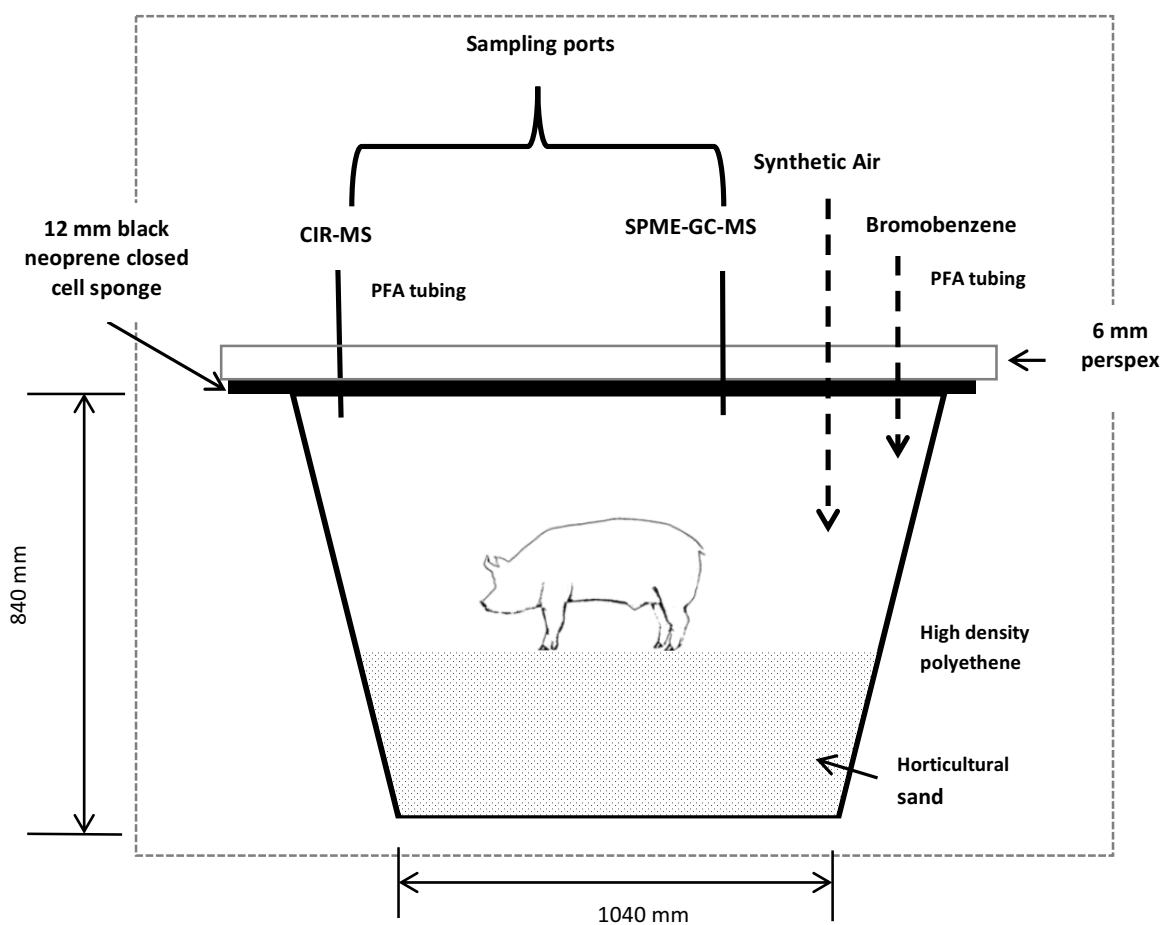


Figure 5.1 Cross-sectional view of the bespoke decomposition chamber during the Exposed Human Analogue trials.

## 5.3 Results and Discussion

### 5.3.1 Physical conditions

Soil temperature during EHA trial 3 was 20.76 °C with a maximum of 21.1 °C and minimum of 20.3 °C, while the maximum and minimum soil temperature of EHA 2 was 22.7 °C and 22.1 °C respectively, with an average of 22 °C. The total temperature change across both EHA trials was less than 1°C, meaning that changes in temperature would not be the most dominant factor to govern the rate of carcass decomposition (Figure 5.2). Nonetheless, accumulated degree days were still calculated from the temperature readings to maintain consistency across the project, as well as to allow comparisons between studies conducted by other carcass decomposition authors.

Regrettably, the volumetric water component (VWC) of the CS650 sensor became saturated beyond day 10 during both EHA trials and as a result, data collection was incomplete. To that end, Figure 5.3 provides an indication of the water content in the sand (in percent) before the CS650 sensor reached maximum capacity. Relative humidity monitored by CS 215 probe measured at 99.8% before the carcass was introduced into the decomposition chamber and remained at this maximum value throughout the decomposition process. Consequently, humidity in CIR-MS was estimated by the use of hydrated hydronium clusters as described in section Figure 3.8.

The VWC suggests that the water content of the sand progressively increased as the carcass underwent decomposition. More importantly, saturation of the sensor beyond day 10 implies the release of significant amounts of liquid decomposition by-products; a trend which is often observed to signify the transition into a new stage of decay [59].

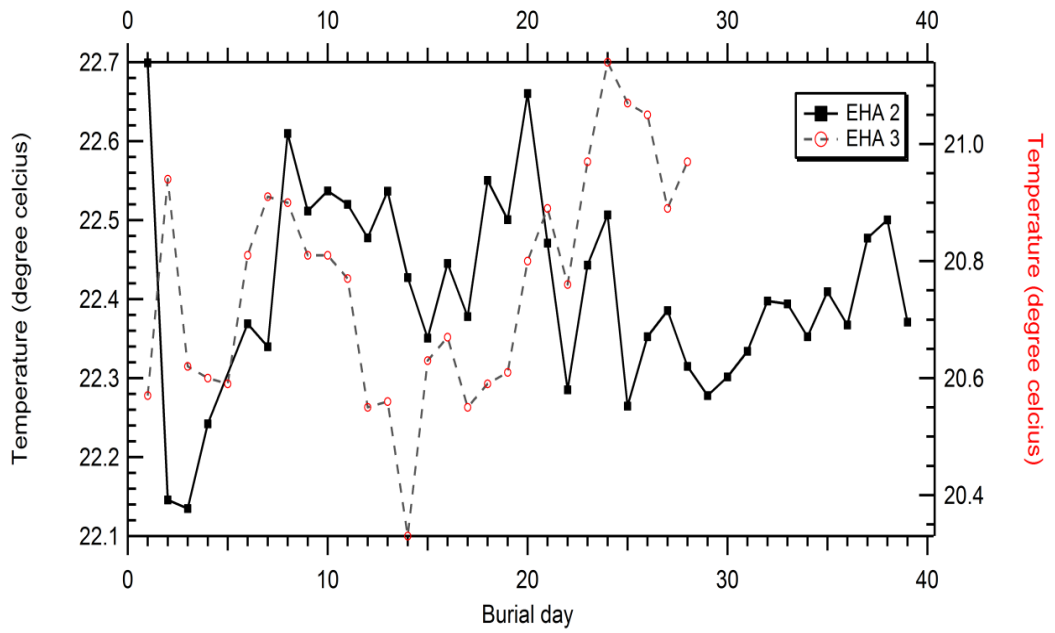


Figure 5.2 Temperature profile of the sand used as the surface for deposition during Exposed Human Analogue (EHA) trials 2 and 3. Measurements were collected hourly by use of Campbell's Scientific CS650 sensor and were averaged daily over a period of 40 days during EHA2 and 30 days during EHA 3.

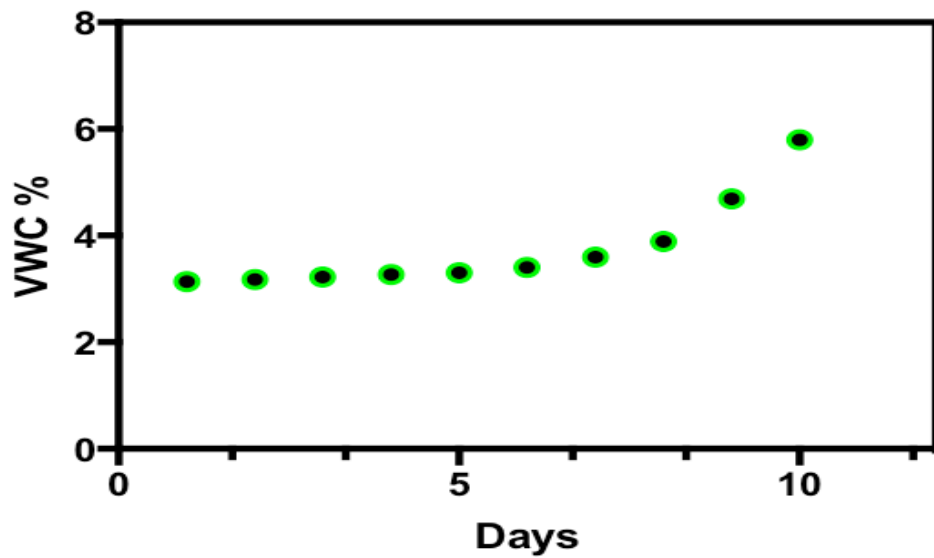


Figure 5.3 Volumetric water content of the decomposition chamber during EHA trial 3 as measured by Campbell Scientific CS650 sensor.

## 5.3.2 CIR-MS

### 5.3.2.1 Competing reagent ions

Typically, CIR-MS operates via proton transfer from the reagent ion  $\text{H}_3\text{O}^+$  to analyte gas  $M$  to form  $M\text{H}^+$ [92], which is subsequently separated by mass to charge ratio in the flight tube region of the mass spectrometer. The CIR-MS instrument used in this project generated  $\text{H}_3\text{O}^+$  when pure  $\text{H}_2\text{O}$  vapour was ionised by the  $\alpha$  particle emitter  $^{241}\text{Am}$ . Primary ions ( $\text{H}_3\text{O}^+$ ) undergo non-dissociative reactive collisions with analyte molecules to form ( $M\text{H}^+$ ) which is represented by a peak in the resulting mass spectrum. The dominant primary ion ( $\text{H}_3\text{O}^+$ ) signal at  $m/z$  19 is typically observed in the spectrum as having a relative abundance in the region of >90%, with minor traces of  $\text{NO}^+$  and  $\text{O}_2^+$  at  $m/z$  30 and  $m/z$  32 respectively (Figure 5.4a).

That said, it is also possible to encounter instances where the primary ion is not  $\text{H}_3\text{O}^+$ . This was the case with the exposed human analogue trials, as  $\text{NH}_4^+$  was detected to be the most abundant ion. Investigation of the use of other ions other than  $\text{H}_3\text{O}^+$  in proton transfer reactions has been discussed in great detail by other authors [110, 111]. During the exposed trials, it became apparent that the headspace gas mixture contained vast amounts of  $\text{NH}_3$ , which was produced as a direct result of carcass decomposition. The source of  $\text{NH}_3$  is demonstrated in Figure 5.4c as it shows a steady increase in intensity as EHA 3 progressed.

The second significant observation was that  $\text{H}_3\text{O}^+$  ions depleted as ammonium surged to become the governing chemical ionisation reagent ion. As a direct consequence,  $\text{H}_3\text{O}^+$  and  $\text{NH}_4^+$  were regarded as being competing reagent ions in the exposed trials. Equations 5.2 and 5.3 explains the reaction pathways occurring in the drift tube as a result of this competitive behaviour. The transfer of a proton from  $\text{NH}_4^+$  is most likely to occur only if it is energetically favourable i.e. if the proton affinity of the analyte  $M$  is higher than that of  $\text{NH}_4^+$  ( $854 \text{ kJmol}^{-1}$ ). Most organic molecules possess proton affinities less than  $\text{NH}_4^+$  with the exception of some nitrogen containing compounds, meaning a simple proton transfer between  $\text{NH}_4^+$  and majority of organic molecules will not be feasible from day 13 onwards in EHA trial 3. Since most organic compounds will not

receive a proton from  $\text{NH}_4^+$ , it is more likely that association reactions are occurring to form  $\text{M.NH}_4^+$  adducts.

Though other chemical ionisation reaction pathways might have been occurring in the drift tube, this work focused primarily on proton transfer reactions from hydronium. That said, there are advantages to working with ammonium as a reagent ion. The main benefits are as follows; 1) it can be used to distinguish between molecules having the same molecular mass; by exploiting the difference in proton affinities of ammonia and water and 2) interpretation of the resulting mass spectra might be simplified as ionisation via ammonium is softer, meaning reduced ion fragmentation [100, 104]

However, despite the advantages of ammonium as a reagent ion, the fluctuating nature of competing ions increased the complexity of data analysis by reducing the ability to determine the distinct phases attributed to carcass decomposition. For example, it became challenging to determine if the changing intensity of a compound was a direct result of, a) change in the physical process that is decomposition, or b) switch in reagent ions. Compounds with proton affinities between  $691 \text{ kJmol}^{-1}$  and  $853 \text{ kJmol}^{-1}$  will not be accurately represented in the mass spectrum from day 13 onwards. As a direct consequence of this, only results generated when hydronium was in excess (day 1-10) will be discussed further. In doing so, the basic principles for product identification and quantification in CIR-MS when operated under hydronium could still be applied. Also, it means that strategy of normalizing to 1 million counts of  $\text{H}_3\text{O}^+$  at  $m/z$  19 was kept consistent across all human analogue trials discussed in this thesis.

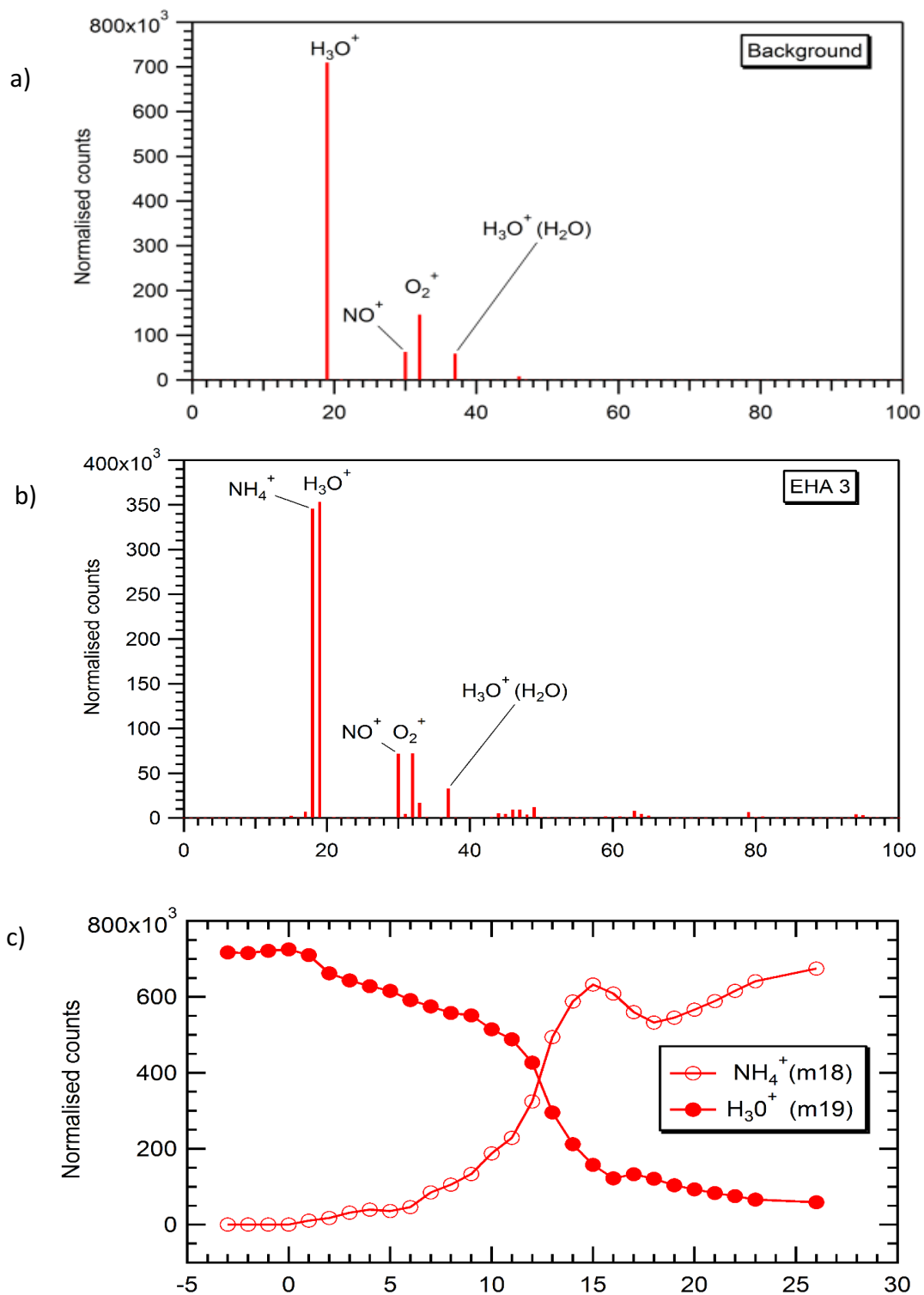
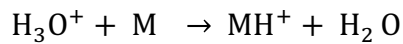
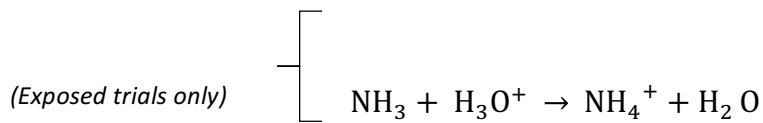


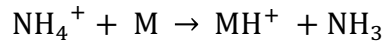
Figure 5.4 Average background mass spectrum generated prior to EHA trial 3 a) Average mass spectrum generated during EHA 3 trial b) and the temporal variations of primary ions m/z 19 (hydronium) and m/z 18 (ammonium) as detected during EHA trial 3 c). The x-axis represents m/z in (a) and (b), while (c) corresponds to experimental day. Negative days denote activity in each channel prior carcass introduction. All counts are normalized to total ion count (TIC) and are derived from the CIR-MS instrument.



Equation 5.1



Equation 5.2



Equation 5.3

### 5.3.2.2 Decomposition VOCs

Analysis of the dataset collected by CIR-MS revealed four characteristic temporal variations within the first 10 days of EHA trial 3. Of these, three subsets were argued to describe the onset of the fresh, bloated, and active stage of decomposition (Figure 5.5). The first 3 subsets comprised of a total of 21 mass channels which represented compounds of varying concentrations. These compounds are believed to be potential markers of decomposition; whereas subset 4 showed the behaviour of hydrated hydronium ions. The data analysis approach applied in the deduction of these mass channels has already been reviewed in section 2.3.5. Background subtraction in the traditional sense could not be applied to this type of work because of the differences in sampling days, nonetheless, inclusion of background contribution in the time profiles (negative days) gives an indication of the behaviour of each mass channel prior to the introduction of the carcass into the decomposition chamber.

The first subset described the behaviour of mass channels 18, 33, 44, 49, 79, 80, 94 and 114 (Figure 5.5a). These compounds showed an increase in intensity from day 0 until day 10. The observed trend implies that these compounds were produced in increasing amounts during decomposition. On the other hand, the compounds of the second subset comprised of mass channels 39, 40, 41, 43, 57, 61, 63, 73, 75, 88 and 89. These compounds showed an initial rise in the first 2-3 days, followed by a dramatic increase from days 5-8. Beyond day 8, intensities declined considerably (Figure 5.5b). Finally, subset three consisted only of mass channel 95, which showed a gradual increase from day 0-2, constant intensity from day 3-4 and a secondary rise from day 5-10 (Figure 5.5c).

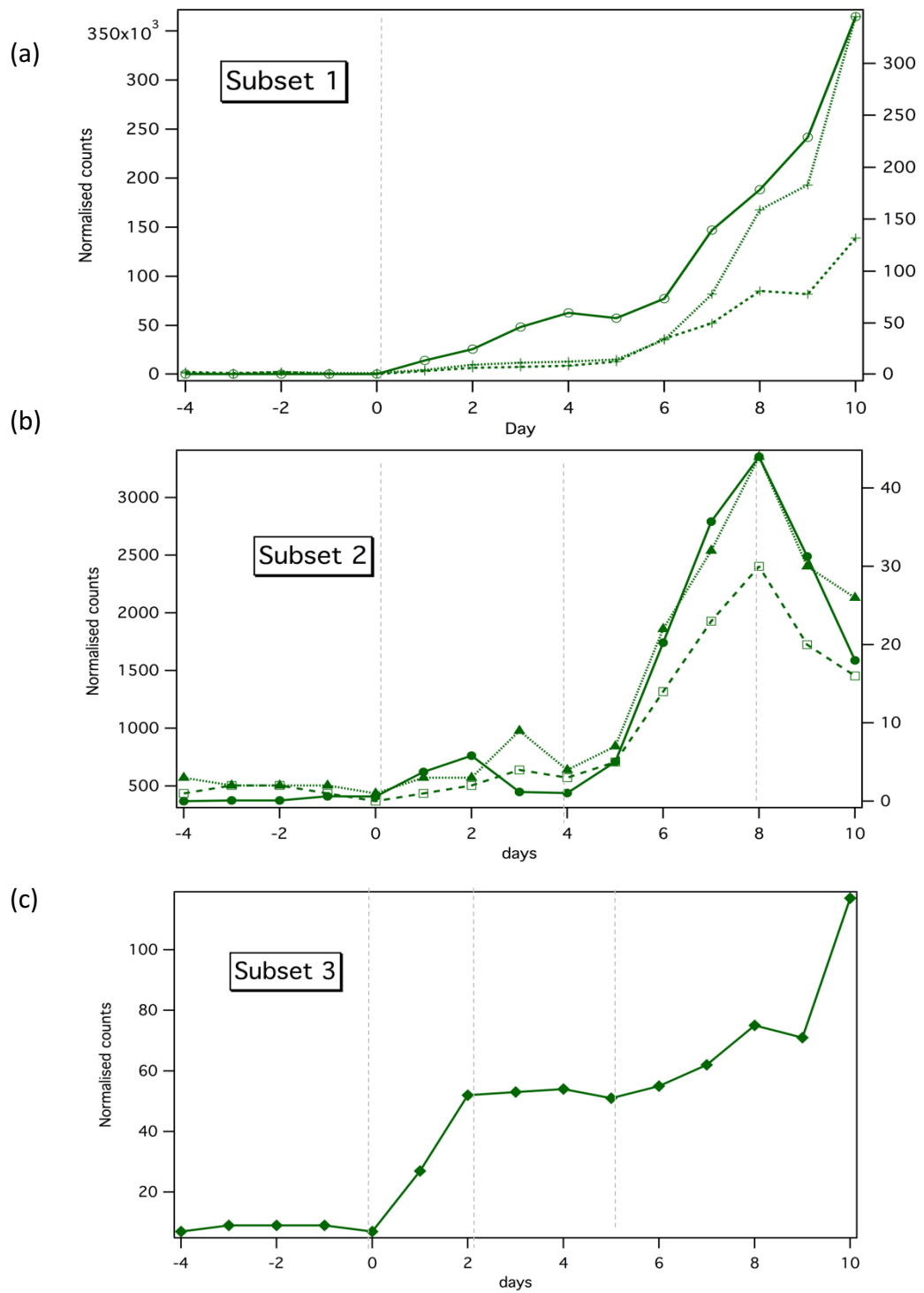


**Figure 5.5** Temporal variation of three subsets argued to describe the process of decomposition in EHA trial 3. Subset 1 consists of mass channels 18, 33, 44, 49, 79, 80, 94, 114 (a), subset 2 consists of mass channels 39, 40, 41, 43, 57, 61, 63, 71, 73, 75, 88, 89, (b) and (c) subset 3 consists of mass channel 95.

The findings depicted in Figure 5.5 suggest that the fresh stage of decomposition in EHA 3 occurred from day 0-2, bloated from days 3-5, and active from day 6 onwards. The VWC data (Figure 5.3) also aligns with the proposed time frame of the active stage of decomposition because it showed that the water content of the sand increased from day 6 onwards. This agrees with the release of accumulated liquid products from the carcass [59].

Unfortunately, owing to the added complications of competing ion ammonium, there was not enough evidence to ascribe a timescale to any other stage of decomposition. Figure 5.6 shows the carcass at the end of the bloated stage (day 5).



**Figure 5.6 Photograph of the bloated carcass on day 5 of EHA trial 3.**

As mentioned in Chapter 2, a drawback of CIR-MS lies in compound identification, especially when employed in non-targeted analysis, such as the work conducted here. As a result, chemical assignment of the spectra can only be tentative. In this work, the activity of the 21 mass channels argued to echo the stages of carcass decay, were compared against results currently available in the literature. Though the instrumentation and techniques may be different, this work is the first time CIR-MS is employed in the study of decomposition VOCs.

Sulphur based compound methanethiol ( $\text{CH}_4\text{S}$ ), is argued to be responsible for the activity in mass channel 49 (subset 1). This is plausible because methanethiol possess a proton affinity significantly higher than that of water, and as such, the transfer of a proton from hydronium would be thermodynamically favourable. Likewise, methanethiol has also been previously detected by other decomposition authors [27, 28], although there is no mention of the stage of decay from which it is released. The data gathered in this trial suggests that methanethiol was released from the fresh, bloated and active stages of decomposition.

Mass channel 63 was tentatively assigned as dimethyl sulphide (DMS) because it was expected to be able to accept a proton from primary reagent ion hydronium. Another equally supportive justification for this assignment was that DMS remains one of the most frequently reported sulphur based compound detected in the study of carcass decomposition [28, 68]; alongside dimethyl disulphide (DMDS) which is also likely to be responsible for the activity in mass channel 95. Dimethyl sulphide has been stated as being associated with the active stage of decay, whereas dimethyl disulphide has been related to all stages, excluding the fresh stage [20, 28, 61, 68]. The data yielded by EHA 3 provides convincing evidence that dimethyl sulphide was released in the active stage, and DMDS in all stages of decomposition.

Altogether, Table 5.1 details compounds suggested as being responsible for the activities observed in the 21 mass channels described by the three subsets above (Figure 5.5). These compounds have all been previously detected in other decomposition work. Compound assignments are tentative and still needs to be validated by additional techniques such as GC-MS, which has the advantage of separating compound based on properties other than molecular mass.

**Table 5.1** Tentative compound assignment of mass channels detected within the three subsets of EHA trial 3 (CIR-MS). Proton affinity figures are reported from NIST unless otherwise stated, and stages of decomposition were collected from the text within several decomposition articles. These have been references symbolically as † (Forbes 2014 [62]), ◇ (Statheropoulos 2011[28]), ⊖ (Perrault 2014 [68]), ▫ (Dekeirsschieter 2009 [27]), • (Swann 2010 [121]), and ‡ (Agapoiu 2015 [58]).

Protonated parent ion	Compound name	Proton affinity (KJ/mol)	Stage of decomposition
49	Methane thiol ▫◇	773.4	N/A
57	Propen-2-al ▫	797	N/A
57	2-Methylprop-1-ene ▫	802.1	N/A
57	But-1-ene ▫	N/A	N/A
57	E-But-2-ene ▫	747	N/A
61	1-propanol ⊖†	786.5	Bloat
61	2-propanol ⊖#◇	793	Advanced Decay, Skeletonisation
61	Acetic acid ⊖#•	783.7	Active Decay, Advanced Decay, Skeletonisation
63	Dimethyl sulphide ⊖◇	830.9	Active Decay
71	But-2-enal ▫	830.8	N/A
71	2-Propenal, 2-methyl◇⊖	808.7	N/A
71	3-Buten-2-one ◇	834.7	N/A
71	Pent-1-ene ▫	N/A	N/A
71	Cyclopropane, 1,2-dimethyl-, trans ‡	N/A	N/A
73	2-Methylpropanal ▫◇	797.3	N/A
73	Butanal ▫	792.7	N/A
73	2-butanone ⊖#◇▫	827.3	Active Decay, Skeletonisation
73	Pentane ⊖#◇	N/A	Skeletonisation
73	Furan, tetra hydro ◇	822.1	N/A
73	Butane, 2-methyl ◇	N/A	N/A

Table 5.1 (continued)

75	Propanoic acid $\ominus+\boxplus^\bullet$	797.2	Advanced Decay, Skeletonisation
75	2-methyl-1-propanol $\ominus\boxplus$	793.7	N/A
75	1-butanol $\ominus\diamond$	789.2	N/A
75	2-butanol $\ominus\diamond$	815	N/A
75	1-Propanol, 2-methyl $\diamond$	793.7	N/A
75	Acetic acid, methyl ester $\ominus$	821.6	N/A
75	Methyl acetate $\ddagger$	821.6	Skeletonisation
75	Acetaldehyde, methoxy $^\ddagger$	N/A	N/A
79	Benzene $\ddagger\diamond$	750	Skeletonisation
79	Dimethyl sulfoxide $\diamond$	884	N/A
80	Pyridine $\boxplus$	930	N/A
88	N-Methyl propanamide $\boxplus$	920.4	N/A
88	N,N-Dimethyl acetamide $\boxplus$	908	N/A
88	Butanamide $\boxplus$	N/A	N/A
89	2-methylpropanoic acid $\ominus+\boxplus^\bullet$	N/A	Active Decay, Advanced Decay, Skeletonisation
89	Butanoic acid $\ominus+\boxplus$	N/A	Active Decay, Skeletonisation
89	Butyric acid $^\bullet$	N/A	N/A
89	2-methyl-1-butanol $\ominus$	N/A	N/A
89	3-methyl-1-butanol $\ominus+\boxplus$	N/A	Advanced Decay, Skeletonisation
89	1-pentanol $\ominus\boxplus$	795	N/A

$\boxplus$ =Forbes 2014 [62],  $\diamond$ = Statheropoulos 2011[28],  $\ominus$ =Perrault 2014 [68],  $\boxplus$ = Dekeirsschieter 2009 [27],  $^\bullet$ =Swann 2010 [121],  $\ddagger$ =Agapoiu 2015 [58]

Table 5.1 (continued)

Protonated parent ion	Compound name	Proton affinity (KJ/mol)	Stage of decomposition
49	Methane thiol $\boxtimes\diamond$	773.4	N/A
57	Propen-2-al $\boxtimes$	797	N/A
57	2-Methylprop-1-ene $\boxtimes$	802.1	N/A
57	But-1-ene $\boxtimes$	N/A	N/A
57	E-But-2-ene $\boxtimes$	747	N/A
61	1-propanol $\ominus^\ddagger$	786.5	Bloat
61	2-propanol $\ominus^\#\diamond$	793	Advanced Decay, Skeletonisation
61	Acetic acid $\ominus^\#\cdot$	783.7	Active Decay, Advanced Decay, Skeletonisation
63	Dimethyl sulphide $\ominus\diamond$	830.9	Active Decay
71	But-2-enal $\boxtimes$	830.8	N/A
71	2-Propenal, 2-methyl $\diamond\ominus$	808.7	N/A
71	3-Buten-2-one $\diamond$	834.7	N/A
71	Pent-1-ene $\boxtimes$	N/A	N/A
71	Cyclopropane, 1,2-dimethyl-, trans $^\ddagger$	N/A	N/A
73	2-Methylpropanal $\boxtimes\diamond$	797.3	N/A
73	Butanal $\boxtimes$	792.7	N/A
73	2-butanone $\ominus^\#\boxtimes$	827.3	Active Decay, Skeletonisation
73	Pentane $\ominus^\#\diamond$	N/A	Skeletonisation
73	Furan, tetra hydro $\diamond$	822.1	N/A
73	Butane, 2-methyl $\diamond$	N/A	N/A

89	2-pentanol $\ominus\diamond$	N/A	N/A
89	3-methylbutan-2-ol $\square$	N/A	N/A
89	Acetic acid, ethyl ester $\ominus\diamond$	835.7	N/A
89	Ethyl Acetate $^+$	835.7	N/A
94	3-Methylpyridine $\square\diamond$	943	Active
94	1-Chloro-butane $\square$	N/A	N/A
95	Phenol $\ominus\#\diamond\square$	817	Active Decay, Advanced Decay
95	Dimethyl sulfone $\diamond$	N/A	N/A
95	Dimethyl disulphide $\#\diamond\ominus\square$	815	Bloat, Active Decay, Advanced Decay, Skeletonisation
114	Benzene, chloro $\diamond$	753.1	N/A

$\#$  =Forbes 2014 [62],  $\diamond$  = Statheropoulos 2011[28],  $\ominus$  =Perrault 2014 [68],  $\square$  = Dekeirsschieter 2009 [27],  $\bullet$  =Swann 2010 [121],  $\#$  =Agapoiu 2015 [58]

### 5.3.3 SPME-GC-MS

#### 5.3.3.1 Decomposition VOCs

A total of 27 decomposition specific compounds were captured and separated by SPME-GC-MS. Almost all chemical classes were detected, although the most prominent groups were sulphur containing compounds, followed by alcohols and ketones (Figure 5.7). In parenthesis are the number of chemical compounds identified in the headspace of EHA 3 trial. Alcohols (5), sulphur containing (9), nitrogen containing (3), ketone (4), aromatic (1), alkane (3), and aldehyde (2).

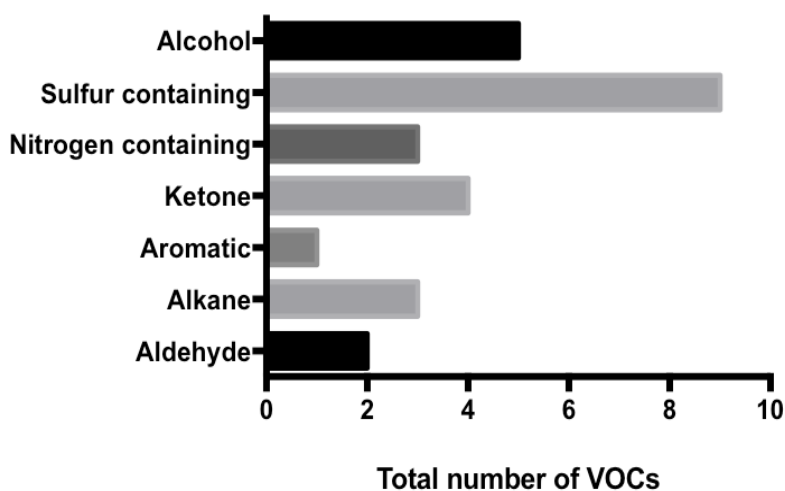


Figure 5.7 Total number of VOCs grouped by chemical class as measured by SPME-GC-MS

Primary alcohols ( $C_3$ - $C_8$ ) were noticed from day 5 until day 12, with the most prevalent being 1-butanol and 1-propanol. Beyond day 13, no alcohols were detected. In the sulphide family, DMS, DMDS and carbon disulphide were seen from day 1 until the end of the trial, but overall the most prevailing sulphur compounds with an excess of ten occurrences were methanethiol, DMS, carbon disulphide, DMDS, dimethyl trisulphide and tetra sulphide dimethyl.

2-azridinylethylamine, trimethylamine, and carbamic acid monoammonium salt represented the nitrogen class. Though ammonia was not directly seen, probably

because the scan range of the quadrupole mass analyser was programmed to scan for masses in the range of 20-400, the contribution of ammonia was inferred from the intensity of carbamic ammonium salt as it is formed from the reaction of carbon dioxide and ammonia [124], both of which were expected to be produced in abundance in the exposed trials. In the ketone family, acetone and 2-butanone were the most abundant with twenty and ten occurrences respectively. Acetone in particular was detected every day of the trial.

Butane, 2-methyl and pentane both occurred three times during EHA 3 trial. Butane, 2-methyl was seen in the first 3 days, while pentane was more sporadic in appearance. Likewise, butanal, 3-methyl in the aldehyde family appeared irregularly. Finally, benzene was the only aromatic identified between day 6 - 9 and day 11-14 (Figure 5.8).

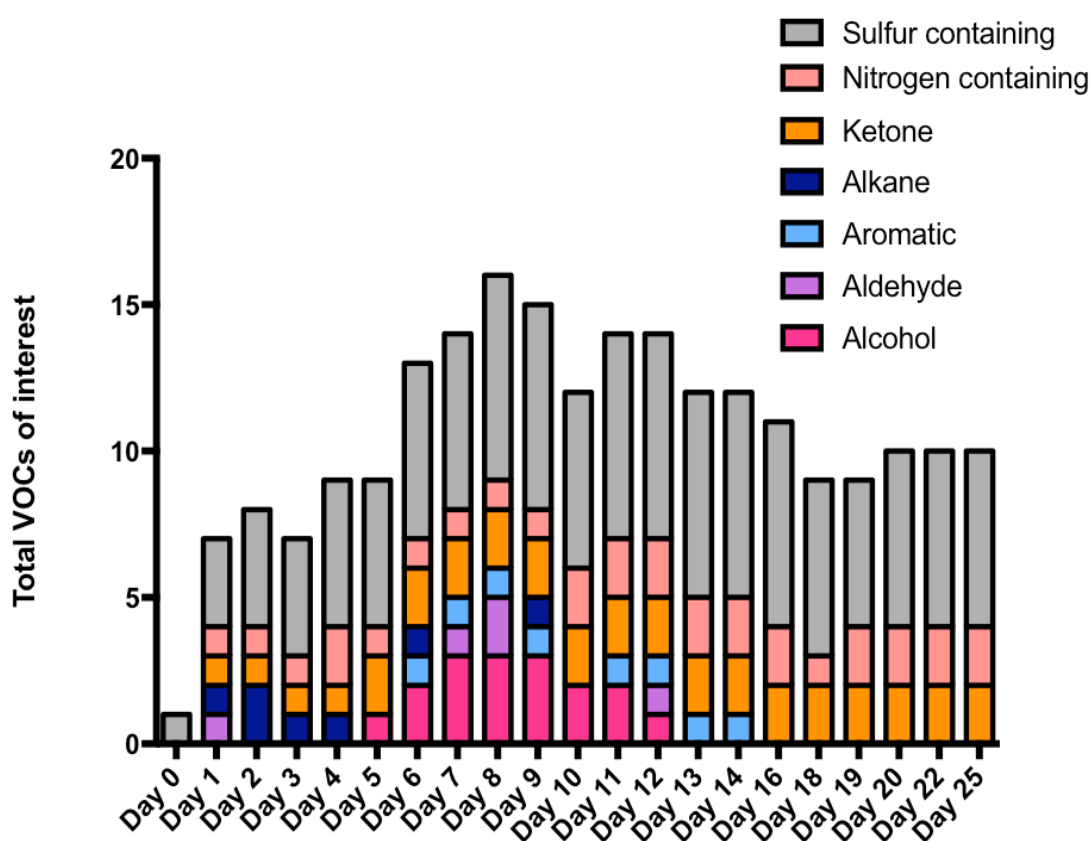


Figure 5.8 Illustrates the distribution of decomposition VOCs when grouped by chemical class as detected by SPME-GC-MS during EHA trial 3.

Table 5.2 Full list of compounds detected by SPME-GC-MS in EHA trial 3. These have been references symbolically as # (Forbes 2014 [62]), ◇ (Statheropoulos 2011[28]), ⊖ (Perrault 2014 [68]), and ⊚ (Dekeirsschieter 2009 [27]).

Compound name	RT	R.Match	% Prob	MW
<i>Alcohols</i>				
1-Propanol ⊖#	1.993	780	56	60
Cyclopropyl methyl carbinol	2.868	710	20.4	86
1-Butanol ⊖◇	3.023	809	45	74
1-Octanol ⊖	11.095	775	12.5	130
1 Hexanol ◇	11.13	765	14	102
<i>Sulphur containing</i>				
Sulphur dioxide #⊚	1.518	899	92.8	64
Methane thiol ⊚◇	1.567	869	97.1	48
Dimethylaminomethyl-isopropyl-sulphide	1.624	764	62	133
DMS ◇⊖	1.81	870	66	62
Carbon disulphide	1.895	896	97	76
DMDS #◇⊖⊚	4.716	764	78	94
Methyl ethyl disulphide ◇	8.438	787	86	108
Dimethyl trisulphide #◇⊖	14.035	798	87.5	126
Tetrasulphide dimethyl ◇	20.454	680	77	158
<i>Nitrogen containing</i>				
Carbamic acid, monoammonium salt	1.433	943	48	78
2-Azridinylethyl)amine	1.433	905	60.2	86
Trimethylamine #◇⊖⊚	1.593	913	86	59
<i>Ketone</i>				
Acetone ◇⊚	1.709	904	91	58
2-Pentanone, 3-methyl-	2.228	809	44	100
2-Butanone #◇⊖⊚	2.233	834	54	72
3-Hexanone ⊖	20.041	682	10.3	100
<i>Aromatic</i>				
Benzene ⊖	2.913	893	48	78
<i>Alkane</i>				
Pentane #◇⊖	2.228	702	16.9	72
Butane, 2-methyl ◇	2.233	753	23	72
Hexane #◇⊖	2.237	820	30.2	86
<i>Aldehyde</i>				
Butanal, 3-methyl ◇	2.859	894	82	86
1-Butanol, 3-methyl- #⊖⊚	4.587	893	57	88

21 out of the 27 compounds detected by SPME-GC-MS in EHA 3 have been previously detected in other exposed experiments around the world [27, 28, 62, 68]. A full list of the compounds seen in this work have been listed in Table 5.2. Of these, 17 compounds were considered as possible key markers of carcass decomposition. Key markers of decomposition were defined as compounds having three or more occurrences during the trial, as well as having a good hit on NIST Library (Reverse Match > 700). The possible key markers of carcass decomposition in exposed human analogue trial 3 were methanethiol, dimethylaminomethyl-isopropyl-sulphide, DMS, carbon disulphide, DMDS, methyl ethyl disulphide, dimethyl trisulphide, dimethyl tetrasulphide, 1-propanol, 1-butanol, butanal 3-methyl, pentane, benzene, acetone, 2-butanone, carbamic acid monoammonium salt and trimethylamine. The available evidence (Figure 5.9) seems to suggest that the fresh stage of decay occurred on day 1, bloated stage from day 2-5, active from day 6-14 and advanced decay from day 22 onwards.

During day 1, autolysis (self-destruction) had commenced. The lack of oxygen within the carcass created a suitable environment for anaerobic organisms from the gastrointestinal tract and respiratory system to break down surrounding cells and tissues. Gases such as hydrogen sulphide, ammonia and carbon dioxide are some of the most common compounds attributed to this stage [54]. In spite of the reduced number of VOCs reported in the literature as being specific to the fresh stage, the presence of acetone, dimethyl sulphide, carbon disulphide, dimethyl disulphide and carbamic acid ammonium salt on day 1 of EHA trial 3 could not be ignored (Figure 5.9). Not only was carbamic acid ammonium salt which signified the presence of carbon dioxide and ammonium detected, but also there was a relatively strong signal observed for acetone on day 1.

By day 2, the carcass began to swell. This period lasted until day 5 (pictured in Figure 5.6). Here, anaerobic microorganisms have begun to destroy soft tissues of the body. The result of this is the accumulation of gas and fluid which are subsequently purged through openings of the carcass (onset of active stage). Following this premise, it is not without logic to expect that the highest number and highest concentrations of volatile organic compounds will be released during the active stage of decomposition. So, the

bloated stage in EHA trial 3 comprised of similar compounds seen in the active phase, but in lower concentrations. The compounds first seen on day 2 (bloated stage) included methanethiol and pentane, although all the compounds previously observed in the fresh stage were also present.

By day 6, the intensity of methanethiol, dimethyl disulphide, dimethyl sulphide, trimethylamine, carbon disulphide and pentane had increased dramatically and continued to do so until days 13 and 14. During this time frame, additional compounds not previously detected in the bloated stage were also seen. Compound such as methyl ethyl disulphide, tetrasulphide dimethyl, dimethyl trisulphide, 1-butanol, 2-butanone, 1-propanol and benzene were not only observed, but highest concentrations were released during this period. This behaviour suggests that the carcass was in the active phase of decomposition. During active decay, bloating has ceased and the abdominal cavity collapses. The skin has also usually broken in one or more places and rapid leeching of liquid and gaseous products of decomposition occurs [59]. This stage is often described as being the most vigorous phase. This is evidenced in EHA 3 trial as the highest number of VOCs were recorded during this stage (Figure 5.10).

Beyond day 15, all compounds followed similar patterns in that their concentrations decreased. 1-propanol, 1-butanol, methyl ethyl disulphide in particular were no longer detected. The only exception to this trend was acetone, which showed signs of increasing in concentrations again from day 22 until the end of the EHA 3 trial on day 25, possibly relating to the onset of advanced decay. The dry phase was not observed in this study as the trial terminated on day 25. Because of this, much of the discussion focuses on the changes observed in the early mid post mortem stages.

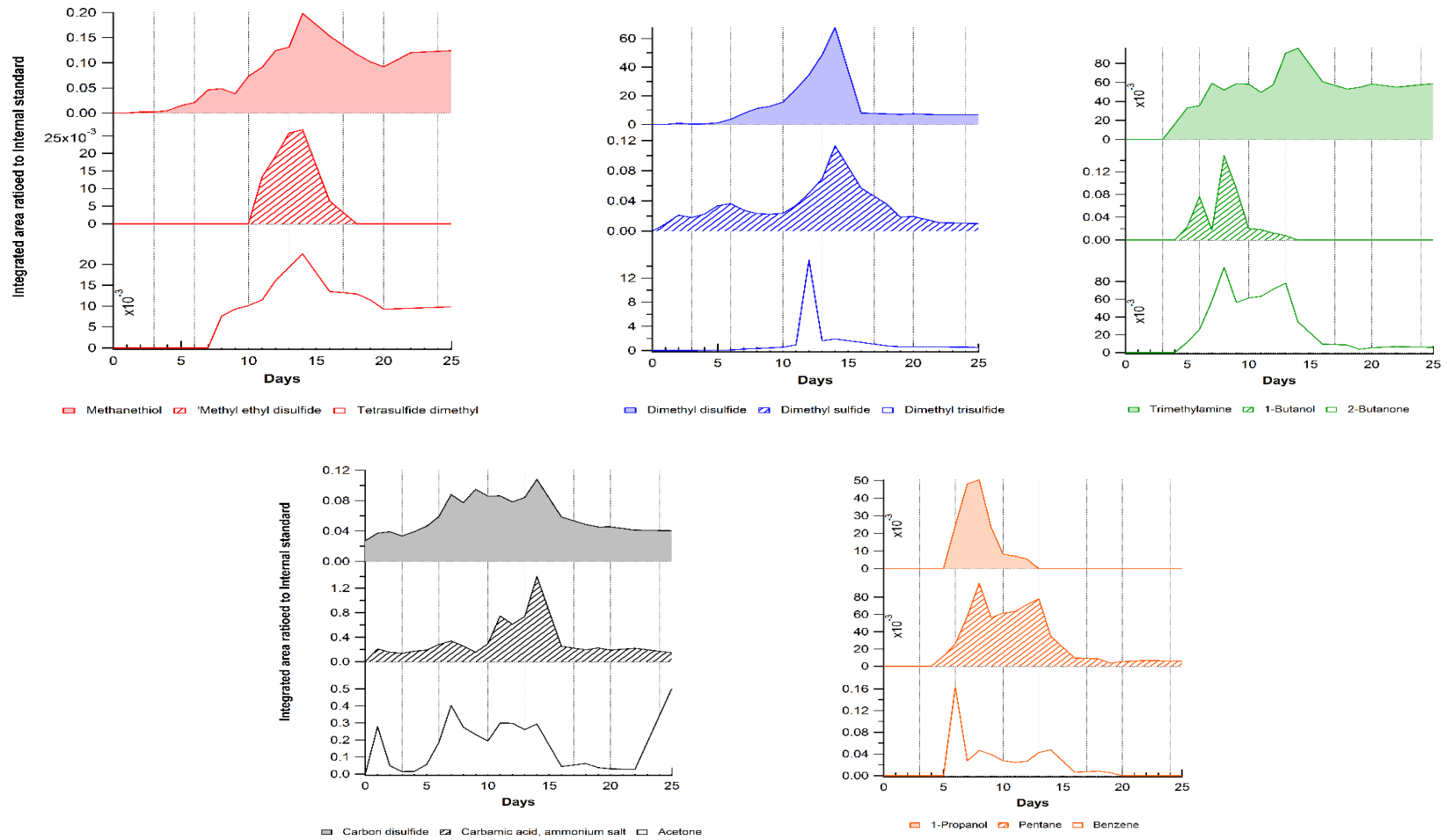


**Figure 5.9 Time profiles of 15 core decomposition VOCs as measured by SPME-GC-MS during EHA trial 3. These include: Methanethiol, Methyl ethyl disulfide, Tetrasulfide dimethyl, Dimethyl disulfide, Dimethyl sulfide, Dimethyl trisulfide, Trimethylamine, 1-butanol, 2-butanone, Carbon disulfide, Carbamic acid ammonium salt, Acetone, 1-propanol, Pentane and Benzene.**

The trends and proposed stages observed in EHA trial 3 are in line with what is expected. For example, the fresh stage contained the fewest amount of VOCs whereas the active stage contained the highest number of VOCs (Figure 5.10), and was also the stage containing the highest concentrations of majority of the core VOCs, specifically sulphur containing compounds. While discussions so far have been based around time periods where maximum concentrations were observed, it is clear from Figure 5.9 that many of the core VOCs listed overlap into more than one stage of decomposition. This overlay highlights the continuum process that is carcass decomposition, and supports the idea that although the process of decomposition as a whole is constantly changing, the underlying core VOCs that could be used as identifiers for each stage need to be quantified to give a more accurate depiction of the onset and duration of each stage of decomposition.

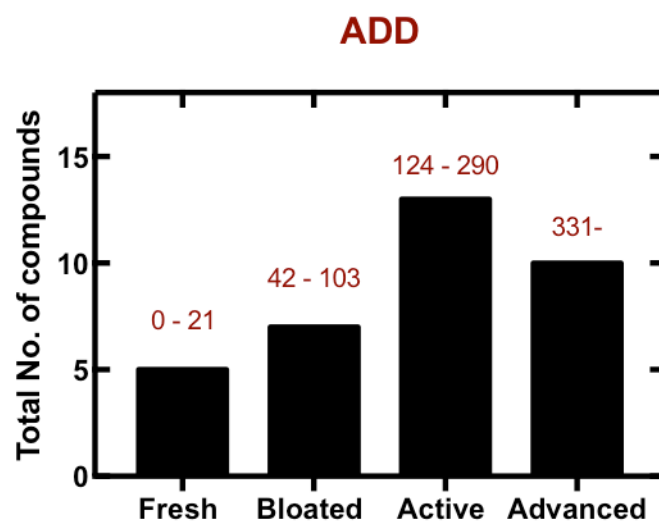


Figure 5.10 Total number of compounds captured during EHA trial 3 as a function of Accumulated Degree Days (ADD)

Despite the fact that 27 different VOCs were identified through the use of SPME-GC-MS during EHA 3, it is important to emphasise that one of the greatest shortcomings of SPME is in the low selectivity of commercially available fibres [87]. To achieve a sensitivity enabling determination of polar and volatile organic compounds, SPME fibres need to be coated with a very specific sorbent with a high affinity for target analysis. EHA 3 trial was conducted by use of SPME fibre with a combination of coatings

(carboxen and polydimethylsiloxane) to maximize extraction efficiency. To add to this, the adsorbent nature of the PDMS/CAR fibre means that analytes may compete for sites on the fibre surface, meaning the fibre has limited capacity. The very basis of SPME relies on the partition mechanism and equilibrium between analyte and sample matrix. To this end, analytes with higher partition coefficients will require longer equilibration times, and thus longer exposure times.

However, with this type of non-targeted analysis, it is necessary to optimise the exposure time otherwise the amount of analyte extracted might exceed detector requirements, not to mention longer exposure times will reduce the number of available sites on the fibre surface for other analytes to adsorb unto. Similarly, the non-polar column DB5-MS limits the separation of polar analytes. Figure 5.11 (days 2 and 4) provides evidence of compounds not retained well to the DB5-MS column in the first 2 minutes of separation.

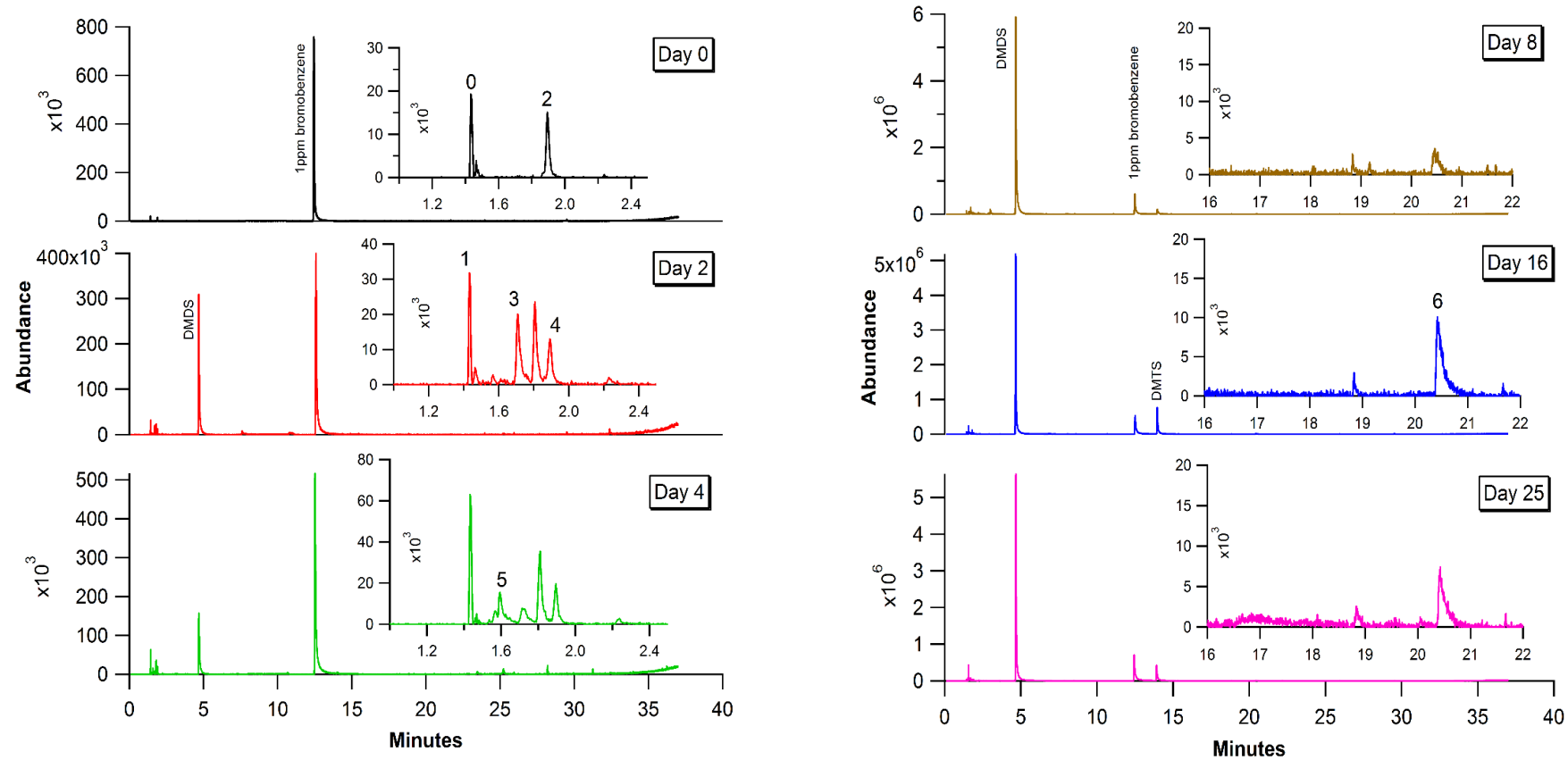


Figure 5.11 Sample chromatograms collected before carcass introduction (day 0), day 2, day 4, day 8, day 16 and day 32 of EHA trial 3 as measured by SPME - GC - MS. Labels 0 refers to remnants of the air peak , 1(carbamic acid ammonium salt, 2 (acetone), 3 (Methanethiol), 4 (carbon disulphide), 5 (Trimethylamine), and 6 (Tetrasulphide dimethyl)

### 5.3.4 Validation of CIR-MS results

Independently reviewed patterns from the time profiles of compounds extracted as key markers from both CIR-MS and SPME-GC-MS dataset were analogous. This finding emphasised the conclusion that it was possible to extract the stages of decomposition exclusively from VOCs measured in the headspace of a decomposing carcass. From EHA trial 3, distinctive trends could be isolated on day 1, between days 2-5, days 6-14, and from day 22 onwards. These were proposed to reflect the fresh, bloated, active and onset of advanced decay respectively. Albeit, only data gathered between days 1-10 by CIR-MS were assessed, the findings from CIR-MS were also in agreement with the elucidation of the fresh, bloated and onset of the active stages of decomposition.

In spite of the shortcomings of CIR-MS, and the added complications of competing reagent ions, seven VOCs were in common between the data gathered by CIR-MS and SPME-GC-MS during EHA trial 3. These mutual compounds were reported to have a reverse match in excess of 700, and were detected regularly by SPME-GC-MS. In CIR-MS significant activities were also observed the corresponding mass channels of these compounds.

More compelling however was the strong correlation of mass channels 49, 60, 73, 61, 75, 59 and 95 from CIR-MS with methanethiol, trimethylamine, 2-butanone, 1-propanol, 1-butanol, acetone and dimethyl disulphide from SPME-GC-MS between days 1-10 of EHA trial 3. The overlay of the compounds seen by GC-MS and the equivalent mass channels in CIR-MS (Figure 5.12), demonstrates cohesiveness between the two techniques.

To that end, results from this comparative study illustrates that CIR-MS is a useful technique that needs to be taken advantage of in the drive towards determining the signature smell of death. Unique mass channels considered to represent possible markers of decomposition were extracted from the CIR-MS dataset and these mass channels were corroborated by results obtained by SPME-GC-MS.

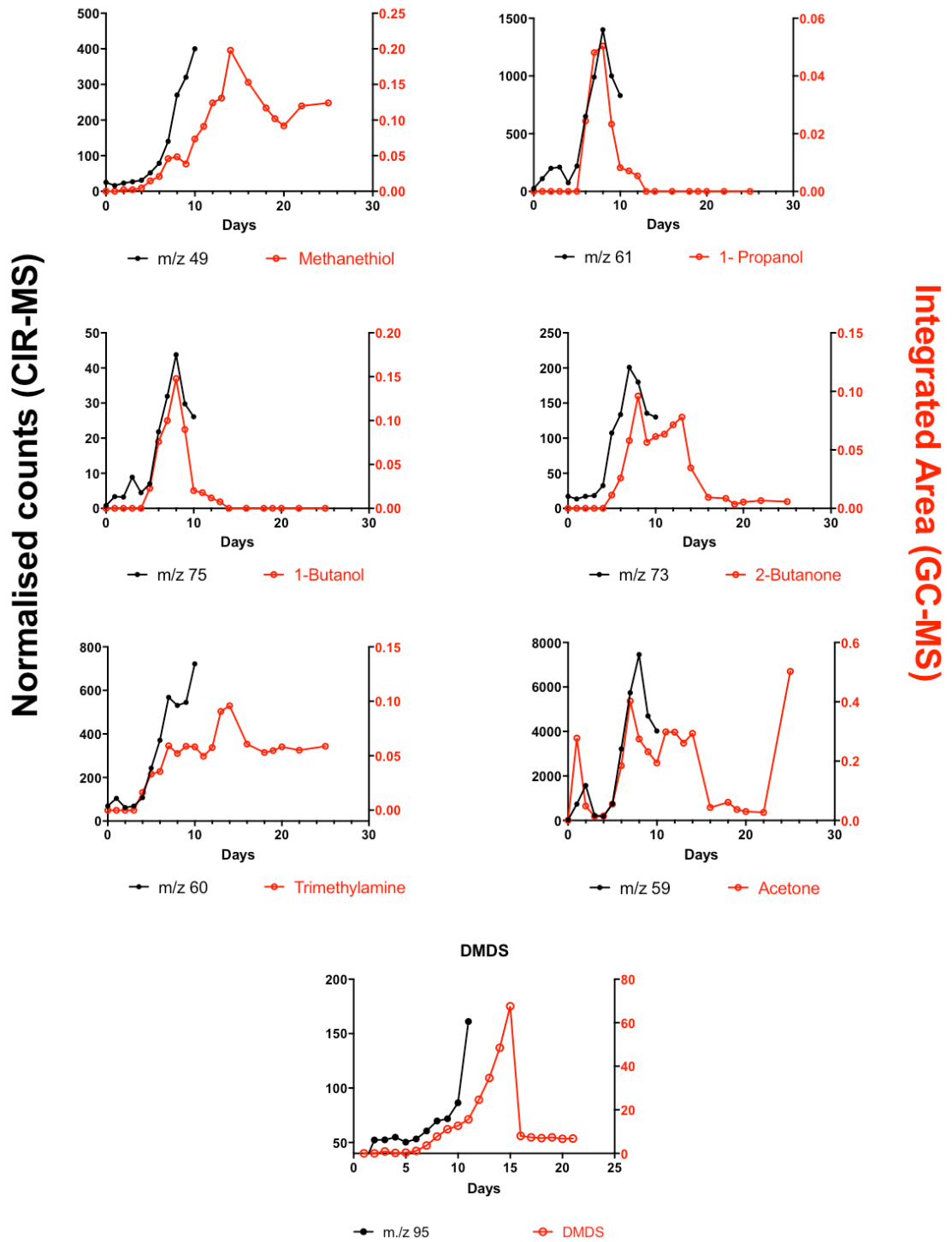


Figure 5.12 Overlay of 7 common VOCs as measured by CIR-MS and SPME-GC-MS during EHA trials 3. Normalised counts represent results generated by CIR-MS. CIR-MS signal was normalized to hydronium, and the integrated area for SPME-GC-MS was ratioed against internal standard bromobenzene. Common compound between CIR-Ms and GC-MS include, methanethiol, 1-propanol, 1-butanol, 2-butanone, trimethylamine and acetone.

### 5.3.5 Reproducibility

At the time of EHA trial 2 (2014), CIR-MS was the principal instrument used to monitor the evolution of decomposition VOCs. Method development for the SPME-GC-MS technique had not been fully conducted at this time: nonetheless, SPME samples were collected in EHA trial 2 and analysed on days the GC-MS instrument was available. In addition, the CAR/PDMS fibre was exposed in the headspace of the carcass chamber for a longer time period (1 hour).

On the other hand, CIR-MS operated at the same settings as EHA trial 3. Initially 10 and 50-fold dilution factors were applied to lessen the interference from competing reagent ion ammonium, however, this was unsuccessful. Regrettably also, the CIR-MS instrument was out of order during the first week of EHA trial 2.

The limitations surrounding data collection during this trial meant the overall decomposition profile of EHA trial 2 was somewhat incomplete. However, in spite of this, it was still possible to extract some similarities between the two exposed experiments.

#### 5.3.5.1 Competing reagent ions in EHA 2 as measured by CIR-MS

To begin with, the competitive nature of primary ions hydronium and ammonium were also presented in this trial. Unlike EHA 3, interferences from ammonium in the CIR-MS dataset of EHA 2 were observed from the onset (day 8) and lasted the entire duration of the study (Figure 5.13). This meant it was problematic to isolate a time period where reagent ion hydronium was in excess.

The results generated from EHA 2 were used instead to justify the exclusion of the dataset collected from day 15 onwards in EHA 3. The profiles of the vast majority of the mass channel monitored by CIR-MS in EHA 3 (beyond day 15) were not as expected. As ammonium was the most prominent primary ion, it was expected that contributions from compounds with lower proton affinity than ammonium would decrease. However,

the opposite was observed. Methanethiol validated to be responsible for the contribution from mass channel 49 and trimethylamine at channel 60 is used to illustrate this point (Figure 5.14).

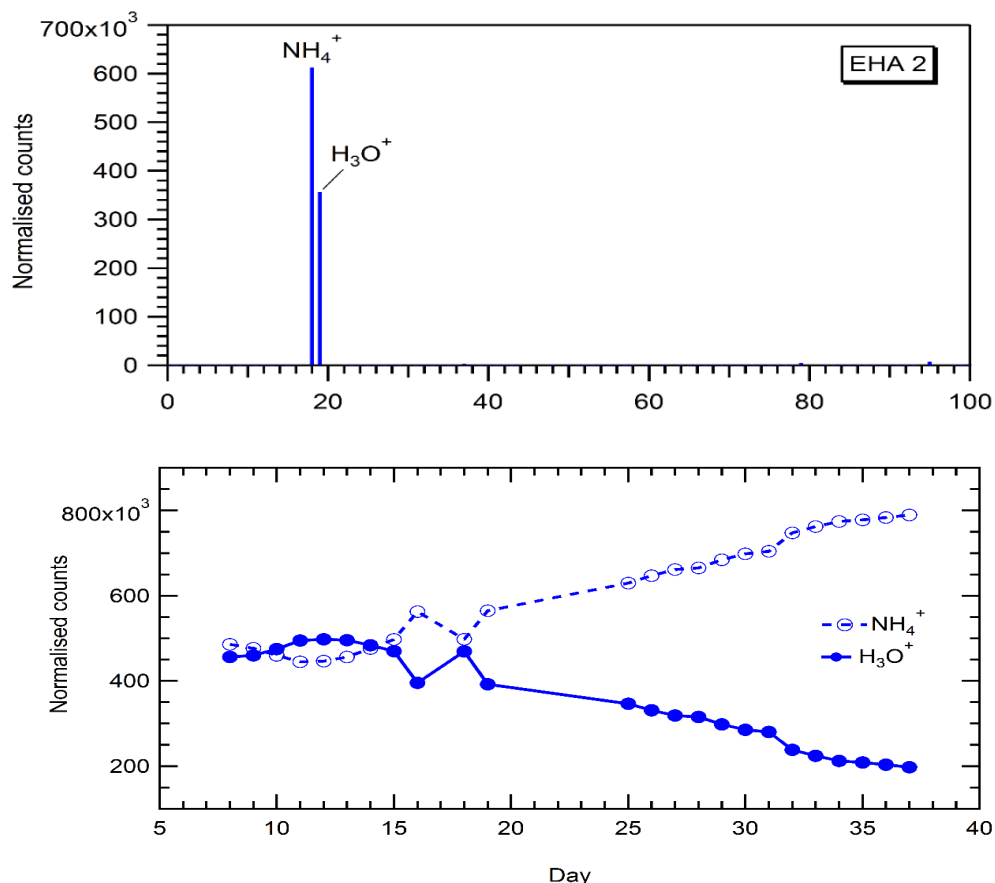


Figure 5.13 Average CIR-MS mass spectrum gathered from EHA trial 2 (a), and (b) the temporal variations of ammonium and hydronium during EHA trial 2

Methanethiol has a proton affinity of 773.4 KJmol<sup>-1</sup> whereas trimethylamine has an affinity of 948.9 KJ mol<sup>-1</sup> (proton affinity of ammonia is 853 KJmol<sup>-1</sup>). Thus, it was expected that methanethiol would not be protonated by ammonium on energetic grounds, whereas the transfer of a proton from ammonium to trimethylamine is favourable energetically. The switch from hydronium to ammonium occurred on day 15 in both exposed trials. Figure 5.14 shows that contributions from both methanethiol and trimethylamine increased from day 15 onwards in EHA trial 3. This phenomenon does not align with proton transfer reaction thermodynamics. In contrast, the behaviour of methanethiol and trimethylamine in EHA trial 2 supports what is expected.

As a consequence, the results from EHA trial 3 from day 15 onwards, were excluded from further analysis, as the ion-molecular chemistry in the drift tube region of the CIR-MS instrument was compromised.

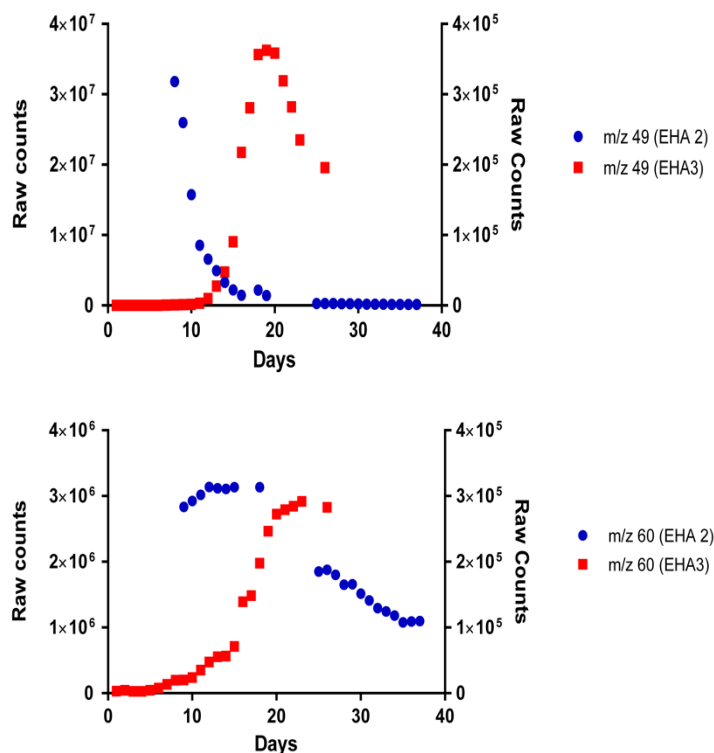


Figure 5.14 The behaviour of methanethiol ( $m/z$  49) and trimethylamine ( $m/z$  60) when under primary ion ammonium (day 15 onwards) in EHA trials 2 and 3. The proton affinity of methanethiol, trimethylamine and ammonium are 773.7, 948.9 and 853  $\text{KJ mol}^{-1}$  respectively.

### 5.3.5.2 SPME-GC-MS results for EHA trial 2

The results collected by SPME-GC-MS during this trial formed part of the method development. As mentioned earlier, the GC-MS was used to analyse headspace VOCs when available; explaining the gaps in data collection. The GC-MS was available for a total of 6 days during this trial (days 4, 5, 6, 12, 13 and 14). The SPME fibre (75  $\mu\text{m}$  CAR/PDMS) was exposed in the headspace of the pig chamber for 1 hour, before being desorbed for 5 minutes into the GC inlet, which was set to operate at 280  $^{\circ}\text{C}$ . Oven

temperature was first held at 40 °C for 2 minutes, then 80 °C at 5 °C /minute and finally 300 °C at increments of 15 °C/min. The GC-MS inlet was set to operate in split mode with a ratio of 10:1 and the total run time was 24.67 minutes.

From Figure 5.15, it can be seen that contributions from polysulphides were present at significant concentrations from early on (day 4). Although a longer exposure allows for longer equilibration between the components in the carcass headspace and the SPME fibre, such high contributions from compounds such as DMDS might exceed the capabilities of the detector. As a consequence, the exposure time was reduced to 20 mins used in EHA 3 trial

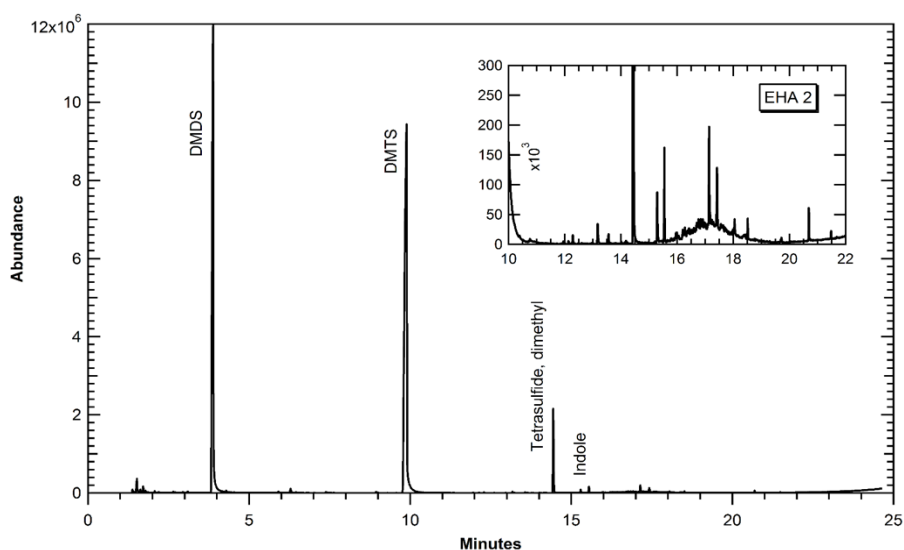


Figure 5.15 Sample chromatogram generated by SPME-GC-MS during EHA trial 2. 1-hour exposure time used

A total of 19 compounds were selected with a high certainty hit from the analysis by SPME-GC-MS in EHA 2 trial. They included phenol, phenol 4-methyl, tetradecane, dimethyl sulphide, dimethyl trisulphide, indole, tetrasulphide dimethyl, toluene, trimethylamine, 2-butanone, methanethiol, methyl ethyl disulphide, nonane, acetone, acetophenone, carbamic acid ammonium salt, carbon disulphide, decane, and dimethyl disulphide. The time profiles of these compounds are shown in Figure 5.16.

Given that the GC-MS instrument was unavailable on most days, it was still possible to deduce the behaviour of these 19 compounds from day 4 through until day 14. It can be implied that there are 3 trends within the CIR-MS dataset collected during EHA trial

2. The first group described the behaviour of phenol, phenol 4-methyl, indole, methyl ethyl disulphide, and dimethyl disulphide as they showed an increase in contributions from day 4 until day 12. The second group shows highest contributions on day 12, followed by a decrease on days 13 and 14. Within this group are compounds tetradecane and nonane. The third group comprised of dimethyl sulphide dimethyl trisulphide, toluene, trimethylamine, 2-butanone, tetrasulphide dimethyl, methanethiol, acetone and carbon disulphide. These compounds were observed at relatively stable concentrations between days 4 and 14 of EHA trial 2.

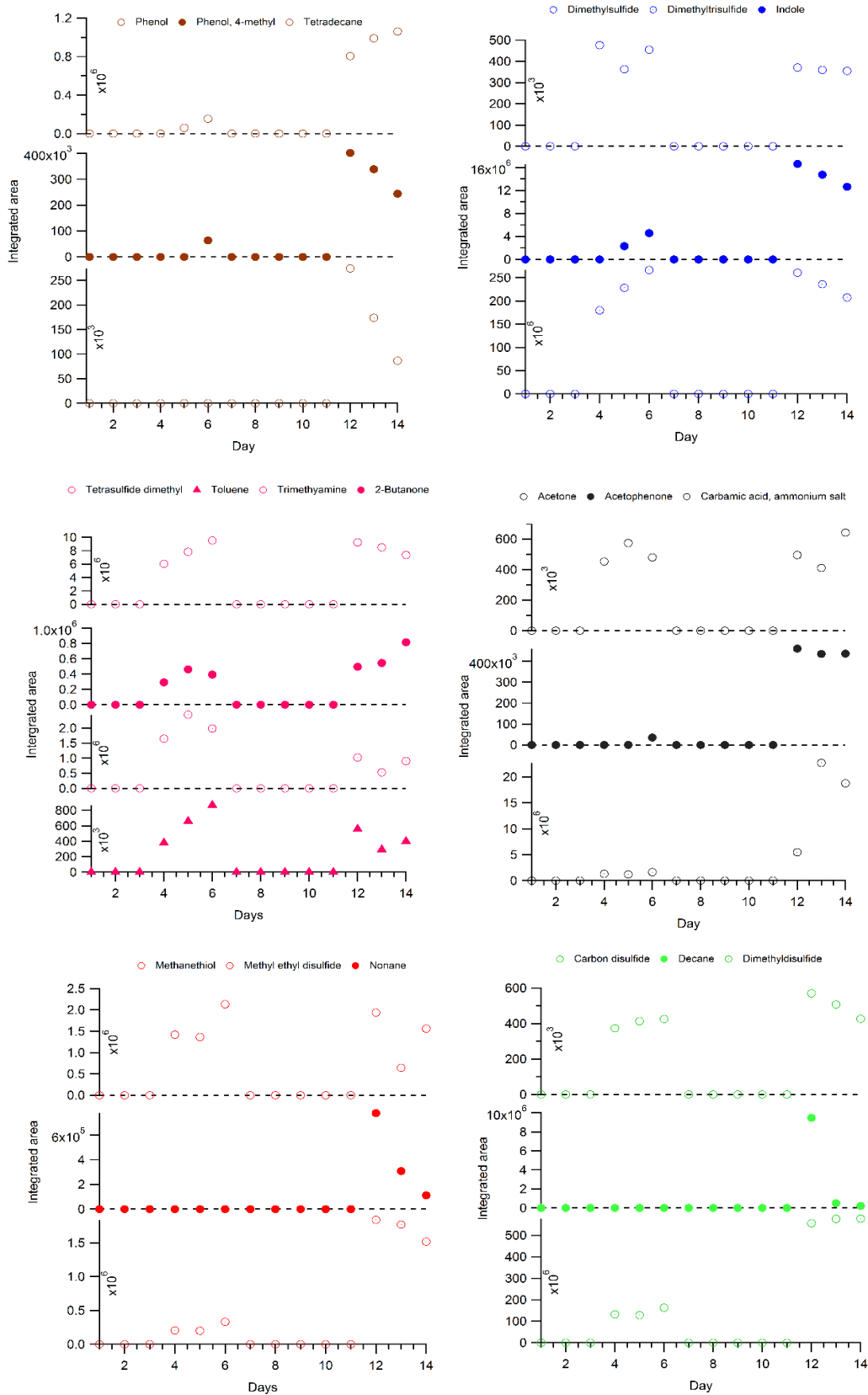


Figure 5.16 Time profiles of 19 compounds detected during EHA trial 2 as monitored by SPME-GC-MS

### 5.3.6 Quantification

As mentioned in section 1.8, one of the objectives of this research was to assess if the sequence of VOCs emitted during the process of carcass decomposition could be used quantitatively as a marker of decay time. Given that seven common VOCs were identified by CIR-MS and SPME-GC-MS in the exposed human analogue trials, this section attempts to extract quantitative information relating to methanethiol, trimethylamine, 2-butanone, 1-propanol, 1-butanol, acetone and dimethyl disulphide.

To achieve this, the equation of the linear fit extrapolated from the calibration curves of each of these VOC markers were used to estimate relative concentrations in units of parts per billion by volume. Calibration curves of these seven VOCs have already been illustrated in Figure 3.11 and Figure 3.21. In the first place, the stability and hence the precision of internal standard bromobenzene was examined. Over the course of EHA trial 3, bromobenzene was relatively stable with a reported precision of 22.7%, calculated from the relative standard deviation (Figure 5.17).

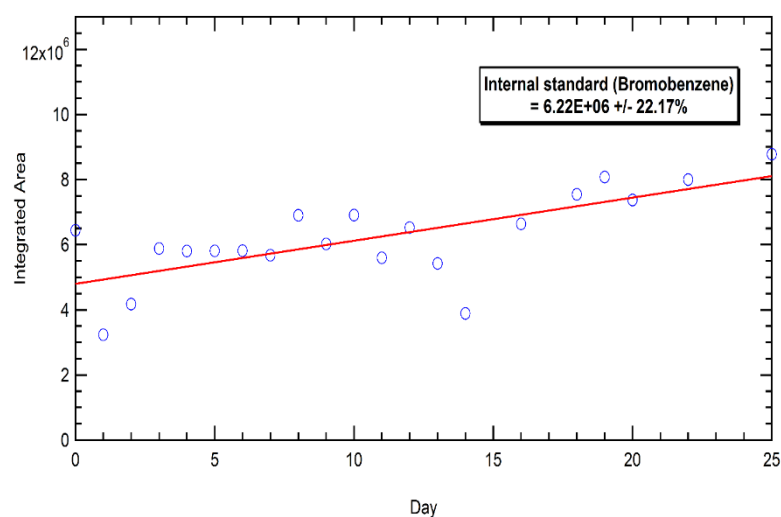


Figure 5.17 Temporal variation of Internal standard bromobenzene (1ppm) during EHA trial 3.

From the results obtained via SPME-GC-MS, it was possible to quantify for five compounds. These were trimethylamine, 2-butanone, 1-propanol, 1-butanol, and acetone (Figure 5.18). Conversely, it was challenging to quantify methanethiol and dimethyl disulphide because the observed concentrations in EHA trial 3 were outside

the linear range of the CAR/PDMS fibre. The only conclusions that could be drawn about methanethiol and dimethyl sulphide were that concentrations were in excess of 1000 ppbV and 4000 ppbV respectively. Highest concentrations of trimethylamine, 1-propanol, 2-butanone, acetone and 1-butanol were approximately 600 ppbV, 250 ppbV, 200 ppbV, 3000 ppbV and 600 ppbV respectively.

In contrast, it was possible to quantify for methanethiol, trimethylamine, 2-butanone, 1-propanol, and DMDS in CIR-MS (Figure 5.19). Highest concentrations of these compounds between day 0 and day 10 of EHA trial 3 were around 800 ppbV, 1000 ppbV, 350 ppbV, 500 ppbV and 40 ppbV respectively. Concentrations of acetone and 1-butanol in EHA trial 3 were outside the range calibrated for and thus could not be derived from the linear fit.

In spite of the similarities between the compounds detected by CIR-MS and SPME-GC-MS, concentration measurements calculated in relation to these seven core VOCs for both CIR-MS and SPME-GC-MS within EHA trial 3 were vastly different. To begin with, the concentration of methanethiol, DMDS, 1-butanol and acetone were exceedingly low in CIR-MS in comparison to the concentrations calculated in SPME-GC-MS. Admittedly, accurate concentrations of methanethiol could not be calculated on SPME due to limitations of the CAR/PDMS fibre, however the concentration of methanethiol was estimated to be in excess of 1000 ppbV on day 2 whereas CIR-MS reported a concentration of only about 100 ppbV on the same day of the trial. This was equally the case with DMDS. A possible explanation for the reduced sensitivity of sulphur containing compounds on CIR-MS could be due to the strong affinity of sulfur to stainless steel, the main component of the CIR-MS instrument. Blake et al [100] noted that some VOCs linger onto the surface of stainless steel causing memory effects in time resolved measurements. This could be the case with methanethiol and DMDS.

Conversely, a higher concentration was calculated for trimethylamine, 2-butanone and 1-propanol from CIR-MS compared to SPME-GC-MS. The reduced concentration calculated for trimethylamine, 2-butanone and 1-propanol might be attributed to polarity, especially as polar compounds do not retain as well on non-polar DB5-MS column.

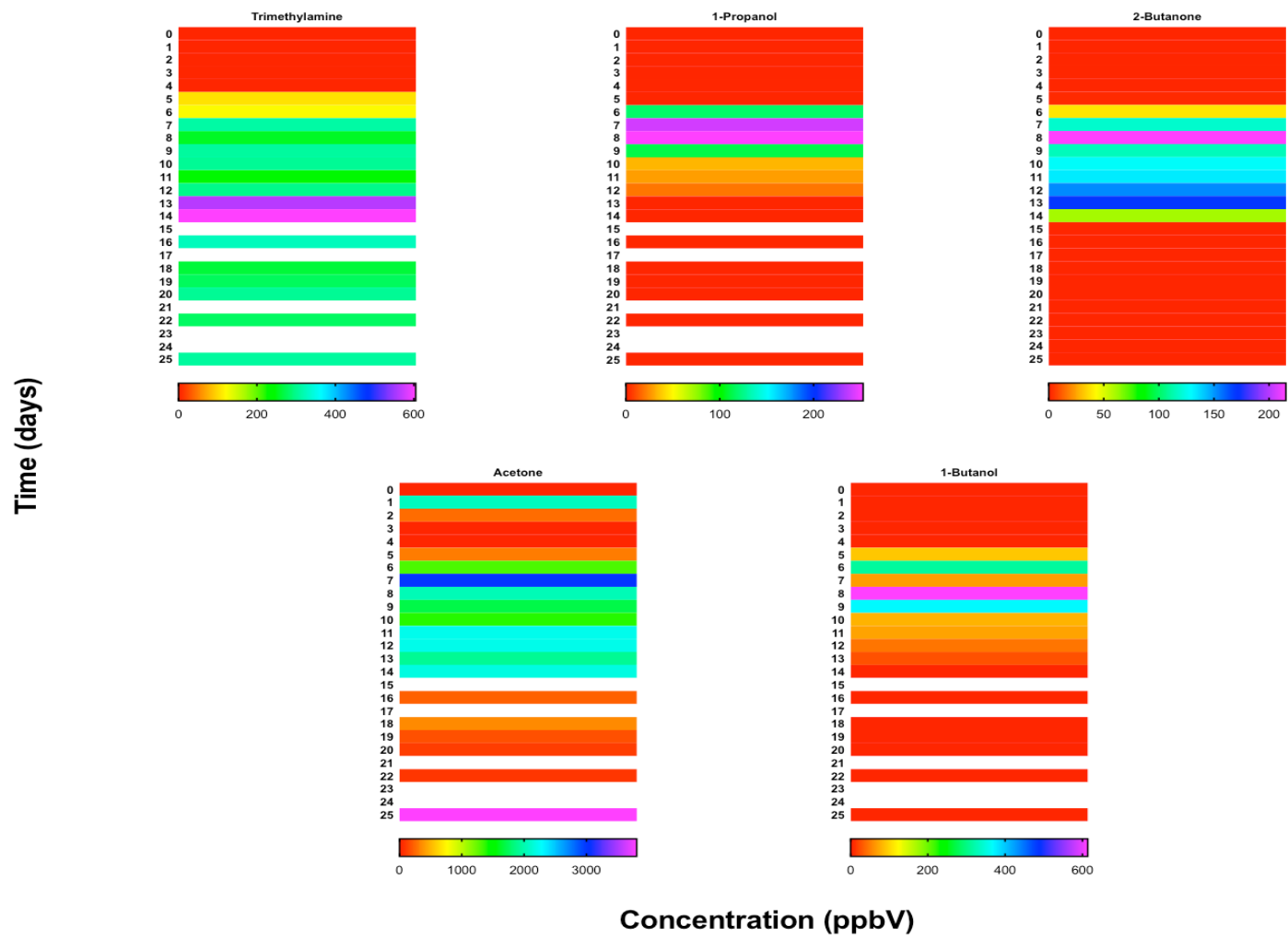


Figure 5.18 Quantification of trimethylamine, 1-propanol, 2-butanone, acetone and 1-butanol as measured by SPME-GC-MS during EHA trial 3

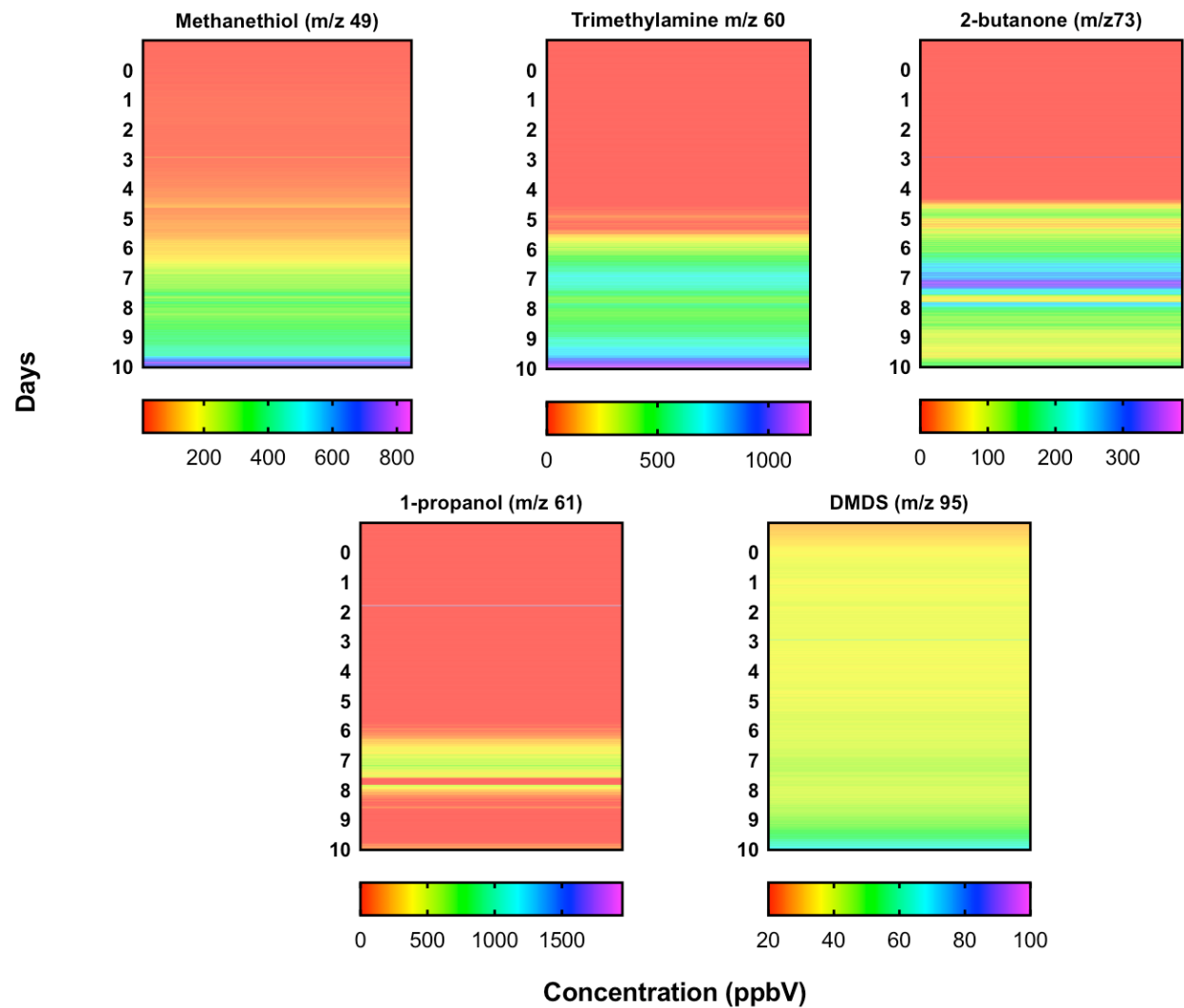


Figure 5.19 Quantification of methanethiol, trimethylamine, 2-butanone, 1-propanol, dimethyl disulphide as obtained by CIR-MS

## 5.4 Chapter 5 summary

The results generated from exposed human analogue trials provide evidence for the need of multiple analytical techniques such as CIR-MS and GC-MS in the study of carcass decomposition. CIR-MS was successful in monitoring the patterns between traces level VOCs attributed to the decomposition process, while GC-MS was effective for compound identification. Overall, this EHA study demonstrated that regardless of methodology, location, a distinct set of VOCs prevails during carcass decomposition.

Each analytical technique employed was not without its challenges, for example, the overwhelming contributions from ammonia in the analyte gas, forced the proton transfer mechanism to shift from hydronium to ammonium dominated, which increased the complexity of data interpretation. From the results generated by SPME-GC-MS, it is clear that polysulphides are the most abundant class of compounds in the exposed trials. The common polysulphides measured across both trials were DMS, DMDS, dimethyl trisulphide, tetra methyl sulphide and carbon disulphide. Other common compounds include trimethylamine, acetone, 2-butanone, methanethiol and carbamic ammonium salt.

Despite the fact that only the results generated by CIR-MS in the first 10 days of EHA trial 3 were discussed, it was still possible to draw similarities between the compounds monitored by CIR-MS and SPME-GC-MS. Compounds such as dimethyl disulphide, methanethiol, trimethylamine, 2-butanone, 1-propanol, 1-butanol, and acetone were monitored by both techniques. Having said that reported concentrations of both the techniques with respect to these seven common compounds did not agree.

The overwhelming contribution from ammonia compromises the ion chemistry in the drift tube region of the CIR-MS, however, CIR-MS could be a good technique to use throughout the decomposition process if hydronium can be maintained as the primary ion.



# 6 CONCLUSIONS

From the onset, the aim of this research project was to contribute to the current body of knowledge surrounding elucidating the profile of decomposition odour. In spite of the rapidly growing literature on the subject, there remains a number of gaps; which this research set out to explore. Broadly speaking, the main objectives of this research project were as follows; 1) assess the feasibility of CIR-MS as an analytical tool in the study of decomposition odour, 2) improve upon the repeatability of carcass decomposition and hence decomposition odour, 3) assess if decomposition related VOCs measured in headspace could be used to denote stages of decay, 4) assess the influence of soil on the release of decomposition VOCs into the headspace matrix, and 5) quantify core VOCs associated with buried and exposed carcass decomposition.

## 6.1.1 Feasibility of CIR-MS in the study of decomposition odour

The results generated from the trials conducted towards this research provides evidence that CIR-MS is a valuable technique that should be incorporated into the study of decomposition odour. Its fast response, sensitivity and focus on trace organic compounds has already found niche applications, of which decomposition odour can be included. The CIR-MS instrument employed in this study focused predominantly on proton transfer reactions between hydronium ions (reagent ion) and trace gases (M). The decision to use hydronium as the reagent ion was based on its low proton affinity and its availability. The low proton affinity of hydronium positioned it as an ideal candidate to transfer a proton to other molecules, especially as most organic compounds poses higher proton affinities than water. This meant PTR reactions were feasible thermodynamically for almost all chemical classes, with the exception of low

molecular weight alkanes which undergo endothermic proton transfer reactions with hydronium [100]. The CIR-MS instrument used in this study was capable of following the succession of VOCs released during decomposition of buried and exposed carcasses. Decomposition VOCs were sampled online, and in the buried trials  $m/z$  63, 79, 94, 95, 96, 97 and 141 were consistently monitored by CIR-MS. Mass channel 63 and 95 were identified by SPME-GC-MS as dimethyl sulphide and dimethyl disulphide respectively. Whereas in the exposed trial (day1-10 of EHA 3), a total of twenty core mass channel extracted from the CIR-MS dataset were proposed to describe the odour profile of surface deposited carcass. Aside from DMDS and DMS, mass channels 49, and 61 were identified as methanethiol and trimethylamine.

The effect of sample humidity can significantly affect the chemistry occurring within the drift tube of the CIR-MS instrument. The humidity effect which was derived from the increase in hydrated hydronium clusters (at  $m/z$  37 and  $m/z$  57) has been described in section 3.2.2. In BHA trial 4, the highest contribution of hydrated water clusters was observed on day 10 (figure 6.1). In spite of this however, there was no significant effect on the resulting mass spectra collected between days 10-15 and day 24-27 (Figure 6.2). These results confirm that the humidity of the CIR-MS instrument was not comprised during the trials.

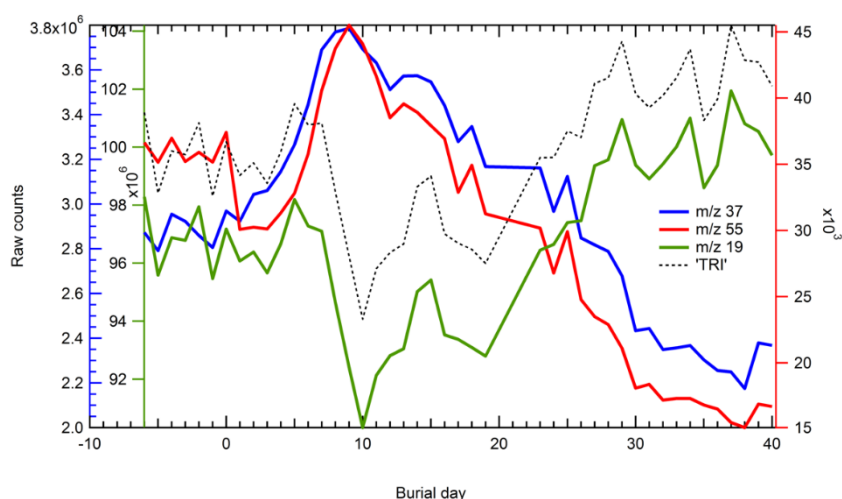


**Figure 6.1** Time profiles of reagent ion at  $m/z$  19, and hydrated hydronium clusters at  $m/z$  37 and 57 during BHA trial 4.

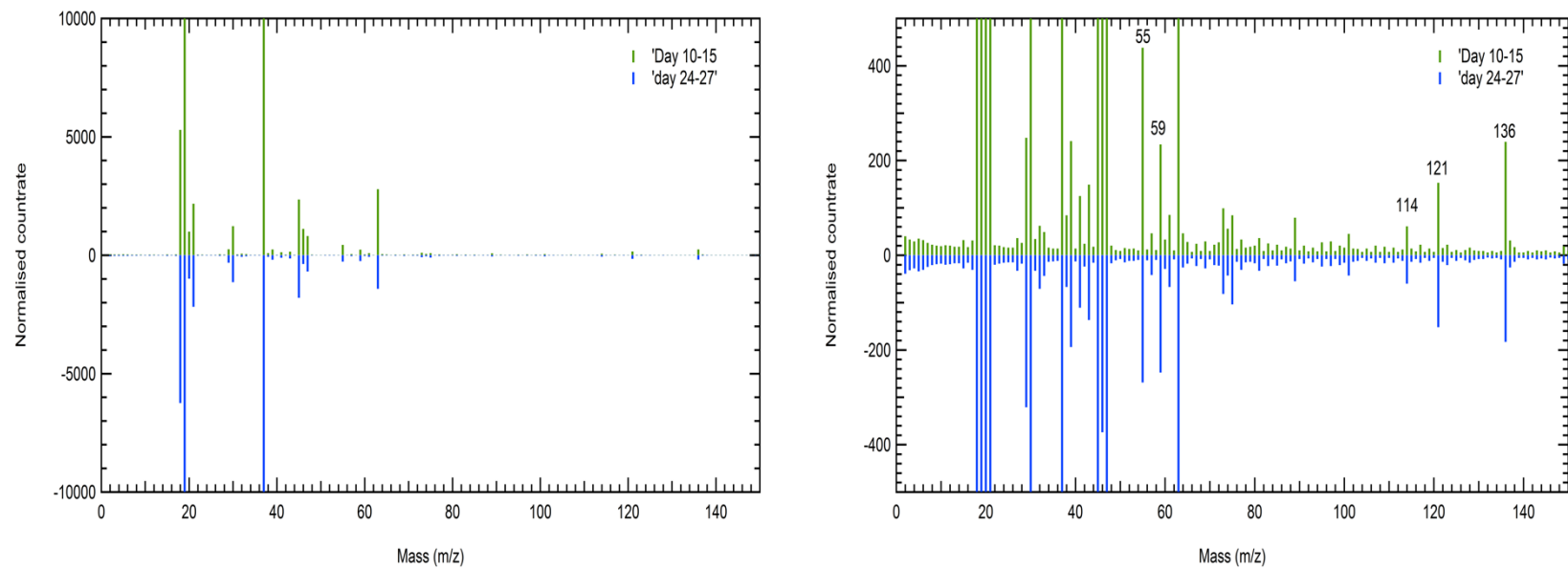


Figure 6.2 Comparison of the mass spectrum obtained during the days 10-15 versus day 24-27 of BHA 4 tria

## **6.1.2 Repeatability of carcass decomposition**

In order to improve upon the repeatability of carcass decomposition and hence increase the reproducibility of decomposition VOCs, trials were conducted in confined environments. The development of a bespoke environmentally controlled decomposition chamber where by environmental factors such as temperature, relative humidity and environmental fauna and flora were restricted proved to be successful in ensuring carcasses underwent decay at the similar rates.

In the buried trials, temperatures were stabilised at 22 °C with a maximum temperature change of less than 1 °C throughout the decay process. Similarly, the temperatures of the exposed trials were constant at approximately 20 °C. Relative humidity was stable at 99% within the decomposition chamber and environmental fauna was restricted through sterilisation of the soil. The net outcome of this was that the main factors governing the rate of decay were the microorganisms originating from the carcass itself.

Seven core mass channels were observed between the buried experiments. These included  $m/z$  63, 79, 94, 95, 96, 97 and 141. More compelling however, was the distinctive pattern observed between days 4-8 of both buried trials which was proposed to signify the active stage of decomposition. Despite the added complications of competing reagent ions in the exposed trials, similar behaviours were reported for hydronium and ammonium. In both exposed trials, ammonium became the most prevalent ion beyond day 15.

## **6.1.3 Stages of decomposition from headspace measurements**

The stages of decomposition during buried and exposed human analogue trials were characterised solely from the patterns extracted from the core VOCs measured in the headspace. The stages were not definitive, especially given that the process of

decomposition is a continuum and stages of decay are known to overlap [54]. Despite this, it was possible to extract information about the fresh and bloated stage of decay which typically occurred within the first 2-3 days following burial, the active stage between days 4-8, advanced stage from day 18 to 23, and dry stage from day 33 onwards. In the exposed trials, the fresh stage is suggested to have occurred in the first 2 days, bloated between days 3 and 5, and active stage from days 6 -10 onwards. A number of compounds observed in the active stages of both trials were in agreement with the literature

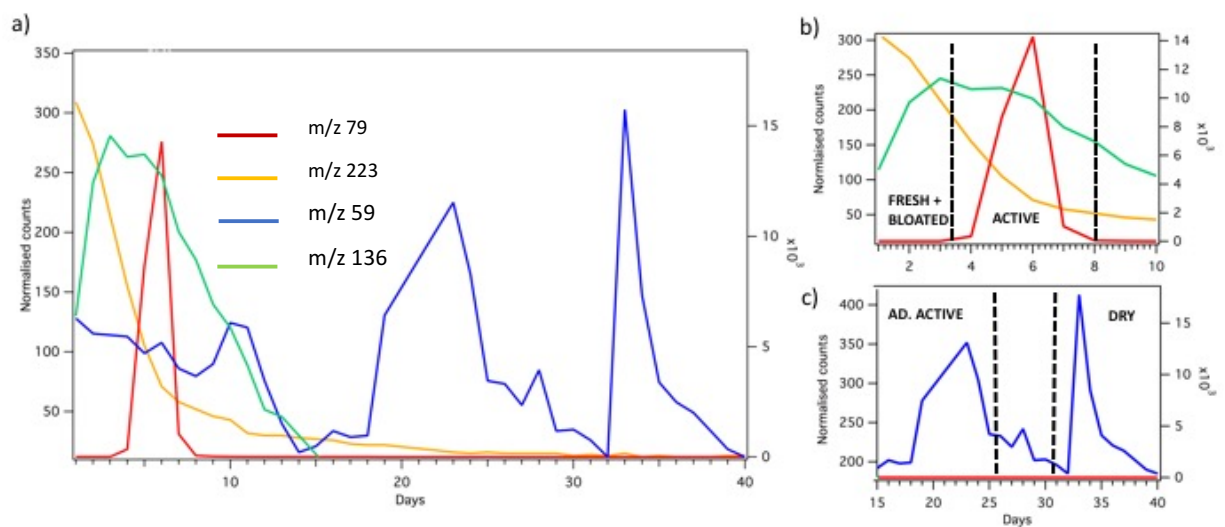


Figure 6.3 Stage of decomposition from the Buried Human Analogue trials

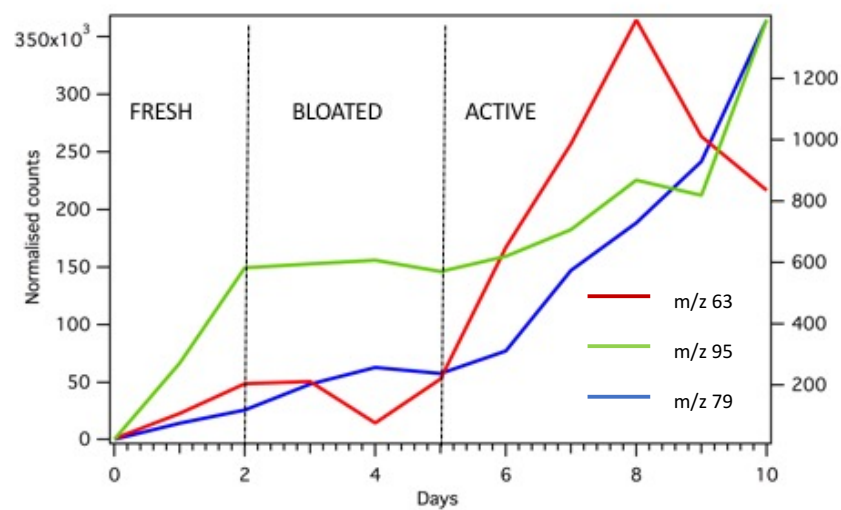


Figure 6.4 Stage of decomposition as measured during the Exposed Human Analogue trails.

#### 6.1.4 Influence of soil on decomposition VOCs.

As expected, the nature of burial affected the migration of decomposition specific VOCs into the headspace region of the chamber. This was particularly clear from the difference in the types of compounds extracted across the full duration of both studies (Figure 4.13 and Figure 5.8). There was no clear pattern in the distribution of VOCs when grouped by chemical class in the buried experiments. Whereas, when soil was excluded entirely (exposed), it became apparent that alkanes were mostly released during the first 4 days, alcohols between days 5 and 12, aromatics between days 6 and 14.

The effect of soil on VOCs was first noticed from the background measurements collected in sequence (Figure 4.4). From these, it was clear that soil acted as a sink for majority of the compounds previously identified in the background chamber. This phenomenon is suggested to have spread across the buried trials and explains why 1-propanol, 1-butanol, methanethiol, 2-butanone, trimethylamine, acetone, were not detected in the headspace of the buried trials. The notion of soil acting as sink to decomposition VOCs has been corroborated by other authors [125].

Despite the restriction soil had on the release of decomposition VOCs into the headspace of the decomposition chamber, polysulphides dimethyl sulphide and dimethyl disulfide were still noticeable between day 4 and 8 of the buried trials. This finding supports the narrative that polysulphides, specifically dimethyl sulphide and dimethyl disulfide, could be used as a marker of decomposition. Dimethyl sulphide was observed across all stages of decay, although highest concentrations were seen during the active stage (day 6). Dimethyl disulfide was a marker for the active stage, though its presence was short-lived (between days 4 and 8).

### **6.1.5 Core VOCs associated with buried and exposed decomposition**

The findings generated from exposed human analogue trial 3 puts forward the claim that methanethiol, trimethylamine, 2-butanone, 1-propanol, 1-butanol acetone and dimethyl disulphide are possible markers of carcass decomposition. While in the buried human analogue trials, polysulphides dimethyl sulphide and dimethyl disulphide could be indicative of the active stage of decomposition during buried decomposition.

## **6.2 Future considerations**

Evidence by the reduced number of reported decomposition specific VOCs monitored in the headspace of the buried carcasses, soil was considered to act as a sink for VOCs. Soil is able to retain products in soil gas, soil moisture, and even on the surface of soil particles [63]. The work conducted here was not meant to be conclusive on the subject of the influence soil has on decomposition products, instead it merely serves to support what is already known, and to highlight that specific decomposition products dimethyl sulphide and dimethyl disulfide still persist in the headspace above the soil used to bury a corpse. More research is still needed to investigate how long these two proposed markers of decomposition persist in the headspace even after removal of the corpse. In addition, it might also be worthwhile to compare the number and types of VOCs released from the soil at elevated temperatures with those released from exposed trials.

Another area worth developing would be the effect of oxygen on the decomposition odour profile, especially in cases where there is a complete depletion of oxygen (anoxic). In the process of decomposition, it could be argued that there is a switch between aerobic and anaerobic metabolic processes. Once the heart function has ceased, levels of oxygen decline, which in turn promotes anaerobic breakdown. Typically, when the bloated stage has ended, and the body begins to deflate, there is a re-introduction of oxygen back into the body, allowing aerobic microorganisms to again function. This interplay between the two processes could have an effect on the rate of

decomposition, and potentially the types of compounds released as a result. This could be particularly relevant for a corpse buried in deeper, more compacted graves where oxygen availability is significantly reduced.

At present, very little evidence is available to emphasize the specific source of decomposition products. Perhaps research could be conducted on individual body parts or organs to pinpoint the sources of the key markers of decay. More so, it is probable that a corpse would be disembodied either intentionally by the suspect (to aid transport during disposal) or naturally by scavengers and predators[54].

There is also scope to feed the effluents of a GC into a PTR-MS as well as EI-MS simultaneously. The GC as always would separate components of decomposition odour on the chromatographic column, however by feeding the effluent into a PTR-MS and EI-MS simultaneously, the probability of identifying the analyte is further increased. Soft ionisation of PTR-MS would allow for identification of the molecular ion, while fragmentation of ions by EI-MS would enhance unambiguous identification of compounds.

Use of a SPME fibre with absorbent properties such as PDMS with a higher linear range would also allow for accurate quantification of methanethiol and dimethyl disulfide, both compounds which are proposed in this study as possible key markers of decomposition. Generally absorbent fibres have a greater capacity and wider linear range although minimum quantification limits are also quite high [117].

Finally, competing reagent ions ammonium and hydronium experienced in the exposed human analogue trials discussed within this thesis restricted the analysis of the CIR-MS dataset collected. Higher dilutions (> 50 fold) was needed to suppress the abundant contributions from ammonia, however achieving this was particularly difficult on the CIR-MS without altering the operational settings such as E/N. Perhaps there is also scope to explore the alternate reaction pathways occurring within the drift tube when competing reagent ions exist. Alternatively, exploring the option of using other reagent ions like  $O_2^+$  or  $NH_4^+$  might be another possibility [111, 112].



# 7

## BIBLIOGRAPHY

1. Oxford University Press, in *Oxford dictionaries*. 2016.
2. Lyman, L., *What taphonomy is, What it isn't, and why taphonomists should care about the difference*. *Journal of Taphonomy*, 2010. 8(1).
3. Pokines, J. and B. Joan, *Manual of Forensic Taphonomy*. 2014.
4. Tibbet, M. and D. Carter, *Soil Analysis in Forensic Taphonomy*. 2008: CRC Press.
5. Haglund, W. and M. Sorg, *Forensic Taphonomy: the postmortem fate of human remains*. 1997, CRC Press: Florida.
6. Stadler, S., *Analysis of the Volatile Organic Compounds produced by the Decomposition of Pig Carcasses and Human Remains*, in *Applied Bioscience*. 2013, University of Ontario Institute of Technology.
7. Killiam, E., *The detection of human remains*. 2004, Springfield Illinois.
8. Jackson, A. and J. Jackson, *Forensic Science*. Third ed. 2011, Edinburgh, England: Pearson Education Limited.
9. Tipple, C.A., et al., *Comprehensive characterization of commercially available canine training aids*. 2014. - p 242- 254.
10. DeGreeff, L.E., B. Weakley-Jones, and K.G. Furton, *Creation of training aids for human remains detection canines utilizing a non-contact, dynamic airflow volatile concentration technique*. *Forensic Science International*, 2012. 217(1–3): p. 32-38.
11. Willis, C.M., et al., *Olfactory detection of human bladder cancer by dogs: proof of principle study*. *BMJ*, 2004. 329(7468): p. 712.
12. Lorenzo, N., et al., *Laboratory and field experiments used to identify *Canis lupus var. familiaris* active odor signature chemicals from drugs, explosives, and humans*. *Analytical and Bioanalytical Chemistry*, 2003. 376(8): p. 1212-1224.
13. Komar, D., *The Use of Cadaver Dogs in Locating Scattered, Scavenged Human Remains: Preliminary Field Test Results*. 1999.
14. Gazit, I. and J. Terkel, *Explosives detection by sniffer dogs following strenuous physical activity*. *Applied Animal Behaviour Science*, 2003. 81(2): p. 149-161.
15. Furton, K.G., et al., *Advances in the use of odour as forensic evidence through optimizing and standardizing instruments and canines*. *Philosophical Transactions of the Royal Society of London B: Biological Sciences*, 2015. 370(1674).
16. Rebmann, A., E. David, and M.H. Sorg, *Cadaver Dog handbook: forensic training and tactics for the recovery of human remains*. CIT0020CIT0020 ed. 2000, Florida: CRC Press.

17. Alexander, M.B., et al., *The Effects of Soil Texture on the Ability of Human Remains Detection Dogs to Detect Buried Human Remains*. Journal of Forensic Sciences, 2016. 61(3): p. 649-655.
18. Oesterhelweg, L., et al., *Cadaver dogs—A study on detection of contaminated carpet squares*. Forensic Science International, 2008. 174(1): p. 35-39.
19. Alexander, M.B., et al., *Application of soil in Forensic Science: Residual odor and HRD dogs*. Forensic Science International. 249: p. 304-313.
20. Stadler, S., et al., *Analysis of synthetic canine training aids by comprehensive two-dimensional gas chromatography–time of flight mass spectrometry*. Journal of Chromatography A, 2012. 1255: p. 202-206.
21. Vass, A.A., *The elusive universal post-mortem interval formula*. Forensic Science International. 204(1): p. 34-40.
22. Byrd, J. and J. Castner, *Forensic Entomology: The utility of arthropods in Legal Investigations*. Vol. 2. 2001: CRC Press.
23. Reichs, K., *Forensic Osteology: Advances in the identification of Human Remains*. 1998, Springfield, Illinois. USA: Charles C Thomas.
24. Knight, B. and I.A.N. Lauder, *Methods of dating skeletal remains*. Human Biology, 1969. 41(3): p. 322-341.
25. Vass, A.A., *Beyond the grave—understanding human decomposition*. Microbiology today, 2001. 28: p. 190-193.
26. Lee Goff, M., *Early post-mortem changes and stages of decomposition in exposed cadavers*. Experimental and Applied Acarology, 2009. 49(1): p. 21-36.
27. Dekeirsschieter, J., et al., *Cadaveric volatile organic compounds released by decaying pig carcasses in different biotopes*. Forensic Science International. 189(1): p. 46-53.
28. Statheropoulos, M., et al., *Combined chemical and optical methods for monitoring the early decay stages of surrogate human models*. Forensic Science International. 210(1): p. 154-163.
29. DeGreeff, L.E. and K.G. Furton, *Collection and identification of human remains volatiles by non-contact, dynamic airflow sampling and SPME-GC/MS using various sorbent materials*. Analytical and Bioanalytical Chemistry, 2011. 401(4): p. 1295-1307.
30. Dekeirsschieter, J., et al., *Enhanced Characterization of the Smell of Death by Comprehensive Two-Dimensional Gas Chromatography-Time-of-Flight Mass Spectrometry (GCxGC-TOFMS)*. PLoS ONE, 2012. 7(6)
31. Spicka, A., et al., *Carcass mass can influence rate of decomposition and release of ninhydrin-reactive nitrogen into gravesoil*. Forensic Science International. 2009(1): p. 80-85.
32. Matuszewski, S., et al., *Effect of body mass and clothing on decomposition of pig carcasses*. International journal of legal medicine, 2014. 128(6): p. 1039-1048.
33. Vass, A.A., et al., *Time since death determinations of human cadavers using soil solution*. Journal of Forensic Science, 1992. 37(5): p. 1236-1253.
34. Simmons, T., R.E. Adlam, and C. Moffatt, *Debugging Decomposition Data—Comparative Taphonomic Studies and the Influence of Insects and Carcass*

- Size on Decomposition Rate*. Journal of Forensic Sciences, 2010. 55(1): p. 8-13.
35. Hewadikaram, K.A. and M.L. Goff, *Effect of Carcass Size on Rate of Decomposition and Arthropod Succession Patterns*. The American Journal of Forensic Medicine and Pathology, 1991. 12(3).
  36. Campobasso, C.P., G. Di Vella, and F. Introna, *Factors affecting decomposition and Diptera colonization*. Forensic Science International, 2001. 120(1): p. 18-27.
  37. Carter, D.O., D. Yellowlees, and M. Tibbett, *Temperature affects microbial decomposition of cadavers (Rattus rattus) in contrasting soils*. Applied soil ecology, 2008. 40(1): p. 129-137.
  38. Michaud, J.-P. and G. Moreau, *A Statistical Approach Based on Accumulated Degree-days to Predict Decomposition-related Processes in Forensic Studies*. 2011. 56(1): p 232.
  39. Higley, L.G., L.P. Pedigo, and K.R. Ostlie, *Degday: A Program for Calculating Degree-days, and Assumptions Behind the Degree-day Approach*. Environmental Entomology, 1986. 15(5): p. 999-1016.
  40. Megyesi, M.S., S.P. Nawrocki, and N.H. Haskell, *Using accumulated degree-days to estimate the postmortem interval from decomposed human remains*. J Forensic Sci, 2005. 50(3): p. 618-26.
  41. Van Belle, L.E., D.O. Carter, and S.L. Forbes, *Measurement of ninhydrin reactive nitrogen influx into gravesoil during aboveground and belowground carcass (Sus domesticus) decomposition*. Forensic Science International, 2009. 193(1-3): p. 37-41.
  42. Marc.S, M. *Frozen environments and soft tissue preservation*. Forensic taphonomy: the postmortem fate of human remains, 1997. 171-180.
  43. Ruffer, M.A., *Studies in palæopathology in Egypt*. The Journal of Pathology and Bacteriology, 1913. 18(1): p. 149-162.
  44. Carter, D.O., D. Yellowlees, and M. Tibbett, *Moisture can be the dominant environmental parameter governing cadaver decomposition in soil*. Forensic Science International. 200(1): p. 60-66.
  45. Forbes, S.L., B.B. Dent, and B.H. Stuart, *The effect of soil type on adipocere formation*. Forensic Science International. 154(1): p. 35-43.
  46. David, C., *Processes associated with cadaver decomposition in soil*, in *School of Pharmacy and Molecular Sciences*. 2005, James Cook University.
  47. European Parliament, C.o.E.U., *Directive 2004/42/CE of the European Parliament and of the council of 21 April 2004 on the limitations of emission of volatile organic compounds due to the use of organic solvents in certain paints and varnishes and vehicle refinishing products and amending Directive 199/13/EC*. 2004, Official Journal of the European Union.
  48. Martin, F. and W. John, *Organic Chemistry*. Toronto: James and Bartlett.
  49. Ralph, P. and H. William, *General chemistry: principles and modern applications*. 2002, New Jersey, Pentice Hall.
  50. Kampa, M. and E. Castanas, *Human health effects of air pollution*. Environmental Pollution, 2008. 151(2): p. 362-367.
  51. Bernstein, J.A., et al., *The health effects of nonindustrial indoor air pollution*. Journal of Allergy and Clinical Immunology, 2008. 121(3): p. 585-591.

52. Fiedler, N., et al., *Health Effects of a Mixture of Indoor Air Volatile Organics, Their Ozone Oxidation Products, and Stress*. Environmental Health Perspectives, 2005. 113(11): p. 1542-1548.
53. Finlayson-Pits, B.J. and J.N.P. Jr, *Chemistry of the upper and lower atmosphere: theory, experiments and applications*. 1999: Academic Press.
54. Vass, A.A., *Odor mortis*. Forensic Science International. 222(1): p. 234-241.
55. Statheropoulos, M., et al., *Environmental aspects of VOCs evolved in the early stages of human decomposition*. Science of The Total Environment, 2007. 385(1–3): p. 221-227.
56. Statheropoulos, M., C. Spiliopoulou, and A. Agapiou, *A study of volatile organic compounds evolved from the decaying human body*. Forensic Science International. 153(2): p. 147-155.
57. Stadler, S., et al., *Characterization of Volatile Organic Compounds from Human Analogue Decomposition Using Thermal Desorption Coupled to Comprehensive Two-Dimensional Gas Chromatography-Time-of-Flight Mass Spectrometry*. Analytical Chemistry, 2013. 85(2): p. 998-1005.
58. Agapiou, A., et al., *Analysis of volatile organic compounds released from the decay of surrogate human models simulating victims of collapsed buildings by thermal desorption–comprehensive two-dimensional gas chromatography–time of flight mass spectrometry*. Analytica Chimica Acta, 2015. 883: p. 99-108.
59. Swann, L.M., S.L. Forbes, and S.W. Lewis, *Analytical separations of mammalian decomposition products for forensic science A review*. Analytica Chimica Acta, 2010. 682(1-2): p. 9-22.
60. Benninger, L.A., D.O. Carter, and S.L. Forbes, *The biochemical alteration of soil beneath a decomposing carcass*. Forensic Science International. 180(2): p. 70-75.
61. Forbes, S.L., et al., *Comparison of the Decomposition VOC Profile during Winter and Summer in a Moist, Mid-Latitude (Cfb) Climate*. PLoS ONE, 2014. 9(11): p. e113681.
62. Forbes, S.L. and K.A. Perrault, *Decomposition Odour Profiling in the Air and Soil Surrounding Vertebrate Carrion*. PLoS ONE, 2014. 9(4): p. e95107.
63. Stokes, K.L., et al., *Decomposition Studies Using Animal Models in Contrasting Environments: Evidence from Temporal Changes in Soil Chemistry and Microbial Activity*. Criminal and Environmental Soil Forensics, 2009: p. 357-377.
64. Cablk, M.E., E.E. Szlagowski, and J.C. Sagebiel, *Characterization of the volatile organic compounds present in the headspace of decomposing animal remains, and compared with human remains*. Forensic Science International, 2012. 220(1–3): p. 118-125.
65. Stadler, S., J.P. Desaulniers, and S.L. Forbes, *Inter-year repeatability study of volatile organic compounds from surface decomposition of human analogues*. International Journal of Legal Medicine, 2015. 129(3): p. 641-650.
66. Perrault, K.A., et al., *Seasonal comparison of carrion volatiles in decomposition soil using comprehensive two-dimensional gas chromatography - time of flight mass spectrometry*. Analytical Methods, 2015. 7(2): p. 690-698.

67. Hoffman, E.M., et al., *Characterization of the volatile organic compounds present in the headspace of decomposing human remains*. Forensic Science International. 186(1): p. 6-13.
68. Perrault, K.A., B.H. Stuart, and S.L. Forbes, *A longitudinal study of decomposition odour in soil using sorbent tubes and solid phase microextraction*. Chromatography, 2014. 1(3): p. 120-140.
69. Forbes, S.L., et al., *Profiling the decomposition odour at the grave surface before and after probing*. Forensic Science International, 2016. 259: p. 193-199.
70. Stefanuto, P.H., et al., *GC×GC–TOFMS and supervised multivariate approaches to study human cadaveric decomposition olfactive signatures*.
71. Furton, K.G. and L.J. Myers, *The scientific foundation and efficacy of the use of canines as chemical detectors for explosives*<sup>1</sup>. Talanta, 2001. 54(3): p. 487-500.
72. Ampuero, S. and J.O. Bosset, *The electronic nose applied to dairy products: a review*. Sensors and Actuators B: Chemical, 2003. 94(1): p. 1-12.
73. Dragonieri, S., et al., *An electronic nose in the discrimination of patients with asthma and controls*. Journal of Allergy and Clinical Immunology, 2007. 120(4): p. 856-862.
74. Dragonieri, S., et al., *An electronic nose in the discrimination of patients with non-small cell lung cancer and COPD*. Lung cancer, 2009. 64(2): p. 166-170.
75. Statheropoulos, M., et al., *Discriminant Analysis of Volatile Organic Compounds data related to a new location method of entrapped people in collapsed buildings of an earthquake*. Analytica Chimica Acta, 2006. 566(2): p. 207-216.
76. Brasseur, C., et al., *Comprehensive two-dimensional gas chromatography–time-of-flight mass spectrometry for the forensic study of cadaveric volatile organic compounds released in soil by buried decaying pig carcasses*. Journal of Chromatography A, 2012. 1255: p. 163-170.
77. Forbes, S.L., B.H. Stuart, and B.B. Dent, *The effect of the method of burial on adipocere formation*. Forensic Science International. 154(1): p. 44-52.
78. Warneke, C., et al., *Measurements of benzene and toluene in ambient air using proton-transfer-reaction mass spectrometry: calibration, humidity dependence, and field intercomparison*. International Journal of Mass Spectrometry, 2001. 207(3): p. 167-182.
79. Schoenly, K.G., et al., *Recreating deaths acre in the school yard: Using Pig Carcasses as Model Corpses To Teach Concepts of Forensic Entomology & Ecological Succession*. The American Biology Teacher, 2006. 68(7): p. 402-410.
80. Catts, E.P. and M.L. Goff, *Forensic entomology in criminal investigations*. Annu Rev Entomol, 1992. 37: p. 253-72.
81. Stokes, K.L., S.L. Forbes, and M. Tibbett, *Human Versus Animal: Contrasting Decomposition Dynamics of Mammalian Analogues in Experimental Taphonomy*. Journal of Forensic Sciences, 2013. 58(3): p. 583-591.
82. Vas, G. and K. Vekey, *Solid-phase microextraction: a powerful sample preparation tool prior to mass spectrometric analysis*. Journal of mass spectrometry, 2004. 39(3): p. 233-254.

83. Arthur, C.L. and J. Pawliszyn, *Solid phase microextraction with thermal desorption using fused silica optical fibers*. Analytical Chemistry, 1990. 62(19): p. 2145-2148.
84. Arthur, C.L., et al., *Environmental analysis of organic compounds in water using solid phase micro extraction*. Journal of High Resolution Chromatography, 1992. 15(11): p. 741-744.
85. Centini, F., A. Masti, and I.B. Comparini, *Quantitative and qualitative analysis of MDMA, MDEA, MA and amphetamine in urine by head-space/solid phase micro-extraction (SPME) and GC/MS*. Forensic Science International, 1996. 83(3): p. 161-166.
86. Peng, S., et al., *Determination of Seven Odorants in Purified Water Among Worldwide Brands by HS-SPME Coupled to GC-MS*. Chromatographia, 2014. 77(9-10): p. 729-735.
87. Shirey, R.E., *SPME Commercial Devices and Fibre Coatings*, in *Handbook of Solid Phase Microextraction*. 2012, Elsevier: Oxford. p. 99-133.
88. Pawliszyn, J., *Theory of Solid-Phase Microextraction*, in *Handbook of Solid Phase Microextraction*. 2012, Elsevier: Oxford. p. 13-59.
89. Schmidt, K., *SPME method development in Analysis of VOCs as potential biomarkers of Cancer*. Journal of Molecular Biomarkers and Diagnosis, 2015. 6(253).
90. Archer, M., *The development of partition chromatography**The development of partition chromatography*. 1955, Norstedt.
91. Szepeszy, L. and D. Morgan, *Gas Chromatography- Theory*, ed. M. E.D. 1963, Budapest: House of Hungary Academy of Sciences.
92. Ellis, A.M. and C.A. Mayhew, *Proton transfer reaction mass spectrometry: principles and applications*. 2013: John Wiley & Sons.
93. Curran, A.M., *The Differentiation of the Volatile Organic Signatures of Individuals Through SPME-GC/MS of Characteristic Human Scent Compounds*. 2010. 50.
94. Von Hoermann, C., et al., *The importance of carcass volatiles as attractants for the hide beetle*. Forensic Science International. 212(1): p. 173-179.
95. Karasek, F.W. and R.E. Clement, *Basic gas chromatography-mass spectrometry: principles and techniques*. 2012: Elsevier.
96. Jonsson, J.A., *Chromatographic theory and basic principles*. 1987: CRC Press.
97. McNair, H.M. and J.M. Miller, *Basic gas chromatography*. 2011: John Wiley & Sons.
98. Wenzel, T., *Separation Science: Chromatography Unit*, D.o.C.-B. College, Editor., Bates College: Lewiston ME 04240.
99. Daniel, H.C., *Quantitative Chemical Analysis*. 2003, NY, USA: W.H Freeman and Company.
100. Blake, R.S., P.S. Monks, and A.M. Ellis, *Proton-transfer reaction mass spectrometry*. Chemical reviews, 2009. 109(3): p. 861-896.
101. Harrison, A.G., *Chemical ionization mass spectrometry*. 1992: CRC press.
102. Karoly, V., *Internal Energy Effects in Mass Spectrometry*. Journal of Mass Spectrometry, 1996. 31: p. 445-463.
103. Field, F.H., *Chemical ionization mass spectrometry*. Accounts of Chemical Research, 1968. 1(2): p. 42-49.

104. Lindinger, W., A. Hansel, and A. Jordan, *On-line monitoring of volatile organic compounds at pptv levels by means of proton-transfer-reaction mass spectrometry (PTR-MS) medical applications, food control and environmental research*. International Journal of Mass Spectrometry and Ion Processes, 1998. 173(3): p. 191-241.
105. Hanson, D.R., et al., *Proton transfer reaction mass spectrometry at high drift tube pressure*. International Journal of Mass Spectrometry, 2003. 223–224: p. 507-518.
106. Laerd. *Laerd Statistics, Statistical tutorials and software guides*. Laerd Statistics, Statistical tutorials and software guides. One-way ANOVA using SPSS Statistics 2015; Available from: <https://statistics.laerd.com/>.
107. Stefanuto, P.-H., P. Katelyn, and S. Sonja, *Reading Cadaveric Decomposition Chemistry with a New Pair of Glasses*. ChemPubSoc Europe, 2014.
108. Pearson, M.P., *The archaeology of death and burial*. 1999, Sutton, UK: Phoenix Mill.
109. Sinha, V., et al., *The effect of relative humidity on the detection of pyrrole by PTR-MS for OH reactivity measurements*. International Journal of Mass Spectrometry, 2009. 282(3): p. 108-111.
110. Boscaini, E., et al., *Characterization of wine with PTR-MS*. International Journal of Mass Spectrometry, 2004. 239(2): p. 215-219.
111. Norman, M., A. Hansel, and A. Wisthaler, *O<sup>2+</sup> as reagent ion in the PTR-MS instrument: detection of gas-phase ammonia*. International Journal of Mass Spectrometry, 2007. 265(2): p. 382-387.
112. Lindinger, W. and A. Jordan, *Proton-transfer-reaction mass spectrometry (PTR-MS): on-line monitoring of volatile organic compounds at pptv levels*. Chem. Soc. Rev., 1998. 27(5): p. 347-375.
113. Hunter, E. and L. Sharon, *Evaluated gas phase basicities and proton affinities of molecules: an update*. Journal of Physical and Chemical Reference Data, 1998. 27(3): p. 413-656.
114. Wu, J., et al., *A stable isotope-labeled internal standard is essential for correcting for the interindividual variability in the recovery of lapatinib from cancer patient plasma in quantitative LC-MS/MS analysis*. Journal of Chromatography B, 2013. 941: p. 100-108.
115. Martos, P.A. and J. Pawliszyn, *Calibration of Solid Phase Microextraction for Air Analyses Based on Physical Chemical Properties of the Coating*. Analytical Chemistry, 1997. 69(2): p. 206-215.
116. Prosen, H. and L. Zupančič-Kralj, *Solid-phase microextraction*. TrAC Trends in Analytical Chemistry, 1999. 18(4): p. 272-282.
117. Robert, S. and M. Raymond, *SPME- Adsorption versus Absorption: Which fiber is best for your application*. 1999, Sigma-Aldrich.
118. Jacobson, L.D., et al., *Odor Emissions and Chemical Analysis of Odorous Compounds from Animal Buildings*. Proceedings of the Water Environment Federation, 2010. 2010(3): p. 864-885.
119. Perrault, K.A., *Novel odour analysis of soils associated with decomposed remains. Novel odour analysis of soils associated with decomposed remains. .* 2015.

120. Damann, F.E. and D.O. Carter, *Human decomposition ecology and postmortem microbiology*. Manual of Forensic Taphonomy, CRC Press, Boca Raton, 2013: p. 37-49.
121. Swann, L., S. Forbes, and S.W. Lewis, *Observations of the temporal variation in chemical content of decomposition fluid: A preliminary study using pigs as a model system*. Australian Journal of Forensic Sciences, 2010. 42(3): p. 199-210.
122. Jonathan, C. and e. al, *Chemical ecology of vertebrate carrion. Carrion Ecology, Evolution, and Their Applications*, ed. B. Raton. 2015, Florida: CRC Press.
123. Yang, X. and T. Peppard, *Solid-phase microextraction for flavor analysis*. Journal of Agricultural and Food Chemistry, 1994. 42(9): p. 1925-1930.
124. Liu, J., et al., *Absorption of carbon dioxide in aqueous ammonia*. Energy Procedia, 2009. 1(1): p. 933-940.
125. Perrault, K., et al., *Detection of decomposition VOCs following removal of remains from a surface deposition site*. Forensic Sci Med Pathol, July 2015. 11(376).